IEEE Standards

691™

IEEE Guide for Transmission Structure Foundation Design and Testing

IEEE Power Engineering Society

Sponsored by the
Transmission and Distribution Committee

and the

American Society of Civil Engineers

Sponsored by the
Transmission Structure Foundation Design Standard Committee

IEEE

Published by
The Institute of Electrical and Electronics Engineers, Inc.
3 Park Avenue, New York, NY 10016-5997, USA

26 December 2001

Print: SH94786
PDF: SS94786

--`,,`-`-`,,`,,`,`,,`---

Copyright The Institute of Electrical and Electronics Engineers, Inc.
Provided by IHS under license with IEEE
No reproduction or networking permitted without license from IHS

Not for Resale

IEEE Guide for Transmission Structure Foundation Design and Testing

Sponsor

Transmission and Distribution Committee
of the
IEEE Power Engineering Society
and
Transmission Structure Foundation Design Standard Committee
of the
American Society of Civil Engineers

Approved 6 December 2000

IEEE-SA Standards Board

Abstract: The design of foundations for conventional transmission line structures, which include lattice towers, single or multiple shaft poles, H-frame structures, and anchors for guyed structures is presented in this guide.
Keywords: anchor, foundation, guyed structure, H-frame structure, lattice tower, multiple shaft pole, single shaft pole, transmission line structure

---

The Institute of Electrical and Electronics Engineers, Inc.
3 Park Avenue, New York, NY 10016-5997, USA

Copyright © 2001 by the Institute of Electrical and Electronics Engineers, Inc.
All rights reserved. Published 26 December 2001. Printed in the United States of America.

Print: ISBN 0-7381-1807-9 SH94786
PDF: ISBN 0-7381-1808-7 SS94786

No part of this publication may be reproduced in any form, in an electronic retrieval system or otherwise, without the prior written permission of the publisher.

Copyright The Institute of Electrical and Electronics Engineers, Inc.
Provided by IHS under license with IEEE
No reproduction or networking permitted without license from IHS
Not for Resale

IEEE Standards documents are developed within the IEEE Societies and the Standards Coordinating Committees of the IEEE Standards Association (IEEE-SA) Standards Board. The IEEE develops its standards through a consensus development process, approved by the American National Standards Institute, which brings together volunteers representing varied viewpoints and interests to achieve the final product. Volunteers are not necessarily members of the Institute and serve without compensation. While the IEEE administers the process and establishes rules to promote fairness in the consensus development process, the IEEE does not independently evaluate, test, or verify the accuracy of any of the information contained in its standards.

Use of an IEEE Standard is wholly voluntary. The IEEE disclaims liability for any personal injury, property or other damage, of any nature whatsoever, whether special, indirect, consequential, or compensatory, directly or indirectly resulting from the publication, use of, or reliance upon this, or any other IEEE Standard document.

The IEEE does not warrant or represent the accuracy or content of the material contained herein, and expressly disclaims any express or implied warranty, including any implied warranty of merchantability or fitness for a specific purpose, or that the use of the material contained herein is free from patent infringement. IEEE Standards documents are supplied "**AS IS**."

The existence of an IEEE Standard does not imply that there are no other ways to produce, test, measure, purchase, market, or provide other goods and services related to the scope of the IEEE Standard. Furthermore, the viewpoint expressed at the time a standard is approved and issued is subject to change brought about through developments in the state of the art and comments received from users of the standard. Every IEEE Standard is subjected to review at least every five years for revision or reaffirmation. When a document is more than five years old and has not been reaffirmed, it is reasonable to conclude that its contents, although still of some value, do not wholly reflect the present state of the art. Users are cautioned to check to determine that they have the latest edition of any IEEE Standard.

In publishing and making this document available, the IEEE is not suggesting or rendering professional or other services for, or on behalf of, any person or entity. Nor is the IEEE undertaking to perform any duty owed by any other person or entity to another. Any person utilizing this, and any other IEEE Standards document, should rely upon the advice of a competent professional in determining the exercise of reasonable care in any given circumstances.

Interpretations: Occasionally questions may arise regarding the meaning of portions of standards as they relate to specific applications. When the need for interpretations is brought to the attention of IEEE, the Institute will initiate action to prepare appropriate responses. Since IEEE Standards represent a consensus of concerned interests, it is important to ensure that any interpretation has also received the concurrence of a balance of interests. For this reason, IEEE and the members of its societies and Standards Coordinating Committees are not able to provide an instant response to interpretation requests except in those cases where the matter has previously received formal consideration.

Comments for revision of IEEE Standards are welcome from any interested party, regardless of membership affiliation with IEEE. Suggestions for changes in documents should be in the form of a proposed change of text, together with appropriate supporting comments. Comments on standards and requests for interpretations should be addressed to:

Secretary, IEEE-SA Standards Board
445 Hoes Lane
P.O. Box 1331
Piscataway, NJ 08855-1331
USA

Note: Attention is called to the possibility that implementation of this standard may require use of subject matter covered by patent rights. By publication of this standard, no position is taken with respect to the existence or validity of any patent rights in connection therewith. The IEEE shall not be responsible for identifying patents for which a license may be required by an IEEE standard or for conducting inquiries into the legal validity or scope of those patents that are brought to its attention.

IEEE is the sole entity that may authorize the use of certification marks, trademarks, or other designations to indicate compliance with the materials set forth herein.

Authorization to photocopy portions of any individual standard for internal or personal use is granted by the Institute of Electrical and Electronics Engineers, Inc., provided that the appropriate fee is paid to Copyright Clearance Center. To arrange for payment of licensing fee, please contact Copyright Clearance Center, Customer Service, 222 Rosewood Drive, Danvers, MA 01923 USA; (978) 750-8400. Permission to photocopy portions of any individual standard for educational classroom use can also be obtained through the Copyright Clearance Center.

--`,,`-`-`,,`,,`,`,,`---

Copyright The Institute of Electrical and Electronics Engineers, Inc.
Provided by IHS under license with IEEE
No reproduction or networking permitted without license from IHS Not for Resale

Introduction

(This introduction is not part of IEEE Std 691-2001, IEEE Guide for Transmission Structure Foundation Design and Testing.)

This design guide is intended for the use of the practicing professional engineer engaged in the design of foundations for electrical transmission line structures. This guide is not to be used as a substitute for professional engineering competency, nor is it to be considered as a rigid set of rules. Of all building materials, soil is the least uniform and most unpredictable; therefore, the methods described in this guide may not be the only methods of design and analysis, nor may they be appropriate in all situations. Design and analysis must be based upon sound engineering principles and relevant experience.

This design guide is the result of a major effort to consolidate the results of published reports and data, ongoing research, and experience into a single document. It is also an outgrowth of the previously published efforts of a joint committee of the American Society of Civil Engineers and the Institute of Electrical and Electronic Engineers, which combined the knowledge, expertise, and experience of both organizations in the field of transmission line structure foundation design. Electrical transmission line structures are unique when compared with other structures, primarily in that no human occupancy is involved and the loading requirements are different from other structure types. The primary loading of most conventional structures or buildings is a dead load or sustained live load and lateral wind forces or seismic loads. The primary loading of a transmission line structure is caused by meteorological loads, such as wind and ice, or combinations thereof [B68].[1] Under normal weather or operating conditions, the loads may be only a fraction of the ultimate capacity of tangent structures, but the application of the design load is short term and sometimes violent as nature unleashes its fury. In addition, a finite probability exists that the design load could be exceeded.

Foundations for transmission line structures are called on to resist loading conditions consisting of various combinations. Lattice tower foundations typically experience uplift or compression and horizontal shear loads. H-frame structures experience combinations of uplift or compression and horizontal shear and moment loads. Single pole structures experience horizontal shear loads and large overturning moments. Foundations for transmission structures must satisfy the same fundamental design criteria as those for any other type of structure—adequate strength and stability, tolerable deformation, and cost-effectiveness. In addition, transmission line structures may be constructed hundreds or thousands of times in a multitude of subsurface conditions encountered along the same route. Therefore, optimization and standardization for cost-effectiveness is highly desirable.

This design guide addresses fundamental performance criteria and the design methods associated with transmission line structure modes of loading, much of which is not found in geotechnical engineering textbooks.

Many alternative approaches can be used for the geotechnical design of foundations for transmission line structures. It is the intent of this design guide to provide several approaches to the design of various foundation types that are consistent with the present state of geotechnical engineering practice. Where several methods are presented for the design of a particular type of foundation, the design engineer should exercise sound engineering judgment in determining which method is most representative of the situation.

[1]The numbers in brackets correspond to those of the bibliography in Annex A.

Copyright © 2001 IEEE. All rights reserved.

Copyright The Institute of Electrical and Electronics Engineers, Inc.
Provided by IHS under license with IEEE
No reproduction or networking permitted without license from IHS
Not for Resale

Participants

At the time this guide was completed, the Foundation Design Standard Task Group of the Line Design Methods Working Group; Towers, Poles, and Conductors Subcommittee; and Transmission and Distribution Committee had the following membership:

Anthony M. DiGioia, Jr., *IEEE Co-Chair*

Fred Dewey
Yen Huang
Jake Kramer
Bob Peters
Pete Taylor

At the time this guide was completed, the Transmission Structure Foundation Design Standards Committee of the ASCE had the following membership:

Paul A. Tedesco, *ASCE Co-Chair*

Wesley W. Allen, Jr.
David R. Bowman
Kin Y. C. Chung
Samuel P. Clemence
Dennis J. Fallon
Safdar A. Gill
Adel M. Hanna
Thomas O. Keller
Fred H. Kulhawy
S. Bruce Langness
Robert C. Latham
Edwin B. Lawless III
Donald D. Oglesby
Marlyn G. Schepers
Wayne C. Teng
Charles H. Trautmann
Dale E. Welch
Robert M. White
Harry S. Wu

When the IEEE-SA Standards Board approved this standard on 6 December 2000, it had the following membership:

Donald N. Heirman, *Chair*
James T. Carlo, *Vice Chair*
Judith Gorman, *Secretary*

Satish K. Aggarwal
Mark D. Bowman
Gary R. Engmann
Harold E. Epstein
H. Landis Floyd
Jay Forster*
Howard M. Frazier
Ruben D. Garzon
James H. Gurney
Richard J. Holleman
Lowell G. Johnson
Robert J. Kennelly
Joseph L. Koepfinger*
Peter H. Lips
L. Bruce McClung
Daleep C. Mohla
James W. Moore
Robert F. Munzner
Ronald C. Petersen
Gerald H. Peterson
John B. Posey
Gary S. Robinson
Akio Tojo
Donald W. Zipse

*Member Emeritus

Also included is the following nonvoting IEEE-SA Standards Board liaison:

Alan Cookson, *NIST Representative*
Donald R. Volzka, *TAB Representative*

Andrew D. Ickowicz
IEEE Standards Project Editor

Copyright © 2001 IEEE. All rights reserved.

Copyright The Institute of Electrical and Electronics Engineers, Inc.
Provided by IHS under license with IEEE
No reproduction or networking permitted without license from IHS
Not for Resale

Contents

1. Overview 1

1.1 Scope 1
1.2 System design considerations 1
1.3 Other considerations 2

2. Loading and performance criteria 3

2.1 Loading 3
2.2 Foundation performance criteria and structure types 5

3. Subsurface investigation and selection of geotechnical design parameters 10

3.1 General 10
3.2 Phases of investigation 10
3.3 Types of boring samples 13
3.4 Soil and rock classification 15
3.5 Engineering properties 18

4. Design of spread foundations 23

4.1 Structural applications 23
4.2 Analysis 31
4.3 Traditional design methods 66
4.4 Construction considerations 73
4.5 General foundation considerations 74

5. Design of drilled shaft and direct embedment foundations 77

5.1 Types of foundations 77
5.2 Structural applications 79
5.3 Drilled concrete shaft foundations 80
5.4 Direct embedment foundations 110
5.5 Precast-prestressed, hollow concrete shafts and steel casings 113
5.6 Design and construction considerations 113

6. Design of pile foundations 115

6.1 Pile types and orientation 116
6.2 Pile stresses 121
6.3 Pile capacity 122
6.4 Pile deterioration 137
6.5 Construction considerations 139

7. Design of anchors 139

7.1 Anchor types 139
7.2 Anchor application 142
7.3 Design analysis 144
7.4 Group effect 163
7.5 Grouts 163

Copyright © 2001 IEEE. All rights reserved.

Copyright The Institute of Electrical and Electronics Engineers, Inc.
Provided by IHS under license with IEEE
No reproduction or networking permitted without license from IHS
Not for Resale

7.6 Construction considerations 164

8. Load tests 167

8.1 Introduction 167
8.2 Instrumentation 169
8.3 Scope of test program 170

Annex A (informative) Bibliography 177

--`,,`-`-`,,`,,`,`,,`---

Copyright © 2001 IEEE. All rights reserved.

Copyright The Institute of Electrical and Electronics Engineers, Inc.
Provided by IHS under license with IEEE
No reproduction or networking permitted without license from IHS

Not for Resale

IEEE Guide for Transmission Structure Foundation Design and Testing

1. Overview

1.1 Scope

The material presented in this design guide pertains to the design of foundations for conventional transmission line structures, which include lattice towers, single or multiple shaft poles, H-frame structures, and anchors for guyed structures. It discusses the mode of loads that those structures impose on their foundations and applicable foundation performance criteria. The design guide addresses subsurface investigations and the design of foundations, such as spread foundations (footings), drilled shafts, direct embedded poles, driven piles, and anchors. The full-scale load testing of the above-listed foundation types is also presented.

This design guide does not include the structural design of the foundations nor the design of the structure. Citations [B5][1] and [B50] provide guidance for the design of lattice towers and tubular steel poles, respectively. The foundation engineer should have an understanding of the magnitudes and time-history of various loading conditions imposed on the foundations in order to provide a suitable foundation to support the transmission line structures under the actual loading conditions that may be reasonably expected in actual service.

1.2 System design considerations

A transmission line is a system of interconnected elements, each individually designed. The overall line must integrate all of these individual design elements into a coordinated structural system.

Every decision made for the system should consider total installed cost, of which foundations are a major consideration. For example, wire tensions are sometimes increased to minimize the number and/or height of the supporting structures. However, if a significant number of angles is in the line, total installed costs may be higher because of increased angle structure and foundation costs. Similarly, when developing structure configurations, a wider base structure could be considered to reduce foundation loads and thereby decrease the foundation cost. This must be evaluated against the added cost of widening the structure.

[1]The numbers in brackets correspond to those of the bibliography in Annex A.

Copyright © 2001 IEEE. All rights reserved.

Copyright The Institute of Electrical and Electronics Engineers, Inc.
Provided by IHS under license with IEEE
No reproduction or networking permitted without license from IHS
Not for Resale

When designing a transmission line, the engineer has the option to design each foundation for site-specific loadings and subsurface conditions or to develop standard designs that can be used at predetermined similar sites. The preferred approach is one that will minimize the total installed cost of the line, and it may also involve a combination of site-specific and standard foundation designs.

A custom design at each site has the advantage of avoiding costly overdesign. However, this approach will require a more extensive subsurface investigation in advance of the design and involve added engineering investment to prepare the many individual designs required. A custom foundation design may be justified at angle structures, or at lightly loaded structures that will not develop the full capacity of a standard structure.

Foundations may be standardized by limiting the number to only one or two designs for each standard structure type, considering each to cover a preselected range of subsurface conditions and foundation loads. The extent of subsurface investigations can be reduced to a level necessary to identify the general subsurface conditions along the line. This approach enables the engineer to select an appropriate standard foundation. Verification of subsurface conditions at each structure site should be made during construction excavation. This approach allows for greater efficiencies in fabrication and assembly of foundation types, such as steel grillages. Using standard foundation designs will result in utilizing foundations having greater load-carrying capacity at some structure locations. Construction excavation may reveal locations that require site-specific foundations because the actual subsurface conditions are outside the limits of the preselected range. The benefits of standardization should be weighted against the cost of site-specific foundation designs and against the additional cost of redesigning the foundation when unusual subsurface conditions are encountered during construction.

The amount and extent of standardization will vary with each foundation type. Steel grillages that are entirely shop fabricated are almost always designed to cover the maximum loads for a given tower type and the majority of subsurface conditions expected along the line. An advantage of the grillage-type foundation is that concrete is not required at the site with the attendant transporting and curing requirements. In addition, grillages may be shipped to the site with the rest of the tower steel. A drilled shaft foundation can be varied to suit the actual soil conditions by providing different depths and/or diameters. Usually, the only change to prefabricated materials, required to modify drilled shaft foundations, is the length or quantity of steel reinforcing bars, and this can usually be readily accomplished at a small additional cost. Likewise, many types of pile foundations can be adapted to actual site conditions by providing standard foundations with various numbers of driven piles of varying lengths, as required.

1.3 Other considerations

Whereas this design guide is primarily aimed at the design of new foundations, the principles are applicable to the investigation of the geotechnical capacity of existing foundations for purposes of determining line capacity or for upgrading or refurbishing the line. If the foundations are upgraded to meet new loading requirements, care must be taken to assure the structural adequacy of the foundation. The investigation and design for restoration of a line after natural or man-made disasters must adhere to the same careful principles of investigation and design as a new line.

Documentation of the design and “as-built” construction data of foundations is vital, particularly if a line is to be refurbished or upgraded at a later date.

Copyright © 2001 IEEE. All rights reserved.

Copyright The Institute of Electrical and Electronics Engineers, Inc.
Provided by IHS under license with IEEE
No reproduction or networking permitted without license from IHS
Not for Resale

2. Loading and performance criteria

2.1 Loading

Each utility normally has a unique agenda of loading cases for the design of transmission line systems. Based on this information, the engineer should analyze the structural system and calculate appropriate combinations of axial, shear, and moment loads acting on every foundation for each loading case. For a given structure type, different load cases may control foundation design depending on line angles and other design factors.

Foundation design methods must be compatible with the foundation type and loading conditions. Similarly, the subsurface exploration program must be compatible with these factors to provide the required geotechnical design data.

The foundation designer should consider the following sources for the determination of foundation loads:

a) Legislated Loads
b) ASCE Guidelines for Electrical Transmission Line Structural Loading [B68]
c) State-Specific Loading Criteria (e.g., California General Order 95)
d) Utility-Specific Loading Criteria

Legislated loads provide minimum structural loading criteria for the design of transmission lines. An example of legislated loads is the National Electric Safety Code (NESC) [B117], which is a legislated code in many U.S. states.

The American Society of Civil Engineers' Committee on Electrical Transmission Structures has published a guide [B68] that provides transmission line designers with procedures for the selection of design loads and load factors. A load resistance factor design (LRFD) format is presented for the development of attachment point loads for the design of any transmission structure. The same design loads and load factors apply to structures made of steel, reinforced concrete, wood, or other materials, as well as to their foundations, with only the resistance factors differing.

Based on specific service area requirements and experience, many utilities have developed their own structural loading agenda. The structural loading agenda may include legislated loads, ASCE, and utility-specific loading criteria.

The foundation design engineer should establish the strength of the foundation relative to the strength of the structure it supports. A foundation could be designed to be stronger than the structure; thus, in the event the structure fails, its replacement can be erected on the same foundation. A foundation could be designed to have the same strength as the structure it supports, thus, developing the full capacity of the structure while minimizing foundation first-cost expenditures. In some cases, the foundation engineer may find that the foundation could be designed to carry loads that are less than the capacity of the structure (where a standard structure is used at less than its design load capacity). In this case, the designer should recognize the probability of a foundation failure if the structure is ever subjected to a load greater than the load required by the structure application. An analysis weighing all values and probabilities should be made to determine the foundation that meets requirements and provides economy.

It is generally recommended that loading cases be separated into steady-state, transient, construction, and maintenance loads. These loading cases are considered separately in the following discussion.

Copyright © 2001 IEEE. All rights reserved.

Copyright The Institute of Electrical and Electronics Engineers, Inc.
Provided by IHS under license with IEEE
No reproduction or networking permitted without license from IHS
Not for Resale

2.1.1 Steady-state loads

Steady-state loads are those loads imposed on a structure for a long or continuous time period. Examples of these types of loads are

- Vertical loads due to the dead weight of the structure, bare weight of conductors and shield wires, insulators, and any hardware, such as suspension clamps and dampers
- Loads due to horizontal or vertical angles in the line
- Differential line tension
- Termination of the line (dead ends)

2.1.2 Transient loads

Transient loads are those loads imposed on a structure for a short time duration. Examples of these types of loads are

- Wind loads on bare or ice-covered conductors, shield wires, structure, insulators, and hardware
- Extreme event loads (including broken wire, hardware failure, loss of structure, etc.)
- Stringing loads due to conductor hanging-up in the stringing block during wire installation, where no work crews are endangered
- Ice loads (including ice shedding and galloping)

2.1.3 Construction loads

Construction loads are those loads imposed during the erection of the structure and wire installation. Examples of these types of loads are

- Horizontal shear loads on a foundation used in tilt-up construction of the structure
- Temporary terminal loads that occur during wire installation
- Wire installation load where work crews are endangered

It is anticipated that construction loads will have a higher load factor than transient loads. Thus, wire installation loads, which endanger work crews, are grouped under construction loads, whereas wire installation loads, which do not endanger work crews, are grouped under transient loads.

2.1.4 Maintenance loads

Maintenance loads are those loads that are a result of line maintenance activities (insulator replacement, etc.).

2.1.5 Design loads

The design loads are the combination of loading conditions used to design the foundations. The time duration that a load is applied to a foundation may often be taken advantage of to reduce foundation costs. An example of this is a foundation in a cohesive soil that can resist design loads for a short duration of time without experiencing significant movements; but when the design loads are applied over the service life of the structure, they will result in excessive displacements. In this situation, the foundation should be designed to resist the maximum combined loading condition; however, displacement could be based on steady-state loads only.

Copyright © 2001 IEEE. All rights reserved.

Copyright The Institute of Electrical and Electronics Engineers, Inc.
Provided by IHS under license with IEEE
No reproduction or networking permitted without license from IHS Not for Resale

In summation, a foundation should be designed to resist the maximum combined design loads acting on it. On the other hand, displacements could be estimated using steady-state loads in the case of foundations constructed in cohesive soils or using the maximum combined design loads in the case of granular soils. Design loads may be steady-state, transient, construction, and maintenance loads. Variations in subsurface conditions from one structure location to another, subsurface variations between foundations of the same structure, uncertainties of the foundation analysis, and foundation construction procedures are additional factors that must be considered in each individual foundation design.

2.2 Foundation performance criteria and structure types

The establishment of performance criteria for the design of safe and economical foundations is essential. In establishing performance criteria, the definition of foundation failure and damage limits should be thoroughly understood by the foundation designer and the structure designer. Foundation failure limit performance criteria are the failure capacity of the foundation and/or the magnitude of displacement (differential and total) at which failure of the structure is imminent. The damage limit performance criteria are the load capacity of the foundation or the displacement (differential and total) that would damage but not fail the structure. Differential settlements may result in foundation elevation differences that cause warping of the structure, inducing unanticipated loads in the structural members and creating difficulties in tower erection. Unfortunately, little work has been done to quantify the levels of failure and damage limit displacements for lattice and H-frame type structures. However, it is known that the amount of allowable total and differential displacement is dependent on the type of structure.

2.2.1 Lattice towers

Lattice tower foundation loads consist of vertical forces (uplift or compression) combined with horizontal shear forces. For tangent and small line angle towers, the vertical loads on a foundation may be either uplift or compression. For terminal and large line angle towers, the foundations on one side may always be loaded in uplift while the foundations on the other side may always be loaded in compression. The distribution of horizontal forces between the foundations of a lattice tower vary with the bracing and geometry of the structure. Care should be taken to include the transverse and the longitudinal load components of all tower members connected to the foundations. A free-body diagram for lattice tower foundation loads is shown in Figure 1.

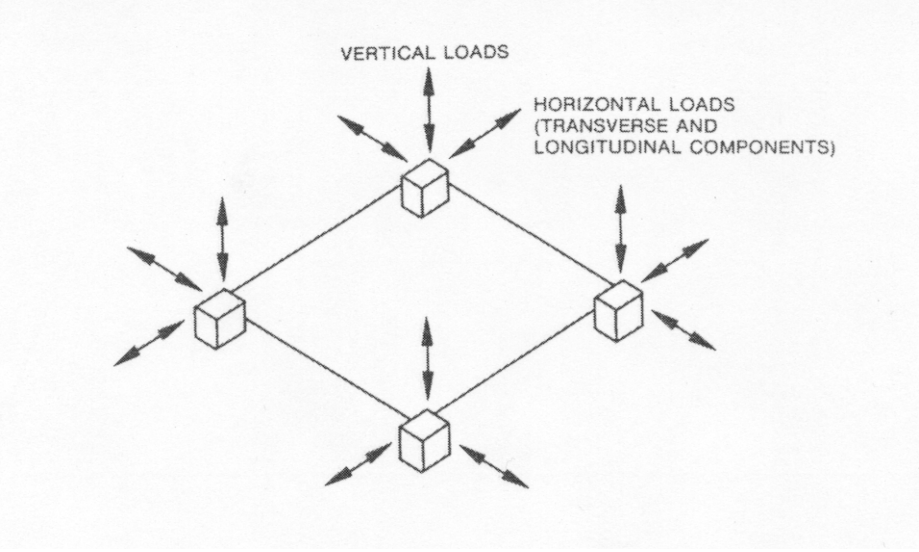

Figure 1—Typical loads acting on lattice tower foundations

Copyright © 2001 IEEE. All rights reserved.

Copyright The Institute of Electrical and Electronics Engineers, Inc.
Provided by IHS under license with IEEE
No reproduction or networking permitted without license from IHS
Not for Resale

When the foundations of a tower displace and the geometric relationship of the four tower foundations remains the same, any increase in load due to this displacement will have a minimal effect on the tower and its foundations. However, foundation movements that change the geometric relationship between the tower's four foundations will redistribute the loads in the tower members and foundations. This will usually cause greater reactions on the foundation that moves less relative to the other tower foundations, which in turn will tend to equalize this differential displacement.

At the present time, the effects of differential foundation movements are normally not included in tower design. Several options are available should the engineer decide to consider differential foundation displacements in the tower design. These options include designing the foundations to satisfy performance criteria that will not cause significant secondary loads on the tower, or designing the tower to withstand specified differential foundation movements.

2.2.2 Single pole structures

Single pole structures can be made of tubular steel, wood, or concrete. These structures have one foundation so that differential foundation movement is precluded. The foundation reactions consist of a large overturning moment and usually relatively small horizontal, vertical, and torsional loads. A free-body diagram for a free-standing single shaft structure is shown in Figure 2.

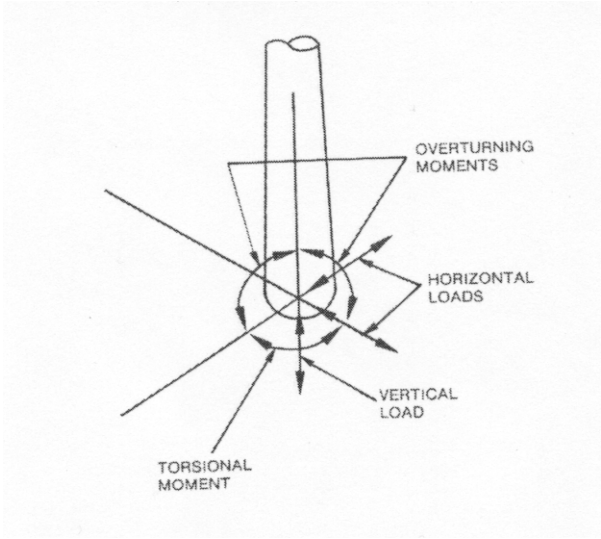

Figure 2—Typical loads acting on foundations for single shaft structures

For single shaft structures, the foundation movement of concern is the angular rotation and horizontal displacement of the top of the foundation. When these displacements and rotations have been determined and combined with the deflections of the structure, the resultant displacement of the conductor support can be computed. Under high wind loading, a corresponding deflection of the conductors perpendicular to the transmission line can be permitted if electrical clearances are not violated. Accordingly, under infrequent temporary loads, larger ground line displacements and rotations of the foundation could also be permitted.

In establishing performance criteria for single-shaft structure foundations, consideration should be given to how much total, as well as permanent, displacement and rotation can be permitted. In some cases, large permanent displacements and rotations might be aesthetically unacceptable and replumbing of the structures and/or their foundations may be required. In establishing performance criteria, the cost of replumbing should be compared with the cost of a foundation that is more resistant to displacement and rotation.

Copyright © 2001 IEEE. All rights reserved.

Copyright The Institute of Electrical and Electronics Engineers, Inc.
Provided by IHS under license with IEEE
No reproduction or networking permitted without license from IHS
Not for Resale

For terminal and large line angle structures, large foundation deflections parallel to the conductor probably are not tolerable. For these structures, the deflection may excessively reduce the conductor-to-ground clearance or increase the loads on adjacent structures. There are also problems in the stringing and sagging of conductors if the deflections are excessive. These problems are usually resolved by construction methods or use of permanent guys.

2.2.3 H-frame structures

The foundation loads for H-frame structures are dependent on the structural configuration and the relative stiffness of the members. Although foundation reactions for moment-resisting H-frames are statically indeterminate, they can be approximated by making assumptions that result in a statically determinate structure. Also, the statically indeterminate structures can be analyzed using any of the classic long-hand analysis methods or by using computer programs. Figure 3 shows a free-body diagram of the foundation loads for an H-frame structure.

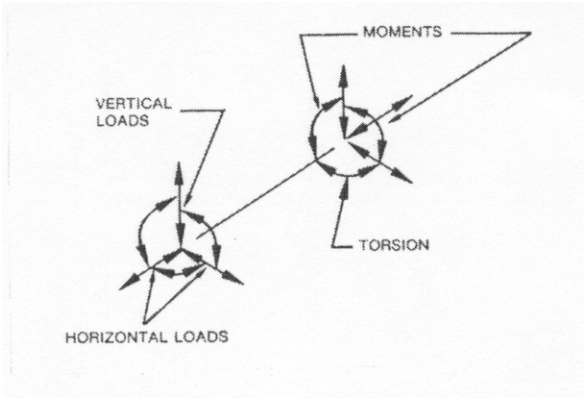

Figure 3—Typical loads acting on foundations for H-frame structures

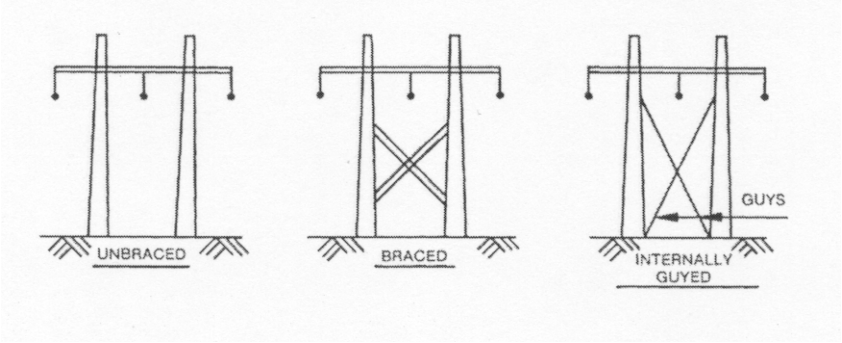

Figure 4—Typical H-frame structures

Many different types of two-legged H-framed structures are in use in transmission lines. This has been particularly true in recent years because visual impact has become of greater concern.

The H-frame structure is particularly applicable for wood, tubular steel, or concrete poles. The cross arm may be pin-connected to the poles, in which case an unbraced structure behaves essentially as two single poles connected by the cross arm. These structures may be unbraced, braced, or internally guyed, as shown in Figure 4.

Copyright © 2001 IEEE. All rights reserved.

Copyright The Institute of Electrical and Electronics Engineers, Inc.
Provided by IHS under license with IEEE
No reproduction or networking permitted without license from IHS
Not for Resale

As with lattice towers, past practice has not normally included the influence of foundation displacement and rotation in H-frame structure design. Significant foundation movements will redistribute the frame and foundation loads. The foundations can be designed to experience movements that will not produce significant secondary stresses in the structure, or the structure can be designed for a predetermined maximum allowable total and differential displacement and rotation.

2.2.4 Externally guyed structures

Three general types of externally guyed structures exist [B49]. For all types, the guys produce uplift loads on the guy foundations and compression loads on the structure foundation. The guys are generally adjustable in length to permit plumbing of the structure during construction and to account for creep in the guy and movement of the uplift anchor.

Several types of externally guyed structures are shown in Figure 5. The guys are located out-of-plane, both ahead and in back of the structure. In this case, the shaft or shafts of the structures usually have a ball-and-socket base connection to the foundation to permit free rotation without transmitting moment to the foundation. This will produce compression loading with a small shear load.

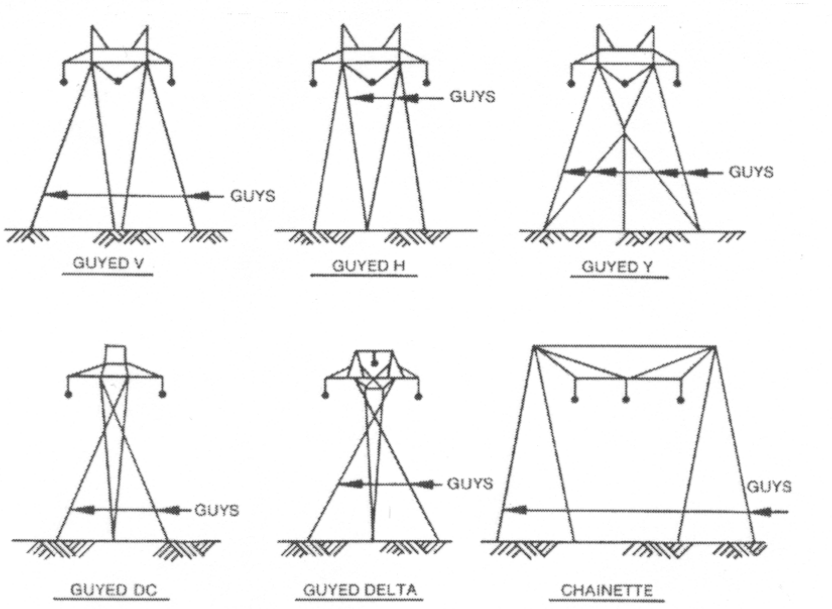

Figure 5—Typical externally guyed structures

This type of guyed structure can generally tolerate large foundation movements if guy stability is maintained. Consideration in establishing performance criteria are similar to those discussed in 2.2.2 for single pole structures.

A single-pole type externally guyed structure is shown in Figure 6. This type of structure is often used as a terminal and large line angle structure and is quite flexible, allowing most of the load to be resisted by tension in the guys and compression in the main shaft.

This type of guyed structure can generally tolerate significant foundation movement as far as its structural integrity is concerned; but like the terminal and large line angle poles discussed in 2.2.2, if excessive guy anchor slippage occurs, conductor-to-ground clearance, security of adjacent structures, and stringing and sagging conductors can become problems.

Copyright © 2001 IEEE. All rights reserved.

Copyright The Institute of Electrical and Electronics Engineers, Inc.
Provided by IHS under license with IEEE
No reproduction or networking permitted without license from IHS
Not for Resale

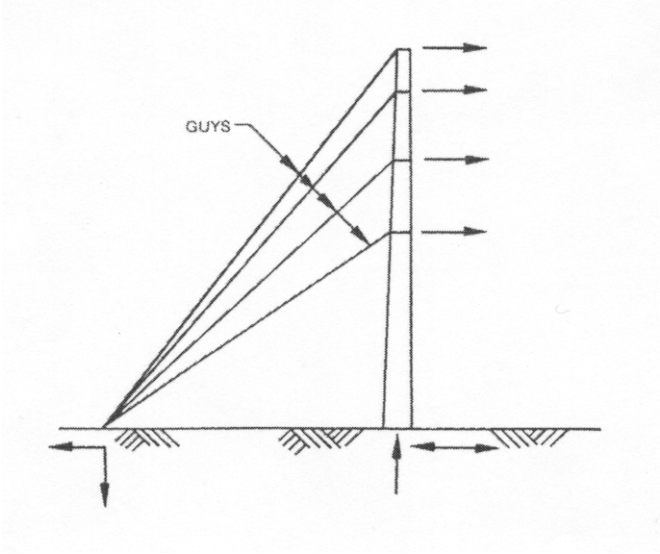

Figure 6—Single-pole, externally guyed structures

Another type of externally guyed structure is a conventional lattice tower guyed to reduce its leg loads and foundation reactions. This approach, which has often been used to upgrade existing towers, can lead to problems, as the relative distribution of the loads between the guys and the tower depend on the guy pretensions and the potential creep of the foundation. The flexibility of the guy, together with the flexibility of the tower, are needed to compute the foundation reactions and anchor loads. The maximum amount of anchor slippage can be selected, and the tower and anchors designed accordingly. The initial and final modulus of elasticity of the guys, together with the creep of the guys, should be considered. The amount of pretension in the guys should be specified and guys prestressed. Load testing of the guy anchors is recommended to ensure against excessive slippage. Figure 7 shows a typical installation.

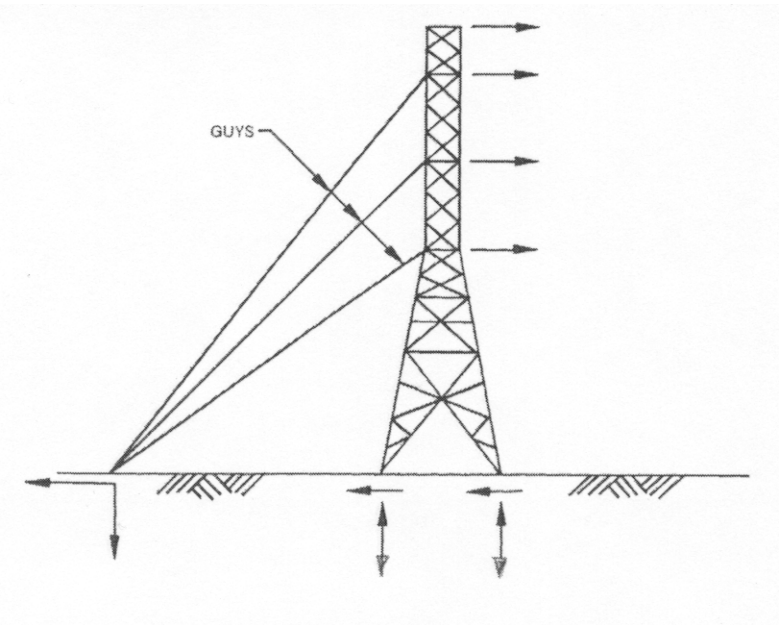

Figure 7—Externally guyed lattice tower

Copyright © 2001 IEEE. All rights reserved.

Copyright The Institute of Electrical and Electronics Engineers, Inc.
Provided by IHS under license with IEEE
No reproduction or networking permitted without license from IHS
Not for Resale

The guyed-lattice tower leg foundations are required to resist horizontal shear forces and vertical compression or uplift loads. As in the case of the lattice towers, discussed in 2.2.1, the load distribution in the component structural elements is sensitive to the foundation performance. Differential displacements of the legs of the tower will result in load redistribution and may affect the integrity of the tower.

3. Subsurface investigation and selection of geotechnical design parameters

3.1 General

Subsurface investigation for electrical transmission tower foundation should be carried out along the right-of-way (r/w) of the transmission line to obtain geotechnical parameters required to successfully design the transmission structure foundations at a minimum cost.

As a minimum, the investigation should provide geotechnical parameters required to establish the ultimate load-bearing capacity of the subsurface material, and to determine the allowable movement of the foundation.

3.2 Phases of investigation

The investigation consists of the following three phases:

— Preliminary investigation to establish feasibilities
— Detailed investigation to finalize designs and details
— Design verification during construction and documentation

3.2.1 Preliminary investigation

The preliminary investigation should consist of collecting existing data relating to local and subsurface conditions, and of making a geotechnical field reconnaissance of the line route. If considered cost-effective, preliminary boring, penetration, and pressuremeter tests can be added to verify and increase the confidence level in existing data and finalize the reconnaissance mapping.

3.2.1.1 Existing data

A considerable amount of data regarding local geology, including distribution of surface water, depth of groundwater, depth and physical characteristics of bedrock, and type and thickness of soil cover, is available from several sources.

Topographic maps and aerial photographs, available from the various U.S. Geological Survey offices and commercial aerial surveying firms, typically provide data on the distribution of surface and ground waters, soil conditions and rock types, the areas of exposed bedrock, and the geomorphologic landform. They also show the location of man-made features such as radio towers, quarries, highways, other transmission lines, and building constructions. Often, due to proximity, useful information along the proposed r/w may be obtained on the foundation conditions by simple extrapolation of the available data.

Other excellent sources of information on the soil distribution and rock types are state and federal geological surveys and the geology departments of nearby universities.

The other potential sources of information are the Natural Resources Conservation Service (NRCS) of the U.S. Department of Agriculture, the U.S. Bureau of Public Roads, and county or regional planning boards. More information concerning sources of geological data may be found in [B165].

 Copyright © 2001 IEEE. All rights reserved.

Copyright The Institute of Electrical and Electronics Engineers, Inc.
Provided by IHS under license with IEEE
No reproduction or networking permitted without license from IHS Not for Resale

3.2.1.2 Field reconnaissance

Another useful means of obtaining information during the preliminary investigation is to perform a field reconnaissance survey of the transmission line route. The reconnaissance should be performed by a geotechnical engineer or an engineering geologist. The purpose of the reconnaissance is to develop a map of the surficial soils showing areas that may offer particular foundation problems such as deep peat or soft organic silt, bedrock outcrops, areas of high groundwater table, and areas of potential slope instability. The soil and rock classifications used in the mapping should be based on engineering properties, not on geological or agricultural distinctions. By comparing the information from the field reconnaissance and existing published information, a preliminary line route map showing basic soil or rock types, inferred depth to bedrock, and elevation of the groundwater table can be developed.

3.2.1.3 Preliminary borings

The development of a surficial map with adequate subsurface interpretation usually is the final step in the preliminary investigation. To achieve such objective, it may be cost-effective to obtain a few preliminary borings in those areas where subsurface interpretation is difficult and where it may affect the foundation design significantly.

Preliminary borings are generally used for soil classification purposes only and disturbed samples are thus satisfactory. The most common methods of obtaining disturbed samples are auger boring and using a heavy walled split-barrel sampler which is driven into the soil at selected intervals in the boring. Test pits and probes can also be used.

When the boring has been advanced to the required depth, the sample is taken by driving the split-barrel sampler into the soil. This Standard Penetration Test (SPT) is covered in ASTM D1586 [B14]. Samples usually are taken at intervals of not more than 1.5 m (5 ft) in depth, and at every change in stratification where such change can be detected by the driller. Closer sampling intervals may be necessary if the soil stratification is complex or thinly stratified. When the scope of the investigation requires that borings be made, it is important to have a knowledgeable person with experience in geotechnical engineering present to ensure correct interpretation of the data obtained from the boring program. Dutch cone tests [B16] or pressuremeter tests [B19] may be used in lieu of the standard penetration tests to determine the in-situ stress, deformability and strength.

Since ground water affects many elements of foundation design and construction, its location should be established as accurately as possible. It is generally determined by measuring to the water level in the borehole after a suitable time lapse. A period of 24 hr is a typical time interval. However, in clays and other soils of low permeability, it may require several days to weeks to determine a meaningful water level. Standpipes or other perforated casings may be used to prevent the borehole from caving during this period.

3.2.2 Design investigation

The purpose of the design investigation is to provide the foundation engineer with sufficient subsurface information to

- Select the types of foundation most suitable at each structure location
- Determine the size and depth of the selected foundations to adequately support the power transmission along the line
- Evaluate potential problems during construction

Copyright © 2001 IEEE. All rights reserved.

Copyright The Institute of Electrical and Electronics Engineers, Inc.
Provided by IHS under license with IEEE
No reproduction or networking permitted without license from IHS
Not for Resale

The information required to achieve these goals includes:

— Type of structure and allowable foundation movements
— Magnitude and duration of structure loadings at the ground line
— Stratigraphy of the subsurface materials
— Elevation of the ground water table
— Engineering properties of the subsurface materials

On any transmission line route these five factors may vary considerably, and the detailed investigation should provide the required information in a cost-effective manner. Ideally, a detailed subsurface investigation would involve boring at each structure site. However, this may not be necessary if the results of the preliminary investigation have shown that subsurface conditions in a specific section of the line route are reasonably uniform.

Indirect methods of subsurface investigation include geophysical exploration techniques such as seismic refraction, electrical resistivity, and gravimetric surveys. These methods generally are used to survey large areas. While not well suited to investigate the small area at each structure location, they may be helpful as supplemental data between boring locations. These indirect methods only assist in defining general stratigraphy.

The designer should be aware of the opportunity to save substantial project cost, since there may be a large number of foundation designs. The saving in cost due to failure to administer adequate subsurface investigation must be weighed, however, against the cost of the risks involved.

Coincident with selecting the locations for the subsurface investigations, decisions should be made concerning the type and depth of exploration. The type of exploration is mainly a function of soil types expected at a given site and the type of foundation being considered for the site. For example, if the structure is located where the expected subsurface material is sand, a boring that obtains disturbed samples and records the standard penetration test results will usually be adequate. On the other hand, the same foundation type located in clay may require a boring that will allow undisturbed samples to be obtained.

Guidance for determining the most satisfactory boring may be obtained from considering the following question: Can the foundation be designed in a cost effective manner from empirical correlations between classification tests and engineering properties of the soil or rock? If so, then boring to obtain disturbed samples with standard or Dutch cone penetration test will be sufficient.

If a cost effective design can be determined only by accurate knowledge of the engineering properties, then undisturbed sample borings must be made, and laboratory or *in situ* tests conducted to determine the required engineering properties. Empirical relationships between engineering properties and classification tests performed on disturbed soil samples can be developed for a specific project. On large projects, this correlation can result in a reduction in boring costs by reducing the number of undisturbed sample borings and engineering property measurements.

The depth of each exploration should extend through any unsuitable or questionable foundation materials, and to a depth sufficient so that imposed stresses below that depth (due to foundation loads) will not result in adverse performance for the types of foundations being considered. As a general guide, unless bedrock is encountered first, explorations should be made to a depth at which the net increase in soil stress from the maximum design load is 10% of the *in situ* vertical effective stress in the soil at the depth. For spread foundations, this translates into depths which are 2.0 to 2.5 times the equivalent diameter of the foundation. The net increase in stress may be computed from the Boussinesq and Mindlin equations [B113]. Poulos [B129] and Westergaard provided various stress distribution charts. Further discussion regarding the depth of the subsurface investigation may be found in [B146] and [B151].

Copyright © 2001 IEEE. All rights reserved.

Copyright The Institute of Electrical and Electronics Engineers, Inc.
Provided by IHS under license with IEEE
No reproduction or networking permitted without license from IHS Not for Resale

3.2.3 Construction verification

The owner should have representation in the field during foundation construction to determine if the actual subsurface conditions are similar to those conditions used in the foundation design. If the subsurface conditions used in the foundation design differ *significantly* from the actual conditions, it may be necessary to enlarge the foundation or change the foundation type.

3.3 Types of boring samples

The purpose of making a boring is to obtain samples of the subsurface materials for visual description, classification, and testing to determine design parameters. Each sample should be visually examined preferrably in the field by a geotechnical engineer or an engineering geologist and the appropriate manual tests performed to allow the soil to be classified according to the Unified Soil Classification System [B37]. ASTM D2488 [B15] may be used for routine field classification.

In making borings, the hole is advanced by drilling with a bit to cut away the soil and circulating drilling fluid through the bit to carry away the cuttings, or the hole is advanced by an auger. Augers, either conventional or hollow-stem type, should be used with caution when sampling below the groundwater table. Upward seepage of water in pervious soils (or even in many silts) may disturb and loosen the soil to such an extent that penetration tests will indicate erroneously low blow-counts and increase the moisture contents of the soil. It is essential that at all times the water level in the borehole be kept above the groundwater table. In granular soils, even above the water table, loading of the soil by the blades of a hollow stem auger may cause higher blow counts in the penetration test than would be measured in other types of boring.

Three kinds of samples can be taken by boring operations: disturbed soil, undisturbed soil, and rock core. The foundation designer should be familiar with the detailed means of subsurface exploration and sampling methods described in [B80].

3.3.1 Disturbed soil samples

Thick-walled samplers may be used for obtaining samples suitable for identification and index property tests. The barrels of such samplers may be solid tubes of the split-barrel type that facilitates removal and examination of samples. Samplers of this type range in diameter from 5 cm to 11 cm (2 in to 4.5 in). They may be used to recover samples in many soils, although there may be difficulties with coarse gravel or rock fragments unless the sampler is equipped with a flap valve or basket retainer. The equipment and procedures for making Standard Penetration Tests (SPT), determining the standard penetration resistance (N), and obtaining split-barrel samples are covered in ASTM D1586 [B14].

The SPT resistance should not be used for estimating the strength and compressibility of cohesive soils (clays). The strength and compressibility of cohesive soils are greatly influenced by their soil structure (particle arrangement) which is a function of mode of deposition, mineralogy, and stress history. Since first described by Casagrande [B36], the importance of the structure of clay has been well documented. The vast majority of clays are sensitive, since their strength is reduced and their compressibility increased when their structure is disturbed. The act of driving a thick-walled sampler, used to measure the SPT resistance, disturbs the clay sufficiently so that this technique is unsuitable for estimating the engineering properties of clays.

The strength and compressibility of cohesionless soils (sands and gravel) usually are not greatly influenced by soil structure, and these soils typically are insensitive. Their strength and compressibility are mainly a function of grain size and density (degree of compactness). Therefore, the SPT resistance can be used to estimate the adequacy of cohesionless soils for supporting the loading associated with transmission tower foundations. In addition to their insensitivity, a second important reason for the applicability of the SPT to cohesionless soils is that these soils are relatively incompressible and have high shear strength; except in unusual cases, the loads imposed by transmission structure foundations will not cause large deformations.

Copyright © 2001 IEEE. All rights reserved.

Copyright The Institute of Electrical and Electronics Engineers, Inc.
Provided by IHS under license with IEEE
No reproduction or networking permitted without license from IHS
Not for Resale

Having stated that the SPT is a useful classification test for cohesionless soils, it is necessary to point out one important exception. The designer must be aware of the special case of cohesionless silts (*they* do not have dry strength). Because of their small particle size, the behavior of silts is influenced by particle arrangement or structure. The strength and compressibility of silts cannot be evaluated from standard penetration tests. Silts should be treated similarly to clays and undisturbed samples should be obtained to permit measurement of strength and compressibility.

A number of the additional factors affecting the results of the SPT have been discussed in the literature. For potential errors inherent in this exploration procedure, see [B48], [B99], [B123]. For example, minor amounts of gravel exceeding 6.35 mm (0.25 in) in size may affect the SPT results. Because of its sensitivity to gravel, the test is not dependable in coarse-grained soils including medium to course gravel.

Customary practice is to take samples at intervals of approximately 1.5 m (5 ft). With the standard sampler, about 45.7 cm (18 in) of soil are usually recovered, which results in about 30% of the soil column being available for examination. This is usually sufficient, although closer spacing of sampling should be used if soils vary markedly with depth. In soil masses where the individual strata are relatively thin, as is frequently the case in estuarine or fluvial deposits, intermittent sampling may give quite misleading results. In such deposits, continuous sampling should be done in a sufficient number of holes to define the stratigraphy more accurately.

At least 15 cm (6 in) of each sample should be sealed in an airtight container and sent to the soils laboratory for further classification and testing. Dependence on a driller for field classification of soils is not good practice, because drillers rarely have the requisite technical training to adequately classify soils.

3.3.2 Undisturbed soil samples

Equipment and procedures for obtaining undisturbed samples of soils of a quality suitable for quantitative testing of strength and deformation characteristics have been given in [B80]. Briefly, taking undisturbed samples requires using a thin-walled sampler with proper clearance at the cutting edge. The sampler must be forced into the soil smoothly and continuously.

To permit taking undisturbed samples in dense soils or soils containing gravel or other hard particles that tend to deform a conventional thin-walled sampler, samplers such as the Denison or Pitcher have been developed in which a thin-walled, nonrotating inner sampler barrel is forced into the soil mass, while the soil surrounding the barrel is removed by a rotating, carbide-toothed outer barrel. Good quality samples in difficult soils can usually be obtained with such equipment.

In most soils of soft to stiff consistency, samples of a quality suitable for quantitative testing can be obtained using thin-walled Shelby tube samplers a minimum of 5 cm (2 in) diameter, providing there is a proper cutting edge [B80]. Normally, the tube is pushed into the soil for a distance of about 15 cm to 20 cm (6 in to 8 in) less than the length of the tube. Preferably the sampler should be pushed downward in one continuous movement. After the sampler has been forced down, the drill rods are rotated to shear the end of the sample and the sample is removed. Friction between the sample and the tube retains the sample as the sampler is withdrawn. A special valve or piston arrangement also may be attached to create a pressure differential (suction) to aid in retaining the sample. To reduce deficiencies with respect to sample length and sample disturbance due to side friction between the sample and the walls of the sampler (while the sampler is being advanced into the soil), various piston and foil samplers have also been developed. These are described in more detail by Hvorslev [B80] and may be used to obtain undisturbed samples in soft soils or soils in which recovery is difficult using a conventional Shelby tube sampler.

Copyright © 2001 IEEE. All rights reserved.

Copyright The Institute of Electrical and Electronics Engineers, Inc.
Provided by IHS under license with IEEE
No reproduction or networking permitted without license from IHS
Not for Resale

3.3.3 Rock coring

Where investigation of the bedrock is necessary, pertinent data to be obtained include:

— Elevation of the rock surface and variation over the site
— Rock type and hardness
— Permeability
— Extent and character of weathering (including alteration of mineral constituents)
— Extent and distribution of solution channels in soluble rocks such as limestones
— Discontinuities such as bedding planes, faults, and joints
— Foliation or cleavage

Identification and classification of rock types for engineering purposes may be limited to broad, basic classes in accordance with accepted geological standards.

The behavior of rock subjected to foundation loadings is a function of the deformation characteristics of the rock mass which are controlled by rock discontinuities such as weathering, joints, and bedding planes. Locating and evaluating the effects of such discontinuities requires carefully planned and executed investigations made by experienced, well-equipped drillers under the guidance of a competent specialist in the field.

Other significant factors affecting the behavior of rock as a foundation material include weathering and hardness. There are no generally accepted criteria for these, although the Rock Quality Designation (RQD) suggested by Deere [B47] is useful. The RQD is defined as the modified core recovery percentage in which all pieces of sound core over four inches in length are counted as recovered. The smaller pieces are considered to be due to close shearing, jointing, faulting, or weathering in the rock mass and are not counted. The RQD may be used for core boring as an indication of the effects of weathering aid discontinuities. It should be noted that if RQD is to be determined, double-tube NX size core barrels with nonrotating inner barrels that produce approximate 5 cm (2 in) ϕ diameter core must be used.

The drillers should proceed with maximum care for maximum possible recovery. Drillers should also pull the core whenever they feel a blockage, grinding, or other indication of poor core recovery. The material that is not recovered is frequently the most significant in deciding upon proper design. The time required to drill each foot, total recovery, physical condition, length of pieces of core, joints, weathering, evidence of disturbance, or other effects should be noted on the drilling log.

Any comments by the driller with regard to the character of the drilling and difficulties encountered should be included. Where massive rocks such as unweathered granite are encountered, good recoveries may be obtained with smaller diameter drills, such as BX and AX sizes. Stepping down to these smaller sizes may be necessary when in bouldery areas of deep weathering.

3.4 Soil and rock classification

Classification of soil and rock samples by visual description and simple manual tests is an important aspect of a subsurface investigation program. The written visual description is the first means of conveying to the engineer the types of subsurface materials along the r/w. This information will be used to determine the parameters selected for designing the foundation.

Based on the visual classification of the soils or rocks, a series of index property tests are performed that further aid in classification of the materials into categories and permit the engineer to decide what field or laboratory tests, if any, will best describe the engineering properties of the soil and rock on a given project.

Copyright © 2001 IEEE. All rights reserved.

Copyright The Institute of Electrical and Electronics Engineers, Inc.
Provided by IHS under license with IEEE
No reproduction or networking permitted without license from IHS
Not for Resale

3.4.1 Soil classification

3.4.1.1 Index properties

Soil classification by index properties (that is, classifying them into broad groups having similar engineering properties) is used primarily to qualitatively describe the soil. Engineering properties (strength, compressibility, and permeability) are usually expensive and time-consuming to determine, especially since they must be measured either *in situ* or from undisturbed samples which are tested in the laboratory. It is impractical and uneconomical to try to measure the engineering properties everywhere throughout a large mass of soil.

Index properties can be measured more economically and quickly than engineering properties. With some exceptions, they can be measured on disturbed samples which can be obtained with less difficulty and expense than undisturbed samples.

Index properties are useful because they can be roughly correlated with the engineering properties. From his knowledge of the empirical correlation between the index properties and engineering properties of soils or rock, the designer can make use of the index properties for the following purposes:

— To select sites that have the most favorable subsoil conditions for a given transmission line
— To make a preliminary estimate of the engineering properties of the soil at a given site
— To select the most critical zones in the subsoils for more extensive investigation of the engineering properties

Useful index properties for cohesionless and cohesive soils are summarized below:

(Cohesionless)	(Cohesive)
Grain size	Water content
Specific gravity	Degree of saturation
Relative density	Atterberg limits
Unit weight	Specific gravity
Degree of saturation	Void ratio
Standard penetration resistance	Undrained strength
Cone penetration test	—

The undrained strength of cohesive soils referred to in this context is the strength measured in the field by means of a pocket penetrometer or vane shear device [B85]. These measurements are made on both undisturbed samples at each end of a tube sample and disturbed samples from a standard penetration test. The measurements, which are quickly and easily performed when combined with the water content and Atterberg limits, provide an excellent means for classifying cohesive soils and selecting specific samples on which engineering property measurements can be made.

The standard penetration resistance is one of the most commonly used index properties for cohesionless soils. A number of empirical relationships between SPT and the compressibility and shear strength of sands have been developed. It should be emphasized that the standard penetration test is an index test and that care must be emphasized when using only the SPT as the basis of a foundation design. The SPT is not listed as an index property test in cohesive soils, since its application to the classification of cohesive soils is subject to serious question, as discussed previously.

Copyright © 2001 IEEE. All rights reserved.

Copyright The Institute of Electrical and Electronics Engineers, Inc.
Provided by IHS under license with IEEE
No reproduction or networking permitted without license from IHS Not for Resale

3.4.1.2 Visual classification

Soil classification, like the index properties, is used to convey qualitative information about the engineering properties. Of the many soil classification systems in use by engineers, geologists, and pedologists, the Unified Soil Classification System [B37] is best suited for conveying significant information about the engineering properties of soils.

Soils are divided into three broad categories in the Unified Soil Classification System: Coarse-grained, fine-grained, and highly organic. A whole spectrum of soil types, overlapping two or all three of these broad categories, can be found in nature. Subdivisions within the broad categories make it possible to classify these more complex soil types.

3.4.2 Rock classification

Generally, the engineering properties of a rock mass cannot be predicted with the precision expected in a soil investigation. Although there are many field and laboratory tests available, there are no widely accepted index properties that correlate with the engineering properties of the rock mass.

As mentioned in 3.3.3, the engineering properties of a rock mass are largely a function of the number, type, spacing, and orientation of rock defects such as

— Joints
— Weathering
— Faults
— Bedding Planes
— Shear Zones
— Foliation
— Solution Channels

The geotechnical engineer or geologist should provide a lithologic description of the rock core, including the geologic name given to the rock type on the basis of its mineralogical composition, texture, and in some cases, its origin. Such names as granite, basalt, sandstone, shale, etc., evolve from such schemes and are generally understood by the foundation design engineer.

In addition to textural description, a generalized description of rock hardness should be included in the rock description. As mentioned previously, even a soft rock generally will have adequate engineering properties to support transmission structure foundations. However, as an aid in describing the rock core, the relative terms soft, medium, or hard should be used to describe rock hardness.

In addition to the lithologic and textural description, additional rock drilling information should be obtained during the coring operation. This information includes

— Rate of drilling with emphasis on the unusual
— Water losses
— Groundwater level
— Core recovery

An index used to evaluate the rock mass in terms of its discontinuities is the RQD; see 3.3.3. An RQD approaching 100% denotes an excellent quality rock mass with properties similar to that of an intact specimen. RQD values ranging from 0 to 50% are indicative of a poor quality rock mass having a small fraction of the strength and stiffness measured for an intact specimen.

Problems arise in the use of core fracture frequencies and RQD for determining the in situ rock mass quality. The RQD and fracture frequency evaluate fractures in the core caused by the drilling process, as well as natural fractures previously existing in the rock mass. For example, when the core hole penetrates a fault zone

Copyright © 2001 IEEE. All rights reserved.

Copyright The Institute of Electrical and Electronics Engineers, Inc.
Provided by IHS under license with IEEE
No reproduction or networking permitted without license from IHS
Not for Resale

or a joint, additional breaks may form that, although not natural fractures, are caused by the natural planes of weakness existing in the rock mass. These breaks should be included in the estimated rock quality. However, some fresh breaks occur during drilling and handling of the core that are not related to the quality of the rock mass. In certain instances, it may be advisable to include all fractures when estimating RQD and fracture frequency. Considerable judgement is involved in the logging of rock core samples.

3.5 Engineering properties

To design foundations for transmission structures or evaluate the foundation performance under the loads applied to the structure, it is necessary that certain geotechnical engineering properties be determined or estimated. The performance of a transmission structure foundation and the dimensions and type of foundation required is governed primarily by the shear strength and compressibility of the supporting soil. Estimated values for the engineering properties required to compute ultimate capacity (for example, bearing, lateral, uplift) or settlement of the foundation may often be obtained from correlations with various index properties of the soil in which the foundation is constructed. Laboratory test procedures are available to measure the shear strength and compressibility of various soil samples [B97].

3.5.1 Index property correlations

Various engineering properties pertaining to the shear strength or compressibility characteristics of both cohesionless and cohesive soils may be estimated from appropriate index properties. While other correlations exist, several useful relationships between engineering properties and index properties are discussed below.

The shear strength of soils is normally expressed by the Mohr-Coulomb equation as:

$$s = c + \sigma_n \tan\phi \quad (1)$$

where

s is shear strength,
c is cohesion,
σ_n is normal stress,
ϕ is angle of internal friction.

In general, the shear strength of a soil determines the ultimate load carrying capacity of a foundation and, consequently, must be estimated to design or analyze potential foundations for transmission structures. The use of the engineering properties, c and ϕ, in determining the capacities of various foundation types will be shown in later sections of this guide.

In cohesionless soils (c = 0), the value of ø and, therefore, the shear strength may be related to the gradation, grain shape, and relative density of the soil mass, among other properties. The influence of grain shape and gradation on the magnitude of ø may be discussed qualitatively. As the angularity of the soil grains increases, the amount of particle interlocking increases. Well-graded soils (those containing roughly equal amounts of a wide range of grain sizes) usually have a lower void ratio since the voids between larger particles are partially filled with the smaller soil particles. Both of these factors result in increases in the value of the angle of internal friction, ϕ.

An approximate quantitative relationship exists between ϕ and the relative density of cohesionless soils, which may be determined from laboratory test procedures or estimated from standard penetration tests conducted during sampling operations in the field.

Copyright © 2001 IEEE. All rights reserved.

Copyright The Institute of Electrical and Electronics Engineers, Inc.
Provided by IHS under license with IEEE
No reproduction or networking permitted without license from IHS
Not for Resale

The Atterberg limits are laboratory tests to determine the influence of moisture content on the consistency of cohesive soils. The liquid limit is defined as the water content at which transition from a plastic state to a liquid state occurs and the plastic limit is the moisture content at which the soil behavior changes from nonplastic to plastic state (test procedures to determine the Atterberg limits have been standardized and are discussed in any basic text on soil mechanics). The plasticity index (the numerical difference between the liquid limit and the plastic limit) provides a measure of the range of water contents over which the soil remains plastic.

Empirical correlations have been obtained which relate index properties to the compressibility of clay soils. For normally consolidated clays (clay soils that have not previously experienced consolidation pressures greater than the existing effective overburden pressure), the compression index, C_c, contained in the consolidation settlement equations presented in Clause 4 may be related to the liquid limit as:

$$C_c = 0.009(W_l - 10) \tag{2}$$

where

W_l is liquid limit in percent.

This discussion illustrates the usefulness of several index properties in estimating various engineering properties. Basic texts on soil mechanics and foundation analysis and design will provide other useful empirical relationships that have been developed to provide estimates of engineering properties required for the analysis and design of the various foundation types used to support transmission structures. The use of index properties to estimate engineering properties should be done with caution, and the engineer should be aware of how the relationships were developed and for what material. Whenever possible, correlation should be verified with appropriate laboratory testing. The empirical relationships should not be accepted as a substitute for laboratory tests to determine the engineering properties of soils along the route of the transmission line. They may, however, often be used to supplement or reduce the amount of laboratory tests conducted and may aid the engineer in selecting the areas along the route where more extensive investigation of engineering properties is required.

3.5.2 Laboratory testing

As mentioned previously, the performance and load carrying capacity of various types of foundations depend upon the shear strength and compressibility of the soil on which the foundation is constructed. Various laboratory tests have been developed to investigate these properties of soil. Brief descriptions outlining several useful laboratory tests are presented in this section to aid in the selection of appropriate tests to determine the engineering properties required in the analytical techniques presented in subsequent sections of this guide.

The shear strength of soils is dependent not only on soil type, but also on test method and loading or drainage conditions imposed during testing of a sample. The two test methods most commonly used to determine the shear strength of soils are the direct shear test and triaxial test.

The direct shear test is one of the earlier methods developed to determine the shear strength of various soils. The test consists of shearing a soil sample across a predetermined failure plane. The soil specimen is enclosed in a box consisting of an upper and lower half. The upper half is usually free to move vertically and can slide horizontally with respect to the lower half of the box. A horizontal force is applied to the upper half of the box either by controlling the loading rate or the rate at which the upper half of the box is displaced horizontally, and both the displacement and load applied to the box are monitored. A stress-displacement curve is obtained by plotting the shear stress versus shear displacement. Failure may be defined either at the peak stress (for dense sand or stiff clays) or at an arbitrary displacement value (for loose cohesionless soil or soft clays). At least three tests using different normal stresses (applied vertically to the top half of the box)

Copyright © 2001 IEEE. All rights reserved.

Copyright The Institute of Electrical and Electronics Engineers, Inc.
Provided by IHS under license with IEEE
No reproduction or networking permitted without license from IHS
Not for Resale

are required to determine the Mohr-Coulomb failure envelope defined by Equation (1); see [B24], [B96] for detailed descriptions of laboratory test procedures.

The direct shear test is relatively simple and inexpensive to perform, but often has been criticized because the failure plane is predetermined. In addition, it is difficult to control sample volume and drainage conditions or to obtain pore pressure measurements during testing. Consequently, some uncertainty may exist with respect to the actual effective stresses existing in the sample during testing and at failure.

The triaxial test eliminates most of these difficulties. This test is conducted inside a cylindrical cell on cylindrical samples encased in rubber membranes. Hydrostatic confining pressure is applied to the sample by application of pressure to the fluid inside the cell. Shear stresses in the sample are usually controlled by applying an additional vertical stress (the deviator stress). Drainage from the sample may be controlled during application of both the confining pressure and deviator stress, and pore pressures generated in the sample during the test may be monitored. To obtain the Mohr-Coulomb failure envelope (and consequently, ϕ and c), several tests are performed using various confining pressures.

The shear strength parameters obtained from triaxial tests are dependent on the consolidation and drainage conditions imposed prior to and during application of the deviator stress. Three conditions under which these tests are conducted are described below:

a) *Unconsolidated-Undrained Test (UU Test)*. No drainage is allowed during application of the confining pressure or the deviator stress. The unconfined compression test is a special case of the unconsolidated-undrained test with confining pressure equal to zero. The deviator stress at failure is the unconfined compressive strength, q_u, which is equal to two times the undrained shear strength, S_u.

b) *Consolidated-Undrained Test (CU Test)*. Drainage is allowed during application of the confining stress. The sample is allowed to consolidate with respect to the applied pressure as observed via drainage measurements. No drainage is allowed during the application of the deviator stress.

c) *Consolidated-Drained Test (CD Test)*. Drainage takes place during the entire test. The deviator stress is applied slowly enough so that pore pressures do not build up during shearing of the specimen.

Detailed descriptions of equipment and test procedures are contained in [B24] and [B96].

For soils of low permeability (such as clays), the CD test may require long periods of time to conduct so that pore pressures will not be generated during shear; consequently, the test would be more expensive to conduct for this type of soil. The drained strength can be evaluated during the quicker CU test if pore water pressures are measured.

With cohesionless soils, which drain relatively freely both during testing and in situ, the CD test is appropriate and does not have the time restraints that are imposed when cohesive soils are tested. Table 1 provides representative values for the angle of internal friction, ø, for various soil types and triaxial test conditions.

Copyright © 2001 IEEE. All rights reserved.

Copyright The Institute of Electrical and Electronics Engineers, Inc.
Provided by IHS under license with IEEE
No reproduction or networking permitted without license from IHS Not for Resale

Table 1 Representative values for angle of internal friction ϕ

Soil	Type of test[a]		
	Unconsolidated-undrained UU	Consolidated-undrained CU	Consolidated-drained CD
Gravel			
Medium size	40°–55°		40°–55°
Sandy	35°–50°		35°–50°
Sand			
Loose dry	28°–34°		
Loose saturated	28°–34°		
Dense dry	35°–46°		43°–50°
Dense saturated	1°–2° less than dense dry		43°–50°
Silt or silty sand			
Loose	20°–22°		27°–30°
Dense	25°–30°		30°–35°
Clay	0° if saturated	3°–20°	20°–42°

NOTES:
1—Use larger values as unit weight, γ, increases.
2—Use larger values for more angular particles.
3—Use larger values for well-graded sand and gravel mixtures (GW, SW).
4—Average values for
Gravels: 35°–38°
Sands: 32°–34°

[a]See a laboratory manual on soil testing for a complete description of these tests, e. g., Bowles (1986b) .

For cohesive soils, the value of the cohesion term, c, in Equation (1) is dependent upon mineral content, triaxial test conditions, and previous (geological) stress history.

The engineering properties governing the compressibility of soils may also be determined from laboratory tests. In general, the settlement of a foundation in cohesionless soils is governed primarily by elastic/plastic compression and is normally computed using expressions derived from the theory of elasticity (see Clause 4). Settlement of foundations in cohesive soils may have both an immediate (elastic) component and a time-dependent consolidation component.

The analysis to estimate the elastic or immediate settlement component of settlement for both cohesionless and cohesive soils requires the determination or estimation of a stress-strain modulus (or modulus of elasticity) and frequently a value for Poisson's ratio. Various methods have been proposed for determining stress-strain moduli from both conventional and cyclic triaxial tests [B27].

Copyright © 2001 IEEE. All rights reserved.

Copyright The Institute of Electrical and Electronics Engineers, Inc.
Provided by IHS under license with IEEE
No reproduction or networking permitted without license from IHS
Not for Resale

Engineering properties governing the consolidation settlement of cohesive soils (for example, clays) are normally determined from laboratory consolidation or oedometer tests. Consolidation of a soil may be defined as the time-dependent reduction in void ratio due to the application of an applied compressive stress, such as might be generated below the foundation of a transmission structure. The compressibility of a cohesive soil is dependent upon the stress history of the soil. If the effective vertical stress below a foundation is less than the maximum effective stress previously experienced by the soil, the settlement will be governed by the recompression index, C_r, determined from laboratory consolidation tests. The void-ratio effective-stress relationship for stress levels exceeding the past maximum effective stress is governed by the so-called virgin compression curve and the compression index, C_c. Detailed discussions of these parameters are presented in various texts on soil mechanics and foundation engineering [B97], [B27], [B123] and a description of test procedures and equipment [B96]. The use of the compression and recompression indexes in estimating consolidation settlement is demonstrated in 4.2.2.2.

The consolidation test and shear strength tests described above are normally conducted on undisturbed samples obtained during the subsurface investigation. It should be emphasized that the results of such laboratory tests are very dependent upon the quality of the samples tested. Consequently, care should be exercised in sampling, handling, and trimming the samples in preparation for testing. Undisturbed samples are difficult to obtain for many cohesionless soils. However, recompacted samples will generally provide useful results provided that care is taken to ensure that the recompacted soil is tested in the same condition (for example, density) as existed in the field.

In addition to the laboratory tests discussed in this section, other specialized tests have been developed to determine the engineering properties of soils. They are treated in laboratory soil testing manuals [B96].

3.5.3 In situ testing

In situ tests that measure the engineering properties of the subsurface materials in place are valuable for designing transmission structure foundations. The most common types of in situ tests that may be useful are

— Vane shear
— Pressuremeter
— Plate loading

The vane shear test is used to measure the undrained shear strength of soft to medium clays. A small, four-bladed vane attached to the end of a rod is pushed into the undisturbed clay at the bottom of a boring. The rod is rotated at the ground surface, and torque and angle of rotation are measured. The measured torque can be related to the shearing resistance developed on the periphery of the cylinder formed by the vanes rotating in the clay. Apparatus and procedures for conducting vane shear tests are described in [B85]. The vane shear test is not suitable in clays containing sand or silt layers, gravel, shells, or organic material.

Comparative studies between the undrained shear strength measured by the vane shear test and laboratory tests on undisturbed samples indicate that the vane shear test can give results either above or below laboratory strength measurements [B152]. Proper interpretation of vane shear test data requires careful sampling and identification of the soil; therefore, the vane shear test should be performed under the direction of a geotechnical engineer.

The pressuremeter is an instrument designed to measure the *in situ* modulus of deformation and may be used to determine the *in situ* state of stress and strength. The pressuremeter consists of an expandable probe that is lowered into a borehole and expanded to contact the sides of the boring. The expandable probe, activated by water pressure, is connected to a volumeter-manometer on the ground surface. After lowering the probe to the desired depth, it is expanded by applying pressure that can be determined by the volume; hence, a curve of pressure versus volume is obtained. This data may be used to determine a horizontal modulus of deformation. It is recommended that pressuremeter testing be performed under the direction of a geotechnical engineer.

Copyright © 2001 IEEE. All rights reserved.

Copyright The Institute of Electrical and Electronics Engineers, Inc.
Provided by IHS under license with IEEE
No reproduction or networking permitted without license from IHS Not for Resale

Menard [B109] has proposed a means of using the pressuremeter to determine the horizontal subgrade modulus. The horizontal subgrade modulus is used to design drilled pier foundations (see Clause 5).

The plate-loading test is a means of estimating the bearing capacity and determining the modulus of vertical subgrade reaction by obtaining a load versus deformation curve from which a modulus of deformation is computed. The general procedure for performing a plate-loading test is described in ASTM D1194-94 [B13]. Particular attention is drawn to Note 3 in [B13], which points out that the deflection of a foundation to a given load is a function of the foundation size and shape and the groundwater table location with respect to the bottom of the foundation.

When plate-loading tests are being considered, an alternative method would be to construct a concrete foundation of one-half or one-third scale at the depth of the final foundation. Data from a field test of this scale will be more readily interpreted and applied to the final foundation design.

It is important that field tests be located at those sites that are representative of the majority of soil conditions on the line route. Generally, if only one test is performed, it will be at a location that is judged to represent the poorest subsurface conditions. If the purpose of the field test is to refine the foundation design for a large number of foundations, then the field test should be performed at a location that is representative of a large number of foundation locations. However, considerable experience and judgement is required in the application of *in situ* test results to the design of foundations.

4. Design of spread foundations

4.1 Structural applications

The spread foundation is suitable and commonly used as support for lattice transmission towers. Less common applications are for single shaft and framed structures. The most frequently used types are steel grillages, pressed plates, cast-in-place concrete, and precast concrete. A description of each of these foundation types is presented in the following.

4.1.1 Foundation types

4.1.1.1 Steel grillages

Figure 8 indicates three typical types of steel grillages. Figure 8, part A, is a pyramid arrangement in which the leg stub is connected to four smaller stubs which are connected to the grillage at the base. The advantage of this type of construction is that the pyramid can transfer the horizontal shear load down to the grillage base by truss action. However, the pyramid arrangement does not permit much flexibility for adjusting the assembly, if needed. In addition, it is difficult to compact the backfill inside the pyramid.

Figure 8, part B shows a grillage foundation which has the single leg stub carried directly to the grillage base. The horizontal shear is transferred through shear members that engage the passive lateral resistance of the adjacent compacted soil. It is important that the bottom shear member and diagonal be connected to the leg stub at an adequate depth below the ground surface to mobilize the passive resistance of the compacted backfill.

Figure 8, part C also has the single leg stub carried directly to the grillage base. This type of grillage foundation has a leg reinforcer which increases the area for mobilizing passive soil pressure as well as increasing the leg strength. The shear is transferred to the soil via the leg and reinforcer and resisted by passive soil pressure.

Copyright © 2001 IEEE. All rights reserved.

Copyright The Institute of Electrical and Electronics Engineers, Inc.
Provided by IHS under license with IEEE
No reproduction or networking permitted without license from IHS
Not for Resale

The base grillage of these three typical foundations consists of steel beams, angles, or channels which transfer the bearing or uplift loads to the soil.

The advantages of steel grillage foundations include: low cost, ease of installation, and immediate tower installation, and they can be purchased with the tower steel, while concrete is not required at the site. The disadvantage is that these foundations may have to be designed before any soil borings are obtained and then may have to be enlarged by pouring a concrete base around the grillage if actual soil conditions are not as good as those assumed in the original design. In addition, large grillages are difficult to set with required accuracy.

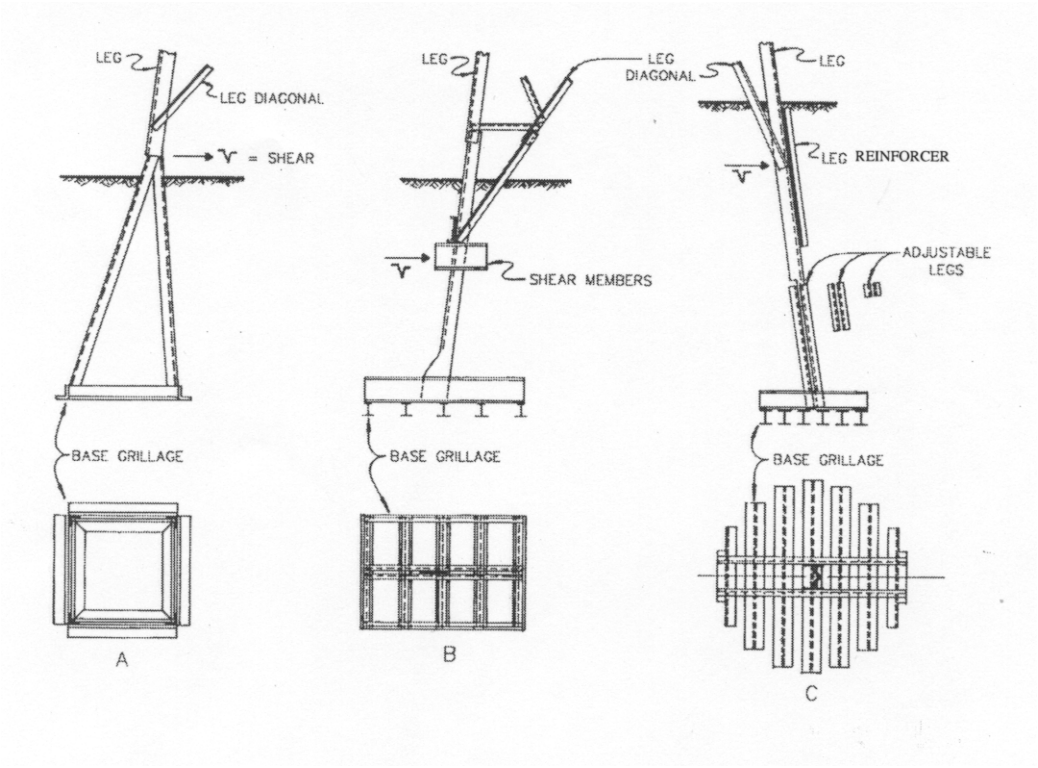

Figure 8—Various steel grillage foundations

4.1.1.2 Pressed plates

A typical pressed plate foundation is shown in Figure 9. This arrangement is similar to the grillages shown in Figure 8, part B except that the base grillage is replaced by a pressed plate. Figure 10 indicates a bipod foundation which has a truss in one direction. In both of the designs shown, the net horizontal shear at the level where the diagonal is attached to the stub is resisted by the passive soil pressure. An apparent disadvantage of this type of foundation is the possibility of loose sand under the dish portion of the plate which could increase settlement.

Copyright © 2001 IEEE. All rights reserved.

Copyright The Institute of Electrical and Electronics Engineers, Inc.
Provided by IHS under license with IEEE
No reproduction or networking permitted without license from IHS
Not for Resale

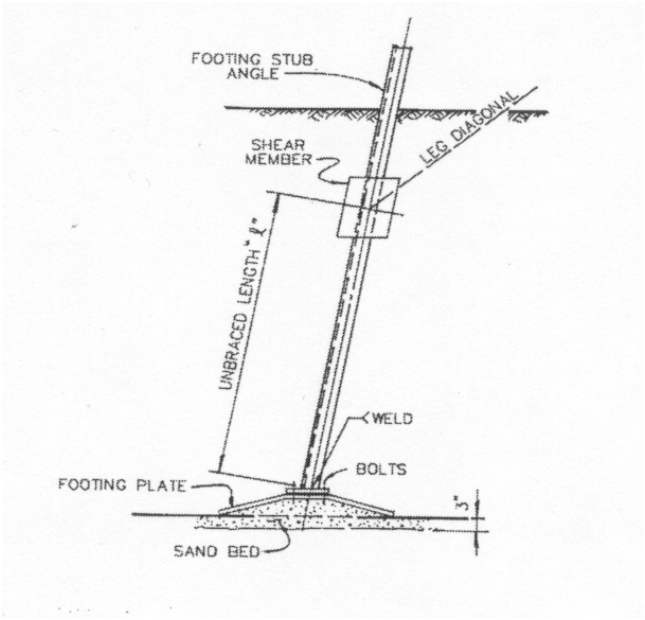

Figure 9—Typical plate foundation

4.1.1.3 Cast-in-place concrete

This type of foundation consists of a base mat and a square or cylindrical pier. It is constructed of reinforced or plain concrete, and several variations exist as indicated in Figure 11. The stub angle can be bent and the pier and mat centered. Alternatively, the mat can be located so that the projection from the stub angle intersects the centroid of the mat, or the pier itself can be battered to the tower leg slope.

Since the mat is required to resist both compression and uplift loads, top and bottom reinforcing steel may be provided to resist the bending moments developed. As required, a construction joint should be provided between the mat and the pier.

Stub angles are embedded in the top of the pier so that the upper exposed section can be spliced directly to the main tower leg and diagonals. The embedded members should be of adequate size to resist the axial loads transmitted from the main leg and diagonals, plus any secondary bending moment from the horizontal shear, if applicable. The embedded member must be embedded in the concrete to a sufficient depth to transmit the load to the concrete. Bolted clip angles, welded stud shear connectors, or bottom plates may be added on the end of the stub angle to reduce this length, as shown in Figure 12. Anchor bolts can also be used in lieu of the direct embedment stub angle, as shown in Figure 11, part C. ANSI/ASCE 10-97, Section 9 [B5] describes the latest embedment design.

4.1.1.4 Precast concrete

This type of foundation is very similar to the cast-in-place concrete foundation, except that the mat is precast elsewhere and delivered to the construction site. Stub angles or anchor bolts may be embedded in the piers during fabrication to provide a connection with the superstructure. The piers may also be cast in the field after the precast mat has been placed and a suitable connection installed prior to pouring the concrete. Care should be exercised to ensure that a uniform contact surface is provided between the precast mat and the soil, and that the soil immediately below the mat is well-compacted.

Copyright © 2001 IEEE. All rights reserved.

Copyright The Institute of Electrical and Electronics Engineers, Inc.
Provided by IHS under license with IEEE
No reproduction or networking permitted without license from IHS
Not for Resale

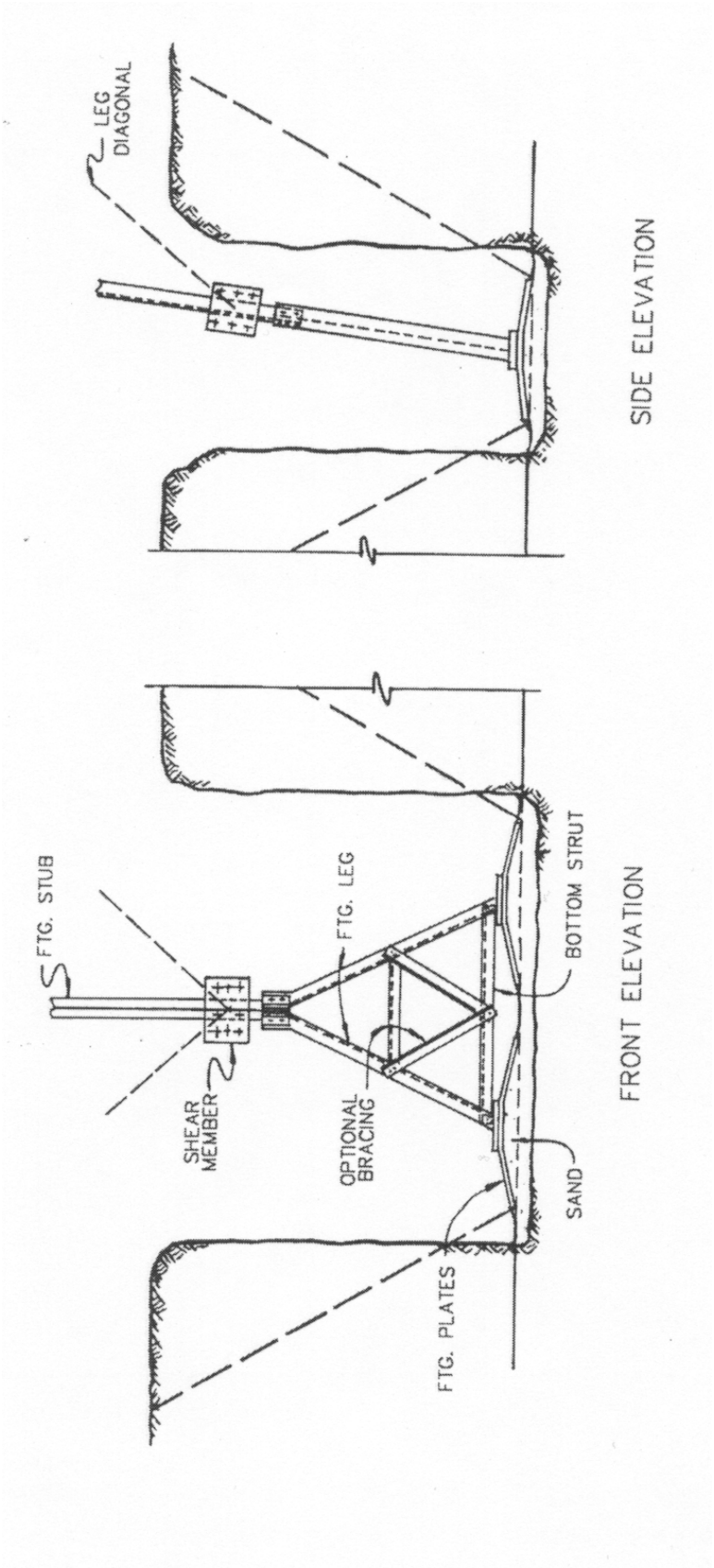

Figure 10—Typical bipod footing

Copyright © 2001 IEEE. All rights reserved.

Copyright The Institute of Electrical and Electronics Engineers, Inc.
Provided by IHS under license with IEEE
No reproduction or networking permitted without license from IHS
Not for Resale

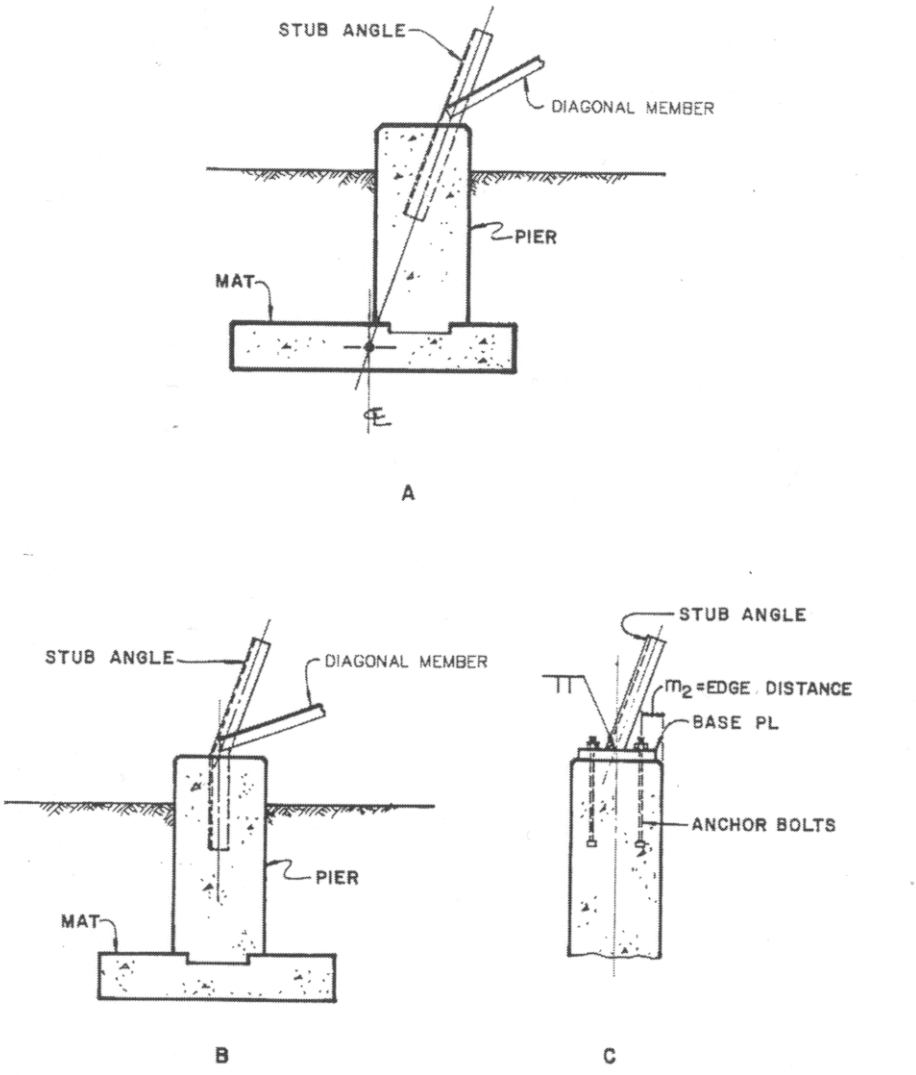

Figure 11—Cast in place concrete foundation

4.1.1.5 Rock foundations

Many areas of the United States have bedrock either exposed at the ground surface or covered with a thin mantle of soil. Relatively simple, economical, and efficient rock foundations may be installed where this type of terrain is encountered. A rock foundation can be designed to resist both uplift and compression loads plus horizontal shear and, in some structure applications, bending moments. Where suitable bedrock is encountered at the surface or close to the surface, a rock foundation, as shown in Figure 13, can be installed.

Copyright © 2001 IEEE. All rights reserved.

Copyright The Institute of Electrical and Electronics Engineers, Inc.
Provided by IHS under license with IEEE
No reproduction or networking permitted without license from IHS
Not for Resale

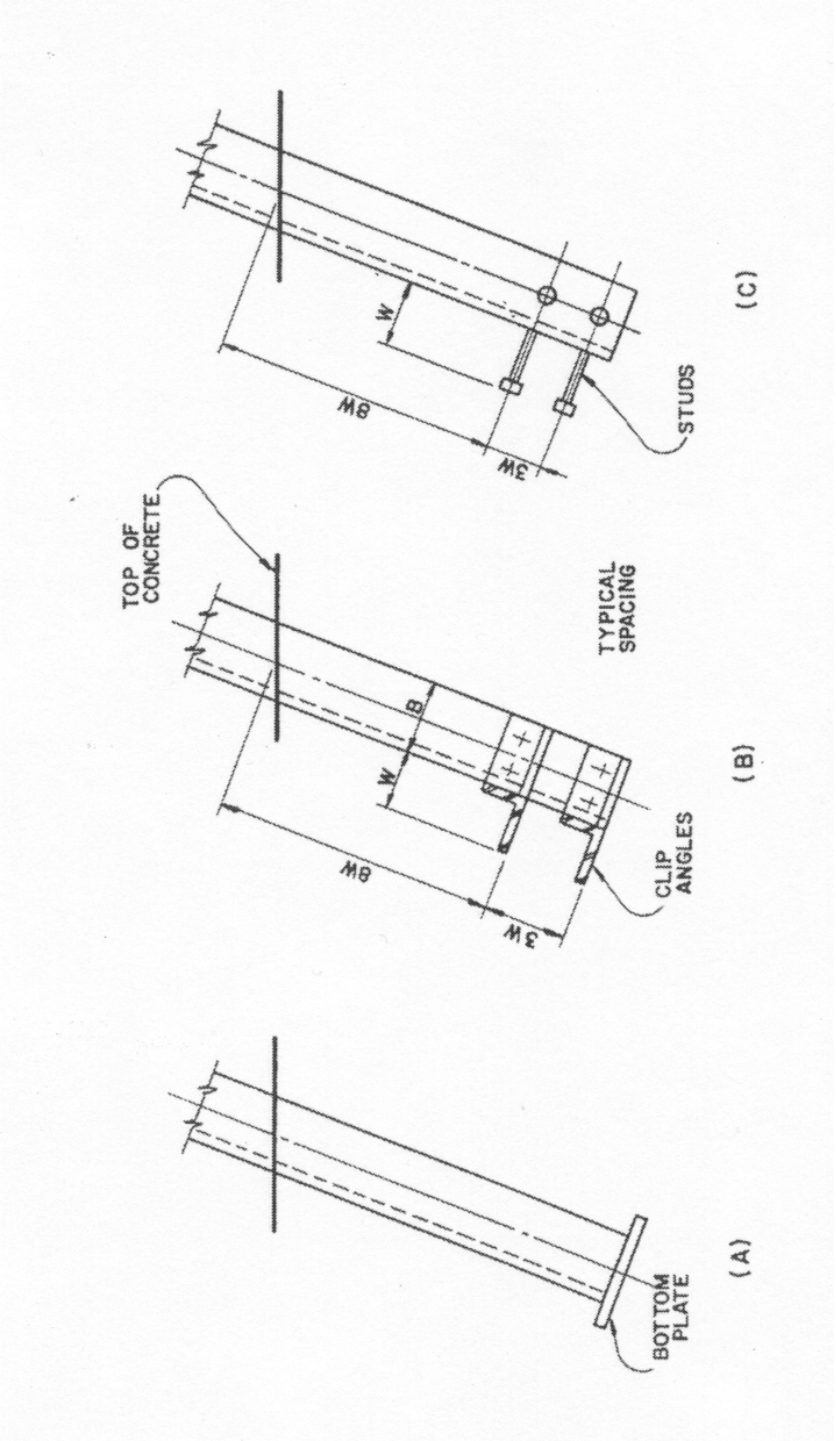

Figure 12—Stub angles

Copyright © 2001 IEEE. All rights reserved.

Copyright The Institute of Electrical and Electronics Engineers, Inc.
Provided by IHS under license with IEEE
No reproduction or networking permitted without license from IHS
Not for Resale

The determination of whether a rock formation is suitable for installation of rock foundations is an engineering judgment based on a number of factors which were discussed previously in Clause 3. Test holes, field inspection of the excavation, knowledge of the local geology, past experience, and load tests should be considered in this evaluation. The Rock Quality Designation (RQD) is useful in helping to evaluate rock suitability [B46].

Since the bearing capacity of rock is usually much greater than the uplift capacity, care must be exercised in designing for uplift [B88]. The rock sockets can be roughened, grooved, or shaped to increase the uplift capacity [B88]. The design of foundations in rock to resist uplift loads is similar to the design of rock anchors discussed in 7.3.1.

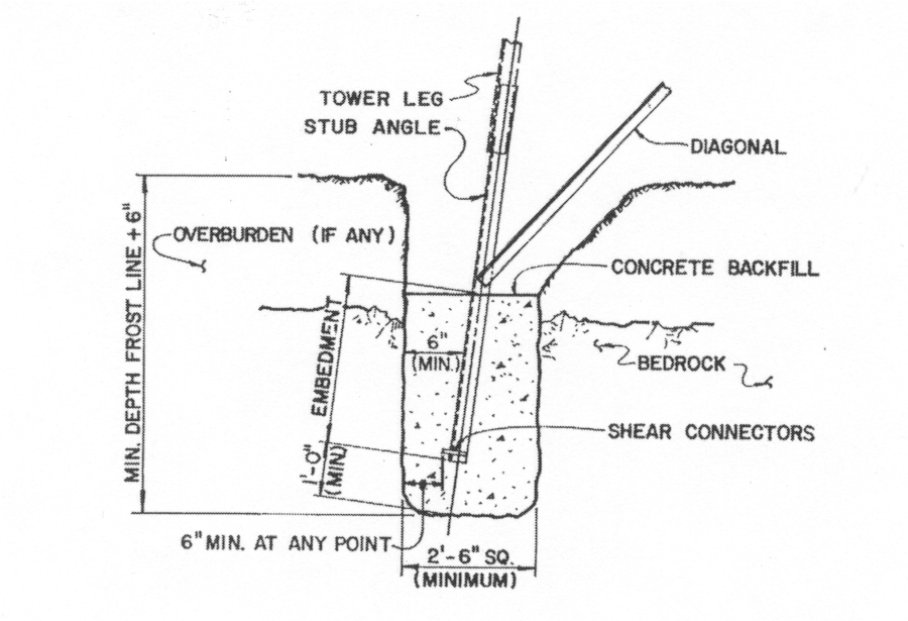

Figure 13—Rock foundation

4.1.2 Foundation orientation

The foundations for lattice towers can be installed with a vertical pier or a pier battered to the same slope as the tower leg, as shown in Figure 14. The pier may be round, square, or rectangular in cross-section and may be of constant section or be tapered to a greater width at the bottom to provide extra strength for the bending moment caused by the horizontal shear at the top of the pier. Generally, the tapered pier will prove to be less economical because of the more complex formwork required.

The pier may also be vertical, as shown in Figure 11, part A, but offset to allow the center of gravity of the stub angle to intersect the centroid of the mat. Alternatively, the pier may be vertical and the stub angle bent, as indicated in Figure 11, part B. The piers and mats can be oriented as shown for Section A-A or for Section B-B in Figure 14. Normally, the orientation of Section A-A gives a better resolution of forces from the two tower faces.

The disadvantage of the vertical pier shown in Figure 14, Section B-B, is the necessity of designing for a large horizontal shear at the top of the pier.

Copyright © 2001 IEEE. All rights reserved.

Copyright The Institute of Electrical and Electronics Engineers, Inc.
Provided by IHS under license with IEEE
No reproduction or networking permitted without license from IHS
Not for Resale

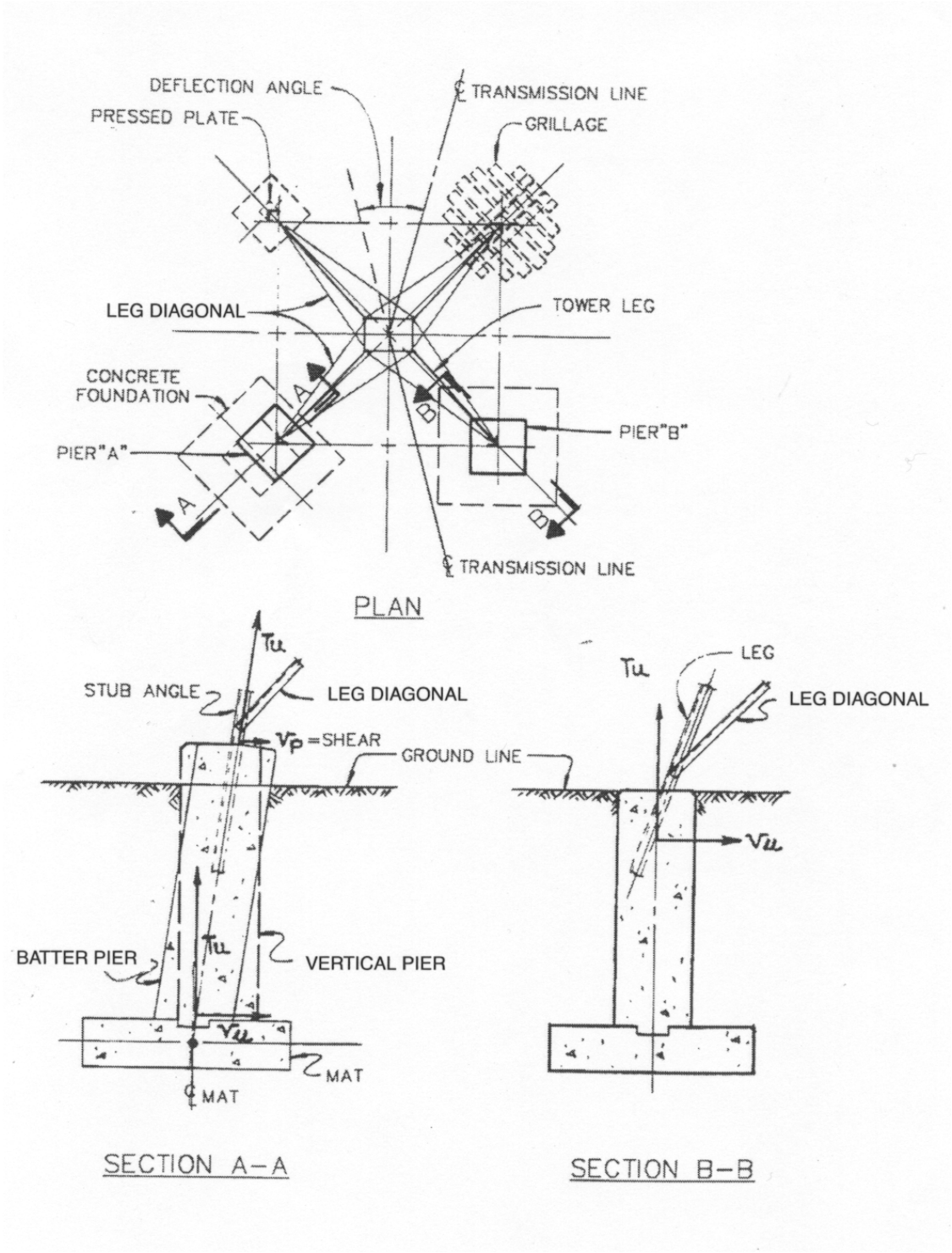

Figure 14—Footing orientation

Copyright © 2001 IEEE. All rights reserved.

Copyright The Institute of Electrical and Electronics Engineers, Inc.
Provided by IHS under license with IEEE
No reproduction or networking permitted without license from IHS
Not for Resale

When the pier is oriented as shown in Figure 14, Section A-A, the axial forces will continue down through the pier to the center of the mat. Consequently, the horizontal shear load at the top of the pier is greatly reduced for dead-end and large line angle towers. The remaining shear load at the top of the pier can be resisted either by passive soil pressure or by pier bending or a combination of both. Therefore, with dead-end and large line angle tower foundations, the piers and mats can be designed more economically as shown in Figure 14, Section A-A. For tangent tower foundations, the differential shear between straight and battered piers is usually not significant.

As shown in Figure 14, the grillage and plate foundations are relatively easy to orient and adjust as required.

4.2 Analysis

The design of spread foundations for transmission towers must consider the following:

— Load direction
— Load magnitude
— Load duration
— Static vs. cyclic loads
— Foundation movement

This section presents methods of estimating the uplift and compression (bearing) capacities and the settlement of spread foundations. Additional details on uplift and compression analysis of spread foundations for transmission structures are contained in References [B82], [B3], [B168], [B148], and [B158].

Although concrete foundations are used in the discussion, the methods presented here are applicable to other spread foundation types. Minor modifications to the methods are suggested as necessary to consider the type or geometry of the foundation.

4.2.1 Compression capacity

The allowable compression capacity of a spread foundation may be controlled either by the stability of the soil-foundation system (bearing capacity) or by the need to limit the total or differential settlement of the structure. The methods to compute the bearing capacity and settlement are given in the following sections.

4.2.1.1 Bearing capacity

The maximum load per unit area that can be placed on a soil at a given depth is the ultimate bearing capacity, q_{ult}. As shown in Figure 15, q_{ult} is the maximum load, Q, divided by the foundation area, B × L, at depth D. Q includes the structure loads, weight of the foundation, and weight of the backfill within the volume B × L × D. In Figure 15, the soil within the shear surface is assumed to behave as a rigid plastic medium which is idealized by an active Rankine zone (I), a radial Prandtl zone (II), and a passive Rankine zone (III). The soil above the foundation base is treated as an equivalent surcharge.

The general solution is the Buisman-Terzaghi equation given below:

$$q_{ult} = cN_c + \frac{1}{2}B\gamma N_\gamma + qN_q \quad (3)$$

where

c is soil cohesion,
B is foundation width,
q is surcharge (γD),

Copyright © 2001 IEEE. All rights reserved.

Copyright The Institute of Electrical and Electronics Engineers, Inc.
Provided by IHS under license with IEEE
No reproduction or networking permitted without license from IHS
Not for Resale

D is foundation depth,
γ is soil unit weight,
N_c, N_γ, N_q are dimensionless bearing capacity factors.

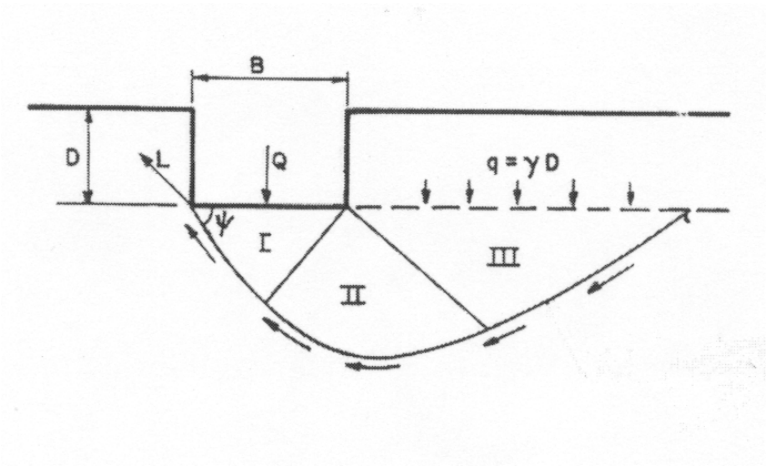

Figure 15—General description of bearing capacity

This equation includes the Prandtl and Reissner solutions for a load on a weightless medium, resulting in:

$$N_q = e^{\pi \tan\phi} \tan^2(45 + \phi/2) \quad (4)$$

$$N_c = (N_q - 1)\cot\phi \quad (5)$$

NOTE—As $\phi \rightarrow 0$, $N_c \rightarrow 5.14$

where

ϕ is soil angle of friction.

Values of N_c and N_q are given in Table 2 and Figure 16. The N_γ term is given as:

$$N_\gamma \approx 2(N_q + 1)\tan\phi \quad (6)$$

which is Vesic's approximation [B162] of the numerical solution by Caquot and Kerisel [B35] that uses $\psi = 45° + \phi/2$ in Figure 15. The solid line (for N_γ) in Figure 16 is Vesic's approximation, which is within 5% for $\phi = 20°$ to 40°.

Equation (3) has been developed for the following idealized conditions:

— General shear failure in the soil
— Horizontal ground surface
— Horizontal, infinitely long, strip foundation at shallow depth
— Vertical loading, concentrically applied

Copyright © 2001 IEEE. All rights reserved.

Copyright The Institute of Electrical and Electronics Engineers, Inc.
Provided by IHS under license with IEEE
No reproduction or networking permitted without license from IHS Not for Resale

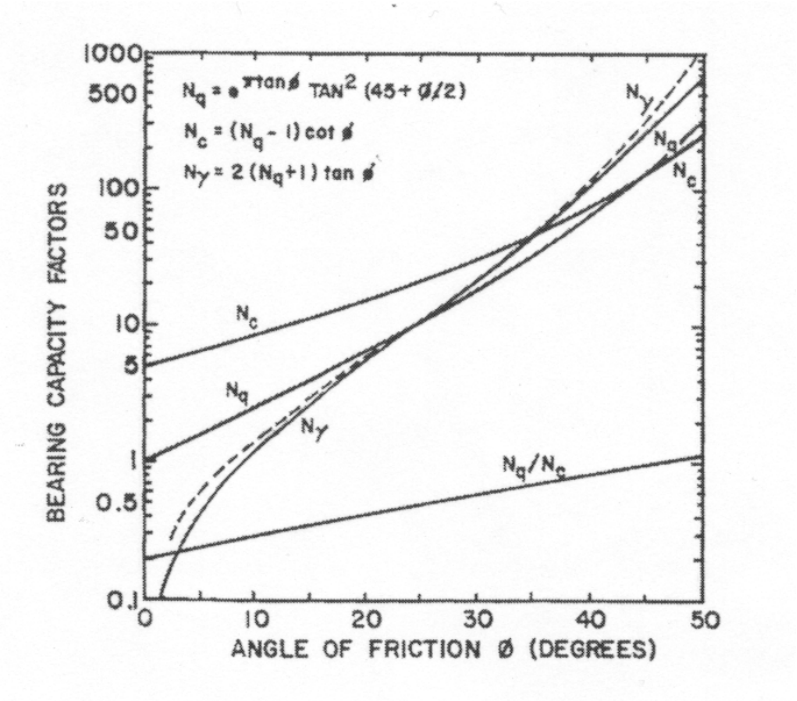

Figure 16—Bearing capacity factors for shall foundations

Table 2—Bearing-capacity factors N_c, N_q and N_γ

ϕ	N_c	N_q	N_γ	N_q/N_c	$\tan\phi$
0	5.14	1.00	0.00	0.20	0.00
1	5.38	1.09	0.07	0.20	0.02
2	5.63	1.20	0.15	0.21	0.03
3	5.90	1.31	0.24	0.22	0.05
4	6.19	1.43	0.34	0.23	0.07
5	6.49	1.57	0.45	0.24	0.09
6	6.81	1.72	0.57	0.25	0.11
7	7.16	1.88	0.71	0.26	0.12
8	7.53	2.06	0.86	0.27	0.14
9	7.92	2.25	1.03	0.28	0.16
10	8.35	2.47	1.22	0.30	0.18
11	8.80	2.71	1.44	0.31	0.19
12	9.28	2.97	1.69	0.32	0.21

Copyright © 2001 IEEE. All rights reserved.

Copyright The Institute of Electrical and Electronics Engineers, Inc.
Provided by IHS under license with IEEE
No reproduction or networking permitted without license from IHS
Not for Resale

Table 2—Bearing-capacity factors N_c, N_q and N_γ (continued)

ϕ	N_c	N_q	N_γ	N_q/N_c	tanϕ
13	9.81	3.26	1.97	0.33	0.23
14	10.37	3.59	2.29	0.35	0.25
15	10.98	3.94	2.65	0.36	0.27
16	11.63	4.34	3.06	0.37	0.29
17	12.34	4.77	3.53	0.39	0.31
18	13.10	5.26	4.07	0.40	0.32
19	13.93	5.80	4.68	0.42	0.34
20	14.83	6.40	5.39	0.43	0.36
21	15.82	7.07	6.20	0.45	0.38
22	16.88	7.82	7.13	0.46	0.40
23	18.05	8.66	8.20	0.48	0.42
24	19.32	9.60	9.44	0.50	0.45
25	20.72	10.66	10.88	0.51	0.47
26	22.25	11.85	12.54	0.53	0.49
27	23.94	13.20	14.47	0.55	0.51
28	25.80	14.72	16.72	0.57	0.53
29	27.86	16.44	19.34	0.59	0.55
30	30.14	18.40	22.40	0.61	0.58
31	32.67	20.63	25.99	0.63	0.60
32	35.49	23.18	30.22	0.65	0.62
33	38.64	26.09	35.19	0.68	0.65
34	42.16	29.44	41.06	0.70	0.67
35	46.12	33.30	48.03	0.72	0.70
36	50.59	37.75	56.31	0.75	0.73
37	55.63	42.92	66.19	0.77	0.75
38	61.35	48.93	78.03	0.80	0.78
39	67.87	55.96	92.25	0.82	0.81
40	75.31	64.20	109.41	0.85	0.84

Copyright © 2001 IEEE. All rights reserved.

Copyright The Institute of Electrical and Electronics Engineers, Inc.
Provided by IHS under license with IEEE
No reproduction or networking permitted without license from IHS
Not for Resale

Table 2—Bearing-capacity factors N_c, N_q and N_γ (continued)

ϕ	N_c	N_q	N_γ	N_q/N_c	tanϕ
41	83.86	73.90	130.22	0.88	0.87
42	93.71	85.38	155.55	0.91	0.90
43	105.11	99.02	186.54	0.94	0.93
44	118.37	115.31	224.64	0.97	0.97
45	133.88	134.88	271.76	1.01	1.00
46	152.10	158.51	330.35	1.04	1.04
47	173.64	187.21	403.67	1.08	1.07
48	199.26	222.31	496.01	1.12	1.11
49	229.93	265.51	613.16	1.15	1.15
50	266.89	319.07	762.89	1.20	1.19

To extend this equation to actual field conditions, modifiers have been developed by a number of authors. Those presented below are based primarily upon the consistent interpretations of the available data by Vesic [B162] and Hansen [B70] and as summarized by Kulhawy, et al. [B88].

In its general form the bearing capacity equation is given as:

$$q_{ult} = \frac{Q}{B'L'} = cN_c\zeta_{cs}\zeta_{cd}\zeta_{cr}\zeta_{ci}\zeta_{ct}\zeta_{cg} \quad (7)$$

$$+ \frac{1}{2}B_\gamma N_\gamma \zeta_{\gamma s}\zeta_{\gamma d}\zeta_{\gamma r}\zeta_{\gamma i}\zeta_{\gamma t}\zeta_{\gamma g}$$

$$+ qN_q\zeta_{qs}\zeta_{qd}\zeta_{qr}\zeta_{qi}\zeta_{qt}\zeta_{qg}$$

The ζ modifiers are doubly subscripted to indicate which term it applies to (N_c, N_γ, N_q) and which phenomenon it describes (s for shape of foundation, d for depth of foundation, r for soil rigidity, i for inclination of the load, t for tilt of the foundation base, and g for ground surface inclination). The B' and L' terms take into account load eccentricity. The equations for ζ modifiers are given in Table 3, with definitions of the geometric terms given in Figure 17. It should be noted that these modifiers only include geometric terms, the soil strength parameters, c and ϕ, and the soil rigidity index, I_r which will be defined subsequently.

Equation (7) represents the most general formulation for the bearing capacity of the foundation for a c-ϕ soil. However, caution must be exercised in evaluating the soil strength parameters because very few natural soils have a true cohesion. Those which do fall into special categories, such as naturally cemented soils, very stiff, overconsolidated clays which show an effective stress cohesion that normally decays with time, and partially saturated cohesive fill, in which the cohesion is lost upon saturation. Part of the problem in evaluating the strength parameters correctly is that the strength envelope for many soils in nonlinear and the in-situ or laboratory testing commonly is limited.

Copyright © 2001 IEEE. All rights reserved.

Copyright The Institute of Electrical and Electronics Engineers, Inc.
Provided by IHS under license with IEEE
No reproduction or networking permitted without license from IHS
Not for Resale

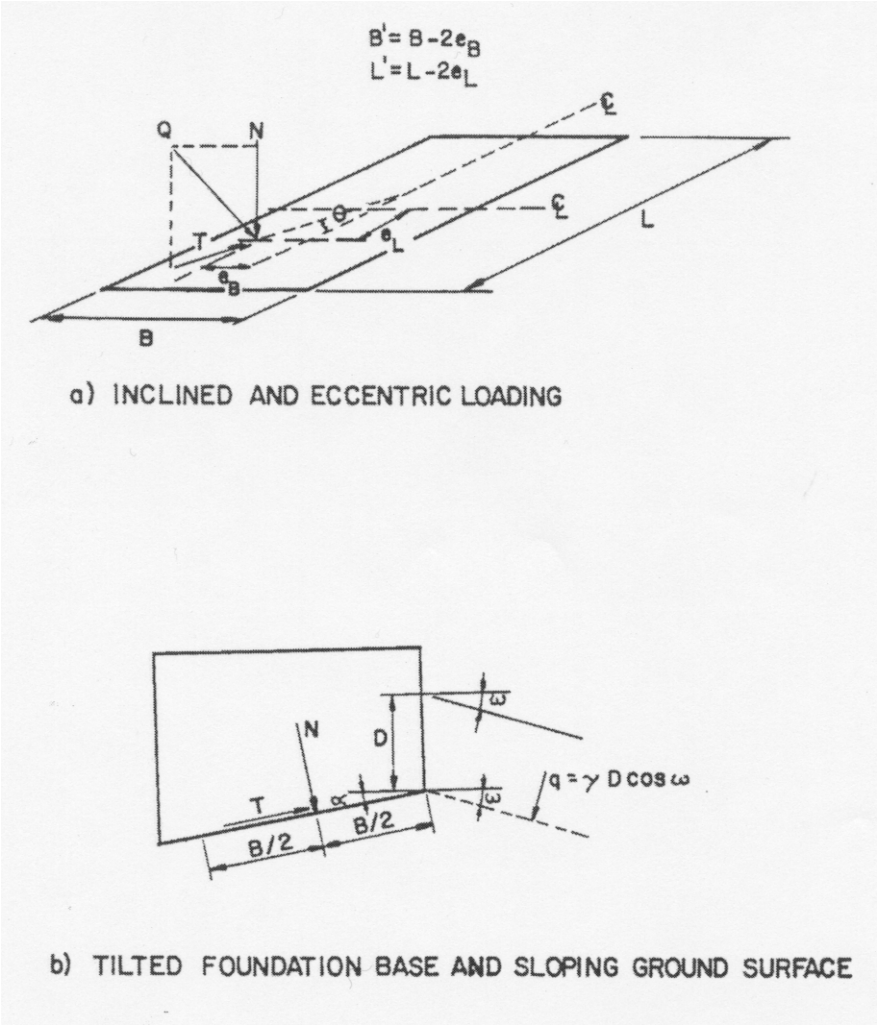

Figure 17—Definitions of geometric terms in bearing capacity equation

Figure 18 shows a common situation which arises. Three tests were conducted on a granular soil at three different normal stresses. The common tendency would be to evaluate this data using the dotted linear approximation. This would be satisfactory if all that one was seeking was the total value of strength within the testing stress range. However, granular soil is cohesionless and the true failure envelope is nonlinear, as shown by the solid line in Figure 18. This nonlinear envelope can be approximated well from the three data points, knowing that the curve must go through the origin. Once this envelope has been established, successive secants from the origin to the envelope are taken to evaluate the variation of ϕ with σ, as shown in Figure 19. For bearing capacity calculations, the value of ϕ to use will be that from Figure 19, consistent with the stress level for the problem at hand.

4.2.1.2 Bearing capacity for drained loading

Equation (7) is used most commonly in either of two derivative forms, which depend primarily on the soil type and rate of loading. The first is for drained loading, which develops under most loading conditions in coarse-grained soils such as sands and for long-term sustained loading of fine-grained soils such as clays. The second is undrained loading, described in the next section.

Copyright © 2001 IEEE. All rights reserved.

Copyright The Institute of Electrical and Electronics Engineers, Inc.
Provided by IHS under license with IEEE
No reproduction or networking permitted without license from IHS
Not for Resale

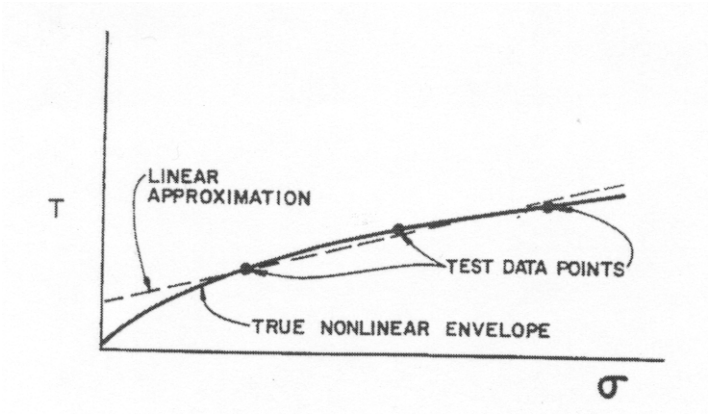

Figure 18—Strength envelope determination

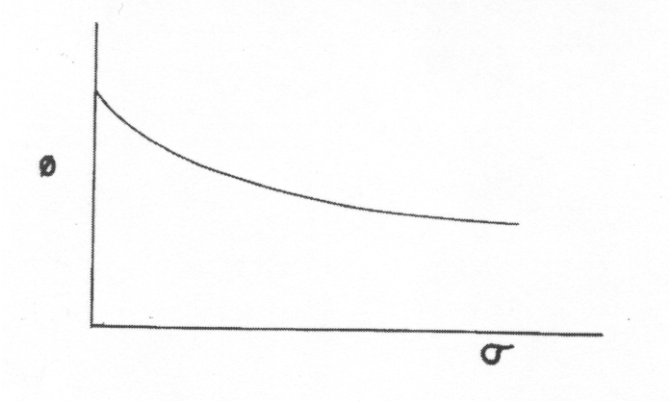

Figure 19—Actual variation of ϕ with σ

For drained loading, c = 0 as described previously, and therefore, Equation (7) becomes:

$$q_{ult} = \frac{Q}{B'L'} = \frac{1}{2}B\gamma N_\gamma \zeta_{\gamma s}\zeta_{\gamma d}\zeta_{\gamma r}\zeta_{\gamma i}\zeta_{\gamma t}\zeta_{\gamma g}$$

$$+ qN_q\zeta_{qs}\zeta_{qd}\zeta_{qr}\zeta_{qi}\zeta_{qt}\zeta_{qg} \quad (8)$$

where

q_{ult}	is ultimate bearing capacity,
Q	is maximum load (including structure load, effective weight of foundation, and effective weight of backfill within the volume $B \times L \times D$),
B	is foundation width or diameter (minimum dimension),
L	is foundation length or diameter,
D	is foundation depth,
B' and L'	are reduced B and L because of load eccentricity,
γ	is average effective soil unit weight from depth D to $D + B$,
q	is effective overburden stress at depth D,
N_γ and N_q	are bearing capacity factors defined in Equation (6) and Equation (4), respectively, and
ζ_{xy}	is bearing capacity modifiers given in Table 3.

Copyright © 2001 IEEE. All rights reserved.

Copyright The Institute of Electrical and Electronics Engineers, Inc.
Provided by IHS under license with IEEE
No reproduction or networking permitted without license from IHS
Not for Resale

Table 3—Bearing capacity modifiers for general solution

Modification	Shape	Value	Notes
Shape	ζ_{cs}	$1 + (B/L)\ (N_q/N_c)$	—
	$\zeta_{\gamma s}$	$1 - 0.4\ (B/L)$	—
	S_{qs}	$1 + (B/L)\ \tan\phi$	—
Depth	ζ_{cd}	$\zeta_{qd} - [(1 - \zeta_{qd})/(N_c \tan\phi)]$	—
	$\zeta_{\gamma d}$	1	—
	ζ_{qd}	$1 + 2\tan\phi\ (1 - \sin\phi)^2\ \tan^{-1}\ (D/B)$	a)
Rigidity	ζ_{cr}	$\zeta_{qr} - [(1 - \zeta_{qr})/(N_c \tan\phi)]$	—
	$\zeta_{\gamma r}$	ζ_{qr}	—
	ζ_{qr}	$\exp\{[(-4.4 + 0.6\ (B/L))\tan\phi] + [(3.07\sin\phi)\ (\log_{10} 2I_{rr})/(1 + \sin\phi)]\}$	—
Load inclination	ζ_{cl}	$\zeta_{ql} - [(1 - \zeta_{ql})/(N_c \tan\phi)]$	b)
	$\zeta_{\gamma i}$	$\{1 - [T/(N + B'L'\ c\ \cot\phi)]\}^{n+1}$	b), c), d)
	ζ_{qi}	$\{1 - [T/(N + B'L'\ c\ \cot\phi)]\}^{n}$	b), c), d)
Base tilt	ζ_{ct}	$\zeta_{qt} - [(1 - \zeta_{qt})/(N_c \tan\phi)]$	b), e)
	$\zeta_{\gamma t}$	$(1 - \alpha\tan\phi)^2$	b), c), e)
	ζ_{qt}	$\approx \zeta_{\gamma t}$	b), e)
Sloping ground surface	ζ_{cg}	$\zeta_{qg} - [(1 - \zeta_{qg})/(N_c \tan\phi)]$	b), g)
	$\zeta_{\gamma g}$	$\approx \zeta_{qg}$	b), g)
	ζ_{qg}	$(1 - \alpha\tan\omega)^2$	b), c), g), h)

a) $\tan^{-1}$ in radians
b) Check for sliding
c) See Figure 17 for notation.
d) $$n = \frac{[2 + L/B]}{1 + L/B}\cos^2\theta + \frac{[2 + B/L]}{1 + B/L}\sin^2\theta$$
e) Limited to $\alpha < 45°$
f) α in radians
g) limited to $\omega < 45°$ and $\omega < \phi$; for $\omega > \phi/2$, check slope stability
h) ω in radians

The ζ terms for shape, depth, load inclination, base tilt, and sloping ground surface are a function only of the geometry and the soil friction angle, ϕ, which should be evaluated at the average effective vertical stress within the shear zone or, more specifically, at a depth D + B/2. It should be noted (footnote b) in Table 3) that a check is warranted to ensure that any lateral load component, T, does not exceed the maximum resistance to sliding, given by:

Copyright © 2001 IEEE. All rights reserved.
Copyright The Institute of Electrical and Electronics Engineers, Inc.
Provided by IHS under license with IEEE
No reproduction or networking permitted without license from IHS
Not for Resale

$$T_{max} = N \tan\delta \tag{9}$$

where

N is axial load component defined in Figure 17,
δ is angle of friction for the soil-foundation interface.

For cast-in-place concrete, $\delta = \phi$; for smooth steel, $\delta = \phi/2$; and for rough steel, $\delta = 3\,\phi/4$ [B94] [B126].

The ζ terms for rigidity include the same geometry and ϕ terms, plus the soil rigidity index, defined as:

$$I_r = \frac{G}{c + \sigma \tan\phi} \tag{10}$$

where

I_r is rigidity index,
G is shear modulus,
c is soil cohesion (equal to 0 for most cases as described previously),
σ is effective vertical stress at depth D + B/2, and
ϕ is soil friction angle as described above.

The shear modulus is commonly expressed in terms of Young's modulus, E, and Poisson's ratio, ν, so that, for drained loading with c = 0, the rigidity index becomes:

$$I_r = \frac{E}{2(1+\nu)} \cdot \frac{1}{\sigma \tan\phi} \tag{11}$$

Young's modulus can be evaluated directly from a number of different field or laboratory tests, corresponding to the stress conditions at depth D + B/2, or can be estimated from correlations in the literature [B137], from empirical techniques [B147], or from case history evaluation [B33]. Of particular interest in this regard is that, for 55 spread foundations in drained uplift, Callanan and Kulhawy found an apparent lower limit for $E/\bar{\sigma}_{vm}$ equal to 200, in which $\bar{\sigma}_{vm}$ equals mean vertical effective stress over depth, D. This apparent limit is a convenient first approximation.

Poisson's ratio approximately ranges from about 0.1 to about 0.4 for granular soils and can be estimated from: [B158]

$$\nu = 0.1 + 0.3\phi_{rel} \tag{12}$$

in which ϕ_{rel} is a relative friction angle given by:

$$\phi_{rel} = \frac{\phi - 25^\circ}{45^\circ - 25^\circ} = \frac{\phi - 25^\circ}{20^\circ} \tag{13}$$

with limits of 0 and 1.

Once the rigidity index is evaluated, it is reduced for volumetric strains [B180] to yield:

$$I_{rr} = I_r/(1 + I_r\Delta) \tag{14}$$

Copyright © 2001 IEEE. All rights reserved.

Copyright The Institute of Electrical and Electronics Engineers, Inc.
Provided by IHS under license with IEEE
No reproduction or networking permitted without license from IHS
Not for Resale

where

I_{rr} is reduced rigidity index, and
Δ is volumetric strain.

Based on Vesic's [B162] guidelines, Trautmann and Kulhawy [B180] showed that Δ can be estimated conveniently by:

$$\Delta \approx 0.005\sigma(1 - \phi_{rel}) \tag{15}$$

with σ defined in Equation (10), in units of tsf, up to a limit of 10 tsf, and ϕ_{rel} as defined in Equation (13).

After the soil rigidity index has been computed, it is compared with the theoretically based critical rigidity index, I_{rc}, given by [B130]:

$$I_{rc} = \frac{1}{2}\exp[(3.30 - 0.45B/L)\cot(45 - \phi/2)] \tag{16}$$

If $I_{rr} > I_{rc}$, the soil behaves as a rigid-plastic material, general shear failure would result, and therefore $\zeta_{cr} = \zeta_{\gamma r} = \zeta_{qr} = 1$. If $I_{rr} < I_{rc}$, the soil stiffness is low, local, or punching shear failure would result, and therefore, ζ_{cr}, $\zeta_{\gamma r}$, and ζ_{qr} will be less than 1 and must be computed to reduce the ultimate bearing capacity.

4.2.1.3 Bearing capacity for undrained loading

For undrained loading, which occurs when loads are applied relatively rapidly to fine-grained soils such as clays, pore water pressures build up in the soil at constant effective stress and lead to the analysis procedure commonly known as the total stress or $\phi = 0$ method. For this $\phi = 0$ method, $N_c = 5.14$, $N_\gamma = 0$, $N_q = 1$, and $\zeta_{qs} = \zeta_{qd} = \zeta_{qr} = \zeta_{qt} = \zeta_{qg} = 1$, therefore, Equation (7) reduces to:

$$q_{ult} = \frac{Q}{B'L'} = 5.14 s_u \zeta_{cs}\zeta_{cd}\zeta_{cr}\zeta_{ci}\zeta_{ct}\zeta_{cg} + \zeta_{qi} \tag{17}$$

in which

q_{ult} is ultimate bearing capacity,
Q is maximum load (including structure load, total weight of foundation, and total weight of backfill within the volume $B \times L \times D$),
B is foundation width or diameter (minimum dimension),
L is foundation length or diameter,
D is foundation depth,
B' and L' are reduced B and L dimensions because of load eccentricity,
s_u is c = average undrained shear strength from depth D to $D + B$,
q is total overburden stress at depth D,
ζ_{xy} is bearing capacity modifiers given in Table 4.

The ζ terms for shape, depth, base tilt, and sloping ground surface are a function only of the geometry while the ζ term for load inclination includes s_u and the geometry. It should be noted [footnote b) in Table 4] that a check is warranted to ensure that any lateral load component, T, does not exceed the maximum resistance to sliding, given by:

$$T_{max} = c_a B'L' \tag{18}$$

Copyright © 2001 IEEE. All rights reserved.

Copyright The Institute of Electrical and Electronics Engineers, Inc.
Provided by IHS under license with IEEE
No reproduction or networking permitted without license from IHS Not for Resale

where

c_a is adhesion for the soil-foundation interface.

For cast-in-place concrete, $c_a \approx s_u$; for smooth steel, $c_a \approx s_u/2$; and for rough steel, $c_a \approx 3\, s_u/4$ [B126] [B137].

The ζ term for rigidity includes the geometry and the soil rigidity index, defined as:

$$I_r = \frac{G}{s_u} = \frac{E}{2(1+\nu)} \cdot \frac{1}{s_u} = \frac{E}{3s_u} = I_{rr} \tag{19}$$

where

I_r is rigidity index,
G is shear modulus,
E is Young's modulus,
ν is Poisson's ratio, which is equal to 0.5 for saturated cohesive soil during undrained loading.

Since $\nu = 0.5$, no volumetric strains occur, and therefore, the reduced rigidity index, I_{rr}, is equal to I_r.

Young's modulus can be evaluated directly from a number of different field or laboratory tests, corresponding to the stress conditions at depth D + B/2, or can be estimated from correlations in the literature [B137], from empirical techniques [B147], or from case history evaluation [B33]. Of particular interest in this regard is that, for 20 spread foundations in undrained uplift, Callanan and Kulhawy [B33] found an apparent lower limit for E/σ_{vm} equal to about 175, in which σ_{vm} is the mean vertical total stress over depth D. This apparent limit is a convenient first approximation.

After the soil rigidity index has been computed, it is compared with the theoretically based critical rigidity index, I_{rc}, given by [B162]:

$$I_{rc} = \frac{1}{2}\exp(3.30 - 0.45B/L) \tag{20}$$

which will vary from 8.64 for a square or circular foundation (B = L) to 13.56 for an infinite strip foundation ($L \rightarrow \infty$). If $I_{rr} > I_{rc}$, the soil behaves as a rigid-plastic material, general shear failure would result, and therefore, $\zeta_{cr} = 1$. If $I_{rr} < I_{rc}$, the soil stiffness is low, local or punching shear failure would result, and therefore, ζ_{cr} will be less than 1 and must be computed to reduce the ultimate bearing capacity.

Copyright © 2001 IEEE. All rights reserved.

Copyright The Institute of Electrical and Electronics Engineers, Inc.
Provided by IHS under license with IEEE
No reproduction or networking permitted without license from IHS
Not for Resale

Table 4—Bearing capacity modifiers for undrained ($\phi = 0$) loading

Modification	Symbol	Value	Footnotes
Shape	ζ_{cs}	1+ 0.20 (B/L)	—
	ζ_{qs}	1	—
Depth	ζ_{cd}	$1 + 0.33 \tan^{-1}$ (D/B)	a)
	ζ_{qd}	1	a)
Rigidity	ζ_{cr}	$0.32 + 0.12$ (B/L) $+ 0.60 \log_{10} I_{rr}$	—
	ζ_{qr}	1	—
Load inclination	ζ_{ci}	$1 - [(nT)/(5.14\ s_u\ B'L')]$	b),c),d)
	ζ_{qi}	$[1 - (T/N)]^n$	b),c),d)
Base Tilt	ζ_{ct}	$1 - [2\alpha/(\pi + 2)]$	b),c),e),f)
	ζ_{qt}	1	b),e)
Sloping ground surface	ζ_{cg}	$1 - [2\alpha/(\pi + 2)]$	b),c),g),h)
	$\zeta_{\gamma g}$	1	b),g),i)
	ζ_{qg}	1	b),g)

a) $\tan^{-1}$ in radians
b) check for sliding
c) See Figure 17 for notation
d) $$n = \left[\frac{2 + L/B}{1 + L/B}\right]\cos^2\theta + \left[\frac{2 + B/L}{1 + B/L}\right]\sin 2\theta$$
e) limited to $\alpha < 45°$
f) α in radians
g) limited to $\omega < 45°$ and $\omega < \phi$; for $\omega > \phi/2$, check slope stability
h) ω in radians
i) $1/2\ B_\gamma N_\gamma \zeta$ term is necessary for $\phi = 0$ loading when $\omega > 0$; for this case, $N_\gamma = -2\sin\omega$ with ω in degrees, $\zeta_{\gamma s} = 1 - 0.4$ (B/L), $S_{\gamma i} = [1 - (T/N)]^{n+1}$, and $\zeta_{\gamma d} = \zeta_{\gamma r} = \zeta_{\gamma g} = 1$.

Copyright © 2001 IEEE. All rights reserved.

Copyright The Institute of Electrical and Electronics Engineers, Inc.
Provided by IHS under license with IEEE
No reproduction or networking permitted without license from IHS
Not for Resale

4.2.2 Settlement of spread foundations

4.2.2.1 Immediate settlement

Immediate settlements are those that occur as soon as the load is applied to the soil mass. While these settlements are not truly elastic, most solutions are based on the assumption that the soil may be modeled as a linear elastic half-space. Consequently, immediate settlements are often referred to as elastic settlements.

Elastic settlements (S_i) of saturated or near saturated clays can be determined by the equation [B137]:

$$S_i = I_w q B(1 - \nu^2)/E \quad \text{[for a one-layer system]} \tag{21}$$

where

I_w is geometric factor which reflects the foundation shape, flexibility, and the point on the foundation for which settlement is being calculated,
q is bearing pressure,
ν is the Poisson's Ratio for the soil,
E is modulus of elasticity of the soil,
B is least lateral dimension of the foundation.

The value of Poisson's Ratio (ν) for saturated clay is commonly assumed equal to 0.5. Typical values for I_w for flexible foundations for a square and circular loaded area are 0.95 and 0.85, respectively. These are average values for the entire area. Various points such as the center, corner, and side of the foundation have different values (e.g., see [B133]).

Equation (21) is applicable to granular soils where the elastic parameters depend substantially upon the confining pressure. An alternative in this case is the method proposed by Schmertmann [B139] which has the additional advantage that it is applicable to layered soils. The settlement is given as:

$$S_i = C_1 C_2 = \sum_{i=1}^{n} (I_z/E)_i \Delta Z_i \tag{22}$$

where

C_1 is the correction factor to incorporate strain relief because of embedment and is given by:

$$C_1 = 1 - 0.5\frac{(\sigma'_o)}{q} \geq 0.5 \tag{23}$$

and σ'_o is the effective overburden pressure at the foundation depth. C_2 is a coefficient of time-dependent increase in settlement for cohesionless soils and may be expressed as:

$$C_2 = 1 + 0.2\log_{10}\frac{t}{0.1} \tag{24}$$

where

t is time in years.

Copyright © 2001 IEEE. All rights reserved.

Copyright The Institute of Electrical and Electronics Engineers, Inc.
Provided by IHS under license with IEEE
No reproduction or networking permitted without license from IHS
Not for Resale

The quantity I_z is a strain influence function which depends only on ν and the location of the point where the strain is located. The strain influence function I_z is approximated by a bilinear function with values of zero at Z/B = 0 and 2, and 0.6 at Z/B = 0.5 (where Z is the vertical distance below the center of the foundation). The displacement for each increment ΔZ_1 of depth below the foundation is then summed in accordance with Equation (22) between Z = 0 and Z = 2B. The value of E at the various Z_i must be known and a useful correlation expresses it in terms of the cone tip resistance (q_c) of the soil. The value of E is obtained as follows:

$$E = 2q_c \tag{25}$$

where q_c and E are both in tons/ft [B139]. Vesic [B162] suggests $E = 2 (1 + D_r^2)q_c$, where D_r is the relative density of the soil deposit. In another approach [B72], the same formula as Schmertmann's is used, but the curves for I_z depend on lateral earth pressures, foundation shape, and Poisson's ratio.

EPRI report EL 6800 [B57] suggests

$$E = \partial(\sigma_1 - \sigma_3)/\partial\varepsilon_a$$

where

$\sigma_1 - \sigma_3$ is deviator stress or principal stress difference,
ε_a is axial strain.

For any particular stress-strain curve, the modulus can be defined as the initial tangent modulus (E_i), the tangent modulus (E_t) at a specified stress level, or the secant modulus (E_s) at a specified stress level.

In the case where the foundation slab cannot be considered rigid, the elastic settlement determination becomes more complex. If the sub-grade can be considered as a Winkler foundation, the displacement can be obtained by assuming that the foundation slab is a plate on an elastic foundation. Numerical methods, such as the finite element method, can also be used to solve this problem.

4.2.2.2 Consolidation settlement

With respect to consolidation settlement, only the sustained or frequent loading condition portion of the total load contributes to settlement. For suspension structures, where the maximum loading results from transient loads, consolidation settlements are probably not significant. For heavy angle or dead-end structures where the steady-state loading is appreciable, consolidation semement should be considered at least for soft or compressible soils. Only the steady-state load should be taken into account.

The compressibility of a clay deposit is dependent on the stress history of the soil. The consolidation settlement of a clay deposit is computed based on this stress history from normally consolidated to overconsolidated.

Normally consolidated clays are those in which the existing effective overburden stress is equal to the maximum effective stress the soil has experienced in the past. When the clay stratum is thick, it should be broken into several layers, and the consolidation of each layer is summed over N layers to obtain the total settlement. The total consolidation settlement (P_c) may then be expressed as:

$$P_c = \sum_{i=1}^{N} \Delta P_{ci} = \sum_{i=1}^{N} \left(\frac{C_{ci}}{1 + e_{oi}}\right) \log_{10} \frac{\sigma'_o + \Delta\sigma}{\sigma'_o} H_i \tag{26}$$

Copyright © 2001 IEEE. All rights reserved.

Copyright The Institute of Electrical and Electronics Engineers, Inc.
Provided by IHS under license with IEEE
No reproduction or networking permitted without license from IHS Not for Resale

where

ΔP_{ci} is settlement in the ith layer,
e_{oi} is initial void ratio of the ith layer,
H_i is the thickness of the ith layer,
σ'_o is the initial effective overburden stress in the ith layer,
Δ_σ is the change in stress in the ith layer due to the foundation load,
C_c is the compression index, as obtained from the slope of the e versus log σ'_c curve or by the use of empirical equations.

The change in stress, Δ_σ in the ith layer may be determined by either Boussinesq or Westergaard methods of evaluating the pressure induced below a loaded area on the ground surface [e.g., [B26]]. The values of C_c and e_o should be determined from appropriate laboratory testing of undisturbed samples. Empirical relationships for C_c have also been proposed for normally consolidated clays and may be used with caution [e.g., [B34]].

Overconsolidated clays are those in which the present effective overburden stress,σ'_o , is less than the maximum previous effective stress, σ'_p, that the soil has experienced. The settlement calculation is performed in the same manner as before, with the total estimated settlement taken as the sum of the settlement in the N layers below the footing. The appropriate expression for the consolidation settlement (P_c) is given as:

a) For $\Delta\sigma \geq (\sigma'_p - \sigma'_o)$

$$P_c = \sum_{i=1}^{N} \Delta P c_i = \sum_{i=1}^{N} \left(\frac{H_i}{1+e_{oi}}\right) c_e \log_{10}\left(\frac{\sigma'_p}{\sigma'_o}\right) + C_c \log_{10}\left(\frac{\sigma'_o + \Delta'_\sigma}{\sigma'_p}\right) i \quad (27)$$

b) For $\Delta\sigma \leq (\sigma'_p - \sigma'_o)$

$$P_c = \sum_{i=1}^{N} \Delta P c_i = \sum_{i=1}^{N} \left(\frac{H_i}{1+e_{oi}}\right) + C_c \log_{10}\left(\frac{\sigma'_o + \Delta'_\sigma}{\sigma'_p}\right) i \quad (28)$$

The variables in these expressions are as defined for the normally consolidated case with the exception of C_e which is the recompression index of the ith layer, and σ_p, which is the preconsolidation stress. Both C_e and σ_p must be determined from laboratory consolidation tests on undisturbed samples.

4.2.2.3 Secondary settlement

When the excess pore water pressure has dissipated under an imposed load condition, primary consolidation is essentially complete. However, the soil may continue to compress indefinitely under the load, although at a much slower rate. The compression taking place after consolidation is termed secondary compression.

Evaluation of the amount of secondary compression may be difficult. However, secondary compression may contribute significantly to the settlement for highly organic soils and may be computed as:

$$P_s = HC_\alpha \log \frac{t_i + \Delta_t}{t_i} \quad (29)$$

Copyright © 2001 IEEE. All rights reserved.

Copyright The Institute of Electrical and Electronics Engineers, Inc.
Provided by IHS under license with IEEE
No reproduction or networking permitted without license from IHS
Not for Resale

where

H is clay layer thickness,
C_α is coefficient of secondary compression,
t_i is time that secondary compression begins,
Δt is time over which settlement will be calculated.

The coefficient of secondary compression is the slope of the straight line portion of the dial reading (settlement) versus log time plot obtained from a laboratory consolidation test after the primary consolidation is complete. The coefficient C_α (Note: this coefficient can be estimated from Ref. [B110]; the value of C_α/C_c for organic clay is given in Ref. [B111]) is normally determined from a consolidation test in which the stress increment (in excess of effective overburden pressure), applied to the sample is equal to the average effective stress increase over the clay layer due to the foundation loads.

4.2.3 Moment foundations

There is, at present, very little available information concerning the response of a spread foundation subjected to axial forces, large shear forces, and large overturning moments. It is possible to analyze the actual state of stress under a spread foundation in an idealized soil by using numerical methods. A second alternative for the analysis of spread foundations is to assume that the foundation is supported on elastic springs. This method requires that the load-deformation characteristics of the springs (subgrade), which are usually expressed in terms of foundation modulus or the modulus of subgrade reaction, be determined or assumed. In general, the load-deformation characteristics are nonlinear except at small values of deformations. A foundation supported on elastic springs can be solved by the finite difference method or by the finite element method. A discussion of both methods is given by Bowles [B25].

A simplified method of analysis is still commonly used. For the great majority of spread foundations, this type of analysis will yield reasonable results, especially when the foundation slab approaches the assumption of infinite rigidity.

The fundamental assumption in the simplified method is that the foundation slab is infinitely rigid and that the soil subgrade is linearly elastic. For the calculation of stress under the foundation, the equations of statics are sufficient, since the two assumptions imply that the stress distribution would be planar.

Consider the foundation, shown in Figure 20, subjected to biaxial overturning moments (M_x and M_y), shear forces (Q_x and Q_y), and an axial compression force (Q_z). The total vertical reaction at the bottom of the foundation is denoted by Q_v where:

$$Q_v = Q_z + W_f + W_s \tag{30}$$

where

Q_z is vertical load applied to the foundation,
W_f is effective weight of the foundation,
W_s is effective weight of the backfill vertically above the foundation slab.

If it is assumed that the friction on the sides of the foundation slab may be ignored, the applied loads may be replaced by an eccentric load of magnitude Q_v. When e_x and e_y denote, respectively, the eccentricity of Q_v with respect to the x- and y-axis, then:

$$e_x = \frac{[M_y + Q_x(P_1 + D)] - A_x a - B_x b}{Q_v} \tag{31}$$

Copyright © 2001 IEEE. All rights reserved.

Copyright The Institute of Electrical and Electronics Engineers, Inc.
Provided by IHS under license with IEEE
No reproduction or networking permitted without license from IHS Not for Resale

and

$$e_y = \frac{[M_x + Q_y(P_1 + D)] - A_y a - B_y b}{Q_v} \quad (32)$$

where

A_x and A_y are passive pressures on the pier,
B_x and B_y are passive pressures on the mat in the x-and y-directions.

The quantities P_1, Q_x, Q_y and D are defined in Figure 20.

A conservative approach is to neglect the passive resistance of the soil, since the magnitude of the passive resistance is dependent on foundation type and construction method. However, for some grillage or pressed plate type foundations, the shear can only be taken by the passive resistance of the soil. For these foundations, care must be exercised in compacting the backfill material.

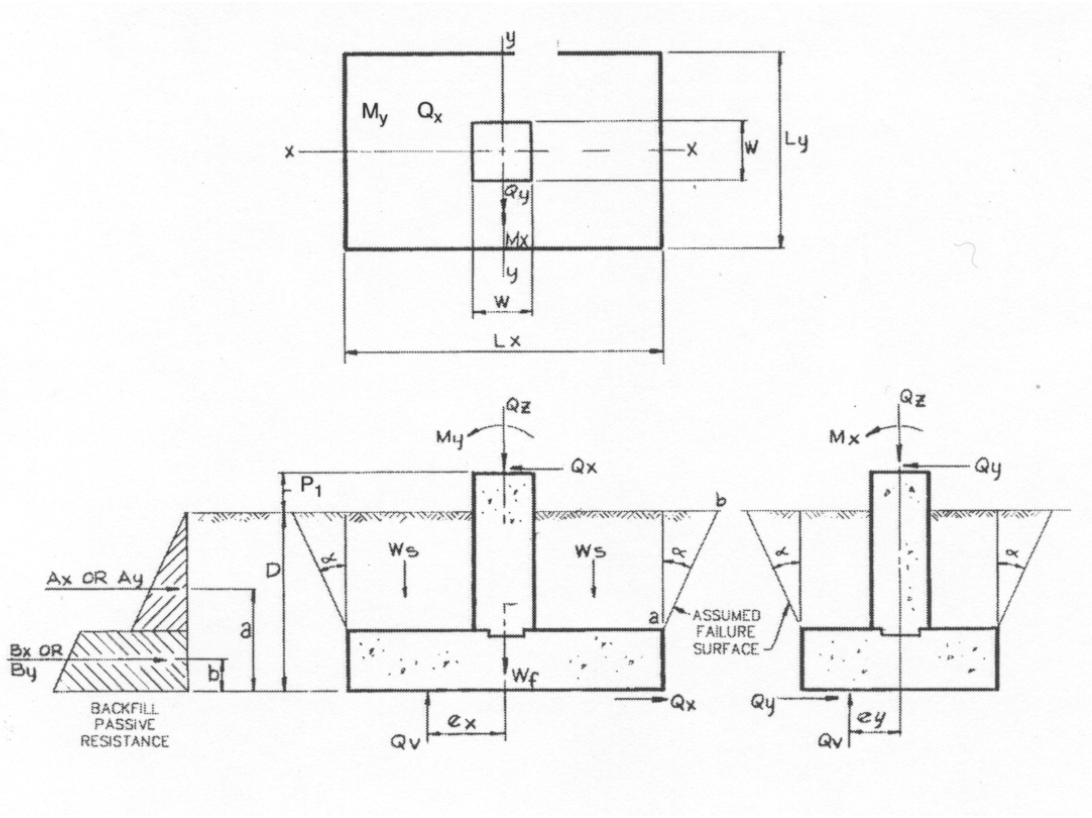

Figure 20—Foundation subjected to axial force, shear and bending moments

Copyright © 2001 IEEE. All rights reserved.

Copyright The Institute of Electrical and Electronics Engineers, Inc.
Provided by IHS under license with IEEE
No reproduction or networking permitted without license from IHS
Not for Resale

When the eccentricity is only on one axis (either the x-or y-axis), the determination of the stress distribution below the foundation mat may be assumed to vary linearly in the axis direction of the eccentricity. The maximum stress will occur at the edge of the foundation mat closest to the applied load and the minimum pressure at the opposite edge of the foundation as shown in Figure 21.

If the resultant load (Q_v) on the mat falls within the middle third of the mat, the maximum and minimum pressures for a rectangular foundation may be expressed as:

$$q_{max,\,min} = \frac{Q_v}{BL}\left(1 \pm 6\frac{e}{L}\right) \tag{33}$$

where B and L are defined in Figure 21.

If the resultant load lies outside of the middle third of the mat, the bearing pressure below a portion of the mat may reduce to zero. Consequently, the whole mat may not be effective in resisting the applied loads, and

$$q_{max} = \frac{2Q_v}{3L[B/2 - e]} \tag{34}$$

This condition may be analyzed as described by Peck, Hanson, and Thornburn [B124]. A conservative design is obtained when the resultant load is located within the middle third of the foundation mat.

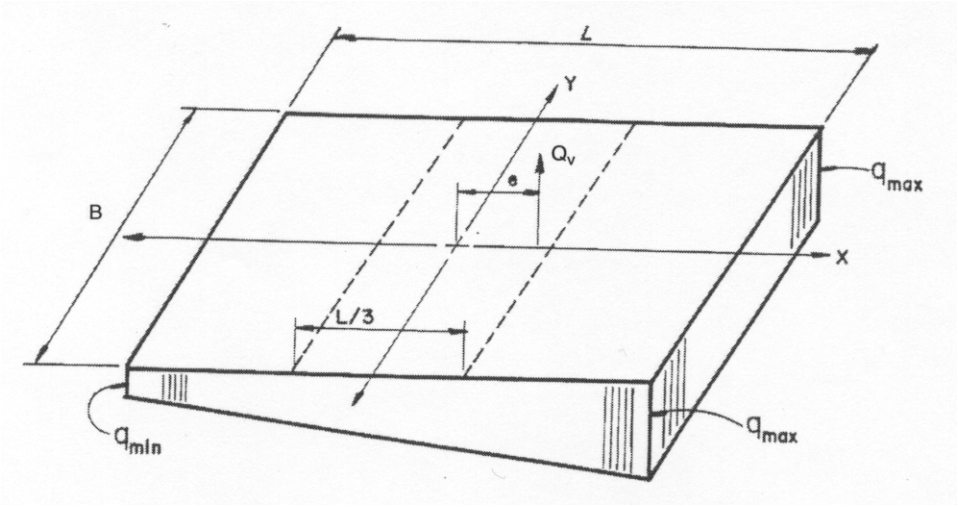

Figure 21—Stress distribution below foundation with eccentricity in one direction

When the moments and shears are on both axes, the calculation of the maximum stress q_{max} (see Figure 22) and the position of the zero stress line involves the solution of a pair of simultaneous nonlinear equations. This is best accomplished by the use of Figure 24, Figure 25, and Figure 26, as outlined in Figure 23. The accuracy obtained by this method is adequate for structural design of the foundation. The maximum stress is:

$$q_{max} = \frac{R_A Q_v}{L_x L_y} \tag{35}$$

where R_A is obtained from Figure 25 after the values of the auxiliary parameters c and d are obtained from Figure 24.

Copyright © 2001 IEEE. All rights reserved.

Copyright The Institute of Electrical and Electronics Engineers, Inc.
Provided by IHS under license with IEEE
No reproduction or networking permitted without license from IHS
Not for Resale

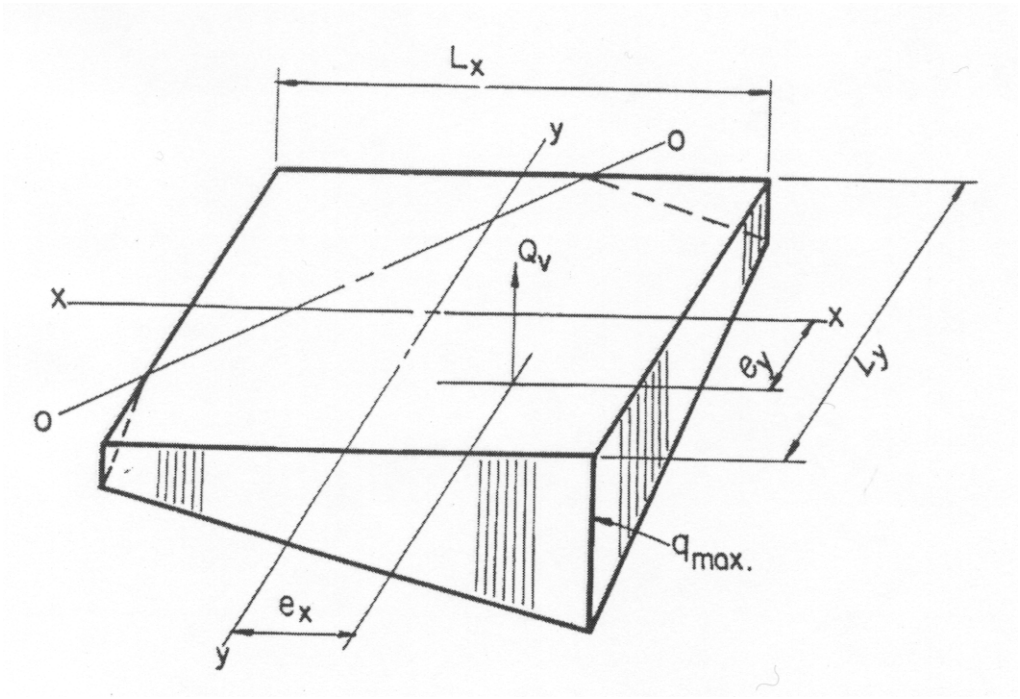

Figure 22—Stress distribution below foundation with eccentricity in two directions

The stability of a foundation with respect to bearing capacity under eccentric loads may be investigated as described in 4.2.1.1. However, the above procedures will give a more accurate approximation of the actual stress distribution below a foundation. Therefore, the stresses can be used to determine shear and moment distribution in the foundation for structural design purposes.

4.2.4 Uplift capacity

The uplift capacity of a spread foundation is often the controlling geotechnical design condition for transmission line structures. When loaded in uplift, a spread foundation can fail in distinctly different modes, which are determined primarily by the construction procedure, foundation depth, soil properties, and in-situ soil stress. The full importance of these factors has not been appreciated until recently, and will be described in the following sections.

4.2.4.1 General behavior

Spread foundations are constructed by making an excavation, placing the foundation, and then backfilling over the foundation. Figure 27 illustrates the basic construction variations possible. Figure 27, Part A is a hypothetical one in which the foundation is in place without disturbing the soil. In this case, the "backfill" and the native soil will have identical engineering properties. Figure 27, Part B through Part E illustrate real installations, with the two main variations of either vertical or inclined excavation walls, and neat or oversized excavations. In these cases, the properties of the backfill and the native soil will differ primarily as a function of the backfill compaction. For example, if the backfill is lightly compacted, the backfill will have a lower strength and state of stress than the native soil. Conversely, if the backfill is compacted very well, the backfill could have a higher strength and state of stress than the native soil.

Copyright © 2001 IEEE. All rights reserved.

Copyright The Institute of Electrical and Electronics Engineers, Inc.
Provided by IHS under license with IEEE
No reproduction or networking permitted without license from IHS
Not for Resale

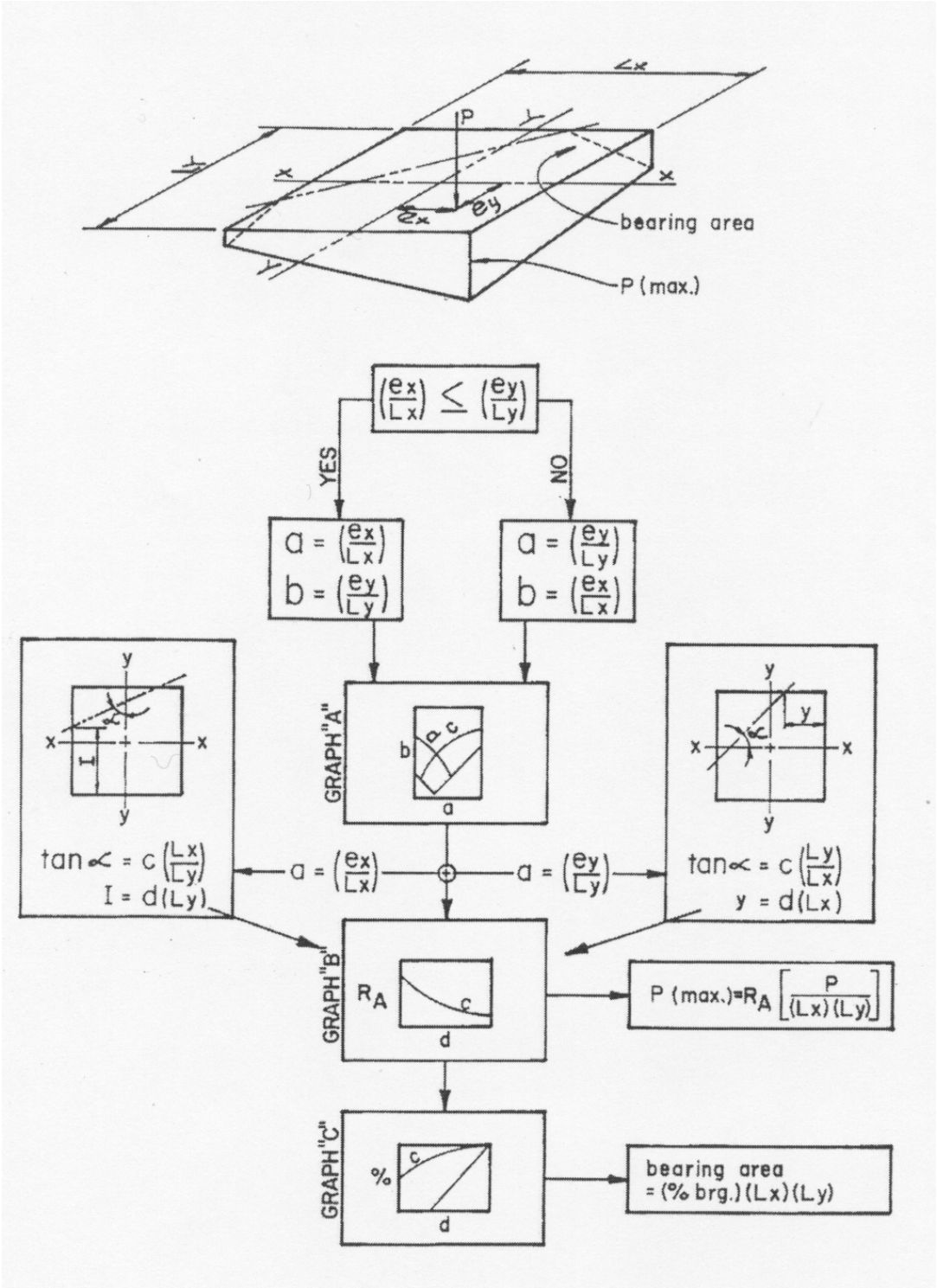

Figure 23—Key diagram for moment on footing

Copyright © 2001 IEEE. All rights reserved.

Copyright The Institute of Electrical and Electronics Engineers, Inc.
Provided by IHS under license with IEEE
No reproduction or networking permitted without license from IHS
Not for Resale

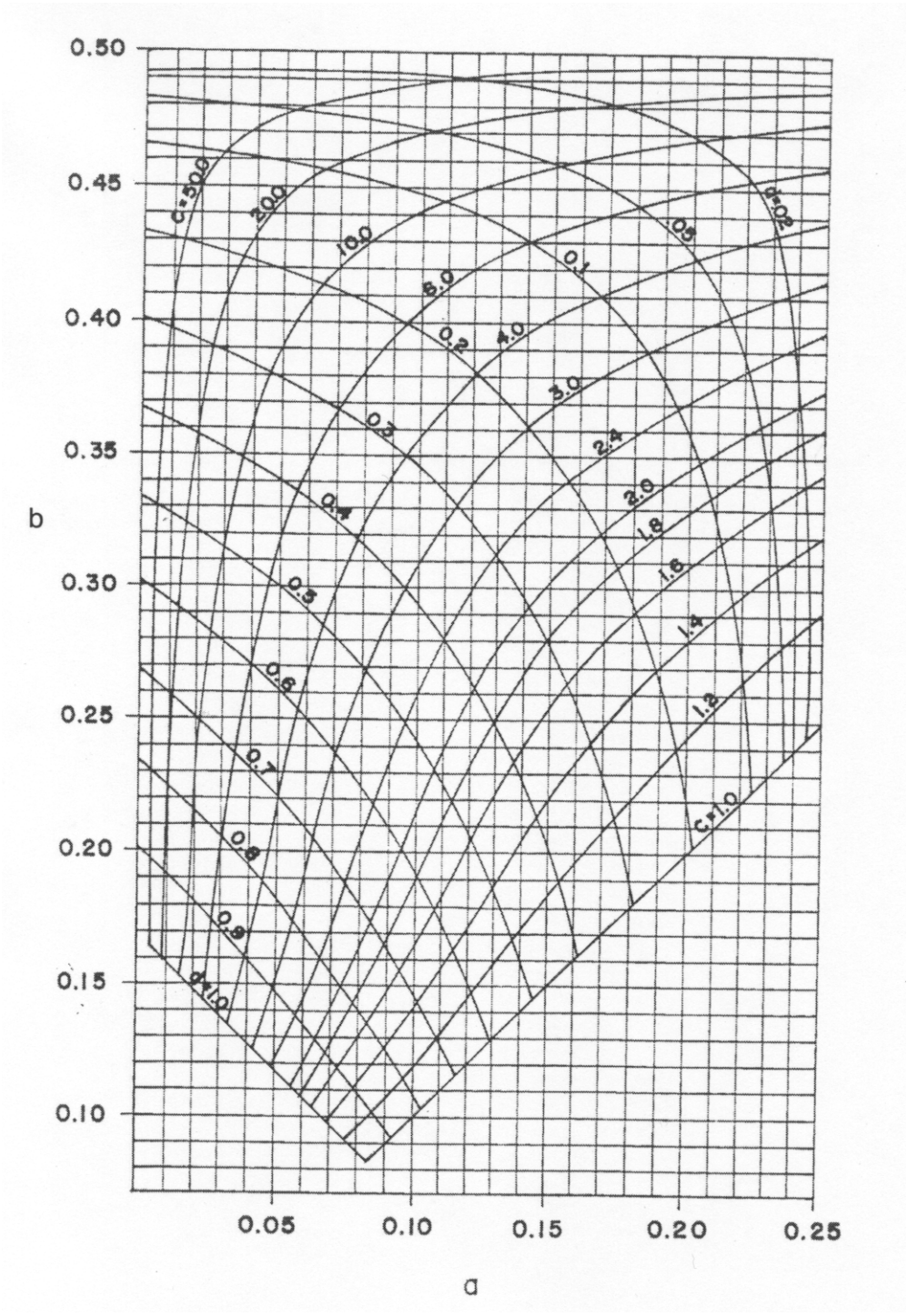

Figure 24—Graph A

Copyright © 2001 IEEE. All rights reserved.

Copyright The Institute of Electrical and Electronics Engineers, Inc.
Provided by IHS under license with IEEE
No reproduction or networking permitted without license from IHS
Not for Resale

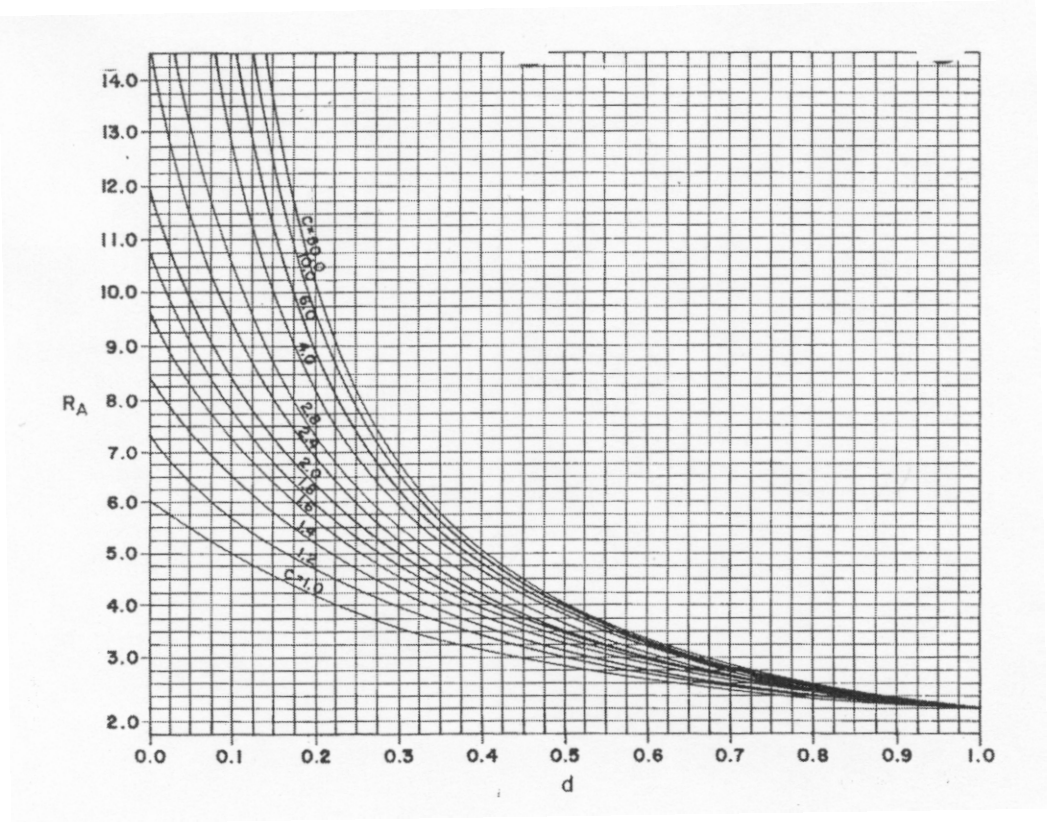

Figure 25—Graph B

A study of the full range of construction, geometry, and soil property variables has led to the generalized model shown in Figure 28 [B137]. This model has been confirmed by critical examination of over 150 full-scale uplift load tests on a variety of spread foundation types in differing soil conditions [B147].

In the majority of cases, a spread foundation in vertical uplift will fail in a vertical shear pattern which is either a cylinder or rectangle, depending on the shape of the foundation. In this mode, the side resistance will be controlled by the weaker of the backfill and native soil. When the native soil is stiff and has a high in situ stress, and the backfill is well-compacted, a variation may occur in which a cone or wedge, or a combined cylinder/rectangle and cone/wedge, failure develops. This mechanism can develop because the backfill and the backfill-native soil interface are stronger than the native soil, and therefore the failure occurs along the kinematically possible failure planes in the native soil. A second variation can occur when the backfill is relatively loose or when the foundation is relatively deep. In these cases, the native soil and the backfill-soil interface are relatively stiff compared with the backfill over the foundation. When this occurs, the vertical shear resistance is greater than the upward bearing capacity resistance of the backfill, and therefore the foundation failure will occur in bearing as a type of “punching.” Both the punching and cone/wedge variations should be evaluated in each design case to determine whether the basic vertical shear pattern is to be modified.

Copyright © 2001 IEEE. All rights reserved.

Copyright The Institute of Electrical and Electronics Engineers, Inc.
Provided by IHS under license with IEEE
No reproduction or networking permitted without license from IHS
Not for Resale

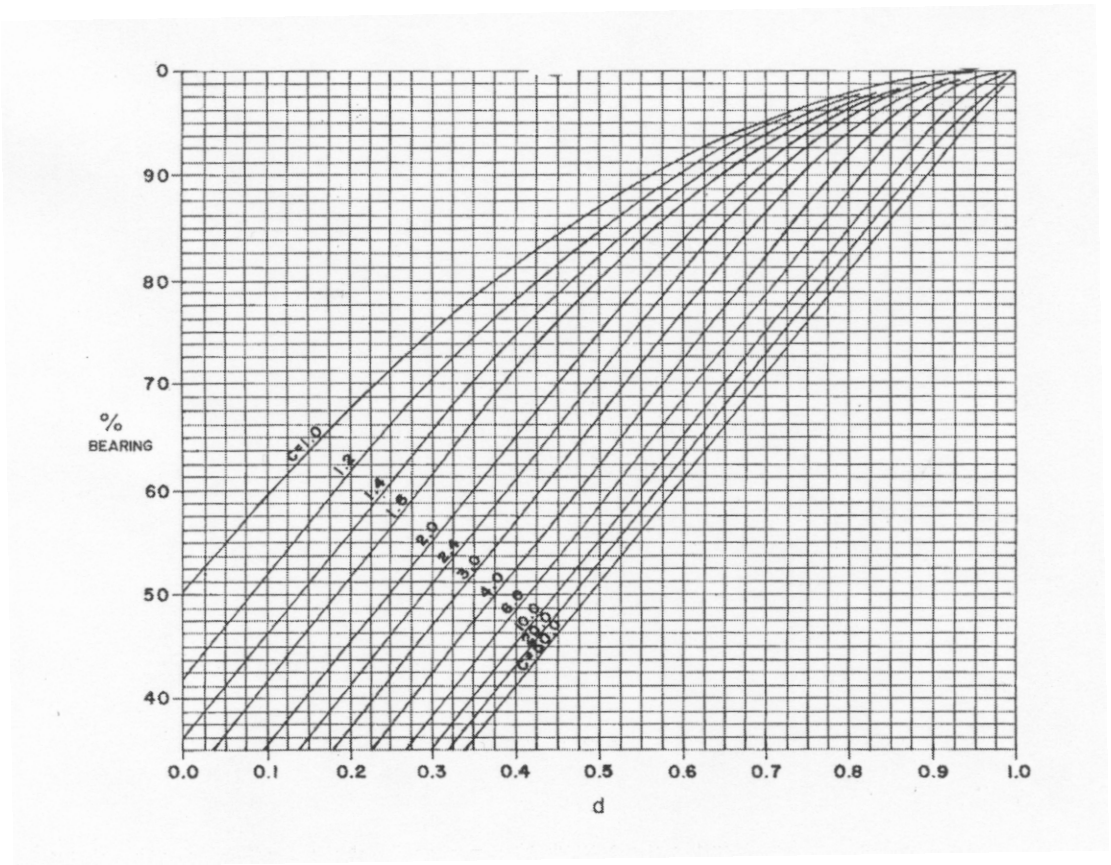

Figure 26—Graph C

4.2.4.2 Traditional design methods

The so called traditional design methods are presented in this guide in 4.3. For all practical purposes, they are either simplified, special case, or empirically-based versions of the general behavioral model described above. However, it is useful to put all of these methods in their proper context.

The traditional methods for uplift design fall into four major categories, as shown in Figure 29. The cone methods assume that the uplift resistance is given only by the weight of soil and foundation within the cone or wedge is defined in Figure 29, Part A. When the cone/wedge angle is zero, this method is a very conservative lower limit to the uplift capacity because it disregards the soil stresses and strength. Cone angles greater than zero are an ad-hoc attempt to incorporate the soil stresses and strength by substituting an equivalent weight of soil. If the equivalence can be made, the computed capacity will be identical. However, different soil characteristics and foundation geometries require different cone angles, and there is no rational basis to establish these angles in a general manner. The same is true for methods which introduce a shearing resistance along the cone/wedge surface.

The shear methods assume that failure occur along a cylindrical/ rectangular shear surface, as shown in Figure 29, part B. These basically are earlier versions of the more complete and general procedure described herein.

Copyright © 2001 IEEE. All rights reserved.

Copyright The Institute of Electrical and Electronics Engineers, Inc.
Provided by IHS under license with IEEE
No reproduction or networking permitted without license from IHS
Not for Resale

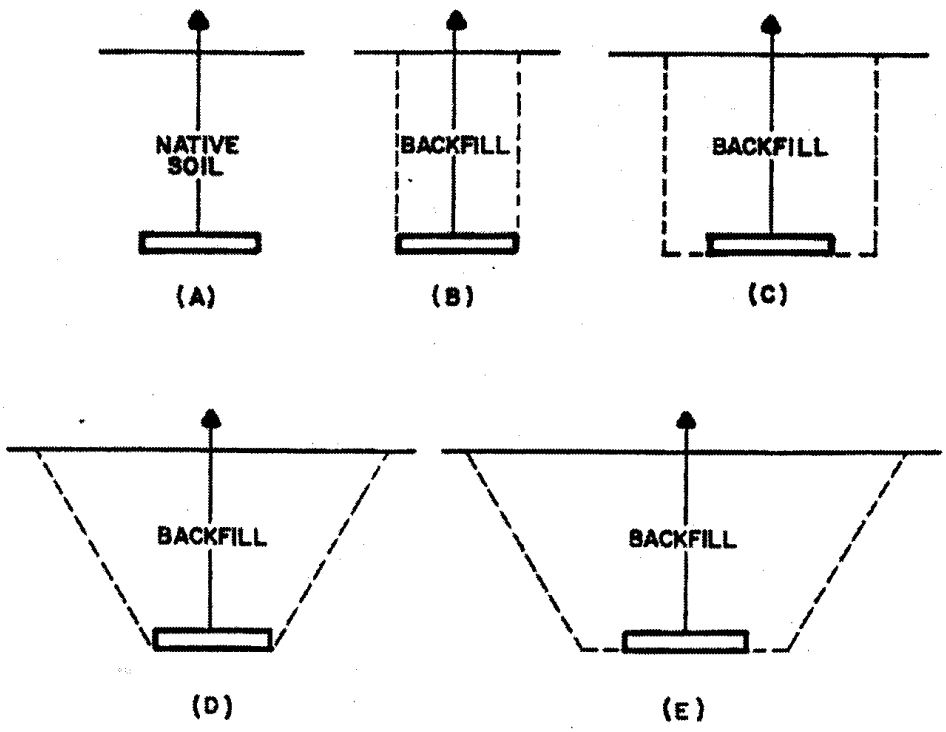

Figure 27—Construction variations with spread-type foundations

The curved surface methods assume that the uplift capacity is given by weight within the curved zone in Figure 29, part C, plus the shearing resistance along the curved surface. The assumption of a curved surface presumes that a cone of failure always occurs, and most of these methods disregard the backfill variations and soil stress. The conditions tend to be reasonable for shallow foundations with soil of medium to dense consistency and stress states corresponding to normally consolidated or lightly overconsolidated. However, these conditions generally are not applicable to deeper foundations, unless ad-hoc modifications are made. Furthermore, these methods tend to overestimate the capacity in loose, normally consolidated soils and underestimate the capacity in dense, heavily overconsolidated soils.

Methods have also been proposed, as shown in Figure 29, part D, which evaluate the uplift capacity as either a bearing capacity or cavity expansion problem. This is basically a special case of the more general behavior pattern described previously.

The points made above illustrate that the traditional methods can be applied for certain ranges of conditions, but all have major limitations in their general applicability. The design procedure described in the following does not have these inherent limitations.

4.2.4.3 Equilibrium conditions

Figure 30 shows the basic conditions for evaluating the uplift capacity of spread foundations.

Copyright © 2001 IEEE. All rights reserved.

Copyright The Institute of Electrical and Electronics Engineers, Inc.
Provided by IHS under license with IEEE
No reproduction or networking permitted without license from IHS
Not for Resale

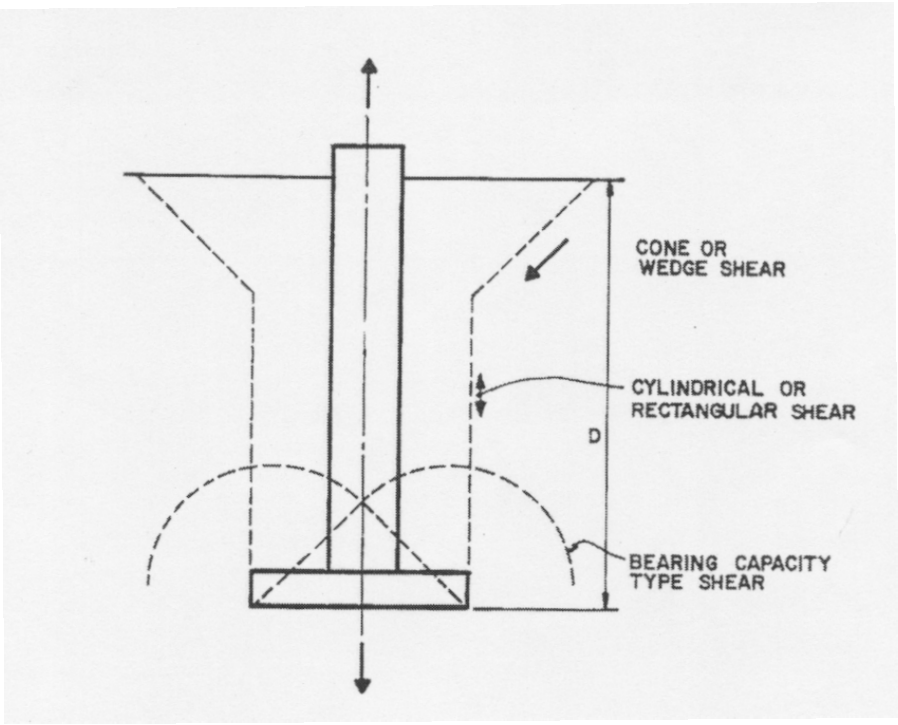

Figure 28—Idealized uplift failure of deep spread-type foundation

From this figure, it can be seen that the uplift capacity, Q_u, is given by:

$$Q_u = W + Q_{su} + Q_{tu} \tag{36}$$

where

W is weight of foundation (W_f) and soil (W_s) within the volume $B \times L \times D$,
Q_{su} is side resistance,
Q_{tu} is tip resistance.

This equation yields the uplift capacity for the cylindrical/rectangular shear mode. Once the terms in this equation have been evaluated, a check is made to determine whether Q_{su} is reduced for a wedge/cone breakout. If breakout is likely, Q_{su} is reduced in Equation (36). Then the punching capacity, Q_{um}, is computed and compared with Q_u. The smaller of Q_u and Q_{um} is then the design capacity. Details of the computations are given separately for both drained and undrained loading, building upon the notation used in 4.2.1.

Copyright © 2001 IEEE. All rights reserved.

Copyright The Institute of Electrical and Electronics Engineers, Inc.
Provided by IHS under license with IEEE
No reproduction or networking permitted without license from IHS
Not for Resale

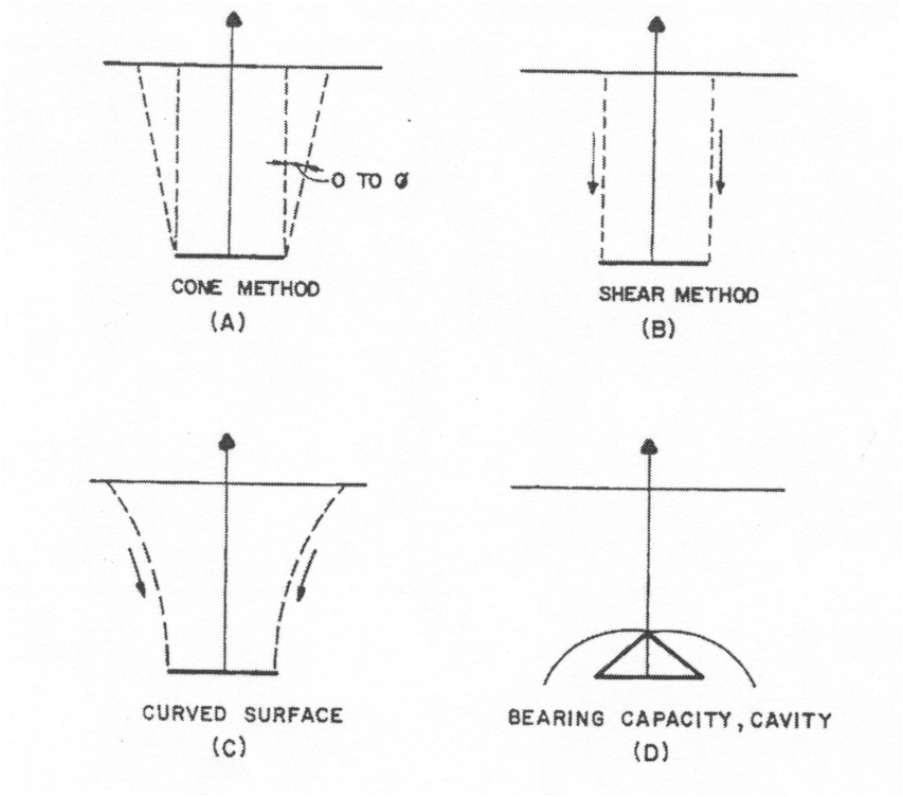

Figure 29—Common uplift capacity models

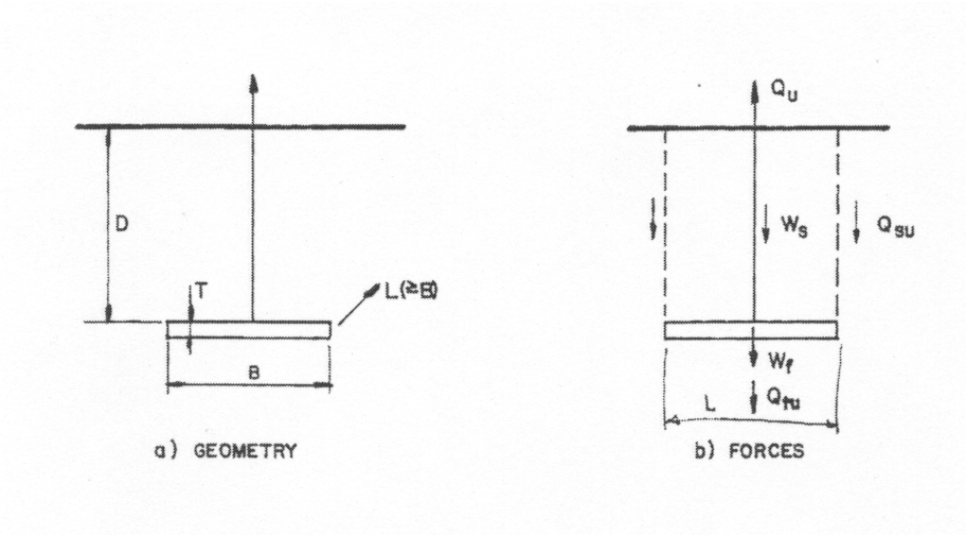

Figure 30—General description for uplift capacity

Copyright © 2001 IEEE. All rights reserved.

Copyright The Institute of Electrical and Electronics Engineers, Inc.
Provided by IHS under license with IEEE
No reproduction or networking permitted without license from IHS
Not for Resale

4.2.4.4 Uplift capacity for drained loading

Drained loading occurs under most loading conditions in coarse-grained soils such as sands and for long-term sustained loading of fine-grained soils such as clays. As described in 4.2.1.2, the soil strength normally will be characterized by c = 0 and a nonlinear ϕ with stress level. Equation (36) is used to evaluate the uplift capacity for the cylindrical/rectangular shear mode, as described below.

The weight term, W, is the effective weight for drained loading, which is the total weight above the water table and the buoyant weight below the water table. Based on Figure 30, W_f is the effective foundation weight and W_s is the effective soil weight, given by:

$$W_s = \bar{\gamma}[B \times L \times (D - t)] \tag{37}$$

$\bar{\gamma}$ is effective soil unit weight.

The tip resistance, Q_{tu}, can develop from bonding of the foundation tip (or base) to the soil or rock below and is given by:

$$Q_{tu} = A_{tip} s_t \tag{38}$$

where

A_{tip} is area of foundation tip ($B \times L$ or $\pi B^2/4$),
s_t is tensile strength of soil bonded to foundation.

The tip resistance is commonly assumed to be zero because of the low tensile strength of soil and soil disturbance during construction. However, for a cast-in-place foundations on sound rock or very stiff soil, with good construction control minimizing soil disturbance, the term may be significant.

The side resistance, Q_{su}, is given as follows:

$$Q_{su} = \int_{\text{surface}} \tau(z)dz \tag{39}$$

where

$\tau(z)$ is unit shearing resistance with depth, z, along the shear surface.

For a rectangular foundation, the side resistance is given as:

$$Q_{su} = 2(B + L)\int_o^D \overline{\sigma_v(z)}\beta(z)dz$$

$$= 2(B + L)\int_o^D \overline{\sigma_v(z)}K(z)\tan\delta(z)dz \tag{40}$$

where

$\overline{\sigma_v(z)}$ is vertical effective stress with depth,
$K(z)$ is operative horizontal stress coefficient with depth,
$\delta(z)$ is interface friction angle with depth,
β is $K\tan\delta$.

Copyright © 2001 IEEE. All rights reserved.

Copyright The Institute of Electrical and Electronics Engineers, Inc.
Provided by IHS under license with IEEE
No reproduction or networking permitted without license from IHS
Not for Resale

In summation form, Equation (40) is expressed as:

$$Q_{su} = 2(B + L) \sum_{n=1}^{N} \bar{\sigma}_{v_n} K_n \tan\delta_n d_n \tag{41}$$

for N layers of thickness d, with $\bar{\sigma}_v$, K, and δ evaluated at mid-depth of each layer.

For a backfilled spread foundation, $\tau = \bar{\sigma}_v K \tan\delta$ must be evaluated separately for the backfill and for the native soil. The lower value will control the behavior and be the one for design. The $\bar{\sigma}_v$ term is evaluated simply as follows:

$$\bar{\sigma}_v = \bar{\gamma} D \tag{42}$$

where

$\bar{\gamma}$ is effective unit weight of backfill or native soil.

The δ term is related to the soil friction angle as follows [B137]:

$$\delta = \bar{\phi}(\delta/\bar{\phi}) \tag{43}$$

in which

$\bar{\phi}$ is effective stress soil friction angle,
$\delta/\bar{\phi}$ is modifier for interface characteristics.

For a backfilled foundation with a soil-soil interface, $\delta/\bar{\phi} = 1$ and, therefore, $\delta = \bar{\phi}$.

The K term is given below [B137] [B147]:

$$K = K_o(K/K_o) \tag{44}$$

where

K_o is in situ coefficient of horizontal soil stress (ratio of horizontal to vertical stress),
K/K_o is modifier to account for construction procedures.

Table 5 provides tentative guidelines for evaluating K. Analysis of existing load test data [B147] shows K values as high as 2.9 with most values between 0.5 and 1.9. Incomplete documentation for the load test data preclude a more precise assessment of K at this time.

The in situ K_o is a necessary term to evaluate the uplift capacity correctly. This term can be evaluated from direct measurements in the field using the pressuremeter, dilatometer, or other in situ techniques, or can be estimated from reconstruction of the geologic stress history [B147] [B137]. Assuming the soil to be normally consolidated, with $K_o = 1 - \sin\phi$, will almost always be a very conservative lower bound because nearly all soil deposits are overconsolidated to some degree.

Copyright © 2001 IEEE. All rights reserved.

Copyright The Institute of Electrical and Electronics Engineers, Inc.
Provided by IHS under license with IEEE
No reproduction or networking permitted without license from IHS Not for Resale

Table 5—Horizontal soil stress coefficients, K, for drained loading

Soil and backfill condition	K	Notes	Approximate % Standard ASTM D698 Compaction of Backfill
Native soil with loose backfill	K_a	a	87-92
Native soil with moderately compacted backfill	1/2 to 1 (K_o in-situ) (min. K = K_a)		92–97
Native soil with well compacted backfill	≥ 1 (K_o in-situ)	b, c	97-102
Backfill, lightly compacted	1 - sin $\bar{\phi}$		87-92
Backfill, moderately compacted	2/3 to 1		92-97
Backfill, well compacted	≥1		97-102
Backfill, very well compacted	>> 1	c, d	> 102

a) $K_a = \tan^2(45 - \bar{\phi}/2)$
b) Use 1 for practical limit at this time
c) Requires very careful construction supervision
d) Use 2 for practical limit at this time

4.2.4.4.1 Modification for cone/wedge breakout

If the average β over the foundation depth is greater than 1 and D/B is less than 6, a cone/wedge breakout is possible. For this combination of parameters, the value of Q_{su} is reduced as follows:

$$Q_{su}(\text{reduced}) = \frac{2+\beta}{3\beta} Q_{su}(\text{computed}) \tag{45}$$

where

β is K tan δ.

This reduced Q_{su} is used in Equation (36) for computing the uplift capacity.

4.2.4.4.2 Upper bound for punching capacity for drained loading

It is always warranted to check whether punching may control the uplift capacity of the foundation. The punching capacity, Q_{um}, is computed as follows:

$$Q_{um} = A_{tip}(qN_q\zeta_{qr}\zeta_{qs}\zeta_{qd}) + \overline{W}_f + Q_{tu} \tag{46}$$

in which all terms have been defined previously in either 4.2.1 or 4.2.2. However, three small differences occur. First, the q term is equal to $\bar{\sigma}_v$ the backfill at B/2 above the foundation (i.e., at D–t–B/2). Second, all strength and deformation parameters are evaluated for this q value. Third, to calculate ζ_{qd} use (D–t)/B rather then D/B. All other terms are as given previously.

If Q_{um} is less than Q_u from Equation (36), then Q_{um} is the design uplift capacity.

Copyright © 2001 IEEE. All rights reserved.

Copyright The Institute of Electrical and Electronics Engineers, Inc.
Provided by IHS under license with IEEE
No reproduction or networking permitted without license from IHS
Not for Resale

4.2.4.5 Example of uplift capacity in drained loading

To illustrate this design method, an example has been prepared. Considering the geometry in Figure 30, assume a steel stub and plate with B = L = 1.07 m (3.3'), D = 2.6 m (8.5'), and t = 0.3 m (1') .

Assume a granular soil, water table at the foundation tip, ϕ = constant at 30° and $\bar{\gamma}_s = \bar{\gamma}_f = 15.7\ \text{kN/m}^3$ (100 pcf) . For this example, W = 46.3 kN (10.4 kips), $Q_{tu} = 0$, Q_{su} will vary as a function of K_o and backfill compaction, no wedge breakout would occur, and Q_{um} for the worst case (normally consolidated) would be 791.7 kN (178 kips). The results of this analysis are given in Figure 31 for several in situ K_o values ranging from normally consolidated to heavily overconsolidated backfill.

This example shows several important points. First, the total uplift capacity can vary dramatically as a function of backfill compaction. Second, it is more important to compact the backfill well when the native soil is very stiff with a high K_o. Third, when the native soil is normally consolidated or close to it, special compaction efforts are not warranted. And fourth, if one assumes conservative design parameters, such as normally consolidated in situ native soil and lightly compacted backfill, the design is going to be very conservative.

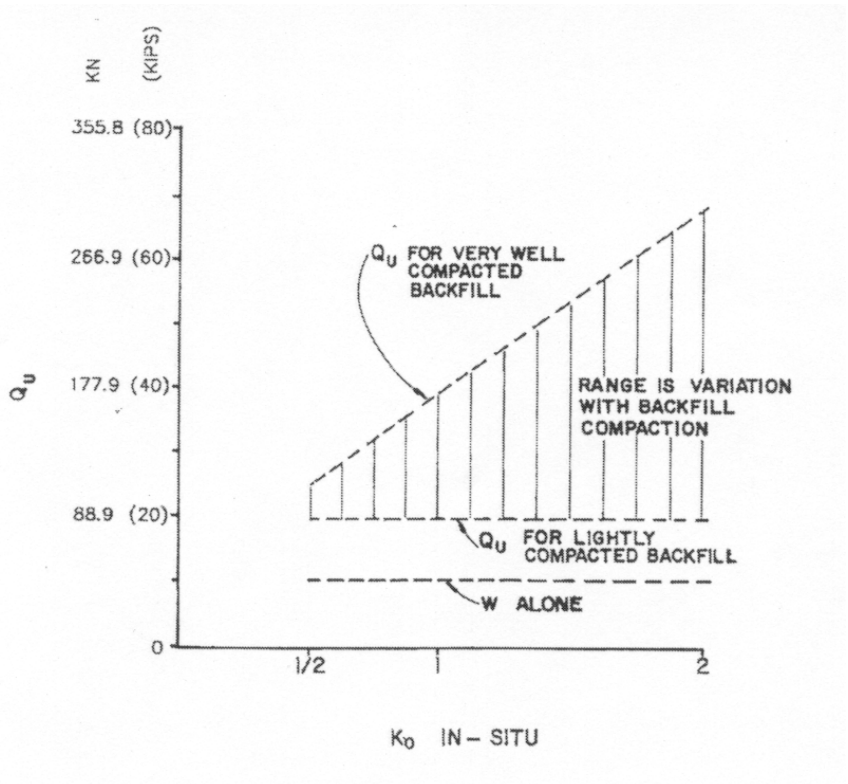

Figure 31—Drained uplift capacity for example problem

4.2.4.6 Uplift capacity for undrained loading

Undrained loading occurs when loads are applied relatively rapidly to fine-grained soils such as clays. As described in 4.2.1, the soil strength normally will be characterized by s_u, the undrained shear strength, with $\phi = 0$ or by the effective stress friction angle, $\bar{\phi}$, taking into account the pore water pressures developed during undrained loading. Equation (36) is used to evaluate the uplift capacity for the cylindrical/rectangular shear mode, as described below.

Copyright © 2001 IEEE. All rights reserved.

Copyright The Institute of Electrical and Electronics Engineers, Inc.
Provided by IHS under license with IEEE
No reproduction or networking permitted without license from IHS
Not for Resale

The weight term, W, is the total weight for undrained loading. Based on Figure 30, W_f is the total foundation weight and W_s is the total soil weight given by:

$$W_s = \gamma[B \times L \times (D - t)] \tag{47}$$

where

γ is total soil unit weight.

The tip resistance, Q_{tu}, can develop from bonding of the foundation tip (or base), as given in 4.2.4.4, or can develop from suction in the saturated fine-grained soil during undrained loading. The tip resistance from suction is given by:

$$Q_{tu} = A_{tip} S_s \tag{48}$$

where

S_s is suction stress at tip. Stas and Kulhawy [B147] have approximated S_s as follows:

$$S_s \approx \frac{W}{A_{tip}} - u_i (\leq 1 \text{ atmosphere}) \tag{49}$$

where

u_i is initial pore water pressure at the tip.

It should be noted that the suction stress decreases with time, in an analogous manner to the consolidation process.

The side resistance, Q_{su}, can be evaluated by an effective stress approach using the same equations and parameters given in 4.2.4.4, except for the K term. Table 6 provides tentative guidelines for evaluating K. Analysis of existing load test data shows K values from 0 to over 3 with no particular concentration of values. Because of this large variation, and the lack of complete documentation for the load test data, the conservative approach outlined above is warranted at this time. As in 4.2.4.4, an estimate of the in situ K_o is necessary.

The side resistance also can be computed by the total stress α method, as described in Clause 5. However, this method was developed for deep foundations, and its use for spread foundations is very poorly documented, at best. Major questions exist as to its reliability, primarily because α really has not been evaluated for compacted backfill.

4.2.4.6.1 Modification for cone/wedge breakout

If the average $\alpha s_u / \bar{\gamma} D$ over the foundation depth is greater than 1 and D/B is less than 6, a cone/wedge breakout is possible. Although no definitive procedure has been developed to address this reduction, a reasonable approximation for this reduction is as follows [B147]:

$$Q_{su}(\text{reduced}) = \frac{(2 + \alpha s_u / \bar{\gamma} D)}{3(\alpha S_u / \bar{\gamma} D)} Q_{su}(\text{computed}) \tag{50}$$

This reduced Q_{su} is used in Equation (36) for computing the uplift capacity.

Copyright © 2001 IEEE. All rights reserved.

Copyright The Institute of Electrical and Electronics Engineers, Inc.
Provided by IHS under license with IEEE
No reproduction or networking permitted without license from IHS
Not for Resale

Table 6—Horizontal soil stress coefficient, k, for undrained loading

Soil and Backfill Condition	K	Notes	Approximate % Standard ASTM D698 Compaction of Backfill
Native soil with lightly compacted backfill	K_a	a	87–92
Native soil with moderately compacted backfill	1/2 to 1 (K_o in-situ) (min. K = K_a)		92–97
Native soil with well compacted backfill	≥1 (K_o in-situ)	b,c	97–102
Backfill, lightly compacted	0 to K_a	a	87–92
Backfill, moderately compacted	K_a to $(1 - \sin\bar{\phi})$	a	92–97
Backfill, well compacted	$(1 - \sin\bar{\phi})$ to 1		97–102
Backfill, very well compacted	≥1	c, d	> 102

a) $K_a = \tan^2(45 - \bar{\phi}/2)$
b) Use 1 for practical limit at this time
c) Requires very careful construction supervision
d) Use 2 for practical limit at this time

4.2.4.6.2 Upper bound for punching capacity for undrained loading

It is always warranted to check whether punching may control the uplift capacity of the foundation. The punching capacity, Q_{um} is computed as follows:

$$Q_{um} = A_{tip}(5.14\ s_u\zeta_{cr}\zeta_{cs}\zeta_{cd} + q) + W_f + Q_{tu} \quad (51)$$

in which all terms have been defined in either 4.2.1 or 4.2.4. However, four small differences occur. First, s_u is the mean value in the backfill at B/2 above the foundation (i.e., at D–t–B/2). Second, q is equal to σ_v in the backfill, also at B/2 above the foundation. Third, all strength and deformation parameters are evaluated for this new q value. Fourth, to calculate ζ_{cd} use (D–t)/B rather than D/B. All other terms are as given previously.

If Q_{um} is less than Q_u from Equation (36), then Q_{um} is the design uplift capacity.

4.2.4.7 Example for uplift capacity in undrained loading

To illustrate this design method, an example has been prepared. Considering the geometry in Figure 30, assume a steel stub and plate with B = L = 1.07 m (3.5 ft), D = 2.6m (8.5 ft), and t = 0.3 m (1 ft). Assume a cohesive soil, water table at the foundation tip, s_u = constant at 24.4 kN/m^2 (500 psf), $\gamma_s = \gamma_f$ = 15.7 kN/m^3 (100 pcf). [With these parameters at D/2, $\bar{\sigma}_v$ = 33.04KN/m^2 (690 psf), K_o= 2.45, and $\bar{\phi}$ = 24.8°.] For this example, W = 46.3 kN (10.4 kips), Q_{tu} = 46.3 kN (10.4 kips), Q_{su} varies as a function of backfill compac-

Copyright © 2001 IEEE. All rights reserved.

Copyright The Institute of Electrical and Electronics Engineers, Inc.
Provided by IHS under license with IEEE
No reproduction or networking permitted without license from IHS Not for Resale

tion, no wedge breakout would occur, and Q_{um} = 182.4kN (41 kips) (assuming conservative parameters). The results of this analysis are presented in Figure 32 as a function of backfill compaction, since the given value of s_u established the soil as moderately overconsolidated.

This example shows several important points. First the total uplift capacity can vary dramatically as a function of backfill compaction. Second, punching can limit the capacity by a significant amount. Third, if one assumes conservative design parameters, such as lightly compacted backfill and neglecting suction, the design is going to be very conservative. And fourth, the α method gives an unrealistically high value for these parameters, and it does not depend on the degree of backfill compaction.

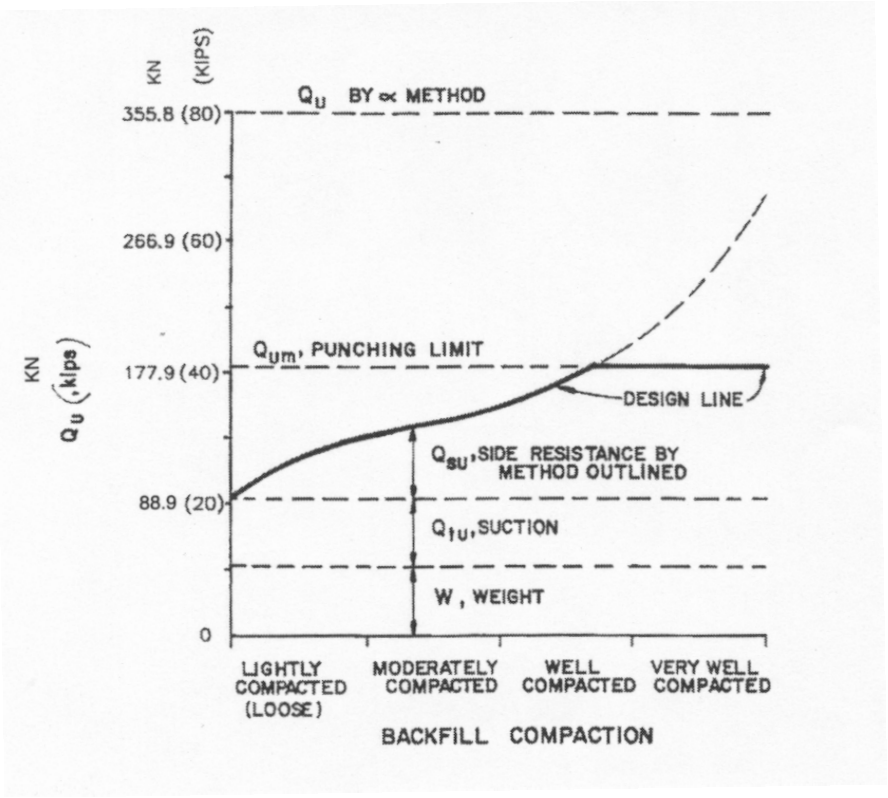

Figure 32—Undrained uplift capacity for example problem

4.2.5 Uplift load-displacement behavior

Based on the results of seventy-five full scale uplift tests on grillages and mats plus eight tests at Hickling and WynCoop Creek, Trautmann and Kulhawy [B158] have analyzed and derived an empirical design procedure for estimating displacements.

The effects of soils (granular or cohesive) and foundation type (grillage, steel plate or concrete slab) had a relatively small effect that can be safely ignored.

4.2.5.1 Hyperbolic equation

Based on the conservative upper limit that will be exceeded with less than 5% probability, the test load-displacement data were fitted with a hyperbolic equation of the form:

Copyright © 2001 IEEE. All rights reserved.

Copyright The Institute of Electrical and Electronics Engineers, Inc.
Provided by IHS under license with IEEE
No reproduction or networking permitted without license from IHS
Not for Resale

$$Y = \frac{X}{a + bX} \tag{52}$$

where

Y is normalized load, Q/Q_u,
X is dimensionless displacement, z/D.

Setting Y equal to 0.5 and 1, Equation (52) can be solved to yield solutions for a and b: where z = upward displacement, D = depth to foundation base, a and b = parameters in hyperbolic equation.

$$a = \frac{X_1 X_2}{(X_2 - X_1)} \tag{53}$$

$$b = \frac{X_2 - 2X_1}{(X_2 - X_1)} \tag{54}$$

where

X_1 is dimensionless displacement at 50% of the failure load, and
X_2 is dimensionless displacement at the failure load.

Substituting values of 0.01 and 0.06 for X_1 and X_2, respectively, into Equations (53) and (54) yields the following general load-displacement relationship:

$$(Q/Q_u) = \frac{(z/D)}{.012 + 0.8(z/D)} \tag{55}$$

or, solving for z/D:

$$z/D = \frac{0.012(Q/Q_u)}{1 - 0.8(Q/Q_u)} \tag{56}$$

4.2.5.2 Design curve for uplift-resisting spread foundations

Figure 33 is a plot of Equation (55) with a limiting load equal to Q_u. This curve represents a 95% upper confidence limit for foundations subjected to uplift loads.

Other factors being equal, a dense sand or stiff clay will exhibit a stiffer load-displacement response than a loose sand or a soft clay. Nearly all of the available data represent tests in which the backfill was compacted to some degree. The data are insufficient, however, to distinguish the effects of compaction quantitatively and to develop corrections for lightly compacted soils. For this reason, the curve in Figure 33 may be unconservative for lightly compacted backfills. Conversely, Figure 33 may be conservative for extremely well-compacted backfills.

Figure 34 shows the recommended load-displacement relationship in comparison to data from randomly selected field load tests and is close to the 50% confidence limit (mean).

Copyright © 2001 IEEE. All rights reserved.
--`,,`-`-`,,`,,`,`,,`---
Copyright The Institute of Electrical and Electronics Engineers, Inc.
Provided by IHS under license with IEEE
No reproduction or networking permitted without license from IHS
Not for Resale

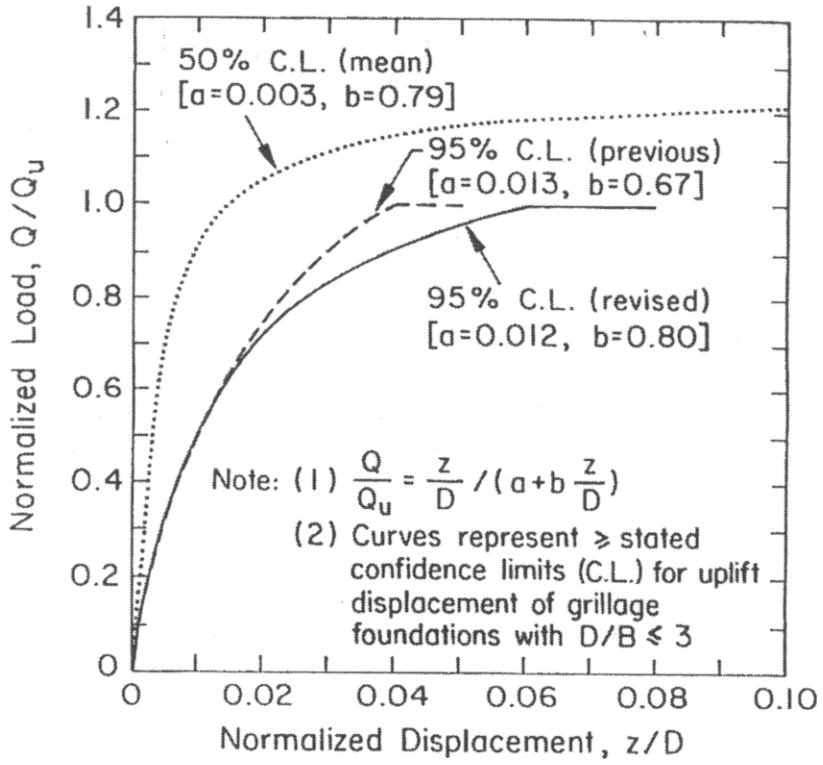

Figure 33—Recommended load displacement relationship

4.2.5.3 Example calculation

Trautmann and Kulhawy [B158] have the following example in which the design of a square grillage foundation for a drained uplift load of 191.3 kN (43 kips) in medium sand is shown. The soil has a total density of 16 kN/m^3 (102 pcf), an angle of shearing resistance of 35°, and the backfill is well-compacted, excavated soil. The horizontal stress coefficient at failure is 1.0. The grillage is 2 m by 2 m (6.56 ft by 6.56 ft) and is buried 2 m (6.56 ft). Partial safety factors of 1.2 and 2 are used for the weight and side resistance terms. The structure is able to tolerate a total foundation displacement of 38 mm (1.5 in), and the groundwater table is below the base of the foundation.

First, the foundation is checked for capacity. The capacity in granular soil is computed by the relation:

$$Q_u = \gamma B^2 D + 2\gamma D^2 B K \tan\phi \quad (57)$$

where

γ is soil density,
B is foundation width,
D is depth to the foundation base,
K is coefficient of horizontal soil stress at failure,
ϕ is angle of shearing resistance.

Copyright © 2001 IEEE. All rights reserved.

Copyright The Institute of Electrical and Electronics Engineers, Inc.
Provided by IHS under license with IEEE
No reproduction or networking permitted without license from IHS
Not for Resale

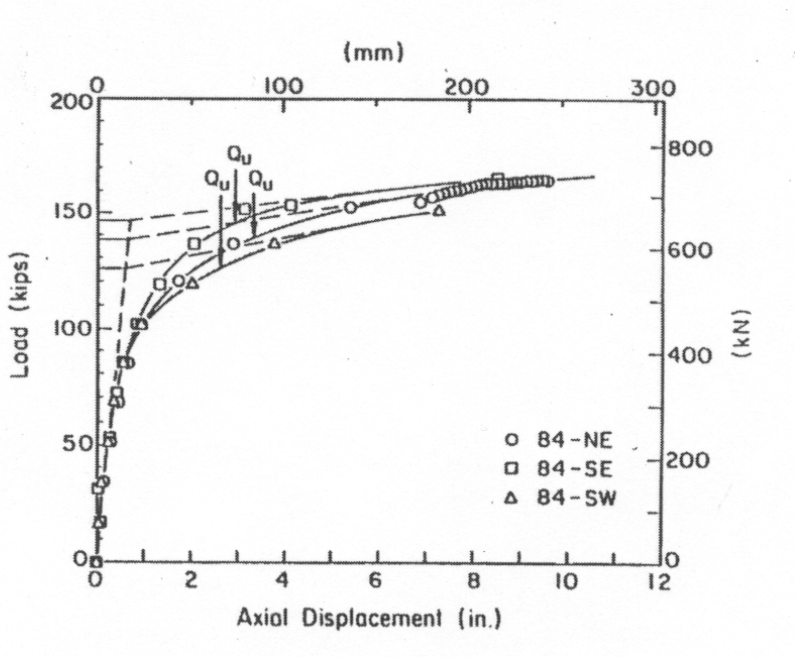

Figure 34—Interpreted failure loads for Hickling Station No. 84 Grillages

The first term represents the weight of the uplifted foundation and backfill, and the second term represents the shearing resistance along the surface extending upward from the perimeter of the foundation. Substituting the given values into the above equation, $Q_u = (16)(2)^2(2) + (2)\ (16)\ (2)^2(2)(1)(\tan 35°) = 128 + 179 = 307$ kN (69 kips). Dividing by the partial safety factors, the allowable load is therefore $Q_a = 128/1.2 + 179/2 = 196$ kN (44.1 kips), and the design satisfies the uplift load criterion.

Next, a check is made for displacements. Entering Figure 33 with $Q/Q_u = 190/(128 + 179) = 0.62$, the normalized displacement for granular soils is found to be approximately 0.014, leading to a displacement at the design load of z = (0.014)(2 m)(1000 mm/m) = 28 mm, (1.1 in) which is less than the limit given for the structure.

4.3 Traditional design methods

The traditional methods that are herein discussed can and still do serve various users well in their range of conditions. The methods are based on experience, tests, and the user's knowledge of their specific conditions.

4.3.1 Earth cone method

The earth cone method is an entirely empirical method which assumes that the failure surface is a truncated pyramid or cone for square and circular foundations, respectively (see Figure 35, part A). The cone or pyramid extends upward from the lower edge of the mat toward the ground surface at an angle ψ. The magnitude of the angle used is determined primarily by soil type. In backfill, values for ψ should be selected by the foundation engineer in accordance with experience, field tests for the specific foundation type and site location, and the degree of predicted compaction. Field tests may also be used to determine the most appropriate value of ψ for use in design of foundations to resist uplift loads.

Copyright © 2001 IEEE. All rights reserved.

Copyright The Institute of Electrical and Electronics Engineers, Inc.
Provided by IHS under license with IEEE
No reproduction or networking permitted without license from IHS
Not for Resale

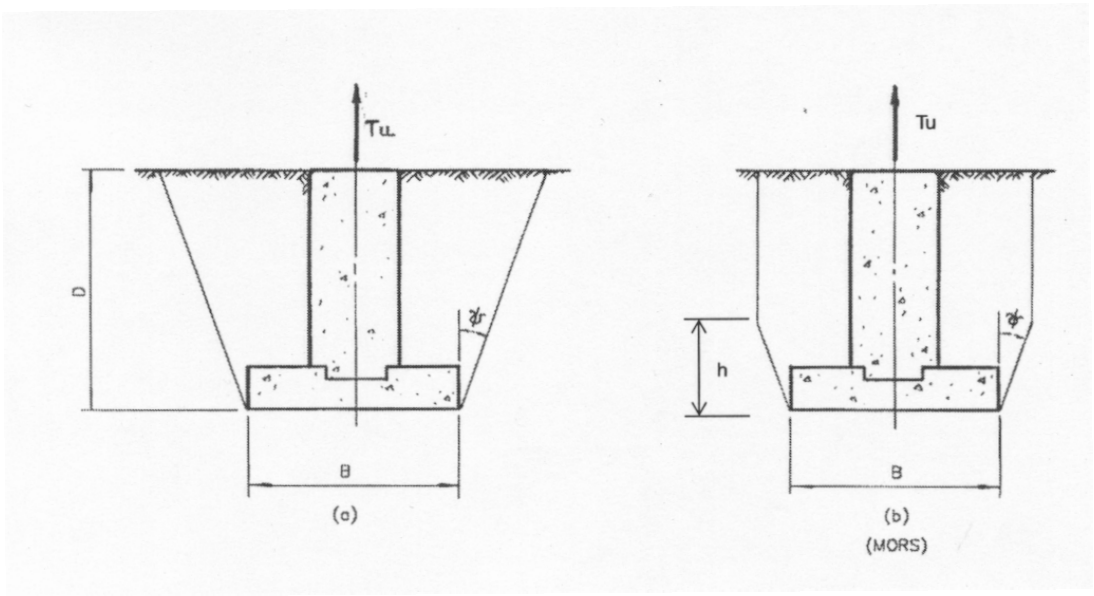

Figure 35—Earth cone method

The ultimate uplift capacity (T_u) is assumed to be derived from the weight of the foundation and the weight of the soil inside the cone or pyramid:

$$T_u = W_f + W_s \tag{58}$$

where

W_f is the weight of the foundation,
W_s is the weight of the soil mass inside the rupture surface.

For that portion of the failure cone or pyramid below the groundwater table, the submerged weight of the foundation and soil should be used to determine the uplift capacity.

It should be noted that the earth cone method ignores any uplift resistance provided by mobilization of shear strength along the failure surface. Consequently, for shallow foundations, the earth cone method is generally acknowledged to underestimate the uplift capacity. However, for deeper embedment, the computed uplift resistance increases rapidly with depth while the results of model and field tests show only 1/4 to 1/7 the increase expected from computed values. This difference between observed and computed values suggests that the method does not accurately model the influence of embedment depth on uplift capacity. Therefore, it would be best to determine ψ by in situ tests.

A variation of the earth cone method was proposed by Mors [B116] as a result of field tests conducted on foundations of various sizes and depths of embedment. A rupture surface of the form shown in Figure 35, part B was assumed by Mors [B116]. The ultimate uplift capacity of a square foundation may then be computed as:

$$T_u = W_f + \gamma(V_1 - V_o) + \frac{1}{6}\gamma D^2 \tan\psi(9B + 2D\tan\psi) \tag{59}$$

Copyright © 2001 IEEE. All rights reserved.

Copyright The Institute of Electrical and Electronics Engineers, Inc.
Provided by IHS under license with IEEE
No reproduction or networking permitted without license from IHS
Not for Resale

where

V_o is the volume of foundation below the ground surface,
V_1 is the area of the base times the depth D,
B is the foundation width,
γ is the unit weight of the soil,
ψ is as defined previously.

If the soil is saturated (i.e., groundwater table at the ground surface), the submerged unit weight should be used to consider the buoyancy effect of the groundwater.

Mors [B116] does not discuss the influence of foundation shape on the uplift capacity; nor is the quantity h in Figure 35, Part B clearly defined to permit ease in developing an expression similar to Equation (54) for circular foundations.

4.3.1.1 Bonneville cone method

One utility's use of the Cone Method is based on tests that indicate a 1-inch deflection for their calculated loads and not the ultimate pullout capacity. Their assumptions are

— 30° Cone
— Soil @ 14.1 kn/m^3 (90 pcf)
— Max depth = 4.6 m (15 ft)
— Uplift pressure on net grillage area = 359.1 kN/m^2 (7.5 ksf)

4.3.2 Shearing or friction method

The shearing or friction method is an empirical method based on the assumption that the rupture surface extends vertically upward from the mat of the foundation as shown in Figure 36. The ultimate uplift capacity results from friction along the failure surface, the weight of the foundation, and the weight of soil above the base of the foundation:

$$T_u = W_f + W_s + F \tag{60}$$

where

W_f and W_s are as defined for the earth cone method and F is the frictional component of uplift resistance.

If cohesion is denoted by c, the angle of intemal friction by ϕ, and the coefficient of lateral earth pressure by K, the frictional resistance for a square foundation may be expressed as:

$$F = 4cBD + 2K\gamma BD^2 \tan\phi \tag{61}$$

where B and D are defined in Figure 36 and γ is the unit weight of the soil (use the submerged unit weight below the groundwater table). The values of c and ϕ should be determined from consolidated undrained or drained laboratory tests conducted on suitable backfill material or in situ soil as appropriate to consider the construction method. For augered foundations, the value of K should be taken as the "at rest" value. If backfill is placed, the degree of compaction and type of soil will determine the value of K.

Copyright © 2001 IEEE. All rights reserved.

Copyright The Institute of Electrical and Electronics Engineers, Inc.
Provided by IHS under license with IEEE
No reproduction or networking permitted without license from IHS Not for Resale

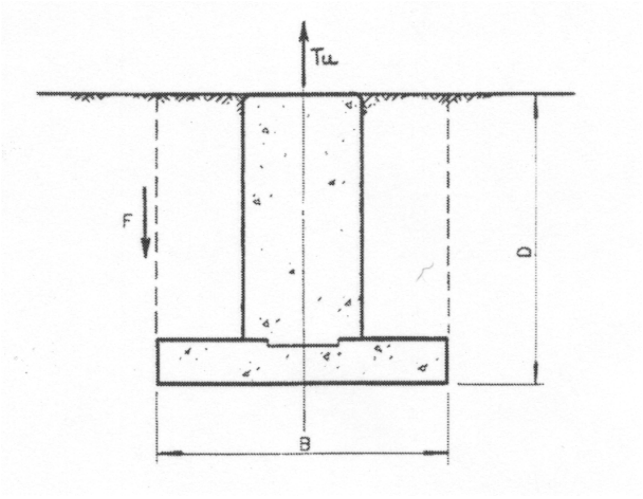

Figure 36—Shearing or friction method

An empirical expression for F was also developed by Motorcolumbus, Baden (Switzerland) based on numerous tests:

$$F = p\sigma D^{x} \tag{62}$$

where

- x is a constant (x = 1.5–2.0),
- p is the circumference of the rupture surface (may be taken as the perimeter of the foundation),
- D is the depth of embedment,
- σ is a shear constant.

The value of the shear constant is dependent on soil type and the depth of the foundation and should be determined from load tests conducted on foundations of similar depth and dimensions. The normal value of shear constants should be decreased by 50% to account for the influence of groundwater.

Under certain construction conditions, the shearing method would seem most appropriate. Matsuo [B106] noted that when the vertical excavation method was used and foundations were cast-in-place against the base of the excavation, rupture surfaces frequently develop along the walls of the excavation. Thus, for this case, the assumption of a vertical rupture surface used in the development of the shearing method appears reasonable.

4.3.3 Meyerhof and Adams' method

Meyerhof and Adams [B112] developed a more general semi-empirical method of estimating uplift capacity for a continuous or strip foundation subjected to vertical load only and then modified it to consider rectangular or circular foundations. As a result of observations and data obtained from model tests conducted in both sands and clays, Meyerhof and Adams [B112] concluded that, for shallow foundations, the uplift capacity increased with increasing depth and that a distinct slip surface occurs in dense sands which extends in a shallow arc from the edge of the foundation to the ground surface.

Copyright © 2001 IEEE. All rights reserved.

Copyright The Institute of Electrical and Electronics Engineers, Inc.
Provided by IHS under license with IEEE
No reproduction or networking permitted without license from IHS
Not for Resale

In clays, a complex system of tension cracks was observed along with significant negative pore water pressures above and below the foundations. For deep foundations, the failure surface is less distinct for both sand and clay and the uplift capacity reaches a limiting value with increasing depth.

Because of the complex form of the failure surfaces, simplifying assumptions were made in developing expressions for the uplift capacity of spread foundations. Meyerhof and Adams [B112] neglected the larger pullout zone observed in tests by assuming a vertical rupture surface, as shown in Figure 37. The influence of the shear resistance along the actual observed failure surface, and the additional weight of soil contained within the rupture surface, were considered by assuming the soil on the sides of the shear plane (Figure 37) to be in a state of plastic equilibrium. The frictional resistance on the shear plane was computed as a function of the passive earth pressure exerted on the plane assuming the curved failure surfaces used by Caquot and Kerisel [B34].

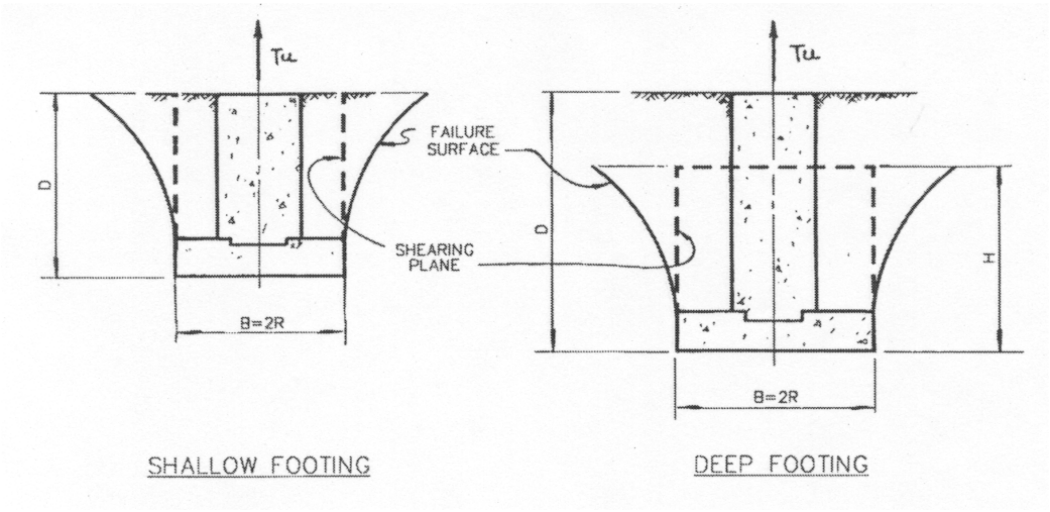

Figure 37—Meyerhof and Adams method (circular footing)

Meyerhof and Adams [B112] developed separate expressions for shallow and deep foundations. Circular and rectangular foundations were considered in both cohesive and cohesionless soils.

Table 7—Foundation parameters for Meyerhof and Adams equation

ϕ (degrees)	20	25	30	35	40	45	48
Limiting $\frac{H}{B}$	2.5	3.0	4.0	5.0	7.0	9.0	11.0
Max. Value of s_f	1.12	1.3	1.6	2.25	3.45	5.50	7.60
M	0.05	0.1	0.15	0.25	0.35	0.5	0.6
K_u	0.85	0.89	0.91	0.94	0.96	0.98	1.00

Copyright © 2001 IEEE. All rights reserved.

Copyright The Institute of Electrical and Electronics Engineers, Inc.
Provided by IHS under license with IEEE
No reproduction or networking permitted without license from IHS
Not for Resale

4.3.3.1 Circular foundations

As shown in Figure 37, the mode of failure is determined by the depth of the foundation. For shallow foundations (D < H), the depth of the foundation D is less than the vertical limit of the failure surface H. When D is greater than the limiting value of H, the failure surface does not reach the ground surface and the foundation is considered to be deep. Table 7 provides limiting values of the ratio H/B for various angles of internal friction ϕ, where B is the diameter of the foundation.

For shallow circular foundations, the ultimate uplift capacity (T_u) may be expressed as the sum of the cohesion and passive earth pressure friction developed on the cylinder extending vertically above the foundation base, the weight of the foundation (W_f) and the weight of soil (W_s) inside the cylinder. The ultimate uplift capacity is given by:

$$T_u = W_f + W_s + \pi BcD + s_f(\pi/2)B\gamma D^2 K_u \tan\phi \quad (63)$$

where

c is the soil cohesion,
s_f is a shape factor governing the passive earth pressure on the side of a cylinder,
K_u as defined by Meyerhof and Adams [B112], is the nominal uplift coefficient of earth pressure on the vertical rupture surface and may be approximated as:

$$K_u = 0.496(\phi)^{0.18} \quad (64)$$

where ϕ is in degrees.

The shape factor, s_f, is determined from the following expression:

$$s_f = 1 + \frac{MD}{B} \leq 1 + \frac{H}{B}M \quad (65)$$

where M is a function of ϕ and is given in Table 7 together with the maximum values of s_f and values of K_u.

Similarly, the ultimate uplift capacity of a deep circular foundation (D ≥ H) may be expressed as:

$$T_u = W_f + W_s + \pi cBH + s_f(\pi/2)\gamma B(2D - H)HK_u \tan\phi \quad (66)$$

where

W_s is the weight of the soil contained in a cylinder of length H.

An upper limit on T_u is imposed by the bearing capacity of the soil above the foundation and is given by:

$$T_u(\text{max.}) = \pi\frac{B^2}{4}(cN_c + \gamma DN_q) + A_s f_s + W_f + W_s \quad (67)$$

where

A_s is the surface area of the cylinder,
f_s is the average unit skin friction of the soil on the cylinder,
N_c and N_q are bearing capacity factors for foundations under compressive loads.

Copyright © 2001 IEEE. All rights reserved.

Copyright The Institute of Electrical and Electronics Engineers, Inc.
Provided by IHS under license with IEEE
No reproduction or networking permitted without license from IHS
Not for Resale

Reasonable agreement was obtained by Meyerhof and Adams [B112] between computed uplift capacities and experimental results for foundations in sand. The theoretical values of the uplift capacities appear to underestimate the actual uplift resistance in dense sand and tend to overestimate the uplift resistance in loose sand.

In clays, Meyerhof and Adams [B112] observed the formation of negative pore water pressures above and below the foundation, particularly with shallow foundations. The drained (long-term) uplift capacity in clay can be considerably less than the undrained (short-term) capacity because of the dissipation of the negative pore water pressure and associated softening of the soil. Meyerhof and Adams recommended that the long-term capacity of shallow foundations in clay be estimated by Equation (63), where drained soil strength parameters (c and ϕ) should be determined from appropriate laboratory tests. For the short-term capacity of shallow foundations, an empirical relationship proposed to estimate uplift capacity is expressed as:

$$T_u = \frac{\pi B^2}{4}(cN_u) + W_f + W_s \tag{68}$$

where

c is cohesion,
N_u is an uplift coefficient,
$W_f + W_s$ is the weight of foundation and soil.

The quantity N_u may be evaluated from:

$$N_u = \frac{2D}{B} \leq 9 \tag{69}$$

where D and B are as previously defined.

4.3.3.2 Rectangular foundations

For rectangular foundations in sand, the ultimate uplift capacity of shallow foundations may be expressed as:

$$T_u = W_s + W_f + 2cD(B + L) + \gamma D^2(2s_f B + L - B)K_u \tan\phi \tag{70}$$

where

B is the width of the foundation, L is the length, and it is assumed that the earth pressure on the two ends is governed by the shape factor (s_f) as calculated by Equation (65).

For the short-term uplift capacity of shallow foundations in clay, Equation (68) may be rewritten for rectangular foundations as:

$$T_u = BLcN_u + W_f + W_s \tag{71}$$

where N_u is defined in Equation (69). For the drained or long-term case, Equation (70) would be appropriate.

The ultimate uplift capacity of deep rectangular foundations may be determined from:

$$T_u = 2cH(B + L) + \gamma H(2D - H)(2s_f B + L - B)K_u \tan\phi + W_s + W_f \tag{72}$$

Copyright © 2001 IEEE. All rights reserved.

Copyright The Institute of Electrical and Electronics Engineers, Inc.
Provided by IHS under license with IEEE
No reproduction or networking permitted without license from IHS Not for Resale

An upper limit on the uplift capacity may be obtained for rectangular foundations in similar fashion to Equation (67):

$$T_u(\max) = BL(cN_c + \gamma DN_q) + A_s f_s + W_f + W_s \quad (73)$$

where A_s, f_s W_f, W_s, N_c, and N_q are as defined for circular foundations in 4.3.3.1 and B is the foundation width and L is the foundation length.

For both circular and rectangular foundations, the influence of the groundwater table should be considered when it is above the base of the foundation. If the soil above the foundation base is submerged, the submerged unit weights should be used for both the foundation and the soil in determining the ultimate uplift capacity. If the groundwater table is between the base of the foundation and the ground surface, the weights of the foundation and the soil should be corrected for buoyancy for that material within the rupture surface and below the water table. The friction component should also be computed based on effective stresses, using the submerged unit weight of the soil for that portion of D or H (Figure 37) below the water surface in the appropriate uplift capacity equation. Above the groundwater table, the total unit weight should be applied.

4.4 Construction considerations

The most critical operation in the construction of spread foundations subjected to uplift is the degree of compaction of the backfill. Particular care in compaction must be taken in areas directly above the base and adjacent to any shear members. The ultimate uplift capacity of a spread foundation varies greatly with the degree of backfill compaction obtained. Therefore, it cannot be overemphasized that this part of the construction is critical and must be reviewed, inspected, and tested. The engineer must verify that the field density of the backfill is at least equal to the assumed design backfill density. The engineer must also take into account the degree of compaction that can actually be attained in the field when originally designing the foundation. The base of the footing should be level and well tamped.

In addition, pressed plate footings are installed on a compacted sand sub-base with a minimum depth of three inches. Additional sand is mounded over the area where the plate is to be set. The plate should be placed on the mound and then worked and tamped into final position in such a manner that no voids exist under the plate.

Metals placed below the ground surface are subject to corrosion action. The degree of corrosion depends on type of metal, type of soil, moisture content of the soil and possible stray electric currents in the soil. At the least metals placed below ground must be given a protective coating. Bitumins are usually used. The coating must be tested prior to backfilling to insure that there are no pinholes.

In even the most careful applications of protective coatings, pinholes may remain, or may be caused by the backfill. Consideration should be given to the advisability of installing a cathodic protection system. In a cathodic protection system, a sacrificial anode is installed in the ground adjacent to and electrically connected to the metal to be protected. This anode is fabricated from a metal lower in the electromotive force series than the protected metal. The anode then corrodes while the protected metal remains whole. In some soils, an electric current must be induced to make the system work, but in most soils, sufficient currents already exist. After some time, the sacrificial anode must be replaced if the system is to remain functional.

For rock foundations, the rock may be excavated by drilling, controlled blasting, or the use of a power-operated rockbreaker or hammer. When blasting, care should be taken to prevent overblasting which may cause extensive shatter or fracture to the adjacent rock mass and, consequently, reduce its capacity to resist uplift.

Copyright © 2001 IEEE. All rights reserved.

Copyright The Institute of Electrical and Electronics Engineers, Inc.
Provided by IHS under license with IEEE
No reproduction or networking permitted without license from IHS
Not for Resale

All backfill should be placed with suitable moisture content in uniform horizontal layers usually not over 8 inches before compaction and thoroughly compacted with mechanical vibrators (granular material) or pneumatic rammers (cohesive material).

The suitable moisture control can be as follows:

— Cohesive material +2% and –2% of the optimum moisture content

Practical compaction densities can be as follows:

— *Undrained loadings*. See Table 6.
— *Drained loading*. See Table 5, or 95% as determined by ASTM D1557 (modified proctor) or 85% of relative density as determined by ASTM D-4253 and ASTM D-4254.

4.5 General foundation considerations

The following considerations are applicable to all foundation types, but are listed here for convenience.

4.5.1 Frost depth

Figure 38 presents an extreme frost depth map of the United States. The base of a spread foundation resting on soil may be conservatively placed a minimum of 152 mm (six inches) below the depth of extreme frost penetration. However, the depth of freezing is highly dependent on local climatic conditions and soil type, and therefore local codes and authorities should be consulted to determine the site-specific conditions, which may be more or less critical than indicated on the map. An estimate of frost depth using the concept of a freeze index is shown in Figure 39 [B80]. This curve is from the U.S. Corps of Engineers with a revision proposed by Brown. The average daily temperatures below freezing can be obtained from the local weather records. The freezing index is equal to the number of days below 32 °F multiplied by the temperature less 32° F. According to Brown, the curve also can be used to estimate the depth of thaw in permafrost areas by replacing the freeze index with a thaw index.

For lightly loaded cylindrical augered foundations, the foundation depth should be checked so that the foundation design also resists the “adfreeze (freezing of soil to foundation) force” caused by frost heave [B125]. This may require the foundation to be deeper than 152 mm (6 in) below the determined frost depth.

4.5.2 Depth criteria for swelling soils

Significant uplift forces may be developed on the base and sides of shallow foundations placed in expansive or swelling soils. Swelling soils consist of clays with a high plasticity indexes (usually >20) which exhibit volume changes because of changes in water content. A curve showing this relationship [B80] is shown on Figure 40. Such soils are encountered in many parts of the United States and are particularly common to the southwest and western states.

Uplift effects of swelling soils can be avoided or reduced by embedding the foundation at a depth below the zone of seasonal moisture change, where practical. The procedure is to place the foundation mat at a sufficient depth so that the uplift forces caused by adhesion on the sides of the mat or pier do not pull it out of the soil or that heave pressures developed on the base of the mat do not lift the entire foundation system.

The swelling potential of expansive soils may also be reduced by treating the soil chemically. Addition of lime, cement, or other admixtures will generally decrease the volume change potential and, consequently, the uplift effects on transmission tower foundations.

Copyright © 2001 IEEE. All rights reserved.
Copyright The Institute of Electrical and Electronics Engineers, Inc.
Provided by IHS under license with IEEE
No reproduction or networking permitted without license from IHS Not for Resale

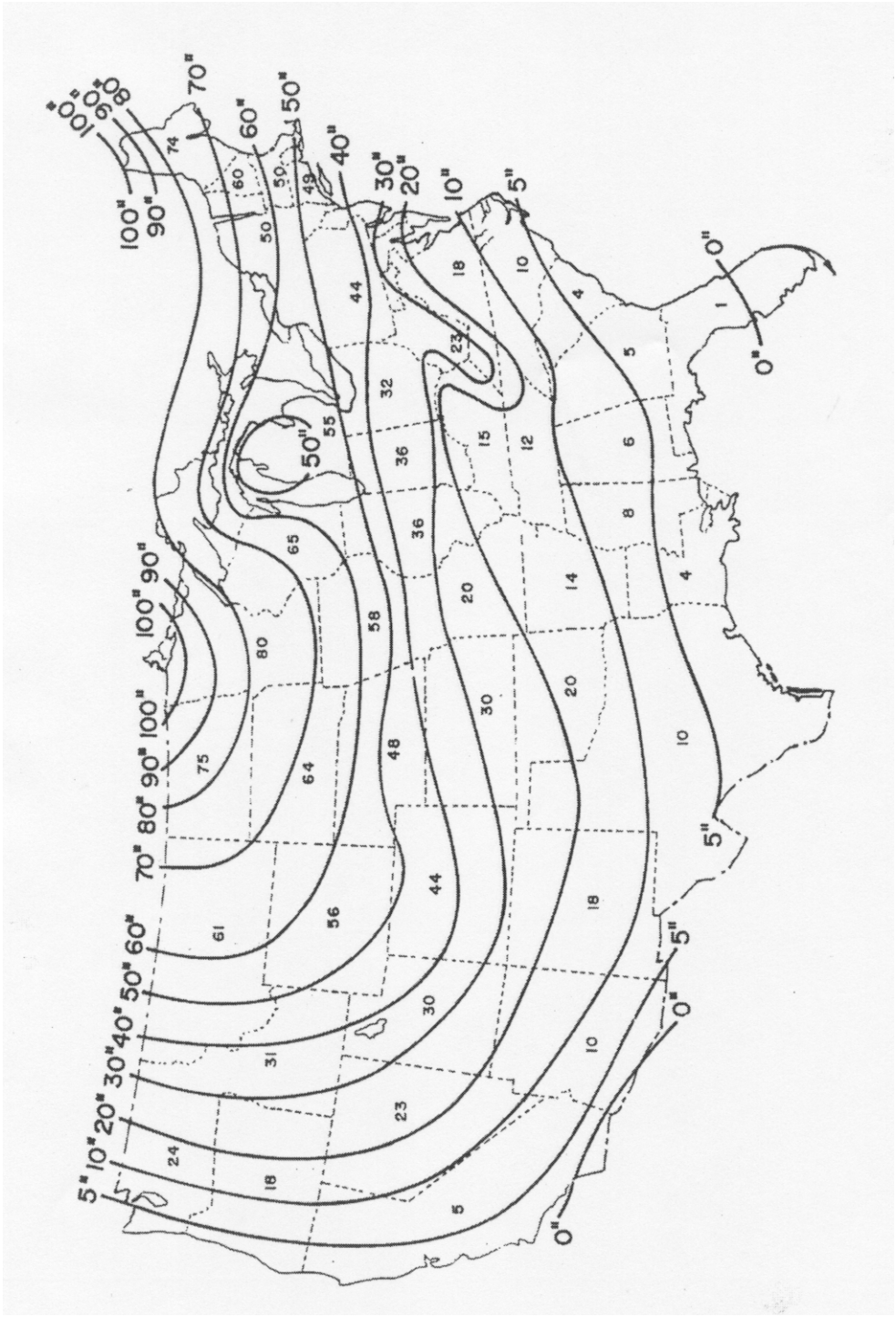

Figure 38—Extreme frost penetration, inches based on state averages

Copyright © 2001 IEEE. All rights reserved.

Copyright The Institute of Electrical and Electronics Engineers, Inc.
Provided by IHS under license with IEEE
No reproduction or networking permitted without license from IHS
Not for Resale

4.5.3 Permafrost

Permafrost is where the ground is permanently frozen. It occurs in regions where the mean temperature for the warmest month is less than 50 °F and the mean annual temperature is less than 32 °F. When the soil freezes, its strength and bearing capacity are increased because of the conversion of at least a portion of the water in the soil to ice. Foundations in these regions require special expertise because the thickness of degradation of the melting permafrost varies. The thickness of the thawing depths depends upon the density and type of soil and soil water content and may be estimated from Figure 39 if the number of freezing degree days are known. These thawing zones can vary from 0.3 m to 6.1 m (1 to 20 feet) and can cause serious foundation problems. When routing a transmission line through permafrost areas, a good reference on terrain is given in reference [B8].

4.5.4 Collapsing soils

The two major categories of collapsing soils in the U.S. are the loessial soils of the northwest and midwest (see Figure 41) and the arid soils of the western and southwestern inter mountain basins. When wetted, these soils can exhibit large volumetric reduction, resulting in as much as several feet of settlement at the ground surface. Foundation design should consider precollapsing the soil or maintaining the design stresses below the collapse stress threshold.

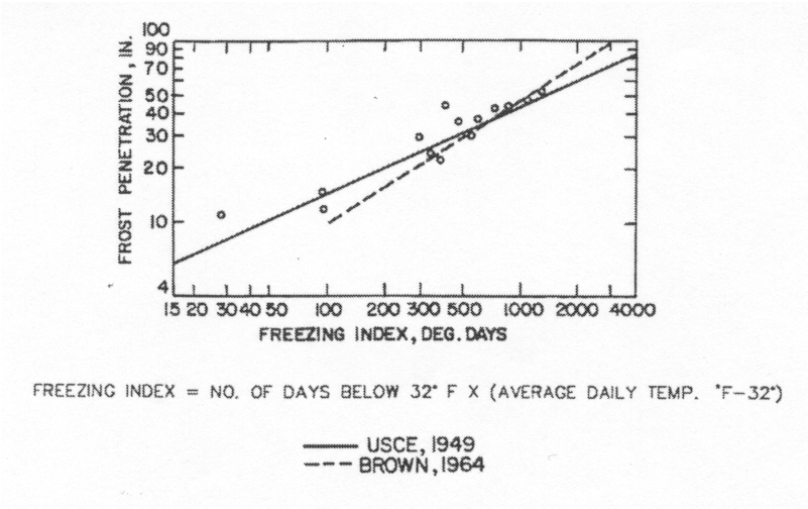

Figure 39—Design curves for maximum frost penetration based on the freezing index

4.5.5 Black shales

Certain areas of the country are underlain by sedimentary rocks collectively known as “black shales.” These rocks can be quite weak when sheared parallel to bedding planes and can cause access and slope stability problems for transmission line structures. In addition, their chemical composition, which may include significant fractions of pyrite, attacks concrete, and, therefore, a moisture barrier is necessary. Black shales may expand when loaded lightly and could heave footings.

Copyright © 2001 IEEE. All rights reserved.

Copyright The Institute of Electrical and Electronics Engineers, Inc.
Provided by IHS under license with IEEE
No reproduction or networking permitted without license from IHS Not for Resale

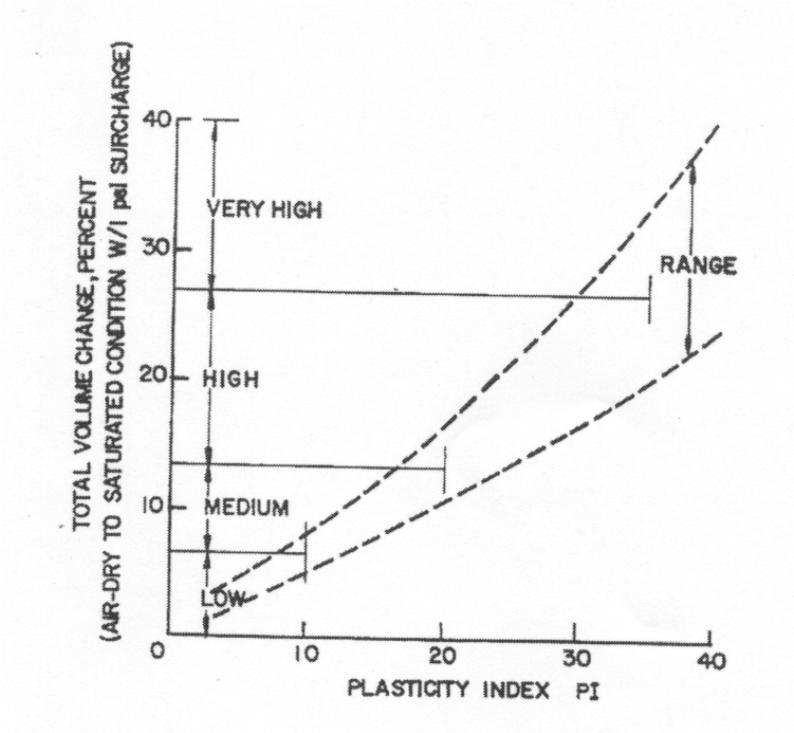

Figure 40—Relationship of a plasticity index to swell potential of a soil

4.5.6 Karst topography

Regions underlain by limestone are subject to dissolution and the formation of sinkholes and underground cavities. The bedrock surface can vary greatly, and therefore special precautions are warranted to ensure that an adequate bearing stratum is achieved in the field.

5. Design of drilled shaft and direct embedment foundations

Drilled shaft and direct embedded pole foundations have been used successfully to support various types of transmission structures. These types of foundations support vertical compression loads through a combination of side and tip resistance and support vertical uplift loads by side resistance and tip suction. Lateral shear loads and overturning moments are supported by lateral, vertical side, and tip resistance.

5.1 Types of foundations

With respect to design methods, three general foundation types are considered in this section: straight and belled drilled concrete shafts[2], direct embedment of wood, concrete or tubular steel poles, and precast-prestressed hollow concrete shafts and steel casings.

[2]Also known as caissons, drilled piles, bored piles, drilled piers.

Copyright © 2001 IEEE. All rights reserved.

Copyright The Institute of Electrical and Electronics Engineers, Inc.
Provided by IHS under license with IEEE
No reproduction or networking permitted without license from IHS
Not for Resale

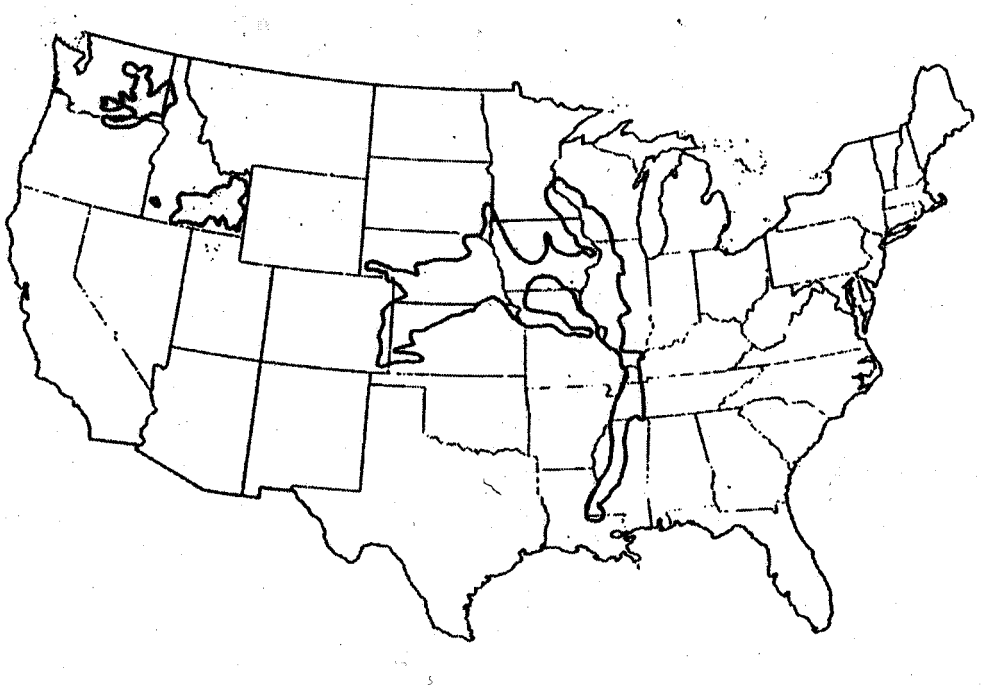

Figure 41—Outline of major loess deposits in the United States

5.1.1 Drilled concrete shafts

The drilled concrete shaft is the most common type of foundation presently being used to support transmission structures. Drilled concrete shafts are constructed by power augering a circular excavation, placing the reinforcing steel and anchor bolts or steel angles, and pouring concrete to form a shaft foundation [B167]. Tubular steel poles and tubular steel H-structures are either attached to the drilled concrete shafts using base plates welded to the pole and anchor bolts embedded in the foundation, or in some cases, directly embedded in concrete. Lattice towers are attached by embedment of a stub angle into the concrete or through the use of base plates and anchor bolts.

Drilled concrete shafts can be constructed in a wide variety of soil types. However, when constructing drilled concrete shafts under certain soil conditions, problems may be encountered. For example, granular soils may collapse into the excavation before concrete can be poured; in soft, cohesive soils, squeezing or shear failure of the soil can occur, producing a reduced diameter; or the excavation may become completely obstructed before the concrete is placed. This soil movement in the excavation can result in ground-surface settlement. Construction below the ground water level requires special attention. Casing or drilling mud, or both, may be required in granular and soft cohesive soils to maintain an open excavation. Also, the concrete should be placed in a continuous manner to avoid cold joints, voids, and other discontinuities that could be detrimental for the foundation.

5.1.2 Direct embedment

Direct embedment refers to wood, steel, or concrete pole foundations constructed by power augering a circular excavation in the ground, inserting the pole directly into the excavation, and backfilling the void between the pole and the sides of the excavation. Thus, the pole acts as its own foundation by transferring loads to the in situ soil via the backfill. This technique has been traditionally used for wood pole foundations in distribution lines and has recently been employed for steel and concrete pole foundations in transmission lines.

Copyright © 2001 IEEE. All rights reserved.

Copyright The Institute of Electrical and Electronics Engineers, Inc.
Provided by IHS under license with IEEE
No reproduction or networking permitted without license from IHS Not for Resale

Where direct embedment is feasible, the cost of the additional length of pole, plus backfill material and associated labor, must be evaluated relative to the cost of concrete, reinforcing steel, anchor bolts, base plates, and the associated labor for drilled concrete shaft foundations. Even when a cost comparison favors a drilled concrete shaft foundation, the reduced time for direct embedment foundation construction may still be beneficial to the overall project. Direct embedment may simplify foundation construction and may be particularly appropriate for remote areas.

The quality of backfill, method of placement, and degree of compaction strongly influence the stiffness and strength of a direct embedment foundation [B28] [B54] [B55] [B73]. Corrosion of an embedded steel pole is also an important consideration. Furthermore, it should be noted that the presence of granular or soft, cohesive soils may cause the same construction problems for direct embedment foundations as for drilled concrete shaft foundation.

5.1.3 Precast-prestressed, hollow concrete shafts and steel casings

Precast-prestressed, hollow concrete shafts can be placed into a circular excavation in much the same manner as direct embedment poles. Hollow concrete shafts and steel casings can also be vibrated, jetted or driven in granular soils that would otherwise require shoring to maintain an open excavation for drilled concrete shafts or direct embedment foundations.

5.2 Structural applications

In general, drilled shaft foundations are applicable to the three major types of transmission structures, that is lattice towers, H-structures (framed, pinned, or braced), and single poles. Direct embedment foundations are applicable to H-structures and single poles. Hollow concrete shafts and steel casings can be used to support lattice towers, H-structures and single poles.

For single-pole structures, both longitudinal and transverse loads and their resultant overturning moments are resisted by the lateral interaction of the foundation with the materials in which it is embedded. The same is true for transverse loads on pinned H-structures and for longitudinal loads on pinned, framed, and braced H-structures. However, for framed and braced H-structures, the transverse overturning moments are resisted primarily by axial loads in the foundation.

Both transverse and longitudinal loads on lattice towers are resisted primarily by axial loads in the foundations, although the foundations will also be subjected to lateral ground-line shears. Figure 42 illustrates the loads applied to the three types of structures and the loads transmitted to their foundations.

Drilled concrete shafts are applicable to all three structure types, but they are particularly appropriate for single shaft structures where high overturning moments are anticipated. For lattice towers, both straight shaft and belled shafts are commonly used. The drilled shafts can be installed vertically or on a batter that has the same true slope as the leg, as shown on Figure 43. Where the shafts are installed with the true leg batter, the shaft shear load is greatly reduced. For H-structures and single-pole structures, the shafts are normally constructed vertically.

Direct embedment foundations are applicable to single-pole structures and H-structures, but they cannot be used in connection with lattice towers. The uplift capacity of directly embedded foundations is related to the quality of the backfill and the side resistance that can be mobilized at the pole-backfill interface and at the backfill-in situ soil interface. Significant tip resistance on tubular steel poles can only be achieved if the pole base is closed with a base plate. Additional bearing capacity for compression loads can be obtained by installing bearing plates.

Copyright © 2001 IEEE. All rights reserved.

Copyright The Institute of Electrical and Electronics Engineers, Inc.
Provided by IHS under license with IEEE
No reproduction or networking permitted without license from IHS
Not for Resale

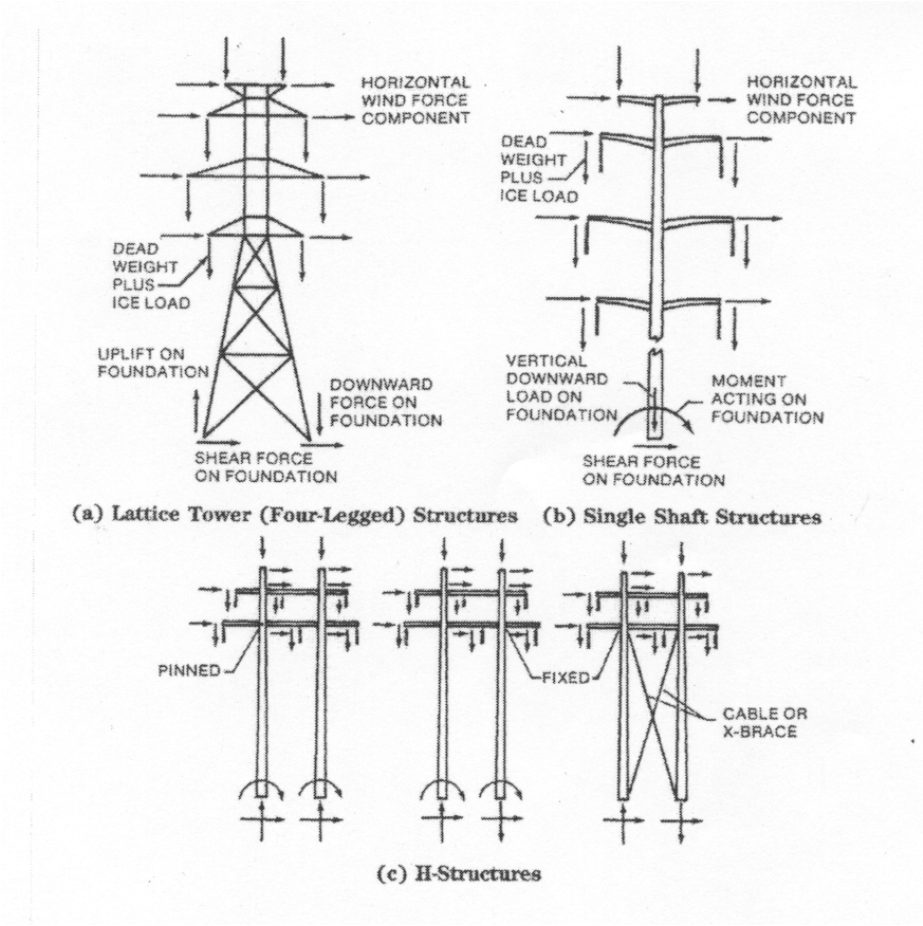

Figure 42—Loads applied to transmission structures and their foundations

Precast-prestressed, hollow concrete shafts or steel casings are applicable where large overturning moments are to be resisted, as in the case of single-pole structures. They may also be used in H-structures and lattice towers.

5.3 Drilled concrete shaft foundations

Lattice towers, H-frame structures, and single-pole structures use drilled concrete shaft foundations. For this type of foundation, the construction sequence includes, as a minimum, auger-drilling a hole, inserting a cage of reinforcing steel and anchor bolts or steel angles, and then backfilling the hole with concrete. Typical shaft diameters for transmission line structures range from about 0.6 m (2 ft) to 3 m (10 ft), with length ranging from about 3 m (10 ft) to about 23 m (75 ft). A minimum diameter of 0.8 m (2.5 ft) is recommended to allow a person to enter the excavated hole if needed.

The precise method of construction depends on both the particular ground conditions and the contractor. If ground conditions are favorable, the hole will remain open with no support, while in poor conditions, casing or slurry may be required to maintain hole stability. High ground water in cohesionless, or sandy, soils generally will require some form of excavation support. Because construction details can influence significantly the capacity of drilled shafts, it is important to carefully evaluate ground conditions relative to construction methods, as an integral part of the overall design procedure.

Copyright © 2001 IEEE. All rights reserved.

Copyright The Institute of Electrical and Electronics Engineers, Inc.
Provided by IHS under license with IEEE
No reproduction or networking permitted without license from IHS
Not for Resale

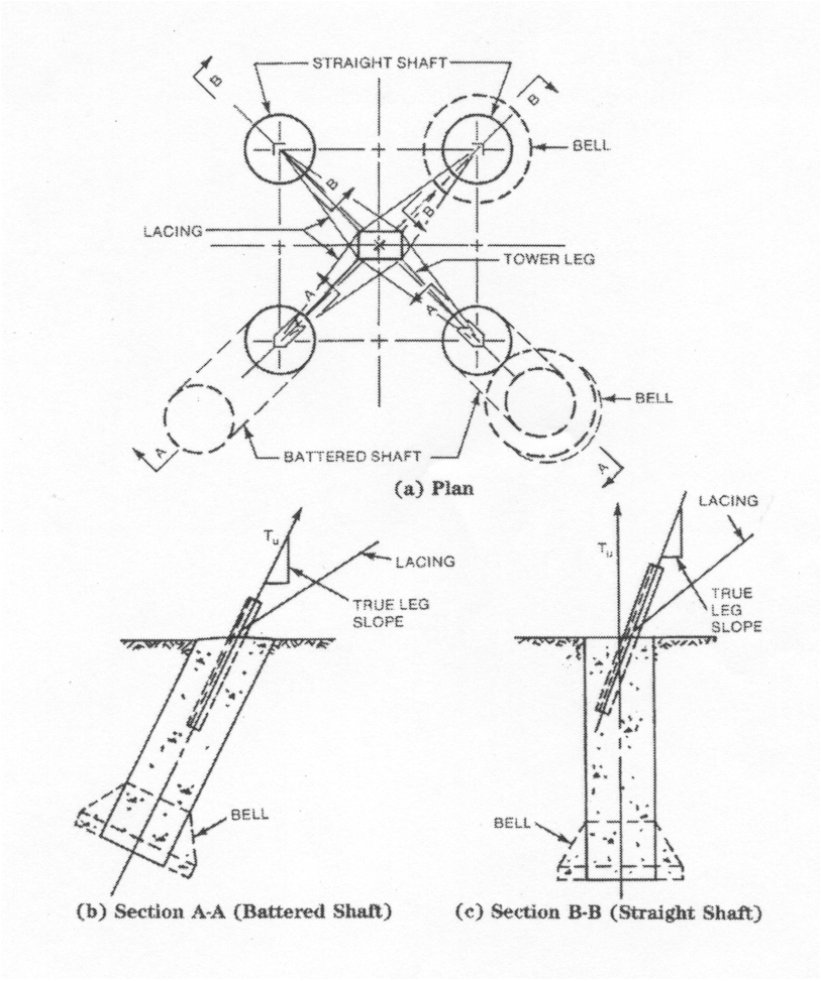

Figure 43—Drilled shaft orientation

5.3.1 Uplift load capacity and displacements

The capacity of drilled shaft foundations for uplift loads follows directly from the analysis of force equilibrium between the applied loads and the weight of the shaft, and both side and tip resistance of the shaft. Several analytical models that attempt to predict the geometry of the failure zone for a drilled shaft under uplift loads are presently being used by the industry. Two of the most popular models are the truncated cone model and the traditional cylindrical shear model. A recent approach to the analysis and design of drilled shafts in uplift is the development of the computer program CUFAD (Compression Uplift Foundation Analysis and Design) available in EPRI's TLWorkstation™ . CUFAD is a cylindrical shear model which includes considerations for potential cone breakout and base suction [B159]. The truncated cone, cylindrical shear and CUFAD analytical method are presented here followed by a statistical evaluation [B53] of their ability for predicting uplift capacity based on the reported behavior of a number of full-scale uplift load tests on straight shafts [B147].

5.3.1.1 Truncated cone model

Figure 44 shows the geometry considered for the truncated cone model. The uplift capacity of the shaft is derived from the weight of the shaft and from the weight of the soil cone adhering to the shaft. In situations

Copyright © 2001 IEEE. All rights reserved.

Copyright The Institute of Electrical and Electronics Engineers, Inc.
Provided by IHS under license with IEEE
No reproduction or networking permitted without license from IHS
Not for Resale

where the shaft penetrates the ground water level, the effective weight of the shaft and of the soil in the cone are used in the model. Also, suction on the base of the shaft is normally neglected. When considering a homogenous soil media, the ultimate uplift capacity, Q_u, can be written as:

$$Q_u = \overline{W} + \overline{Q_{sw}} \tag{74}$$

where

$\overline{W}$ is effective weight of the shaft

$\overline{Q_{sw}}$ is effective weight of the soil cone adhering to the shaft

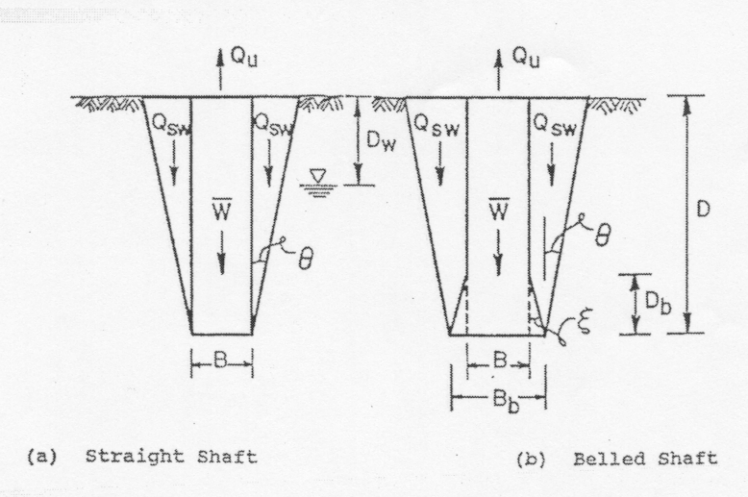

Figure 44—Truncated cone drilled shaft model for uplift loads

For a straight shaft the resisting weight components are:

$$\overline{W} = \frac{\pi B^2}{4}\{\gamma_c D_w + \bar{\gamma}_c (D - D_w)\} \tag{75}$$

$$\overline{Q_{sw}} = \pi \bar{\gamma}_s D\left\{\frac{B^2}{2} + \frac{BD\tan\theta}{2} + \frac{D^2\tan^2\theta}{3}\right\} \tag{76}$$

where

γ_c is total unit weight of concrete,

$\bar{\gamma}_c$ is effective unit weight of concrete,

$\bar{\gamma}_s$ is effective unit weight of soil,

B is diameter of straight shaft,

D is length of straight shaft below ground surface,

D_w is depth to the water table,

θ is angle between the face of the cone and the vertical.

Copyright © 2001 IEEE. All rights reserved.

Copyright The Institute of Electrical and Electronics Engineers, Inc.
Provided by IHS under license with IEEE
No reproduction or networking permitted without license from IHS
Not for Resale

For a belled shaft, Equation (76) is modified by accounting for the additional soil hollow cylinder around the shaft as follows:

$$Q_{sw} = \pi\bar{\gamma}_s D\left\{\frac{B_b^2}{2} + \frac{B_b D\tan\theta}{2} + \frac{D^2\tan^2\theta}{3} + \frac{B_b^2 - B^2}{4}\right\} \quad (77)$$

where

B_b is diameter of the belled section of the shaft

The additional weight contribution of the bell area concrete, $\Delta\overline{W}$, to the weight of the shaft can be calculated by the following expression:

$$\Delta\overline{W} = \pi(\bar{\gamma}_c - \bar{\gamma}_s)D_b^{\,2}\left\{\frac{B\tan\xi}{2} + \frac{D_b\tan^2\xi}{3}\right\} \quad (78)$$

where

ξ is angle between the bell surface and the vertical axis of the shaft,
D_b is height of the bell.

As previously mentioned, Equation (74) considered a drained state of failure and uses an effective stress approach (since both terms of the expression use effective unit weight values); thus the ground water level effect has to be properly incorporated in $\bar{\gamma}_s$ in Equation (76), Equation (77), and Equation (78).

5.3.1.2 Traditional cylindrical shear model

For a straight drilled shaft, this model assumes that the failure surface is generated at the interface between the shaft and the soil on the side of the shaft. For a belled shaft, the model assumes that the failure surface is either along the concrete-soil interface or is a cylinder having a diameter equal to the bell diameter (see Figure 45).

Straight shafts-

Undrained loading. Traditionally, in addition to the total weight of the shaft, the shear resistance developed along the side of the shaft, Q_{su}, has to be considered and tip suction is neglected [B145]. For a homogenous cohesive soil, the uplift capacity for undrained loading is then given by:

$$Q_u = W + Q_{su} \quad (79)$$

The value of Q_{su}, the shaft side resistance under undrained loading conditions, can be calculated from:

$$Q_u = \alpha s_u(\pi BD) \quad (80)$$

where

α is adhesion factor,
s_u is undrained shear strength of the soil.

Copyright © 2001 IEEE. All rights reserved.

Copyright The Institute of Electrical and Electronics Engineers, Inc.
Provided by IHS under license with IEEE
No reproduction or networking permitted without license from IHS
Not for Resale

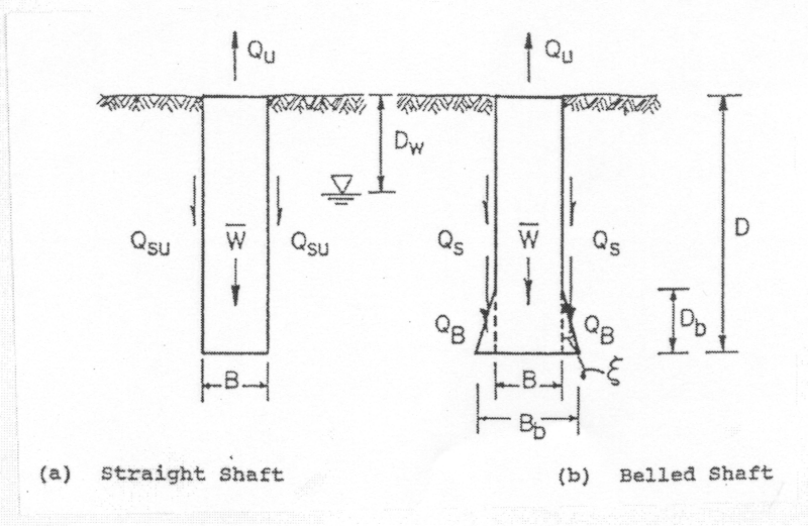

Figure 45—Cylindrical shear drilled shaft model for uplift loads

Note that in the equation the shear resistance developed along the side of the shaft has been accounted for by correlating it with the undrained shear strength of the soil, through the adhesion factor, α. Figure 46 presents different correlations between α and s_u. The curve proposed by Tomlinson [B155] is based on results obtained largely from compression tests on precast concrete piles driven in clay soils. The side resistance of each foundation was estimated by subtracting the estimated tip contribution from the observed ultimate capacity of the pile. Sowa [B145] obtained values of adhesion factor, α, from uplift tests conducted on cast-in-situ concrete piles in clay soils. The side resistance of each foundation was estimated by subtracting the effective weight of the foundation from the observed uplift capacity, and there was no consideration of tip suction. The values obtained were in general agreement with the correlation proposed by Tomlinson. The relationship proposed by Stas and Kulhawy [B147] also is shown in Figure 46. This relationship was obtained from a regression analysis of an extensive data base collected for this purpose of drilled shafts in cohesive soils. The side resistance of each foundation was estimated by subtracting the total weight of the foundation and the estimated tip suction contribution from the measured uplift capacity. An extensive discussion on this last approach is presented in Reference [B89]. It is recommended that the value determined by Sowa be used with Equation (80) since Sowa's values were determined using Equation (79). The values obtained from the relationship by Stas and Kulhawy should be used with the CUFAD model presented in 5.3.1.3.

Equation (80) can be rewritten as the sum of contributions from one or more soil layers, given as follows:

$$Q_{su} = \pi B \sum_{i=1}^{n} s_{ui} t_i \tag{81}$$

where

t_i is thickness of layer i.

It is important to note that the α values presented in Figure 46 are based on averaging the undrained shear strength along the entire depth of the shaft.

Copyright © 2001 IEEE. All rights reserved.

Copyright The Institute of Electrical and Electronics Engineers, Inc.
Provided by IHS under license with IEEE
No reproduction or networking permitted without license from IHS
Not for Resale

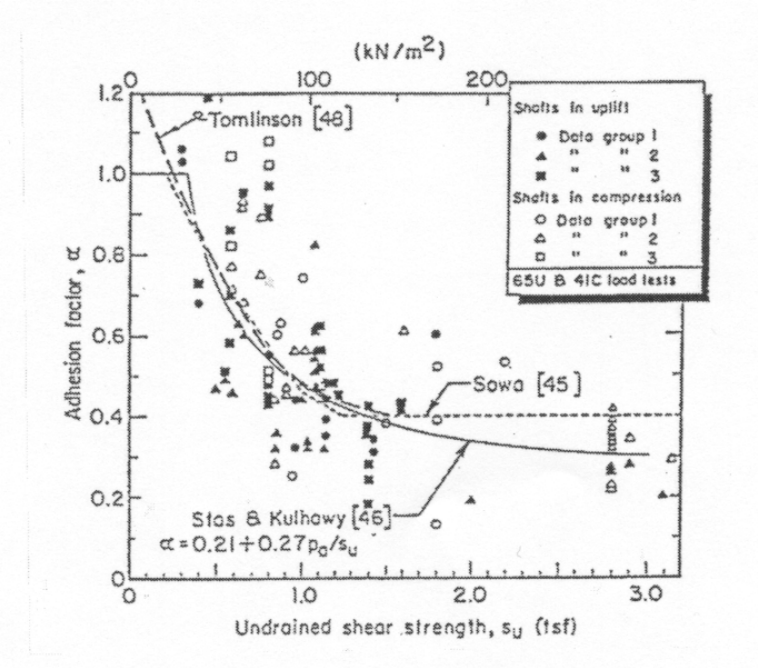

Figure 46—Correlation of adhesion factor with undrained shear strength (from [B147])

Drained loading. Under drained failure conditions for homogeneous soils, Equation (79) for the traditional cylindrical shear model becomes:

$$Q_u = \overline{W} + \overline{Q_{su}} \tag{82}$$

where

$$\overline{Q_{su}} = (\bar{\gamma}_s K \tan\delta)(\pi B D^2/2) \tag{83}$$

where

K is coefficient of horizontal soil stress,
δ is friction angle between shaft material and surrounding soil.

Under layered soil conditions or in situations where the shear strength parameters change with depth, Equation (83) is usually modified to generate a summation of incremental contributions with depth as follows [B159]:

$$\overline{Q_{su}} = \pi B \frac{K}{K_o} \sum_{i=1}^{n} K_{oi} \bar{\sigma}_{vi} \tan\left(\bar{\phi}_i \frac{\delta_i}{\bar{\phi}_i}\right) t_i \tag{84}$$

where

K/K_o is ratio of operative to at-rest coefficient of horizontal soil stress,
$\bar{\sigma}_{vi}$ is vertical effective stress at the midpoint of layer i,
K_{oi} is at-rest coefficient of horizontal soil stress for layer i,

Copyright © 2001 IEEE. All rights reserved.

Copyright The Institute of Electrical and Electronics Engineers, Inc.
Provided by IHS under license with IEEE
No reproduction or networking permitted without license from IHS
Not for Resale

$\bar{\phi}_i$ is effective stress friction angle for layer i,

$\delta_i/\bar{\phi}_i$ is ratio of the friction angle at the soil-concrete interface to the effective stress friction angle of the soil alone for layer i,

t_i is thickness of layer i.

The at-rest coefficient of horizontal soil stress, K_o, is the ratio of the effective horizontal stress to the effective vertical stress. While somewhat difficult to measure directly, it is one of the most important variables affecting the side resistance of drilled shafts. In addition, its value can vary with depth, commonly having higher values near the ground surface as a result of post-depositional desiccation of the soil, preloading by glacial ice in northern regions, or the erosion of previous soil overburden.

K_o values can be determined in three ways. First, an in-situ measurement can be made with instruments such as the pressuremeter, dilatometer, or K_o stepped blade. Second, values can be estimated on the basis of the geologic history of the soil [B108]. Third, K_o can be estimated from empirical correlations with field and laboratory test indices [B147] [B90]. Typical values range from about 0.3 for some strong, normally consolidated soils, to more than 3 for some heavily overconsolidated soils. The values given by the commonly used equation, $K_o = 1 - \sin\bar{\phi}$ are normally much too conservative for soil layers near the surface, because most near-surface soils are overconsolidated to some degree.

The parameter K/K_o describes the extent to which the original horizontal stresses are modified as a result of construction and shear during loading. The analysis of field load tests [B95] indicates a range from about 2/3 to about 1 for drilled shafts. The upper end of the range is associated with dry construction, while the lower end of the range is associated with slurry construction, which, when not done well, can leave a thick sidewall cake. Casing construction under water represents an intermediate case.

The parameter $\delta/\bar{\phi}$ represents the degree of frictional contact between the shaft surface and the native soil [B95]. For cast-in-place concrete shafts in direct contact with the soil, a value of one is suggested. Precast or steel shafts, as well as slurry construction, would lead to reduced values in the range of 0.7 to 0.9.

The parameter $\bar{\phi}$ represents the effective stress friction angle of the soil. Typical values range from 25° to 45° for granular soils and 10° to 25° for cohesive soils. The friction angle can be determined by correlation with the results of various in situ tests [B92] or can be measured in the laboratory on undisturbed samples.

Belled shafts. The ultimate uplift capacity, Q_u, for belled shafts can be assumed equal to the sum of the shear resistance along the portion of the shaft above the bell, Q_{su}, given by Equation (80) or Equation (81), for undrained loading, or Q_{su}, given by Equation (83) or Equation (84), for drained loading, and on the soil stratigraphy (one layer or multi-layered subsurface), the shearing resistance of the bell, Q_B, and the weight of the shaft, (effective weight under drained load conditions and total weight under undrained load conditions), as follows:

— Undrained loading:

$$Q_u = Q_{su} + Q_b + W \tag{85}$$

where Q_{su} and W are as defined previously and

$$Q_b = \frac{\pi}{4}(B_b^2 - B^2)N_c\omega s_u \tag{86}$$

— Drained loading:

$$Q_u = \bar{Q}_{su} + \bar{Q}_b + \bar{W} \tag{87}$$

Copyright © 2001 IEEE. All rights reserved.

Copyright The Institute of Electrical and Electronics Engineers, Inc.
Provided by IHS under license with IEEE
No reproduction or networking permitted without license from IHS Not for Resale

where $\overline{Q}_{su}$ and $\overline{W}$ are as defined previously and

$$\overline{Q}_b = \frac{\pi}{4}(B_b^2 - B^2)\bar{\sigma}_v N_q \tag{88}$$

where

B_b is bell diameter,
B is shaft diameter,
$\bar{\sigma}_v$ is effective vertical stress estimated at mid-depth of the bell,
ω is shear strength reduction factor due to underreaming disturbance as presented in [B167],
N_c, N_q are bearing capacity factors [B95] [B130] [B167].

A second model exists for evaluating the uplift ultimate capacity of a belled shaft and is called the friction cylinder method. This model assumes that, at failure, a vertical cylinder of soil is formed above the bell whose diameter is equal to the diameter of the bell. Using this model, the ultimate uplift capacity for layered soil conditions can be expressed as:

— Undrained loading:

$$Q_u = \pi B_b \sum_{z=0}^{D} s_u \Delta D + W_s + W \tag{89}$$

where

W_s is total weight of the soil enclosed in the cylinder

— Drained loading:

$$\overline{Q}_u = \pi B_b \sum_{z=0}^{D} K\bar{\sigma}_v(\tan\bar{\phi})\Delta D + \overline{W}_s + \overline{W} \tag{90}$$

where

$\overline{W}_s$ is effective weight of the soil enclosed in the cylinder.

Although the above models have been proposed, the side resistance of belled shafts under uplift loads is not well understood. However, limited field data suggest that simple modifications to the analyses developed for straight-sided shafts can provide reasonable designs. Observations [B86] have shown that for belled shafts in which D/B is less than about 5, shear takes place along an essentially vertical surface extending upward from the base of the bell. In this case, side resistance can be computed as for straight-sided shafts, using the diameter to the centroid of the bell as the shear surface diameter.

For shafts where D/B is greater than about 10, observations indicate that the bell has a relatively small influence on side resistance, so that shaft side resistance can be conservatively computed using Equation (81) and Equation (84) for undrained and drained loading conditions, respectively.

For intermediate depths, the side resistance for design can be approximated by using an interpolated diameter. Summarizing these observations:

$$B_{mod} = B_c \text{ [for D/B < 5]} \tag{91}$$

Copyright © 2001 IEEE. All rights reserved.

Copyright The Institute of Electrical and Electronics Engineers, Inc.
Provided by IHS under license with IEEE
No reproduction or networking permitted without license from IHS
Not for Resale

$$B_{mod} = B + \left(\frac{D}{5B} - 1\right)(B_b - B) \text{ [for } 5 \leq \text{D/B} \leq 10\text{]} \quad (92)$$

$$B_{mod} = B \text{ [for D/B} > 10\text{]} \quad (93)$$

where

B_{mod} is diameter modified for bell effects,
B_c is diameter to the centroid of the bell.

5.3.1.3 CUFAD

CUFAD [B159] evaluates the uplift resistance of the shaft as the sum of the weight of the shaft, W, tip suction, Q_{tu}, and side resistance, Q_{su}, as follows:

$$Q_u = Q_{su} + Q_{tu} + W \quad (94)$$

Two basic soil types are used in CUFAD. The first, denoted "SAND" is specified as an entirely frictional, or cohesionless material, with strength under both drained (long-term) and undrained (short-term) loading that is characterized by the effective stress friction angle, $\bar{\phi}$.

The second type of soil, denoted "CLAY", behaves as a frictional material during drained (long-term) loading and as cohesive material during undrained ($\phi = 0$) loading. The drained strength is given by the effective stress friction angle, ϕ, and the undrained strength is given by the undrained shear strength, s_u.

Two other materials can be used for the top layer at a multilayer site. The first, denoted "WATER", has no affect on side or tip resistance of the foundation but allows for the analysis of underwater sites.

The second, denoted "INERT", has no shear strength under drained or undrained loading but does have weight and contributes to the vertical stresses in the underlying soil layers. This type of layer can be used to represent a depth of frost, expansive soil, or other seasonal conditions where it may be desirable to neglect the side resistance for uplift capacity calculations.

Side resistance for all shafts is computed based on the traditional cylindrical shear method. However, under certain conditions of high horizontal stress and relatively short shaft length, the side shear mechanism described above may change to a cone breakout mechanism [B149]. Measured values of the normalized depth of the breakout cone, z/D, are shown for several series of field and laboratory tests in Figure 47, together with proposed tentative limits of occurrence. Subsequent work [B160] has confirmed these limits. Side resistance within the cone breakout limits is computed using a strength reduction factor for soils that simulate the effect of cone breakout failures.

CUFAD evaluates cone breakout for drilled shafts by first dividing the embedment soil into a number of elemental layers and then computing the value of ß (drained loading) or $\alpha\, s_u YD$ (undrained loading), where ß is given as:

$$\beta_i = K_{oi}\left(\frac{K}{K_o}\right)\tan\left(\bar{\phi}_i \frac{\delta_i}{\phi_i}\right) \quad (95)$$

in which all parameters are evaluated at the midpoint of an elemental layer i. In this equation, K/K_o is an average for the entire length of the foundation.

Copyright © 2001 IEEE. All rights reserved.

Copyright The Institute of Electrical and Electronics Engineers, Inc.
Provided by IHS under license with IEEE
No reproduction or networking permitted without license from IHS Not for Resale

These values then are summed and averaged over the depth of the shaft as follows:

— Undrained loading

$$(\alpha s_u/\bar{\gamma}_s D)_{\text{avg}} = \left[\frac{1}{n}\sum_{i=1}^{n}(\alpha s_u/\bar{\gamma}_s)\right]/D \tag{96}$$

in which β_{avg} and $(\alpha s_u/\bar{\gamma}_s D)_{\text{avg}}$ are average values over the depth of the shaft and n is the number of elemental layers.

— Drained loading

$$\beta_{\text{avg}} = \left(\frac{1}{n}\right)\sum_{i=1}^{n}\beta_i \tag{97}$$

A weighted average, ß', then is taken for the values of ß and $(\alpha s_u/\bar{\gamma} D)$, according to the expression:

$$\beta' = (L_s\beta_{\text{avg}} + L_c\alpha s_u/\bar{\gamma} D_{\text{avg}})/(L_s + L_c) \tag{98}$$

where

L_s is cumulative thickness of free draining layers,
L_c is cumulative thickness of undrained layers.

As indicated in Figure 47, the conditions for the cone breakout can be summarized by:

$(D/B < 6)$ and β_{avg} or $(\alpha s_u/\bar{\gamma} D)_{\text{avg}} > 1$

For cone breakout, the value of Q_{su} is reduced according to the approximate formula:

$$Q_{\text{sum}} = \frac{2+\beta'}{3\beta'}Q_{su} \tag{99}$$

where

Q_{sum} is side resistance in uplift modified for cone breakout

CUFAD also incorporates tip resistance in uplift at the user's discretion. This force can, in principle, result from tensile strength of soils or suction. However, the tensile strength of most soils is so low under normal conditions and construction practice that it is usually ignored for design. Also, suction stresses dissipate with time and therefore are ignored for drained loading conditions. Details are described elsewhere [B159].

5.3.1.4 Statistical analysis of models

Table 8 through Table 11 present the statistical analysis results of applying the different analytical models to the full-scale load test data base summarized in Reference [B147] for straight drilled shafts in undrained loading [B53] and Table 12 presents results for straight drilled shafts in drained loading [B53].

Copyright © 2001 IEEE. All rights reserved.

Copyright The Institute of Electrical and Electronics Engineers, Inc.
Provided by IHS under license with IEEE
No reproduction or networking permitted without license from IHS
Not for Resale

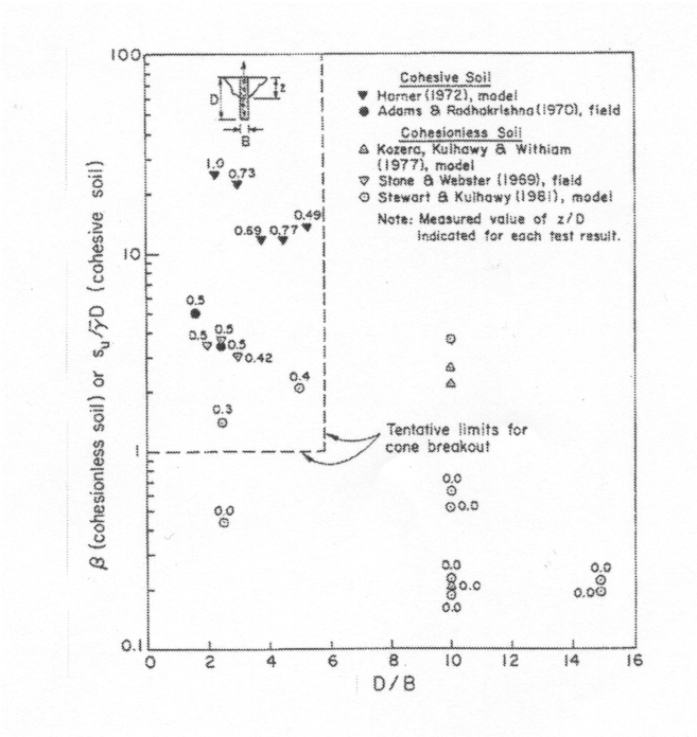

Figure 47—Conditions for cone breakout of drilled shafts (from [B159])

Table 8—Undrained uplift loading on straight shafts—Group 1: 12 tests [B53]

Method	Normal distribution			Lognormal distribution		
	$\bar{r}$	V_r(%)	R^2	$\bar{r}$	V_r(%)	R^2
Cone(θ = 15°)	0.45	59	0.66	0.45	51	0.88
Cone(θ = 30°)	0.97	89	0.33	0.94	62	0.69
Cylindrical	0.98	14	0.88	0.98	22	0.91
CUFAD	0.81	22	0.83	0.81	22	0.91

Copyright © 2001 IEEE. All rights reserved.

Copyright The Institute of Electrical and Electronics Engineers, Inc.
Provided by IHS under license with IEEE
No reproduction or networking permitted without license from IHS
Not for Resale

Table 9—Undrained uplift loading on straight shafts—Group 2: 26 tests [B53]

Method	Normal distribution			Lognormal distribution		
	$\bar{r}$	$V_r(\%)$	R^2	$\bar{r}$	$V_r(\%)$	R^2
Cone(θ = 15°)	0.73	100	0.56	0.70	84	0.89
Cone(θ = 30°)	2.56	123	0.56	2.44	122	0.91
Cylindrical	1.20	30	0.98	1.21	33	0.97
CUFAD	1.02	33	0.92	1.03	34	0.94

Table 10—Undrained uplift loading on straight shafts—Group 3: 27 tests [B53]

Method	Normal distribution			Lognormal distribution		
	$\bar{r}$	$V_r(\%)$	R^2	$\bar{r}$	$V_r(\%)$	R^2
Cone(θ = 15°)	0.25	36	0.91	0.25	36	0.96
Cone(θ = 30°)	0.77	42	0.88	0.77	42	0.95
Cylindrical	0.99	32	0.90	0.99	31	0.97
CUFAD	0.89	26	0.96	0.90	26	0.97

Table 11—Undrained uplift loading on straight shafts—All cases: 65 tests [B53]

Method	Normal distribution			Lognormal distribution		
	$\bar{r}$	$V_r(\%)$	R^2	$\bar{r}$	$V_r(\%)$	R^2
Cone(θ = 15°)	0.48	109	0.44	0.45	75	0.90
Cone(θ = 30°)	1.52	144	0.34	1.35	92	0.84
Cylindrical	1.07	31	0.95	1.07	30	0.99
CUFAD	0.93	31	0.93	0.93	30	0.98

Copyright © 2001 IEEE. All rights reserved.

Copyright The Institute of Electrical and Electronics Engineers, Inc.
Provided by IHS under license with IEEE
No reproduction or networking permitted without license from IHS
Not for Resale

Table 12—Drained uplift loading on straight shafts—All cases: 13 tests

Method	Normal Distribution			Lognormal Distribution		
	$\bar{r}$	V_r(%)	R^2	$\bar{r}$	V_r(%)	R^2
Cone(θ = 15°)	1.16	138	0.32	1.48	206	0.77
Cone(θ = 30°)	4.09	168	0.28	5.81	331	0.76
Cylindrical	1.02	26	0.93	1.01	31	0.98
CUFAD	0.99	24	0.93	1.00	30	0.98

The uplift load tests for undrained loading of straight shafts were divided into three groups based on the overall quality of the input data [B147]. Group 1 (12 tests) included cases in which the undrained shear strength was measured by field vane, unconfined compression, undrained direct shear, or triaxial tests, the ground water level was reported or could be inferred from the boring description and water content profile with depth. Group 2 (26 tests) included cases in which the undrained shear strength was measured by laboratory shear vane or torvane and/or the ground water level was known or inferred. Group 3 (27 tests) consisted of all remaining cases, including those in which the type of undrained shear strength test was not reported. The 13 straight shaft drained uplift load test cases, for which a statistical analysis was developed here, were not subdivided. In these tables, $\bar{r}$ corresponds to the average of the ratio of the predicted (R_n) to the observed ultimate capacity (R_{test}), Vr is the coefficient of variation of r, and R^2 corresponds to a correlation coefficient of the results. The observed ultimate capacities were taken as those defined in Reference [B147]. Two probability distribution functions (PDF) are shown fitting the data: the normal (Gaussian) distribution and the lognormal distribution. The coefficient of correlation, R^2, for the ultimate capacity ratio values was estimated by means of a regression analysis using a least square fit on the statistical data obtained by the method of moments.

The results shown in Table 8 through Table 12 indicate that the truncated cone model with θ=15˚ underpredicts the average ultimate capacity under undrained conditions and overpredicts it under drained conditions for all groups and for both PDFs. As shown in Table 8, for θ = 30° and for both PDFs, the model predicts the Group 1 tests quite well (Table 8), greatly overpredicts the average ultimate uplift capacity for Group 2 (Table 9), underpredicts it for Group 3 (Table 10), and grossly overpredicts it for drained conditions (Table 12). In general the model yields a very wide and unacceptable dispersion, which reflect in high values of V_r. The R^2-values for this model are significantly higher for the lognormal PDF than for the normal PDF, indicating a better fit with the latter.

The traditional cylindrical shear model was applied to the undrained shear test data (Table 8 through Table 11), using α values proposed by Sowa [B145] (see Figure 46). The α values proposed by Sowa were used since the model being evaluated does not include tip resistance, which is the basis of Sowa's α values. For all test groups and both PDFs, the mean values of r for undrained loading are close to 1.0 (0.98 to 1.21) and the model has a relatively moderate dispersion, i.e., the V_r varies from 14% to 32% for the normal PDF and 13% to 33% for the lognormal PDF. The drained test data (Table 12) were analyzed applying K values calculated in Reference [B147]. The model slightly overpredicts the average capacity for both the normal and lognormal PDFs ($\bar{r}$ = 1.02 and 1.01, respectively). Again, values of V_rS are relatively small under drained conditions.

The statistical data for CUFAD show that the value of $\bar{r}$ under undrained conditions ranged from 0.81 to 1.02 and that the coefficient of variation, V_r, ranged from 22% to 33% when using a normal distribution approach. The $\bar{r}$-value ranged from 0.81 to 1.03 and V_r varied from 22% to 34% when considering a lognormal distri-

Copyright © 2001 IEEE. All rights reserved.

Copyright The Institute of Electrical and Electronics Engineers, Inc.
Provided by IHS under license with IEEE
No reproduction or networking permitted without license from IHS Not for Resale

bution. The value of $\bar{r}$ was equal to 0.99 and 1.0 for the normal and lognormal PDFs, respectively, under drained conditions and the corresponding values of V_r were 24% and 30% for the normal and lognormal distributions, respectively. The R^2-values obtained for each of the groups analyzed indicate that the lognormal PDF fits the data slightly better than the normal PDF.

The statistical analysis on the available data for straight drilled shafts under uplift loads suggests that the lognormal PDF best fits the results for ultimate capacity. Also, as shown in Figure 48 and Table 8 through Table 11, the traditional cylindrical model and CUFAD give the best predictions. The truncated cone method is the least reliable method among the three.

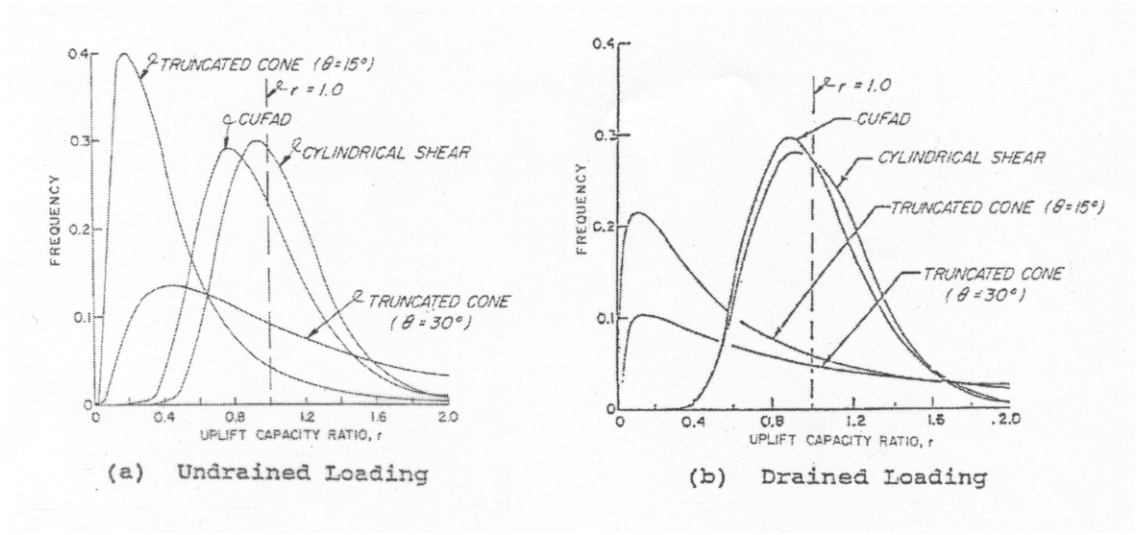

Figure 48—Lognornal distribution for drilled shafts under uplift loads:
(a) Undrained loading conditions (65 load test cases) (from Table 11 [B54])
(b) Drained loading conditions (13 load test cases)

It is interesting to note that the performance of the cylindrical shear and CUFAD models improves with more accurate geotechnical data, as reflected in lower values of V_r, for the Group 1 tests (Table 8). This trend indicates that the dispersion of the models is much better when design parameters are measured via a thorough subsurface exploration program at each site. In addition, the V_r values for each model tend to improve when applying the lognormal PDF, but both the normal and lognormal PDFs yield similar statistical results when the model dispersion is small.

5.3.1.5 Foundation displacements

In addition to studying the conditions under which a foundation will be stable, criteria for allowable uplift displacements should be met. Data from many field full scale uplift tests on drilled shaft foundations have shown that in nearly all cases, full uplift capacity is mobilized with less than 13 mm (0.5 in) of displacement [B147]. Because almost all transmission structures can accommodate this much movement without distress [B33] [B95], designs that satisfy stability will normally be acceptable for both strength and deformation considerations.

Copyright © 2001 IEEE. All rights reserved.

Copyright The Institute of Electrical and Electronics Engineers, Inc.
Provided by IHS under license with IEEE
No reproduction or networking permitted without license from IHS
Not for Resale

5.3.2 Compression load capacity and displacements

The compression load capacity of a drilled shaft is composed of side and tip resistance. The available load test data suggest no consistent difference in the side resistance for uplift and compressive loadings. However, a number of theories have been derived for the tip resistance (bearing capacity) of drilled shafts under compression. One of the most widely used approaches is presented here. This approach is implemented in CUFAD [B159].

5.3.2.1 Ultimate capacity

Figure 49 shows the geometry and free-body diagram for a drilled shaft foundation under an applied axial compression load.

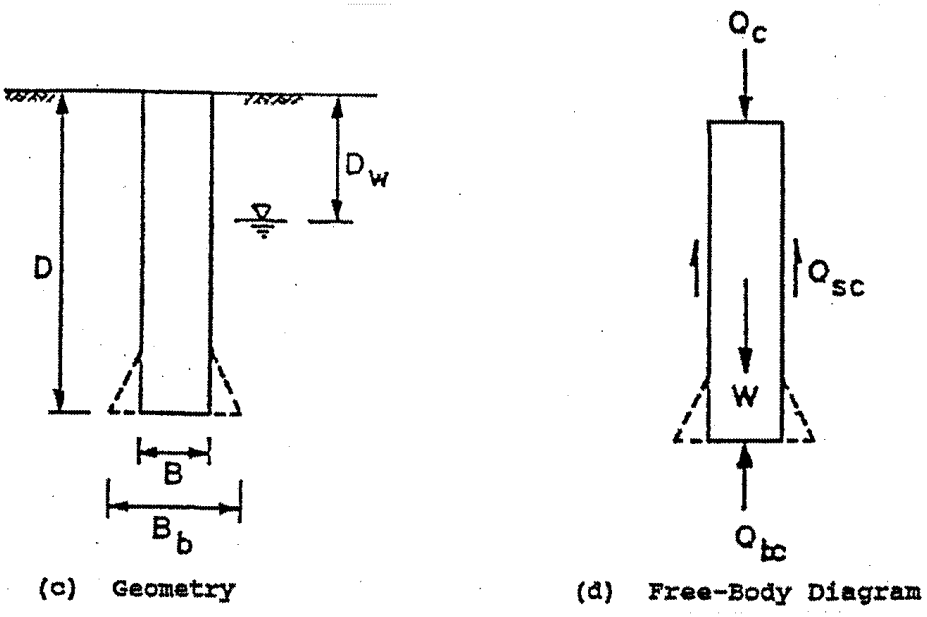

Figure 49—Compression analysis of drilled shaft foundations

The ultimate compression capacity is given by the equilibrium equation:

$$Q_c = Q_{tc} + Q_{sc} - W \quad (100)$$

where

Q_c is ultimate compressive capacity,
Q_{tc} is tip resistance in compression,
Q_{sc} is side resistance in compression,
W is weight of the foundation.

The foundation weight does not depend on the direction of loading, and therefore either the effective foundation weight or the total foundation weight should be used for drained or undrained conditions, respectively. Equation (75) gives the value of the effective weight for a straight shaft.

Copyright © 2001 IEEE. All rights reserved.

Copyright The Institute of Electrical and Electronics Engineers, Inc.
Provided by IHS under license with IEEE
No reproduction or networking permitted without license from IHS
Not for Resale

The available data suggests no consistent difference in the side capacity for uplift and compressive loadings, except that the cone breakout mechanism for short shafts is not possible in compression [B95]. The approach indicated by the cylindrical shear model in 5.3.1.2 can be used to compute Q_{sc} in Equation (100) for compression loading, Equation (81) for undrained loading and Equation (84) for drained loading.

The tip resistance in compression, Q_{tc}, is a bearing capacity problem that can be written as follows:

$$Q_{tc} = q_{ult} A_b \tag{101}$$

where

q_{ult} is maximum bearing capacity at the foundation base,
A_b is area of the foundation base.

Drained Loading. In general, the drained bearing capacity is given by [B130]:

$$q_{ult} = 0.5 B \bar{\gamma}_s N_\gamma \zeta_{\gamma r} \zeta_{\gamma s} \zeta_{\gamma d} + \bar{q} N_q \zeta_{qr} \zeta_{qs} \zeta_{qd} \tag{102}$$

For a circular foundation, $\zeta_{\gamma s} = 0.6$ and $\zeta_{\gamma d} = 1$, resulting in:

$$q_{ult} = 0.3 B \bar{\gamma}_s N_\gamma \zeta_{\gamma r} + \bar{q} N_q \zeta_{qr} \zeta_{qs} \zeta_{qd} \tag{103}$$

where

$\bar{\gamma}_s$ is average effective soil unit weight between D and D+B,
N_γ is bearing capacity factor for friction,
N_q is bearing capacity factor for overburden,
$\bar{q}$ is in situ effective vertical stress at a depth of D + B/2,
ζ is bearing capacity modification factors for soil rigidity, foundation shape, and foundation depth.

The bearing capacity factors for drained loading are given by

$$N_q = [\exp(\pi \tan \bar{\phi})] \tan^2(45° + \bar{\phi}/2) \tag{104}$$

$$N_\gamma \cong 2(N_q + 1) \tan \bar{\phi} \tag{105}$$

Several calculations are necessary to evaluate the ζ modification factors indicated in Equation (102). First, it is necessary to compute the critical rigidity index, I_{rc}:

$$I_{rc} = 0.5 \exp[2.85 / \tan(45° - \bar{\phi}/2)] \tag{106}$$

Next, the soil rigidity index, I_r, is computed from:

$$I_r = E / [2(1 + \upsilon) \bar{q} \tan(\bar{\phi})] \tag{107}$$

where

E is Young's modulus,
υ is Poisson's ratio.

Copyright © 2001 IEEE. All rights reserved.

Copyright The Institute of Electrical and Electronics Engineers, Inc.
Provided by IHS under license with IEEE
No reproduction or networking permitted without license from IHS
Not for Resale

The Young's modulus, E, can be evaluated from field or laboratory tests or can be estimated [B33] [B147]. Poisson's ratio ranges from about 0.1 to 0.4 for granular soils and can be estimated from [B159]:

$$\upsilon = 0.1 + 0.3\bar{\phi}_{rel} \tag{108}$$

where

$\bar{\phi}_{rel}$ is relative friction angle estimated by:

$$\bar{\phi}_{rel} = (\bar{\phi} - 25°)/(45° - 25°) \tag{109}$$

and has the limits of 0 and 1. Finally, the rigidity index is reduced for volumetric strains to yield:

$$I_{rr} = I_r/(1 + I_r\Delta) \tag{110}$$

where

I_{rr} modified rigidity index, and Δ can be approximated by [B159]:

$$\Delta = 0.05\bar{q}(1 - \bar{\phi}_{rel}) \text{ (for } \bar{q} \text{ in tsf, up to 10 tsf maximum)} \tag{111}$$

The ζ modification factors are given by:

$$\zeta_{\gamma r} = \exp\{[-3.8\tan\bar{\phi}]\} + [(3.07\sin\bar{\phi})(\log_{10}2I_{rr})/(1 + \sin\bar{\phi})] \tag{112}$$

subject to the condition that $\zeta_{\gamma r} \leq 1$. Also:

$$\zeta_{qr} = \zeta_{yr} \tag{113}$$

$$\zeta_{qs} = 1 + \tan\bar{\phi} \tag{114}$$

$$\zeta_{qd} = 1 + 2\tan\bar{\phi}(1 - \sin\bar{\phi})^2\tan^{-1}(D/B) \tag{115}$$

in which $\tan^{-1}$ (D/B) is expressed in radians.

Undrained Loading. For drilled shafts in granular or cohesionless soils, undrained conditions are likely to be of only minor importance because excess pore water stresses dissipate rapidly with respect to the duration of the load. For these soils, the undrained bearing capacity can be considered equal to the drained capacity.

For cohesive soils, such as clays and silts, undrained bearing capacity can be computed as [B95]:

$$q_{ult} = N_c s_u \zeta_{cr}\zeta_{cs}\zeta_{cd} + q \tag{116}$$

where

N_c is bearing capacity factor for cohesion,
q is total overburden stress at a depth D.

Copyright © 2001 IEEE. All rights reserved.

Copyright The Institute of Electrical and Electronics Engineers, Inc.
Provided by IHS under license with IEEE
No reproduction or networking permitted without license from IHS Not for Resale

For a circular foundation under these conditions, $N_c = 5.14$ and $\zeta_{cs} = 1.2$, so that:

$$q_{ult} = 6.17 s_u \zeta_{cr} \zeta_{cd} + q \tag{117}$$

The other ζ factors are given by:

$$\zeta_{cr} = 0.44 + 0.6 \log_{10} I_{rr} \tag{118}$$

subject to the condition that $\zeta_{cr} \leq 1$. I_{rr} is calculated using Equation (110) and Equation (121) (below). Also,

$$\zeta_{cd} = 1 + 0.33 \tan^{-1}(D/B) \tag{119}$$

in which $\tan^{-1}$(D/B) is expressed in radians. To evaluate whether ζ_{cr} will be less than 1, corresponding to local or punching shear failure, several calculations are required. First, it is necessary to compute the critical rigidity index. For circular foundations and undrained conditions, $\phi = 0$, and Equation (106) reduces to:

$$I_{rc} = 0.5 \exp(2.85) = 8.64 \tag{120}$$

The soil rigidity index is given by:

$$I_r = E/2(1 + \upsilon) S_u \tag{121}$$

However, since Poisson's ratio, $\upsilon \cong 0.5$ for saturated clays in undrained loading, the expression can be simplified to:

$$I_r = E/3 S_u \tag{122}$$

Accordingly, volumetric strains are zero, and $\zeta_{cr} < 1$ if $I_{rc} < 8.64$.

5.3.2.2 Foundation displacements

It is well-documented that, although the side shear capacity of drilled shafts generally is fully mobilized with less than 13 mm (0.5 in) of displacement, the tip capacity requires considerably more displacement, typically about 10% of the shaft diameter. Differential displacements of this magnitude are greater than most transmission line structures can tolerate, and therefore the tip capacity should be reduced to reflect the resistance offered at tolerable displacements. The conservative linearized approximation shown in Figure 50 can be used, in which the tip capacity is estimated along a secant drawn between the origin and the point at which maximum bearing capacity develops. For practical purposes, the weight and side resistance terms can be assumed to develop with the onset of displacement. Accordingly, the total compressive capacity is given by:

$$Q_c = \left(\frac{10 d_{\text{allow}}}{B}\right)(Q_{tc} - W) + Q_{sc} \tag{123}$$

where

d_{allow} is the allowable total foundation settlement.

Consolidation settlements in cohesive soils may require a considerably more detailed approach and should be evaluated by an experienced geotechnical engineer.

Copyright © 2001 IEEE. All rights reserved.

Copyright The Institute of Electrical and Electronics Engineers, Inc.
Provided by IHS under license with IEEE
No reproduction or networking permitted without license from IHS
Not for Resale

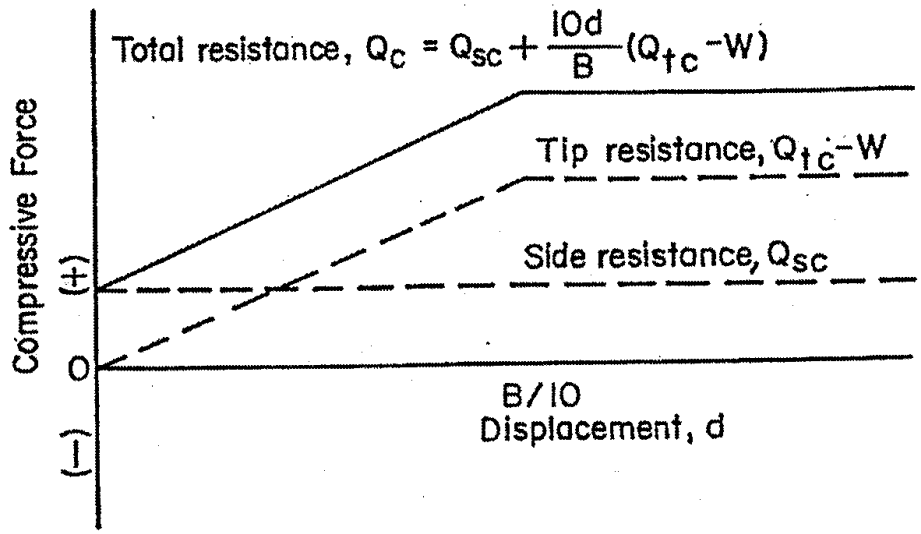

Figure 50—Summation of capacity terms for compression loading

5.3.3 Lateral and moment load capacity and displacements

Various design philosophies are currently used by the utility industry for lateral and moment loaded drilled shaft design. Some designers permit the drilled shaft foundation to reach some percentage of its ultimate geotechnical capacity at the maximum design load. Some designers limit soil pressures, as determined from elastic analysis, to allowable values under a working load, while others design to certain deflection and/or rotation criteria at various load levels. Regardless of the criteria used in design, the shaft-soil foundation must be safe against both total collapse (ultimate structural and geotechnical capacities) and excessive movement (shaft deflection and/or rotation).

The response of the drilled shaft foundations under lateral and moment loads is highly nonlinear. At relatively low load levels the deflection of the foundation consists of an elastic or recoverable component and a plastic or non-recoverable component. Such a combination of recoverable and non-recoverable deflections is commonly referred as elastic-plastic deformation. As load levels increase, the plastic component of total deflection increases until the ultimate capacity of the foundation (ultimate plastic load) is reached and static equilibrium under the applied load can no longer be maintained if a higher load is applied to the shaft. The deflection behavior of the drilled shaft is at this point fully plastic and the load applied to the foundation is referred to as the ultimate geotechnical capacity.

A simplified representation of the potential forces acting on the perimeter of a laterally loaded drilled shaft is shown in Figure 51. Lateral and moment loads applied to the top of the drilled shaft are resisted by a combination of forces including: lateral forces acting perpendicular and tangential to the surface of the shaft, vertical side shear forces acting on the surface of the shaft, a shear force acting parallel to the surface of the base of the shaft, and a base force acting upward perpendicular to the base of the shaft.

As the shaft tends to move under the system of applied lateral and moment loads, active and passive pressures may be envisioned as acting on opposing sides of the shaft. Above the center of rotation, the surface of the shaft is pressed into the soil on the front side of the shaft (mobilizing passive soil resistance) and moves away from the soil on the backside (reducing the soil pressure toward the active earth pressure condition).

Copyright © 2001 IEEE. All rights reserved.

Copyright The Institute of Electrical and Electronics Engineers, Inc.
Provided by IHS under license with IEEE
No reproduction or networking permitted without license from IHS
Not for Resale

Below the center of rotation, the opposite condition exists; passive pressure is developed on the backside of the shaft and active pressure on the front side of the shaft.

However, it may be noted that in general, the passive forces are much larger than the active forces. Furthermore, based on the results of full-scale load tests conducted on drilled shafts in both cohesive and granular soils, a gap tends to develop above the center of rotation on the back side of the shaft and it is assumed to occur below the center of rotation on the front side of the shaft [B43]. Consequently, the system of forces acting on the shaft may be simplified as shown in Figure 51.

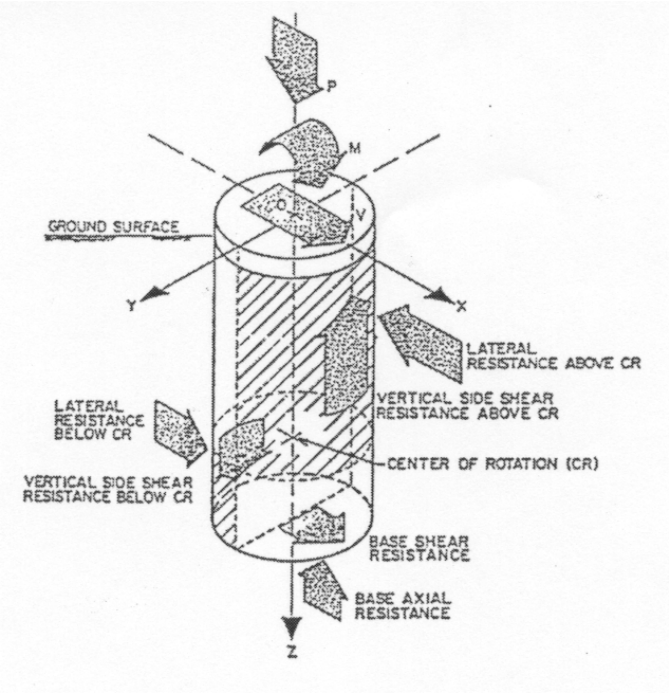

Figure 51—Potential forces acting on a drilled shaft foundation

The lateral resistance (force) developed on front of the shaft and above the center of rotation and the lateral resistance (force) developed on back of the shaft and below the center of rotation, can be computed as the sum of the contributions from the radial compressive stress and from the horizontal component of the shear stress, over the face of the shaft.

The vertical side shear and base shear forces are developed due to the movement of the shaft relative to the surrounding soils. As the shaft rotates, its surface slides downward on the front side relative to the soil, generating upward shear forces on the front and above the center of rotation, and downward shear forces on the back and below the center of rotation of the shaft. Similarly, the base of the shaft translates backwards in the opposite direction of the applied loads and a base shear force is developed which acts in the same direction as the applied loads.

The base normal force acts perpendicular to the base of the shaft and represents the reaction of the soil due to the loads applied at the top of the shaft, the weight of the shaft, and the net force associated with this vertical side shear resisting forces. Due to the rotation of the base of the shaft, the magnitude of the pressure at the front edge of the base of the shaft is greater than at the back edge of the base. If the rotation is sufficient, only a portion of the base may remain in contact with the soil.

Copyright © 2001 IEEE. All rights reserved.

Copyright The Institute of Electrical and Electronics Engineers, Inc.
Provided by IHS under license with IEEE
No reproduction or networking permitted without license from IHS
Not for Resale

Analytical models to predict the nonlinear load-deflection behavior and ultimate load capacity of drilled shaft foundations should ideally consider the contribution of all of the significant acting forces. Historically, most of the ultimate capacity and load-deflection models have been based on the assumption that the interaction between shaft and soil can be characterized by net lateral (horizontal) soil pressures and a corresponding pressure/deflection relationship. Other forces associated with stresses on the base of the shaft and the vertical side shear stresses on the perimeter of the shaft have been neglected.

A variety of ultimate capacity [B51] [B32] [B31] [B30] [B59] [B71] [B105] [B101] [B121] [B127] [B131] and load-deflection [B51] [B32] [B31] [B30] [B44] [B45] [B52] [B43] [B67] [B96] [B103] [B120] [B133] [B134] [B136] [B153] models have been proposed for rigid (short) and for flexible (long) drilled shafts. The simplest of these models has assumed that the shaft is rigid, the load-deflection relationship is linear, and that the soil surrounding the embedded length of the foundation is homogeneous. Other solutions have attempted to model (either collectively or separately) the flexibility of the shaft, soil stratification, and the nonlinear load-deflection response of the soil-shaft system. However, in general, only the lateral resisting forces have been considered. The analytical models which are the most commonly used in practice today are those developed by Broms [B32] [B31] [B30], Hansen [B71], Reese [B103] [B133] [B136], and the computer code MFAD (Moment Foundation Analysis and Design) developed by Davidson [B43], and Bragg et al. [B28] [B51]. These models are briefly presented here followed by a statistical evaluation [B53] of their ability for predicting lateral and moment load capacity based on the reported behavior of a number of full scale straight drilled shaft tests [B43].

5.3.3.1 Broms' method

Broms utilizes a single layer approach for cohesive [B30] and cohesionless soils [B31]. For cohesive soils under undrained loading, Broms uses the distribution shown in Figure 52, part b where s_u is the undrained shear strength of the soil and B is the shaft diameter. For cohesionless soils (drained conditions), Broms utilizes the lateral earth resistance distribution shown in Figure 52, part c where γ_s is the effective unit weight (force/length^3) of the soil, D is the embedment depth of the shaft, and K_p is the Rankine's passive earth pressure coefficient [B105]. As shown in Figure 52, part c, the high lateral earth pressures developed at the back of the shaft near its base are approximated by a concentrated load acting at the toe of the shaft. The ultimate lateral and moment load and concentrated force at the base of the shaft can be determined from the equations of equilibrium.

5.3.3.2 Hansen's method

Hansen [B71] has proposed the following equation for the ultimate lateral resistance, p_{ult} (force/length), at a given depth acting on the shaft:

$$p_{ult} = \bar{q}K_qB + cK_cB \tag{124}$$

where

$\bar{q}$ is effective overburden pressure at a certain depth,
c is cohesion,
K_q is earth pressure coefficient for overburden pressure,
K_c is earth pressure coefficient for cohesion.

The earth pressure coefficients K_q and K_c are functions of the angle of friction of the soil as well as the depth to shaft diameter ratio at the point in question. Charts for K_q and K_c are presented in References [B71] and [B130]. Note that under undrained conditions, the first term becomes zero since $K_q = 0$ when $\phi = 0$ and c is replaced by the undrained shear strength of soil, s_u. Hansen's equations are directly applicable to multi-layered soil profiles as shown in Figure 53. The ultimate lateral and moment capacity for a given drilled shaft can be determined for the equations of equilibrium.

Copyright © 2001 IEEE. All rights reserved.

Copyright The Institute of Electrical and Electronics Engineers, Inc.
Provided by IHS under license with IEEE
No reproduction or networking permitted without license from IHS Not for Resale

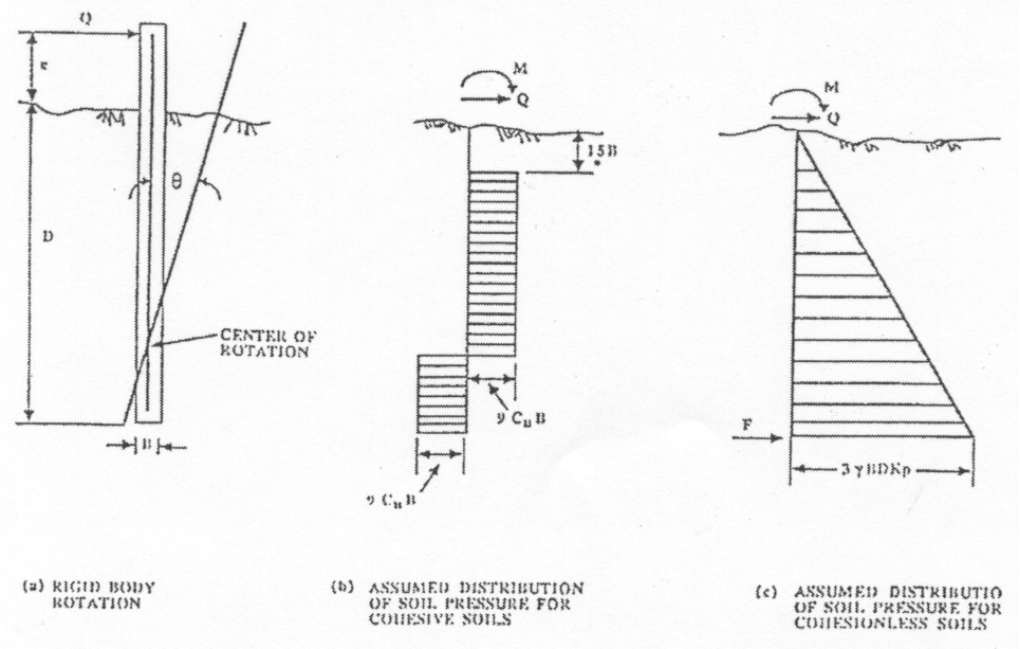

Figure 52—Idealized ultimate capacity method for laterally loaded drilled shaft as per Broms [B30] [B31]

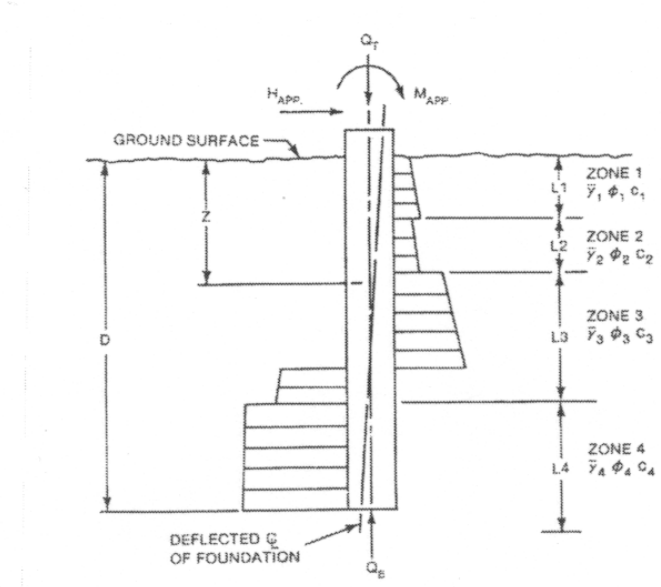

Figure 53—Ultimate lateral pressure for a multilayered subsurface profile [B71]

Copyright © 2001 IEEE. All rights reserved.

Copyright The Institute of Electrical and Electronics Engineers, Inc.
Provided by IHS under license with IEEE
No reproduction or networking permitted without license from IHS
Not for Resale

5.3.3.3 Reese's method

Reese [B136] has proposed equations for the ultimate lateral resistance for a soil which is idealized as being purely cohesive (undrained condition), i.e., $\phi = 0$, where ϕ is the angle of internal friction of the soil. Thus, referring to Equation (124), the ultimate resistance, p_{ult}, can be defined by $s_u K_c B$. At depths in excess of approximately three shaft diameters, Reese calculated a value of 12 for K_c and a value of 2 at ground surface.

Matlock [B101] has posed the following equations for ultimate lateral resistance, p_{ult} (force/length), in soft cohesive soils.

$$p_{ult} = \bar{q}B + 3cB + 0.5zc \leq 9cB \tag{125}$$

where

z is depth in question.

The limiting lateral soil pressures (9cB) is identical to the ultimate lateral soil pressure posed by Broms [B30]. Equation (125) was also recommended by Reese and Welch [B136] relative to developing p-y curves for stiff clays.

Parker and Reese [B121] recommend that the ultimate lateral resistance, p_{ult} (force/length), in sand be taken as the lowest value from the following two equations:

$$p_{ult} = \bar{\gamma}_s z[B(K_p - K_a) + zK_p(\tan\bar{\alpha}\tan\bar{\beta}) + zK_o\tan\bar{\beta}(\tan\bar{\phi} - \tan\bar{\alpha})] \tag{126}$$

$$p_{ult} = \bar{\gamma}_s zB[K_p^3 + 2K_p^2K_o\tan\bar{\phi} - K_a + 2K_o\tan\bar{\phi}] \tag{127}$$

where

$\bar{\gamma}_s$ is average effective unit weight above the point in question,
K_p is Rankine passive earth pressure coefficient [B97],
K_a is Rankine active earth pressure coefficient [B97],
K_o is at-rest earth pressure coefficient,
$\bar{\phi}$ effective friction angle for the sand.

$\bar{\alpha}$ and $\bar{\beta}$ define the geometry of the failure mechanism and are functions of the relative density of the soil and the angle of internal friction (see Figure 54).

The ultimate resistance formulations by Reese and Welch [B136] for stiff clay, Matlock [B101] for soft clay, and Parker and Reese [B121] for sands, as well as nonlinear models incorporating these ultimate pressures have been developed for conditions in which the lateral force is the predominant applied force (i.e., small eccentricity) and are referred to hereafter, for convenience, as "Reese's method".

Copyright © 2001 IEEE. All rights reserved.

Copyright The Institute of Electrical and Electronics Engineers, Inc.
Provided by IHS under license with IEEE
No reproduction or networking permitted without license from IHS Not for Resale

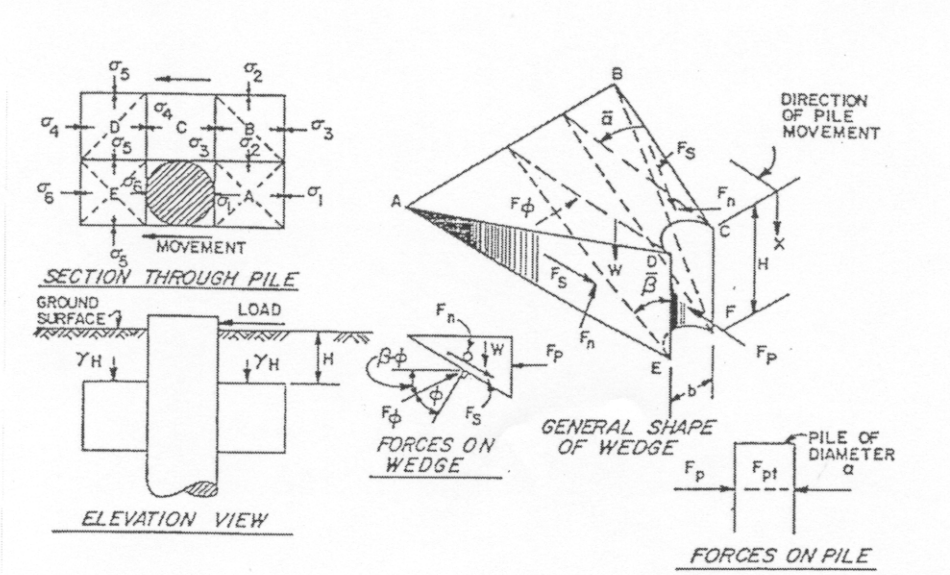

Figure 54—Reese's assumed deep and surface failures in sand [B133]

5.3.3.4 MFAD

A design/analysis model for drilled shafts subject to lateral and moment loads was developed [B43] and has been translated into a computer code, MFAD, available in EPRI's TLWorkstation™. The model considers both flexible and nearly rigid shafts embedded in multi-layered subsurface profiles. The model idealizes the soil as a continuous sequence of independent springs, as in the beam on elastic foundation problem addressed by Hetenyi [B74]. It consists of a so-called nonlinear four-spring, subgrade modulus approach in which each of the four significant sets of resisting forces shown in Figure 51 (lateral resistance, vertical side shear, base shear, and base normal force or base moment) have been represented as discreet springs. Referring to Figure 55, nonlinear lateral translational springs are used to characterize the lateral force-displacement response of the soil, vertical side shear moment springs are used to characterize the moment developed at the shaft centerline by the vertical shear stress at the perimeter of the shaft induced by shaft rotation, a base translational spring is used to characterize the horizontal shearing force-base displacement response, and a base moment spring is used to characterize the base normal force-rotation response.

The four-spring ultimate capacity model incorporates previous work by Hansen [B71] and by Ivey [B83]. The ultimate lateral force, P_{ult}, for a given layer is determined from the ultimate lateral bearing capacity theory developed by Hansen [B71]. For a circular shaft, this force can be said to be the integrated sum of normal stresses and horizontal shearing stresses along the shaft perimeter. A vertical shearing stress is posed such that the vector resultant of the vertical and horizontal shearing stresses correspond to the fully mobilized shear strength of the soil at the shaft-soil interface [B83].

The ultimate shearing force and moment at the base of the shaft are determined from an equation of vertical equilibrium combined with assumptions concerning the percentage of the base in contact with the subgrade and the distribution of the base normal stresses.

Copyright © 2001 IEEE. All rights reserved.

Copyright The Institute of Electrical and Electronics Engineers, Inc.
Provided by IHS under license with IEEE
No reproduction or networking permitted without license from IHS
Not for Resale

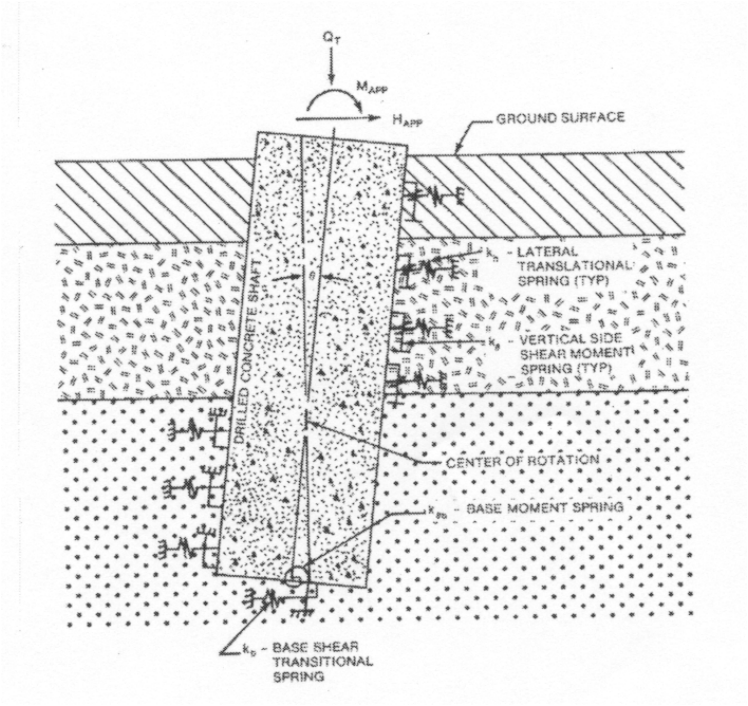

Figure 55—MFAD four-spring subgrade modulus model

5.3.3.5 Statistical analysis of models

A statistical analysis of the four models described above was performed by DiGioia et al. [B53] and involved computing the ultimate moment capacity predicted by each model for seventeen full scale load tests and comparing the predicted ultimate moment capacity (R_n) with the measured moment (R_{test}) at two-degree rotation. The predicted ultimate moment capacities were computed using subsurface data available for each test site which included standard penetration resistance data, pressuremeter data, and laboratory density and strength data. Based on the quality of the subsurface data, the load tests were divided into two groups. The first group, the EPRI load tests, involved detailed subsurface investigations at each site, including extensive laboratory test data [B43]. The eleven EPRI tests are designated as Group 1 tests in Table 13. The remaining 6 load tests conducted by ITT and Ontario-Hydro [B43] did not provide measured strength and density data, and therefore standard penetration resistance data were used to establish strength and density parameters. These tests are designated as Group 2 in Table 13. The definition of measured ultimate lateral and moment capacity for the load tests is given in Reference [B43].

The results of the statistical analysis are summarized in Table 13 for normal and lognormal distributions. In this table, $\bar{r}$ corresponds to the average of the ratio of the predicted (R_n) to the ultimate capacity (R_{test}), V_r is the coefficient of variation of r, and R^2 corresponds to a correlation coefficient of the results. Figure 56 shows the lognormal results obtained considering all seventeen cases.

Copyright © 2001 IEEE. All rights reserved.

Copyright The Institute of Electrical and Electronics Engineers, Inc.
Provided by IHS under license with IEEE
No reproduction or networking permitted without license from IHS
Not for Resale

Copyright The Institute of Electrical and Electronics Engineers, Inc.
Provided by IHS under license with IEEE
No reproduction or networking permitted without license from IHS

Table 13—Ultimate lateral capacity models [B53]

Group	Number of Tests	Brohms			Hansen			Reese			MFAD		
		$\bar{r}$	V_r(%)	R^2	$\bar{r}$	V_r(%)	R^2	$\bar{r}$	V_r(%)	R^2	$\bar{r}$	V_r(%)	R^2
Normal Distribution													
1	11	0.67	45	0.92	0.78	38	0.89	0.65	41	0.88	0.9	33	0.87
2	6	1.07	N/S	—	0.68	N/S	—	0.56	N/S	—	1.27	N/S	—
All	17	0.82	43	0.94	0.75	37	0.91	0.62	44	0.94	1.09	31	0.95
Lognormal distribution													
1	11	0.84	53	0.91	0.79	38	0.94	0.65	41	0.94	1.00	36	0.87
All	17	0.84	53	0.90	0.75	37	0.96	0.62	48	0.97	1.10	34	0.91

NOTES

a) N/S: Not sufficient data to compute V_r values.
b) N/A: Not available.
c) R^2: Coefficient of correlation estimated when considering all 17 tests and based on regression analyses of the data.

Copyright © 2001 IEEE. All rights reserved.

Not for Resale

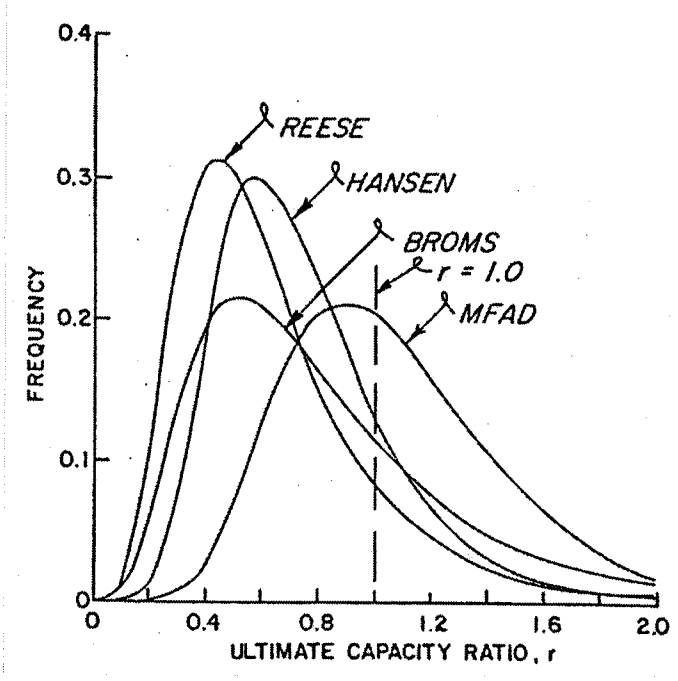

Figure 56—Lognormal distributions for laterally loaded drilled shaft analytical models [B53]

An examination of Table 13 leads to the following conclusions considering the normal PDF results:

— For the Group 1 tests, the lateral-resistance-alone models (using Hansen's, Broms', and Reese's methods) underpredict the ultimate moment capacities by 22% to 35%, on the average ($\bar{r}$ ranges from 0.65 to 0.78).

— For the Group 1 tests, MFAD predicts ultimate moment capacity very well, since its calibration was based on these tests.

— For the Group 1 tests, the coefficients of variation, V_r, varied from a low of 33% for MFAD to 45% for the Broms' model.

— For all the data, where the average quality of geotechnical data is less than for Group 1 tests, the lateral-resistance-alone models continue to underpredict ultimate capacities and MFAD slightly overpredicts ultimate capacities but continues to have the lowest coefficient of variation, V_r.

— For all the data, the coefficient of correlation, R^2, varies from 0.91 for Hansen's model to 0.95 for MFAD. The R^2-values were estimated by means of regression analysis using a least square fit on the statistical data obtained by the method of moments.

The results obtained when applying the lognormal PDF to all of the cases (See Table 13 and Figure 56) lead to the following conclusions:

Copyright © 2001 IEEE. All rights reserved.

Copyright The Institute of Electrical and Electronics Engineers, Inc.
Provided by IHS under license with IEEE
No reproduction or networking permitted without license from IHS
Not for Resale

— The lognormal PDF models the data better than the normal PDF in that the R^2-values for the lognormal PDF are equal to or higher than those for the normal PDF. The R^2-values were obtained by means of a regression analysis using a least square fit on the statistical data obtained by the method of moments. Also, the lognormal PDF eliminates negative r-values.

— For those cases where the width of the frequency distribution is narrower, the statistical parameters obtained by the two distributions are similar.

— The model that shows the largest difference between normal and lognormal PDF is that proposed by Broms. Whereas the mean, $\bar{r}$, increased from 0.82 for the normal PDF to 0.84 for the lognormal PDF, the coefficient of variation increased from 43% to 53%, respectively for the above mentioned distributions, implying a much larger scatter in model predictions for the lognormal PDF than for the normal PDF.

— The models by Hansen, Reese, and MFAD show small differences for the mean and coefficient of variation between the normal and lognormal PDFs and the conclusions derived from the results obtained for the normal PDF are essentially still valid.

— The data base (17 cases) is not large enough to draw a definitive conclusion on which of the two distributions should be used for laterally loaded drilled shafts, but it seems that the lognormal distribution has clear advantages with respect to the normal distribution.

5.3.3.6 Foundation displacements

The stress-strain behavior of soil is highly nonlinear. In this regard, Reese and his co-workers have developed so-called p-y curves, where y is the shaft deflection and p is the soil reaction pressure (force/unit length). For example, Matlock [B101] has proposed the following equation for soft clays:

$$\frac{p}{p_{ult}} = 0.5\left(\frac{y}{y_{50}}\right)^{\frac{1}{3}} \tag{128}$$

where

y_{50} is deflection at one-half of the ultimate lateral pressure

Reese and Welch [B136] have proposed the following equation for stiff clays:

$$\frac{p}{p_{ult}} = 0.5\left(\frac{y}{y_{50}}\right)^{\frac{1}{4}} \tag{129}$$

Equation (128) and Equation (129) are fully defined once p_{ult} and y_{50} are known. Matlock [B101] has proposed Equation (125) for calculating p_{ult} and has suggested that y_{50} can be computed using the following equation:

$$y_{50} = 2.5\varepsilon_{50}B \tag{130}$$

where

ε_{50} is strain corresponding to one-half of the maximum principal stress difference (sometimes called the deviator stress), determined from an unconsolidated, undrained triaxial strength test.

The principal stress difference can be determined from an unconsolidated, undrained triaxial strength test.

Copyright © 2001 IEEE. All rights reserved.

Copyright The Institute of Electrical and Electronics Engineers, Inc.
Provided by IHS under license with IEEE
No reproduction or networking permitted without license from IHS
Not for Resale

Parker and Reese [B121] have proposed the following p-y curve for sand:

$$\frac{p}{p_{ult}} = \tanh\left(\frac{E_{si}y}{p_{ult}}\right) \tag{131}$$

P_{ult} is defined by Equation (126) or Equation (127), And E_{si} is the initial slope of the p-y curve where

$$E_{si} = \frac{E_m}{1.35} \tag{132}$$

and E_m is the initial slope of the soil stress-strain curve obtained by conducting a consolidated, drained triaxial strength test.

The highly nonlinear load-deflection response of drilled shaft foundations is modeled in MFAD using a nonlinear relationship between lateral pressure and lateral deflection based upon a variant of the so-called p-y curves in conjunction with a finite element beam formulation [B39]. A schematic p-y curve is shown in Figure 57, part a, in which the lateral pressure, p is shown to be nonlinear related to the lateral deflection, y. A tangent to this curve can be said to correspond to a tangent value of the horizontal subgrade modulus. Since a linear model can only intersect the load-deflection curve at one point, a nonlinear approach is necessary to predict shaft deflection at all load levels. The following equation is used for the nonlinear lateral spring pressure-deflection relationship in MFAD:

$$p = 0.6p_{ult}\left(\frac{2k_h y}{p_{ult}}\right) \tag{133}$$

where

p_{ult} is ultimate lateral pressure developed by Hansen [B71].

$$k_h = \frac{5.7E_p}{B}(D/B)^{-0.40} \tag{134}$$

where

E_p is modulus of deformation of the soil measured with a pressuremeter test.

The other three springs of the four-spring model (vertical side shear moment spring, base shear spring, and base moment spring) were modeled as elastic-perfectly plastic springs as shown in Figure 57, parts b, c, and d. The slopes of the elastic part of these curves are defined by Equation (135), Equation (136), and Equation (137), as follows:

Vertical side shear moment spring

$$K_\theta = 0.55E_pB \tag{135}$$

Base Shear force spring:

$$K_b = \frac{2.1E_p}{B}(D/B)^{-0.15} \tag{136}$$

Copyright © 2001 IEEE. All rights reserved.

Copyright The Institute of Electrical and Electronics Engineers, Inc.
Provided by IHS under license with IEEE
No reproduction or networking permitted without license from IHS Not for Resale

Base moment spring:

$$K_{\theta b} = 0.24 E_p B (D/B)^{0.40} \quad (137)$$

Each of the above spring constants (e.g., $K_{\theta b}$) has units of force or moment per unit area. Thus, for example, the total moment acting on the base of the shaft can be computed as:

$$M_b = K_{\theta b} A_b \theta_b \quad (138)$$

where

A_b is area of the base.
θ_b is rotation of the base (in radians).

The linear elastic-perfectly plastic presentation of the vertical side shear moment spring, the base shear spring, and the base moment spring was considered sufficiently accurate for these springs since their contribution to resisting the applied moment and shear load is significantly less than that of the lateral spring. The results of 14 full-scale field load tests conducted on prototype drilled shaft foundations [B43] indicated that these three springs together contributed between 20% to 44% of the shaft foundation stiffness and between 10% and 25% of the ultimate lateral capacity. The nonlinear representation of the lateral spring provided reasonable predictions of the measured load-deflection curves for the tests [B43].

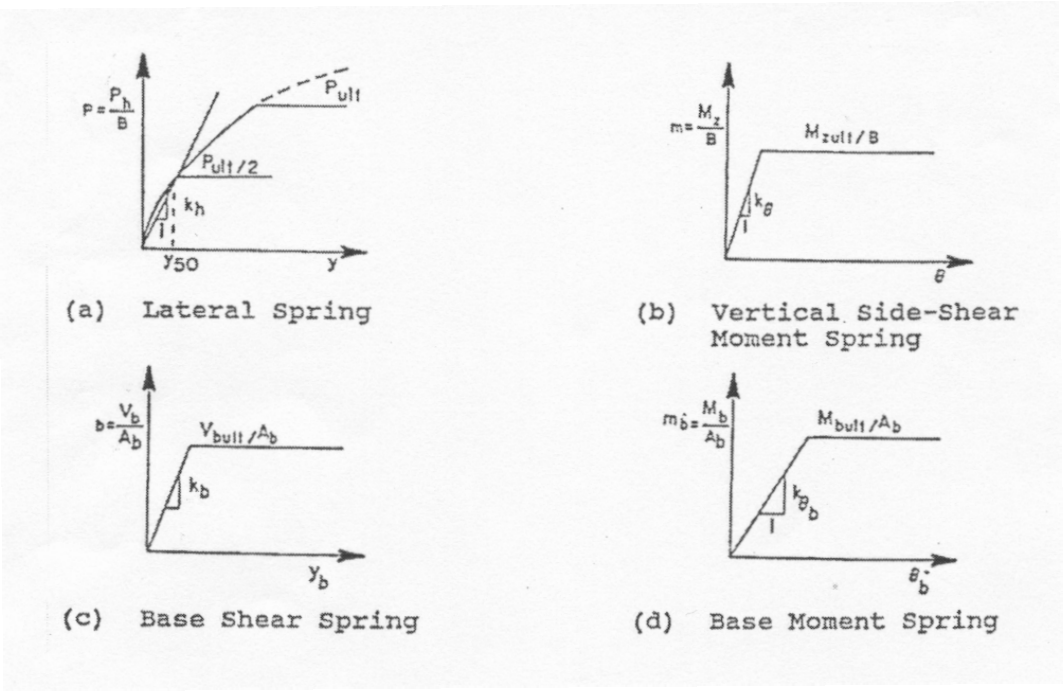

Figure 57—Schematic representation of nonlinear springs in MFAD [B43]

Copyright © 2001 IEEE. All rights reserved.

Copyright The Institute of Electrical and Electronics Engineers, Inc.
Provided by IHS under license with IEEE
No reproduction or networking permitted without license from IHS
Not for Resale

5.4 Direct embedment foundations

The response of direct embedment foundations to compression, uplift, and lateral loads is similar to that of drilled concrete shafts. As outlined above, some of the analytical techniques used in drilled shaft design are relevant to direct embedment design. The principal differences between direct embedment foundations and drilled concrete shaft foundations are (1) the backfill which intervenes between the pole and the in situ soil; and (2) the stiffness of the embedded portion of the pole relative to that of a drilled concrete shaft. Drilled shafts transfer loads directly to the in situ soil. However, direct embedment foundations transfer loads to the backfill which in turn transfer the loads to the in situ soil.

In the cases of uplift and compression, the ultimate capacities are significantly influenced by the type of backfill material and degree of compaction of the backfill. The ultimate shear resistance of drilled shaft foundations is determined by the available shearing strength between the in situ native soil and the surface of the concrete shaft (as described in preceding sections). However, the ultimate capacity of a direct embedment foundation is a function of the available shear strength, not only at the structure shaft-backfill interface, but also potentially at the backfill-native soil interface. Since the annulus between the direct embedment foundation and the native soil is typically thin [usually on the order of 152–203 mm (6–8 in)], the ultimate shear strength of the foundation may be governed by the available shear strength (adhesion and/or friction) at either the surface of the foundation or at the boundary between the backfill and the native soil. If the combined adhesion and frictional resistance of the backfill against the foundation is greater than the shear strength of the native soil, the failure surface controlling the uplift/compression capacity could develop in the native soil adjacent to the backfill surface. However, if the shear strength of the backfill is less than that of the native soil, the tendency would be for the failure surface to develop at the surface of the foundation.

Consequently, it is apparent that the uplift/compression performance of a direct embedment foundation is dependent not only on the native soil characteristics but also on the type of backfill and the corresponding degree of compaction. For cohesive soil backfills, the undrained shear strength, and, thus, the adhesion between the structure shaft and the backfill will be directly related to the stiffness of the backfill after compaction. When granular soils are used as backfill material, the frictional resistance along the structure shaft will depend on the coefficient of lateral earth pressure. If the backfill is compacted to a density comparable to the in situ soil, the coefficient of lateral earth pressure will in general approach the at-rest value of the in situ material. A lesser degree of compaction will result in a value of the lateral earth pressure coefficient which is less than the in situ value. When the annulus is backfilled with concrete, the structure shaft and concrete may be treated as a drilled shaft having a diameter equal to the augered hole diameter.

In the case of direct embedment foundations subjected to lateral and moment loads, the ultimate capacity and load-deflection response of the foundation depends on the relative strength and stiffness of the foundation shaft, backfill and in situ soil. This behavior is complex and is not always subject to simple analytical modeling. However, in certain cases, simplified analysis/design approximations are possible based upon observations made from full-scale lateral load tests conducted on direct embedment foundations:

— If the backfill is considerably stiffer and stronger than the in situ soil, then the backfill may act as part of the foundation and the shaft and backfill react to applied moment and shear loads by moving together with respect to the in situ soil. The ultimate capacity of the foundation will be governed by a failure mechanism developed predominantly in the in situ soil.

— If the backfill is much weaker than the in situ soil, then the embedded structure will respond to shear and moment loads by moving with respect to the backfill and little of the applied load will be resisted by the in situ soil until considerable deformation has occurred.

— If backfill and in situ soil strength and stiffness are comparable, the behavior involves a complex interaction between the two media.

Copyright © 2001 IEEE. All rights reserved.

Copyright The Institute of Electrical and Electronics Engineers, Inc.
Provided by IHS under license with IEEE
No reproduction or networking permitted without license from IHS Not for Resale

Past practices for the design/analysis of direct embedment foundations subjected to shear and moment loads have involved using methodologies developed for the design of drilled shafts by making simplifying assumptions concerning the influence of the backfill on the performance of the foundation. For instance, granular materials, placed in thin layers and compacted, are often used as a backfill and may be stiffer and stronger than many natural soils. If the granular backfill is, in fact, much stronger and stiffer than the in situ soil, the backfill and embedded pole may be treated as an equivalent shaft having a diameter of the drilled hole and bearing on the in situ soil. If the backfill is considerably less strong and stiff than the in situ soil, it is reasonable to compute foundation response by modeling the embedded pole as a shaft bearing on a homogeneous soil having displacement and strength parameters of the backfill. For intermediate cases, it may be possible to average the parameters of backfill and in situ soil. The deflection should also be estimated for the intermediate case by adding the deflections calculated by: (1) treating the embedded pole as a shaft bearing on the backfill; and (2) treating the embedded pole and backfill as a shaft bearing on the in situ soil.

A more rigorous design/analysis model for laterally loaded direct embedment foundations has been developed [B28]. The foundation model (shown in Figure 58) consists of a modified version of the MFAD four-spring subgrade modulus model presented earlier for drilled shaft foundations. Additional springs have been added in-series to the lateral translation spring and the vertical side shear spring to account for the influence of the backfill strength and stiffness on the lateral force-displacement response and the vertical shear stress-vertical displacement response of the foundation backfill-in situ soil system. The base resisting forces have been removed based on the small bottoms of wood and concrete poles and on the thin end plate of steel poles. As in the case of drilled shaft foundations, the nonlinear lateral spring pressure-deflection relationship is given by Equation (133). However, the horizontal subgrade modulus expression has been modified such that:

$$k_h = \left[\frac{5.7 E_a (D/B_o)^{-\beta}}{1 + \left(\frac{E_a}{E_s}\right)\left(\frac{B}{B_o}\right)^{-\beta} - \left(\frac{B}{B_o}\right)^{-\beta}} \right] \frac{1}{B_o} \tag{139}$$

where

E_a is modulus of elasticity of the annulus backfill as evaluated from triaxial strength tests,
E_s is deformation modulus of the in situ soil (determined with a pressuremeter),
B_o is diameter of the foundation,
B is diameter of the augered hole,
D is depth below the ground surface to the base of the foundation.
β is 0.40.

The ultimate strength of the lateral spring was selected as the smaller of the ultimate pressure of the in situ soil computed using Hansen's method [B71] or based on a theoretical model of a shear failure confined to the interior of the backfilled annulus [B28].

The vertical side shear moment spring was modeled as an elastic-perfectly plastic spring as shown in Figure 57, part b, for the drilled shaft foundation. The subgrade modulus, representing the linear elastic portion of the curve was modified to account for the backfill as follows:

$$K_{\sigma d} = \frac{0.55 E_a B_o (B/B_o)^2}{\left(\frac{B}{B_o}\right)^2 + \left(\frac{E_a}{E_s}\right) - 1} \tag{140}$$

Copyright © 2001 IEEE. All rights reserved.

Copyright The Institute of Electrical and Electronics Engineers, Inc.
Provided by IHS under license with IEEE
No reproduction or networking permitted without license from IHS
Not for Resale

where E_s, E_a, B and B_o are as defined for Equation (139). The ultimate strength of the vertical side shear spring was selected as the smaller of the available shear resistance of the foundation-backfill interface or the backfill-in situ soil interface using the same methodology as drilled shaft foundations [B28].

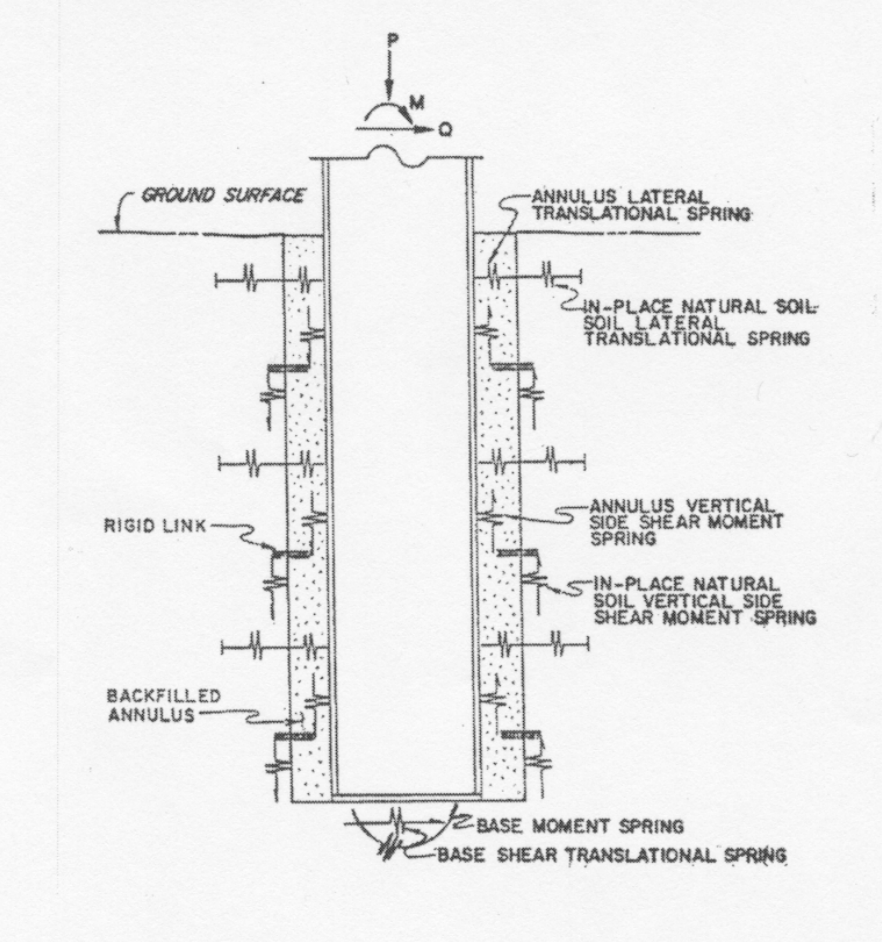

Figure 58—MFAD two-spring subgrade modulus model for direct embedment pole foundations [B28]

A field testing program, consisting of 10 full-scale foundation load tests in soil, was conducted to evaluate the predictive capabilities of the analytical model contained in MFAD (additionally, 2 tests were conducted with the poles partially embedded in rock). Seven of the soil embedded load tests were conducted using tubular steel poles, two load tests were conducted using prestressed concrete poles, and one load test was conducted using a wood pole. The two concrete poles were embedded in silty clay using the native soil as backfill and the remaining eight tests utilized various crushed stone backfills. The test poles varied in length from 19.8 to 34.5 m (66 to 115 ft), 686 to 991 mm (27 to 39 in) in diameter, and the embedded length varied from 1.5 to 3.5 m (5 to 11-1/2 ft). The embedded portion of the poles were instrumented for load measurements, and extensive geotechnical investigations which included in situ and laboratory tests were conducted for the test sites. Groundline deflection and rotation values were also obtained. Thus, these tests would be similar to the previously described Group 1 EPRI tests conducted for drilled shafts.

Copyright © 2001 IEEE. All rights reserved.

Copyright The Institute of Electrical and Electronics Engineers, Inc.
Provided by IHS under license with IEEE
No reproduction or networking permitted without license from IHS
Not for Resale

A fully plastic ultimate capacity can be said to be achieved when little additional load is sufficient to produce considerable additional deflection. This condition was achieved for nine of the tests conducted [B28]. For one of the tests, the maximum applied moment was extrapolated from the applied moment versus measured groundline lateral deflection curve. A statistical analysis was made for the ratio of the predicted ultimate capacity (R_n) to the maximum applied groundline moment (R_{test}) for the 10 foundation tests conducted in soil [B54]. The ratio r of R_n to R_{test} ranged from 0.64 to 1.04 with $\bar{r}$ equal to 0.81 and V_r equal to 12%. The direct embedment analytical model is conservative and under predicts the ultimate geotechnical capacity of the test foundations on the average by approximately 19%. The model is probably slightly less conservative than these data indicate because in seven of the load tests a thick steel base plate was welded to the base of the test pole and thus the base did contribute some resistance to the applied loads, which was not considered in the computed R_n-values.

5.5 Precast-prestressed, hollow concrete shafts and steel casings

The method of design and analysis of precast-prestressed, hollow concrete shafts and steel casing depends on the method of installation. Precast concrete shafts and steel casings can be directly embedded such that the design approach discussed in 5.4 would apply.

5.6 Design and construction considerations

Many aspects in the design of drilled shafts, direct embedded poles, precast-prestressed hollow concrete shafts and steel casings have not been standardized and depend largely on regional experience and previous practice [B132] [B135]. Additional research will be needed to resolve several of the issues raised by these differences found in practice. Several of the more common variations are included below.

5.6.1 Drilled shafts

5.6.1.1 Concreting

Several details of the concreting procedure can influence drilled shaft capacity. In loose, granular soils, drilled without casing or slurry, concrete placement by tremie may be required to prevent falling concrete from disturbing the walls of the hole. Good communication is required between field personnel and designers to permit identification of these conditions.

There is evidence indicating that the use of expansive concrete can increase side capacity by increasing the normal stress on the interface between the shaft and the surrounding soil. For test shafts in stiff clay, it has been found that expansive concrete increased side resistance 50% over concrete made with Type I cement [B142]. While considerable additional research is needed to quantify the effects of expansive concrete in the range of soils found in the United States, as well as the influence of cracking, this relatively inexpensive option should be considered as a possible means of increasing sidewall friction.

If a casing is used to maintain an open hole during shaft construction, it is important to provide adequate clearance between the reinforcing cage and the casing. If less than 75 mm (3 in) of clearance is specified, large aggregate in the concrete can jam between the casing and the cage, causing the cage to pull out with the casing. In some cases, it may be necessary to leave the casing in place.

A minimum of 102 mm (4 in) slump is required to permit adequate flow of the concrete around the reinforcing cage. Vibration at depth is generally difficult and not required for concrete placement if an adequate slump is specified.

Copyright © 2001 IEEE. All rights reserved.

Copyright The Institute of Electrical and Electronics Engineers, Inc.
Provided by IHS under license with IEEE
No reproduction or networking permitted without license from IHS
Not for Resale

5.6.1.2 Shear rings

Shear rings are sometimes used to develop an increased effective diameter for drilled shafts while reducing the overall volume of concrete. Test results from research preformed to verify the quantitative effects of shear rings in the performance of drilled shafts socketed into very weak rock indicate that increasing the roughness of the socket wall can result in a significant increase in shaft resistance [B74].

5.6.1.3 Belled shafts

Belled shafts are commonly used to increase compressive bearing capacity while minimizing the use of concrete. However, since the construction of belled shafts can be difficult along a line where subsurface conditions can vary greatly, their use for transmission line work is more limited. Belling a vertical shaft in granular soil is, at best, difficult, if not impossible. In general, belled shafts are most effective where it is necessary to make use of the strength afforded by a highly overconsolidated upper crust of cohesive soil. In these soils, strength decreases with depth, and increased depth can add little to overall shaft capacity.

The common goal of contractors in constructing belled shafts is to avoid having to hand-clean the bell hole, a task which is both time-consuming and dangerous for the contractor and expensive for the owner. Therefore, firm, cohesive soils are necessary to ensure the successful construction of bells.

Bells are commonly constructed with a 60° angle between the side and base of the bell. However, it has been demonstrated that a 45° bell could provide adequate structural strength for a shaft constructed in a very stiff clay [B143]. Forty-five-degree bells can be reamed with a truck-mounted drill rig, while 60° bells generally require a crane-mounted rig. Thus, although 60° bells are common, 45° bells may be considerably less expensive and should be used where possible.

5.6.2 Direct embedment

Because the construction method for direct embedment foundations differs from that used in cast-in-place concrete shafts, direct embedment deserves special consideration. The backfill clearly constitutes an important element of the direct embedment foundation. Granular backfill can be readily compacted and is generally preferable to a cohesive backfill. To obtain proper compaction, the backfill should be placed in layers of 15 cm (6 in) or less and compacted to the specified density. Various granular backfill materials have been utilized for direct embedment foundations; for example, crushed limestone, sand, and shells. The possibility of using a cement-stabilized backfill is discussed in Reference [B73]. The mix could be installed dry, with water for hydration supplied by ground or rain water. Crushed limestone backfills tend to harden with time as water seeps through the backfill [B54]. The selection of a backfill may also depend on the electrical resistances of the potential backfills.

The uplift capacity of direct embedment foundations is related to the quality of the backfill and the adhesive and frictional forces that can be mobilized at the structure-backfill interface or at the backfill- in situ soil interface. For compression loads, significant end-bearing capacity can only be achieved if the direct embedded pole is closed with a base plate.

5.6.3 Precast-prestressed, hollow concrete shafts and steel casings

Under certain soil conditions, precast-prestressed hollow concrete shafts can be vibrated into place, in which case the problems associated with driving concrete piles should be considered. For example, concrete piles are subject to impact damage from the hammer. There is no conclusive evidence that driving in cohesionless soils produces significant densification for straight-sided shafts. Shafts driven in cohesive soils can produce a significant smear zone of softened, weak soil adjacent to the shaft. Given time prior to structural load, the soil may set up, possibly due to moisture migration, and gain strength, although it will probably never again achieve its undisturbed in situ strength. Thus, a strength reduction for soil parameters should be considered in design.

Copyright © 2001 IEEE. All rights reserved.

Copyright The Institute of Electrical and Electronics Engineers, Inc.
Provided by IHS under license with IEEE
No reproduction or networking permitted without license from IHS Not for Resale

5.6.4 General considerations

5.6.4.1 Negative skin friction

In soils that are still consolidating, such as fill and underconsolidated clays, negative skin friction, or downdrag, can cause significant loads on foundations. This can also occur from a lowering of the ground water table. The magnitude of the downdrag loads can be estimated with the same methods described in 5.3 for shaft side resistance capacity.

5.6.4.2 Expansive soils and rocks

Soil or rock having a high swell potential can create considerable tensile force in reinforced concrete foundations. These forces result from drying of the near-surface soils and can cause tensile failure of the concrete if it is not properly reinforced. Swell of soils, such as montmorillonitic clays, and rocks, such as pyritic shales, is a complex process that depends on a variety of parameters, including the material mineralogy, seasonal and climatic cycles, chemical changes, stress relief, and alteration of the soil moisture and ground water regime. Careful evaluation is required by an experienced geotechnical engineer to determine the potential influence of expansive materials.

5.6.4.3 Mine subsidence

In areas of active or past subsurface mining, ground subsidence and excessive differential settlement is a potential problem. The routing studies for lines crossing such areas should include a thorough evaluation of all mines, and if subsidence is likely to be a problem, rerouting or stabilization may be required. Information on locating mines is given in Reference [B157].

5.6.4.4 Cavernous limestone regions

Soil properties and the soil/rock interface are highly variable in cavernous limestone (karst) regions. These regions can be identified by geologic reconnaissance methods, as described in Reference [B157]. If karst conditions are present, it may be necessary to prove the integrity of acceptable foundation materials at each individual drilled shaft location by percussion drilling or other means. Flexibility of design, careful field inspection, and a procedure for field design alterations are commonly required because of the highly variable subsurface conditions that may be found.

5.6.4.5 Seasonal influence on soil strength

In northern climates, seasonal freeze/thaw cycles can reduce side capacity by disturbing the soil/concrete interface during soil movements. Similar effects can accompany soil wetting and drying in areas of expansive soil. If such conditions are present, it may be prudent to disregard the side capacity to a depth consistent with the effects of seasonal influence.

6. Design of pile foundations

A pile is a structural element that is used to transmit loads through soft soils to underlying competent soils or bedrock. Piles are also used to prevent scour from undermining tower foundations. Piles are typically installed by driving or by augering.

Piles provide high axial load capacity and relatively low shear or bending moment capacity. Therefore, pile foundations are normally used more often for lattice towers, which have low shear and high axial loads, than for H frame structures or single shaft structures which have high moment and shear loads.

Copyright © 2001 IEEE. All rights reserved.

Copyright The Institute of Electrical and Electronics Engineers, Inc.
Provided by IHS under license with IEEE
No reproduction or networking permitted without license from IHS
Not for Resale

6.1 Pile types and orientation

Typical pile types are timber, prestressed concrete, cylinder, cast-in-place shell, and steel H or pipe sections. Other proprietary types are available. Selection of the appropriate pile type is a function of load and strength requirements, cost of construction, and cost of materials. Illustrations and physical characteristics of several pile types are shown in Figure 59, Figure 60 and Figure 61. A discussion of the most common pile types follows. More information regarding pile characteristics may be found in [B66] and [B161].

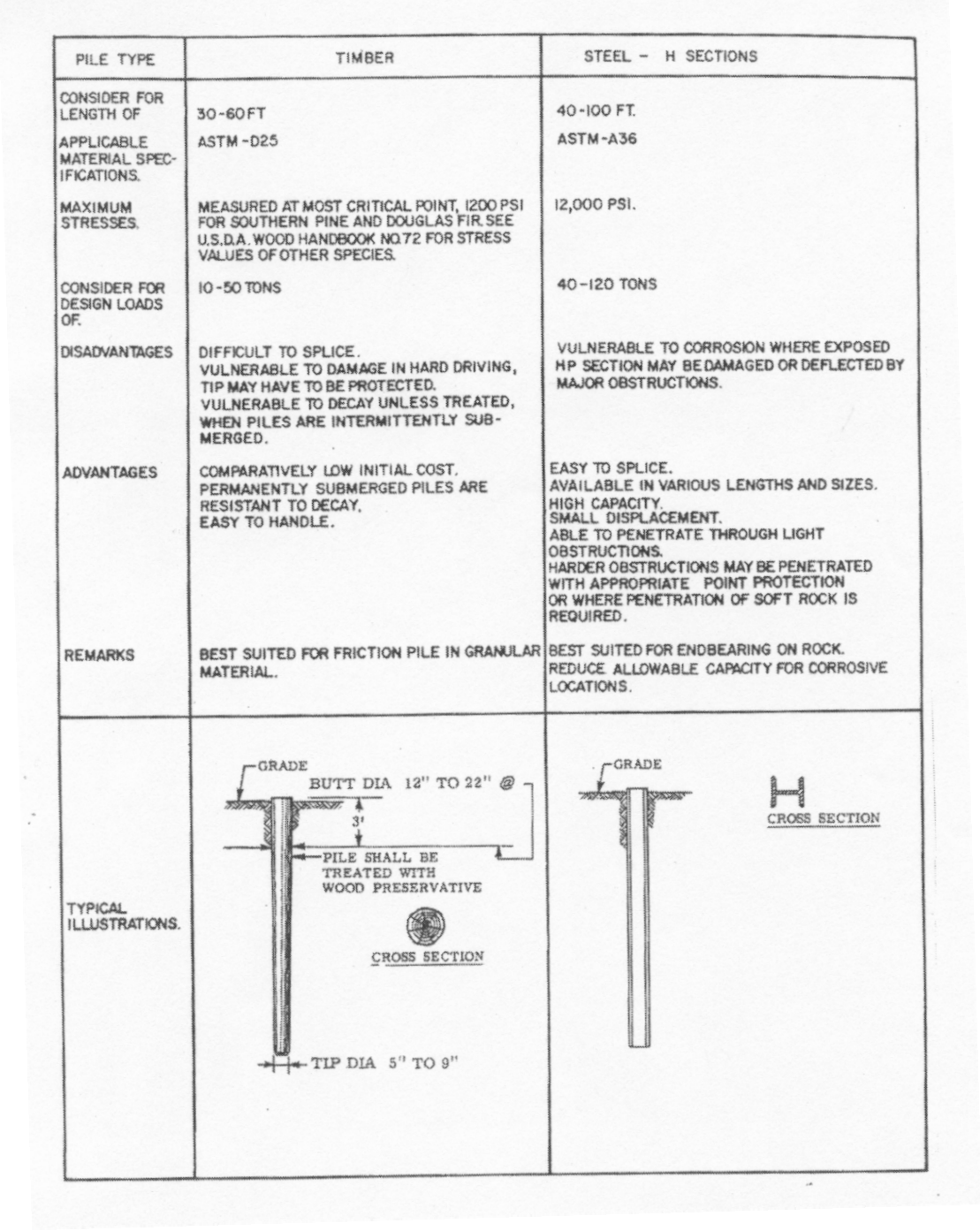

Figure 59—Typical pile types [B161]—Timber and steel H section

Copyright © 2001 IEEE. All rights reserved.
Copyright The Institute of Electrical and Electronics Engineers, Inc.
Provided by IHS under license with IEEE
No reproduction or networking permitted without license from IHS
Not for Resale

PILE TYPE	PRECAST CONCRETE (INCLUDING PRESTRESSED)	CAST-IN-PLACE CONCRETE (THIN SHELL DRIVEN WITH MANDREL)
CONSIDER FOR LENGTH OF	40-50 FT. FOR PRECAST 60-100 FT. FOR PRESTRESSED.	10-120 FT. BUT TYPICALLY IN THE 50-80 FT. RANGE
APPLICABLE MATERAL SPECIFICATIONS.	ACI 318 FOR CONCRETE ASTM A15-FOR REINFORCING STEEL	ACI CODE 318-FOR CONCRETE.
MAXIMUM STRESSES.	FOR PRECAST-33% OF 28 DAY STRENGTH OF CONCRETE. FOR PRESTRESSED- $F_c = 0.33\ F'_c - 0.27\ F_{pe}$ (WHERE: F_{pe} IS THE EFFECTIVE PRESTRESS STRESS ON THE GROSS SECTION).	33% OF 28-DAY STRENGTH OF CONCRETE, WITH INCREASE TO 40% OF 28 DAY STRENGTH. PROVIDING: (A) CASING IS A MINIMUM 14 GAUGE THICKNESS (B) CASING IS SEAMLESS OR WITH WELDED SEAMS (C) RATIO OF STEEL YIELD STRENGTH TO CONCRETE 28 DAY STRENGTH IS NOT LESS THAN 6. (D) PILE DIAMETER IS NOT GREATER THAN 17".
	SPECIFICALLY DESIGNED FOR A WIDE RANGE OF LOADS.	SPECIFICALLY DESIGNED FOR A WIDE RANGE OF LOADS.
DISADVANTAGES	UNLESS PRESTRESSED, VULNERABLE TO HANDLING. RELATIVELY HIGH BREAKAGE RATE ESPECIALLY WHEN PILES ARE TO BE SPLICED. HIGH INITIAL COST. CONSIDERABLE DISPLACEMENT. PRESTRESSED DIFFICULT TO SPLICE.	DIFFICULT TO SPLICE AFTER CONCRETING. REDRIVING NOT RECOMMENDED. THIN SHELL VULNERABLE DURING DRIVING TO EXCESSIVE EARTH PRESSURE OR IMPACT. CONSIDERABLE DISPLACEMENT.
ADVANTAGES	HIGH LOAD CAPACITIES. CORROSION RESISTANCE CAN BE ATTAINED. HARD DRIVING POSSIBLE.	INITIAL ECONOMY. TAPERED SECTIONS PROVIDE HIGHER BEARING RESISTANCE IN GRANULAR STRATUM CAN BE INTERNALLY INSPECTED AFTER DRIVING RELATIVLY LESS WASTE STEEL MATERIAL. CAN BE DESIGNED AS END BEARING OR FRICTION PILE, GENERALLY LOADED IN THE 40-100 TON RANGE.
REMARKS	CYLINDER PILES IN PARTICULAR ARE SUITED FOR BENDING RESISTANCE. GENERAL LOADING RANGE IS 40-400 TONS.	BEST SUITED FOR MEDIUM LOAD FRICTION PILES IN GRANULAR MATERIALS.
TYPICAL ILLUSTRATIONS	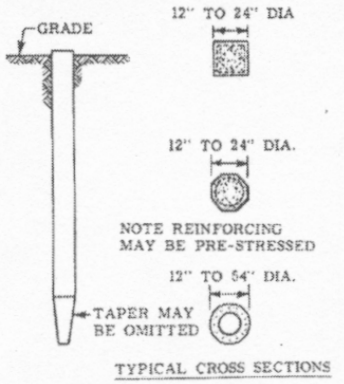 TYPICAL CROSS SECTIONS	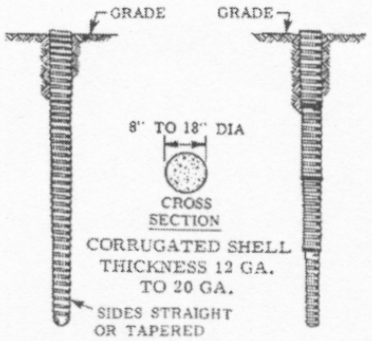

Figure 60—Typical pile types [B161]—Precast and cast-in place concrete

Copyright © 2001 IEEE. All rights reserved.

Copyright The Institute of Electrical and Electronics Engineers, Inc.
Provided by IHS under license with IEEE
No reproduction or networking permitted without license from IHS
Not for Resale

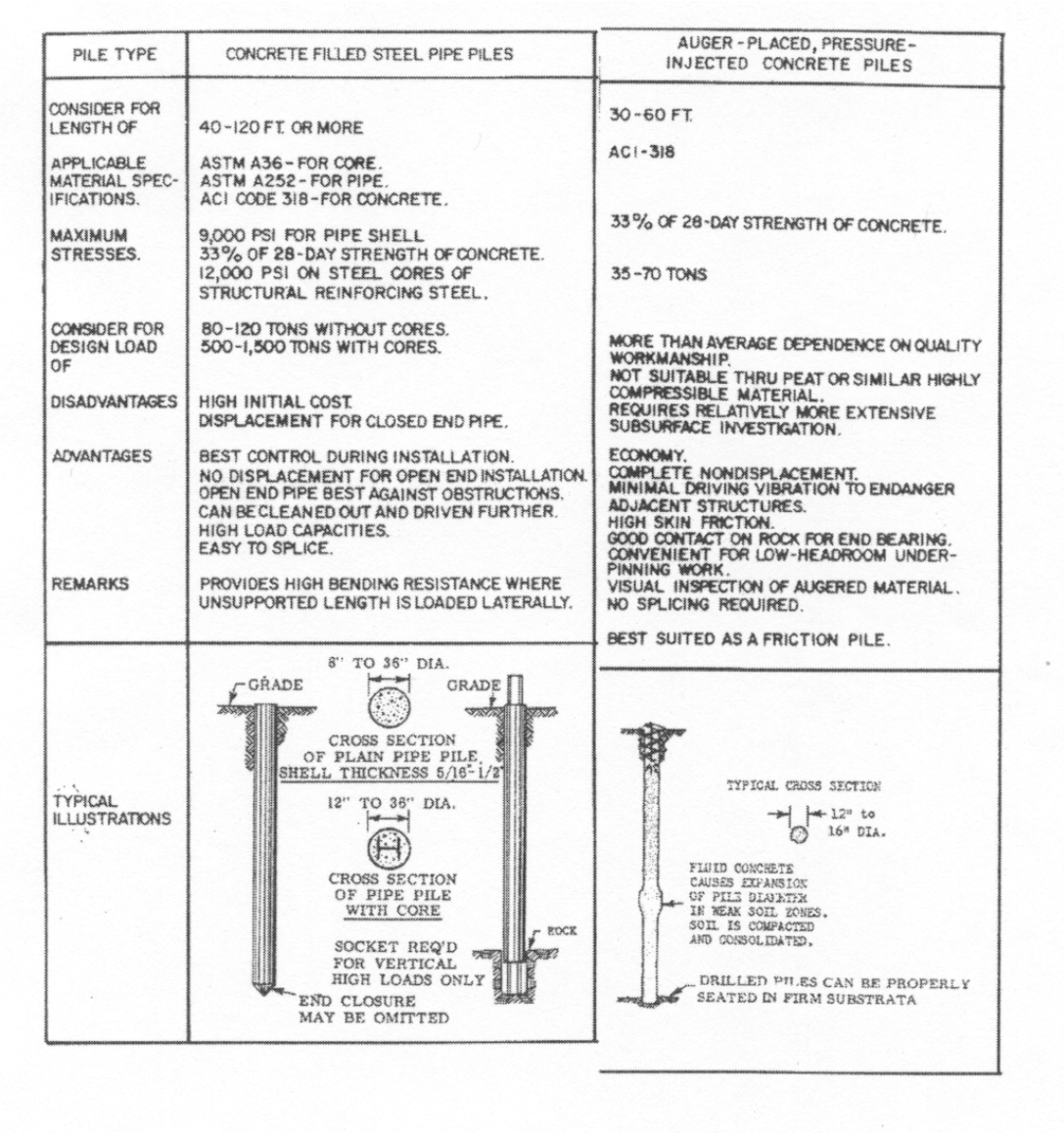

Figure 61—Typical pile types [B161]—Concrete-filled pipe and Augercast concrete

6.1.1 Timber piles

Timber piles are typically pressure treated Southern Pine or Douglas Fir. Douglas Fir piling comes from the Northwest in single pieces up to 36 m (120 ft) on special order, but 18 m (60 ft) and shorter lengths of southern pine are readily available. Timber piles normally do not exceed 36 000 kg (40 tons) in capacity. They are very difficult to splice, so it is necessary to select appropriate pile lengths in advance of pile driving. Timber piles tend to break when over driven, and consequently the contractor must be cautious in selecting driving equipment and the driving criteria must be mutually agreeable to the contractor and the engineer. Most timber piles are pressure treated to preserve the wood. Untreated timber piling deteriorates quickly above the groundwater table.

Copyright © 2001 IEEE. All rights reserved.

Copyright The Institute of Electrical and Electronics Engineers, Inc.
Provided by IHS under license with IEEE
No reproduction or networking permitted without license from IHS
Not for Resale

6.1.2 Prestressed concrete piles

Prestressed concrete piles are formed, poured and cured in a casting yard. A compressive stress is locked into the pile during manufacture to enable the pile to withstand tensile stresses. Piles are usually square, round, or octagonal in section, with or without taper, and reinforced to permit handling. They may be cast with a hole in the center to enable them to be advanced by jetting.

Splicing of prestressed concrete piles is difficult and expensive: therefore an accurate prediction of pile length is necessary to efficiently utilize this pile type.

6.1.3 Cylinder piles

A special type of prestressed concrete pile is the cylinder pile. It ranges in diameter from 0.762 m to 1.37 m (30 to 54 in), and is cast in up to 18.3 m (60 ft) lengths that may be spliced together to make any required length. The cylinder pile has a vertical load capacity of up to several hundred tons, and can absorb and transmit horizontal forces of considerable magnitude. The large bending capacity of cylinder piles makes them particularly well adapted to single pole and H frame structures, if appropriate construction equipment is available.

6.1.4 Cast-in-place shell piles

Cast-in-place, concrete filled shell piles are formed by driving a steel shell with a heavy walled steel mandrel. The shell is filled in place with concrete, and a reinforcing cage is easily installed if required. The shells are easily spliced, may be inspected after driving, and the excess shell that is cut off may be reused.

6.1.5 Steel H piles

Steel H piles are particularly well suited for hard driving into a dense bearing stratum and have a large section modulus about one axis to resist bending moments. These piles may be reinforced with prefabricated pile points to protect them during hard driving. Pile lengths are unlimited since they may be spliced and the cutoff ends are reusable. Steel H piles are susceptible to corrosion. Each site should be evaluated for corrosion potential and the required protection methods determined when considering the use of this pile type.

6.1.6 Steel pipe piles

Steel pipe piles are similar to H piles in that they may be spliced, have reusable cut ends, and are subject to corrosion. Pipe piles are better suited to resist bending moments from any direction because of the uniform section modulus. They may be driven either close-ended or open-ended (and later cleaned out by drilling or jetting, if desired) to minimize soil displacement or facilitate penetrating dense strata. These piles may be reinforced with prefabricated pile points to protect them during hard driving. Pipe piles may be visually inspected before concreting.

6.1.7 Pile orientation

The pile caps for lattice towers are usually constructed as shallow as possible, with the resultant force from the tower stub angle intersecting the center of gravity of the pile group. Figure 62 illustrates a typical pile foundation without a grade beam, and Figure 63 illustrates the addition of a grade beam to distribute shear loads between foundations. A grade beam is the preferred method to eliminate differential lateral movement. The inclined or batter piles shown in Figure 62 and Figure 63 resist the lateral loads imposed by the tower legs.

Copyright © 2001 IEEE. All rights reserved.

Copyright The Institute of Electrical and Electronics Engineers, Inc.
Provided by IHS under license with IEEE
No reproduction or networking permitted without license from IHS
Not for Resale

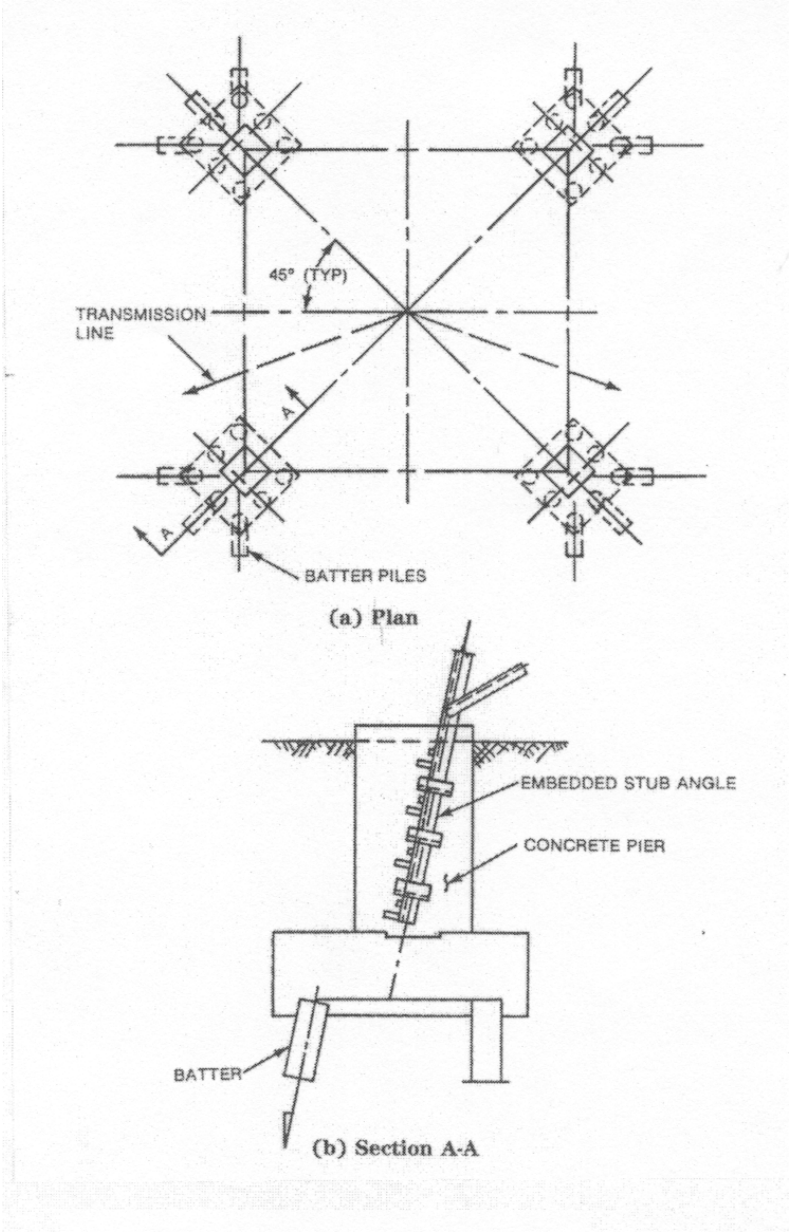

Figure 62—Pile foundation without a grade beam

6.2 Pile stresses

The following sources of stress in a pile should be considered when selecting the pile type, material, and size:

a) *Design loads*. Live, wind and dead loads will cause compression, tension, shear or bending stresses in a pile. Both tension and compression stresses in piles will be diminished along the length of the pile, depending upon the distribution and magnitude of the shearing resistance between the soil and periphery of the pile.

Copyright © 2001 IEEE. All rights reserved.

Copyright The Institute of Electrical and Electronics Engineers, Inc.
Provided by IHS under license with IEEE
No reproduction or networking permitted without license from IHS
Not for Resale

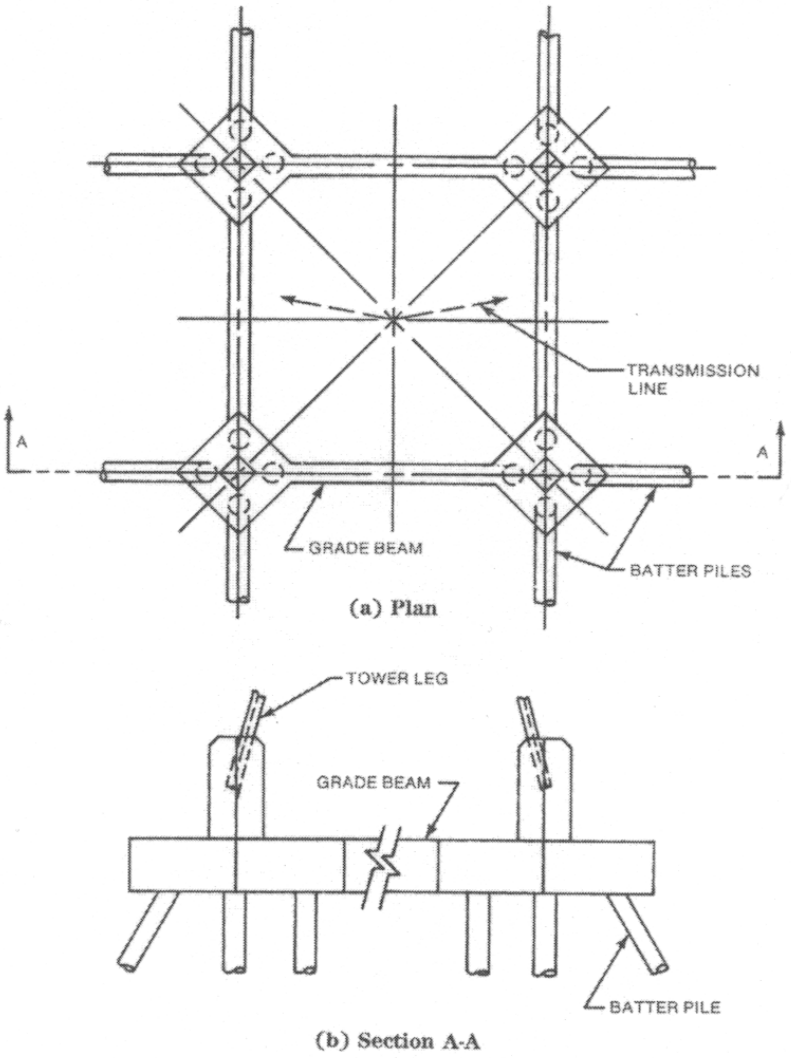

Figure 63—Pile foundation with grade beam

b) *Handling stress*. Piles that are lifted, stored and transported may be subject to substantial handling stresses. Bending and buckling stresses should be investigated for all conditions, including lifting, storing, transporting, and impact.

c) *Driving stresses*. Driving stresses are complex functions of pile and soil properties, influenced by the required driving resistance, size and type of pile driving equipment, and method of installation. Both tension and compression stresses occur and could exceed the yield strength of the pile material. Dynamic compressive stresses during driving are considerably greater than the stresses incurred by the maximum design load. Analysis of driving stresses has been made possible by development of the wave equation. A thorough discussion of the wave equation theory and application is included in [B58] and [B144].

Copyright © 2001 IEEE. All rights reserved.

Copyright The Institute of Electrical and Electronics Engineers, Inc.
Provided by IHS under license with IEEE
No reproduction or networking permitted without license from IHS
Not for Resale

d) *Tension stresses due to swelling soils*. Piles are sometimes subjected to temporary axial tensile stresses due to swelling of certain types of clays when the moisture content increases. Swelling clays should be provided for in the design or minimized in the installation procedures.

e) *Compression or bending stresses due to negative skin friction*. Negative skin friction resulting from the consolidation of compressible soils through which the pile extends and can produce additional compressive or bending loads on the pile. Consolidation is generally caused by an additional load being applied at the ground surface, and continues until a state of equilibrium is reached. Under negative skin friction conditions, the critical section of the pile may be located at the surface of the bearing strata. The magnitude of the load applied to the pile as a result of negative skin friction is limited by certain factors; shearing resistance between the pile surface and the soil, shear strength of the soil, pile shape, and thickness of the compressible stratum. Bending stresses on vertical piles can be caused by unbalanced loading of a surcharge, such as a fill. Also, battered piles subjected to down drag will experience bending stresses.

   Stresses due to swelling soils or negative skin friction may be estimated by assuming that the maximum friction that can be mobilized may be computed as discussed in 6.3.1 for either cohesive or non-cohesive soils. These stresses will be applied to the pile in the zone where either swelling or consolidation may be occurring.

6.3 Pile capacity

The main reason piles are used is to transfer loads through poor soils to competent soils. The soil resistance contributing to the support of the pile in compression loading should only be considered below any unsuitable soil layers. For example, a pile driven through a dense sand layer overlying a soft clay layer and finally into a deep gravel layer, should be designed to mobilize all necessary support only in the gravel layer. Similarly, piles which may be subjected to scour should be designed assuming the only useful resistance will be below the expected scour depth.

Piles subjected to uplift loads can include the full soil profile when estimating the pile capacity in uplift.

Typically the uplift capacity of a pile is governed by the ultimate shearing resistance between the soil and the pile along its length (commonly called side resistance or skin friction). The compression capacity of a pile is governed by skin friction in the bearing stratum plus the ultimate capacity of the soil or rock beneath the pile tip. The size of the pile element required to transmit the load to the soil is based upon allowable stresses in the pile material either under static loads or during pile driving. Commonly used methods to evaluate the capacity of the pile soil system include static analysis, dynamic analysis, and pile load tests.

6.3.1 Static methods of analysis

Pile driving changes the engineering properties of the soils in the vicinity of the piles; consequently the soil properties at the conclusion of pile driving may differ considerably from those existing prior to the installation. Therefore, estimating pile capacities on the basis of soil parameters obtained prior to pile installation using the currently available semi-empirical methods of analysis will result in only a rough approximation of the capacity of the actual pile foundation. The pile design for transmission tower foundations should be conservative if load tests are not performed.

6.3.1.1 Bearing capacity

a) Single pile in cohesionless soil (drained loading)

The ultimate bearing capacity Q_u of a single pile in cohesionless soil may be expressed as the sum of the tip bearing resistance Q_t and the skin friction Q_s:

Copyright © 2001 IEEE. All rights reserved.

Copyright The Institute of Electrical and Electronics Engineers, Inc.
Provided by IHS under license with IEEE
No reproduction or networking permitted without license from IHS Not for Resale

$$Q_u = Q_t + Q_s$$

— Tip Resistance

The estimation of the tip resistance has received considerable attention from researchers over the years. A discussion of the historical development of the bearing capacity of piles is covered in [B79]. Most of the theories for the ultimate bearing capacity of the pile tip have a form similar to the following:

$$Q_t = (\gamma' b N_\gamma S_\gamma + c_u N_c S_c + \sigma' N_q S_q) A_t$$

where

γ'	is effective unit weight
A_t	is area of the pile tip
b	is pile tip diameter
N_γ, N_c, N_q	are bearing capacity factors
S_γ, S_c, S_q	are Shape factors
σ'	is effective vertical stress at the pile tip
c_u	is undrained shear strength

The second term is equal to 0 for cohesionless soils and the first term is relatively small and may be ignored for large depth to width ratios. Consequently, the expression for point bearing capacity for cohesionless soils can be reduced to the following:

$$Q_t = A_t \sigma' N_q S_q$$

or

$$Q_t = A_t \sigma' N_q^*$$

where

N_q^* is bearing capacity factor which includes the necessary shape factor.

Most theories for bearing capacity require the estimation of the angle of friction, ϕ. It is well documented that as the effective stress increases the angle of friction decreases. Coyle et al., [B40], Kulhawy et al., [B137] and Vesic [B148] have proposed that N_q is not a constant but that it also decreases with increasing effective stress or depth of pile tip. This results in an ultimate tip resistance which increases at a diminishing rate as the depth of penetration increases, as shown in Figure 64. Vesic proposed a method for estimating the pile point bearing capacity based on the theory of expansion of cavities. According to this theory,

$$Q_t = A_t \sigma_0' N_\sigma^*$$

Copyright © 2001 IEEE. All rights reserved.

Copyright The Institute of Electrical and Electronics Engineers, Inc.
Provided by IHS under license with IEEE
No reproduction or networking permitted without license from IHS
Not for Resale

where

σ_0' is mean normal effective stress at the level of the pile tip.

$$\sigma'_o = \frac{1 + 2K_0}{3}\sigma'$$

σ' is effective vertical stress at the pile tip and,
K_0 is coefficient of earth pressure at rest,
$= 1 - \sin \phi$
N_σ^* is bearing capacity factor.

$$N_\sigma^* = \frac{3N_q^*}{1 + 2K_0}$$

$$N_\sigma^* = f(I_{rr})$$

I_r is rigidity index, and for conditions of no volume change, i.e., dense sand, saturated clay,
$I_{rr} = I_r$ and may be approximated by the following values:

Soil type	I_{rr} [B137]
Sand	70–150
Silts and clays (drained)	50–100
Clays (undrained)	100–200

Values of both N_c^* and N_σ^* are given in Table 14 for various values of ϕ and I_r.

Copyright © 2001 IEEE. All rights reserved.

Copyright The Institute of Electrical and Electronics Engineers, Inc.
Provided by IHS under license with IEEE
No reproduction or networking permitted without license from IHS
Not for Resale

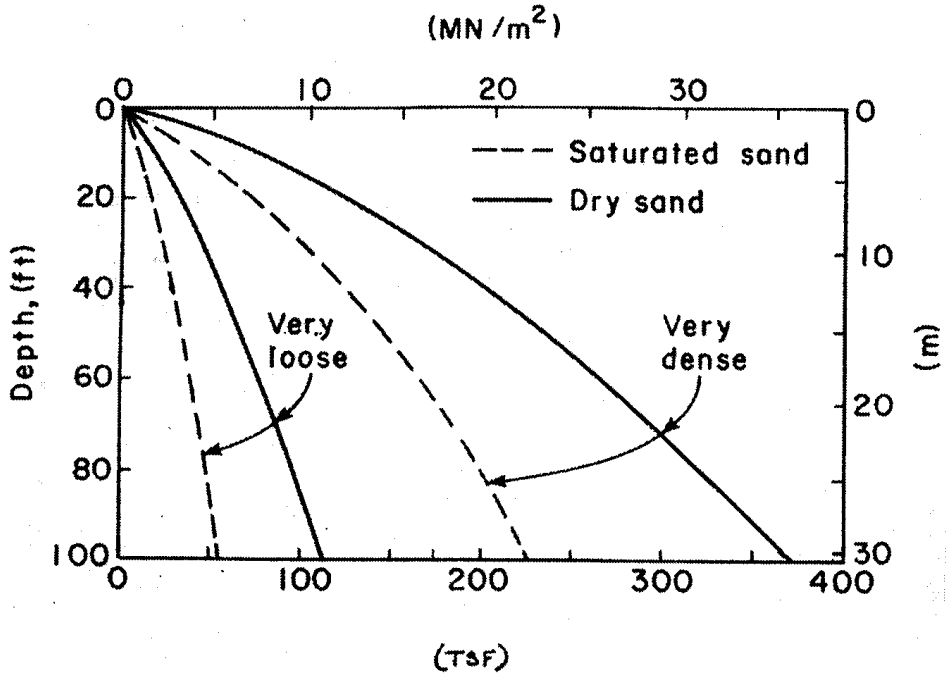

Figure 64—Ultimate tip resistance versus depth [B139]

Table 14—Bearing capacity factors for deep foundations [B148]

ϕ	I_r									
	10	20	40	60	80	100	200	300	400	500
0	6.97	7.90	8.82	9.36	9.75	10.04	10.97	11.51	11.89	12.19
	1.00	1.00	1.00	1.00	1.00	1.00	1.00	1.00	1.00	1.00
1	7.34	8.37	9.42	10.04	10.49	10.83	11.92	12.57	13.03	13.39
	1.13	1.15	1.16	1.18	1.18	1.19	1.21	1.22	1.23	1.23
2	7.72	8.87	10.06	10.77	11.28	11.69	12.96	13.73	14.28	14.71
	1.27	1.31	1.35	1.38	1.39	1.41	1.45	1.48	1.50	1.51
3	8.12	9.40	10.74	11.55	12.14	12.61	14.10	15.00	15.66	16.18
	1.43	1.49	1.56	1.61	1.64	1.66	1.74	1.79	1.82	1.85
4	8.54	9.96	11.47	12.40	13.07	13.61	15.34	16.40	17.18	17.80
	1.60	1.70	1.80	1.87	1.91	1.95	2.07	2.15	2.20	2.24
5	8.99	10.56	12.25	13.30	14.07	14.69	16.69	17.94	18.86	19.59
	1.79	1.92	2.07	2.16	2.23	2.28	2.46	2.57	2.65	2.71

Copyright © 2001 IEEE. All rights reserved.

Copyright The Institute of Electrical and Electronics Engineers, Inc.
Provided by IHS under license with IEEE
No reproduction or networking permitted without license from IHS
Not for Resale

Table 14—Bearing capacity factors for deep foundations [B148] (continued)

ϕ	I_r									
	10	20	40	60	80	100	200	300	400	500
6	9.45	11.19	13.08	14.26	15.14	15.85	18.17	19.62	20.70	21.56
	1.99	2.18	2.37	2.50	2.59	2.67	2.91	3.06	3.18	3.27
7	9.94	11.85	13.96	15.30	16.30	17.10	19.77	12.46	22.71	23.73
	2.22	2.46	2.71	2.88	3.00	3.10	3.43	3.63	3.79	3.91
8	10.45	12.55	14.90	16.41	17.54	18.45	21.51	23.46	24.93	26.11
	2.47	2.76	3.09	3.31	3.46	3.59	4.02	4.30	4.50	4.67
9	10.99	13.29	15.91	17.59	18.87	19.90	23.39	25.64	27.35	28.73
	2.74	3.11	3.52	3.79	3.99	4.15	4.70	5.06	5.33	5.55
10	11.55	14.08	16.97	18.86	20.29	21.46	25.43	28.02	29.99	31.59
	3.04	3.48	3.99	4.32	4.58	4.78	5.48	5.94	6.29	6.57
11	12.14	14.90	18.10	20.20	21.81	23.13	27.64	30.61	32.87	34.73
	3.36	3.90	4.52	4.93	5.24	5.50	6.37	6.95	7.39	7.75
12	12.76	15.77	19.30	21.64	23.44	24.92	30.03	33.41	36.02	38.16
	3.71	4.35	5.10	5.60	5.98	6.30	7.38	8.10	8.66	9.11
13	13.41	16.69	20.57	23.17	25.18	26.84	32.60	36.46	39.44	41.89
	4.09	4.85	5.75	6.35	6.81	7.20	8.53	9.42	10.10	10.67
14	14.08	17.65	21.92	24.80	27.04	28.89	35.38	39.75	43.15	45.96
	4.51	5.40	6.47	7.18	7.74	8.20	9.82	10.91	11.76	12.46
15	14.79	18.66	23.35	26.53	29.02	31.08	38.37	43.32	47.18	50.39
	4.96	6.00	7.26	8.11	8.78	9.33	11.28	12.61	13.64	14.50
16	15.53	19.73	24.86	28.37	31.13	33.43	41.58	47.17	51.55	55.20
	5.45	6.66	8.13	9.14	9,93	10.58	12.92	14.53	15.78	16.83
17	16.30	20.85	26.46	30.33	33.37	35.92	45.04	51.32	56.27	60.42
	5.98	7.37	9.09	10.27	11.20	11.98	14.77	16.69	18.20	19.47
18	17.11	22.03	28.15	32.40	35.76	38.59	48.74	55.80	61.38	66.07
	6.56	8.16	10.15	11.53	12.62	13.54	16.84	19.13	20.94	22.47
19	17.95	23.26	29.93	34.59	38.30	41.42	52.71	60.61	66.89	72.18
	7.18	9.01	11.31	12.91	14.19	15.26	19.15	21.87	24.03	25.85
20	18.83	24.56	31.81	36.92	40.99	44.43	56.97	65.79	72.82	78.78
	7.85	9.94	12.58	14.44	15.92	17.17	21.73	24.94	27.51	29.67
21	19.75	25.92	33.80	39.38	43.85	47.64	61.51	71.34	79.22	85.90
	8.58	10.95	13.97	16.12	17.83	19.29	24.61	28.39	31.41	33.97
22	20.71	27.35	35.89	41.98	46.88	51.04	66.37	77.30	86.09	93.57
	9.37	12.05	15.50	17.96	19.94	21.62	27.82	32.23	35.78	38.81
23	21.71	28.84	38.09	44.73	50.08	54.66	71.56	83.68	93.47	101.83
	10.21	13.24	17.17	19.99	22.26	24.20	31.37	36.52	40.68	44.22

Copyright © 2001 IEEE. All rights reserved.

Copyright The Institute of Electrical and Electronics Engineers, Inc.
Provided by IHS under license with IEEE
No reproduction or networking permitted without license from IHS
Not for Resale

Table 14—Bearing capacity factors for deep foundations [B148] (continued)

ϕ	I_r									
	10	20	40	60	80	100	200	300	400	500
24	22.75	30.41	40.41	47.63	53.48	58.49	77.09	90.51	101.39	110.70
	11.13	14.54	18.99	22.21	24.81	27.04	35.32	41.30	46.14	50.29
25	23.84	32.05	42.85	50.69	57.07	62.54	82.98	97.81	109.88	120.23
	12.12	15.95	20.98	24.64	27.61	30.16	39.70	46.61	52.24	57.06
26	24.98	33.77	45.42	53.93	60.87	66.84	89.25	105.61	118.96	130.44
	13.18	17.47	23.15	27.30	30.69	33.60	44.53	52.51	59.02	64.62
27	26.16	35.57	48.13	57.34	64.88	71.39	95.02	113.92	128.67	141.39
	14.33	19.12	25.52	30.21	34.06	37.37	49.88	59.05	66.56	73.04
28	27.40	37.45	50.96	60.93	69.12	76.20	103.01	122.79	139.04	153.10
	15.57	20.91	28.10	33.40	37.75	41.51	55.77	66.29	74.93	82.40
29	28.69	39.42	53.95	64.71	73.58	81.28	110.54	132.33	150.11	165.61
	16.90	22.85	30.90	36.87	41.79	46.05	62.27	74.30	84.21	92.80
30	30.03	41.49	57.08	68.69	78.30	86.64	118.53	142.27	161.91	178.98
	18.24	24.95	33.95	40.66	46.21	51.02	69.43	83.14	94.48	104.33
31	31.43	43.64	60.37	72.88	83.27	92.31	126.99	152.95	174.49	193.23
	19.88	27.22	37.27	44.79	51.03	56.46	77.31	92.90	105.84	117.11
32	32.89	45.90	63.82	77.29	88.50	98.28	135.96	164.29	187.87	208.43
	21.55	29.68	40.88	49.30	56.30	62.41	85.96	103.66	118.39	131.24
33	34.41	48.26	67.44	81.92	94.01	104.58	145.46	176.33	202.09	224.62
	23.34	32.34	44.80	54.20	62.05	68.92	95.46	115.51	132.24	146.87
34	35.99	50.72	71.24	86.80	99.82	111.22	155.51	189.11	217.21	241.84
	25.28	35.21	49.05	59.54	68.33	76.02	105.90	128.55	147.51	164.12
35	37.65	53.30	75.22	91.91	105.92	118.22	166.14	202.64	233.27	260.15
	27.36	38.32	53.67	65.36	75.17	83.78	117.33	142.89	164.33	183.16
36	39.37	55.99	79.39	97.29	112.34	125.59	177.38	216.98	250.30	279.60
	29.60	41.68	58.68	71.69	82.62	92.24	129.87	158.65	182.85	204.14
37	41.17	58.81	83.77	102.94	119.10	133.34	189.25	232.17	268.36	300.26
	32.02	45.31	64.13	78.57	90.75	101.48	143.61	175.95	203.23	227.26
38	43.04	61.75	88.36	108.86	126.20	141.50	201.78	248.23	287.50	322.17
	34.63	49.24	70.03	86.05	99.60	111.56	158.65	194.94	225.62	252.71
39	44.99	64.83	93.17	115.09	133.66	150.09	215.01	265.23	307.78	345.41
	37.44	53.50	76.45	94.20	109.24	122.54	175.11	215.78	250.23	280.71
40	47.03	68.04	98.21	121.62	141.51	159.13	228.97	283.19	329.24	370.04
	40.47	58.10	83.40	103.05	119.74	134.52	193.13	238.62	277.26	311.50

Copyright © 2001 IEEE. All rights reserved.

Copyright The Institute of Electrical and Electronics Engineers, Inc.
Provided by IHS under license with IEEE
No reproduction or networking permitted without license from IHS
Not for Resale

Table 14—Bearing capacity factors for deep foundations [B148] (continued)

ϕ	I_r									
	10	20	40	60	80	100	200	300	400	500
41	49.16	71.41	103.49	128.48	149.75	168.63	243.69	302.17	351.95	396.12
	43.74	63.07	90.96	112.68	131.18	147.59	212.84	263.67	306.94	345.34
42	51.38	74.92	109.02	135.68	158.41	178.62	259.22	322.22	375.97	423.74
	47.27	68.46	99.16	123.16	143.64	161.83	234.40	291.13	339.52	382.53
43	53.70	78.60	114.82	143.23	167.51	189.13	275.59	343.40	401.36	452.96
	51.08	74.30	108.08	134.56	157.21	177.36	257.99	321.22	375.28	423.39
44	56.13	82.45	120.91	151.16	177.07	200.17	292.85	365.75	428.21	483.88
	55.20	80.62	117.76	146.97	172.00	194.31	283.80	354.20	414.51	468.28
45	58.66	86.48	127.28	159.48	187.12	211.79	311.04	389.35	456.57	516.58
	59.66	87.48	128.28	160.48	188.12	212.79	312.03	390.35	457.57	517.58
46	61.30	90.70	133.97	168.22	197.67	224.00	330.20	414.26	486.54	551.16
	64.48	94.92	139.73	175.20	205.70	232.96	342.94	429.98	504.82	571.74
47	64.07	95.12	140.99	177.40	208.77	236.85	350.41	440.54	518.20	587.72
	69.71	103.00	152.19	191.24	224.88	254.99	376.77	473.42	556.70	631.25
48	66.97	99.75	148.35	187.04	220.43	250.36	371.70	468.28	551.64	626.36
	75.38	111.78	165.76	208.73	245.81	279.06	413.82	521.08	613.65	696.64
49	70.01	104.60	156.09	197.17	232.70	264.58	394.15	497.56	586.96	667.21
	81.54	121.33	180.56	227.82	268.69	305.37	454.42	573.38	676.22	768.53
50	73.19	109.70	164.21	207.83	245.60	279.55	417.82	528.46	624.28	710.39
	88.23	131.73	196.70	248.68	293.70	334.15	498.94	630.80	744.99	847.61

NOTE—Upper number is N_c*, lower number is N_σ*.

Copyright © 2001 IEEE. All rights reserved.

Copyright The Institute of Electrical and Electronics Engineers, Inc.
Provided by IHS under license with IEEE
No reproduction or networking permitted without license from IHS
Not for Resale

— Side Resistance

The determination of ultimate side resistance (f_s) for piles in sand is commonly determined by the following equation:

$$Q_s = A_s f_s = A_s K \sigma' \tan\delta$$

where

K is lateral earth pressure coefficient,
σ' is vertical effective overburden pressure,
$\tan\delta$ is coefficient of friction between the pile and the soil,
A_s is area of pile surface (for H piles, use the enclosing envelope).

In this equation the two unknowns are K and tan δ.

Considerable study has been done by several researchers to relate δ to ϕ for various interface materials and the results are given below:

Interface friction angles [B137]	
Interface materials	δ/ϕ
Sand/rough concrete	1.0
Sand/smooth concrete	0.8–1.0
Sand/rough steel	0.7–0.9
Sand/smooth steel	0.5–0.7
Sand/timber	0.8–0.9

The development of K is very complex, being related both to past stress history of the soil deposit as well as the displacement and method of installation of the foundation element. Kulhawy [B137] has proposed correlations of K/K_o as shown below:

Horizontal soil stress coefficents [B137]	
Foundation and method of installation	**K/K_0**
Jetted pile	0.5–0.67
Drilled shaft	0.67–1
Driven pile, small displacement	0.75–1.25
Driven pile, large displacement	1–2

Copyright © 2001 IEEE. All rights reserved.

Copyright The Institute of Electrical and Electronics Engineers, Inc.
Provided by IHS under license with IEEE
No reproduction or networking permitted without license from IHS
Not for Resale

K_o is the lateral earth pressure coefficient which existed prior to installation of the foundation element. Evaluation of K_o is complicated because insitu measurements are not routine and are subject to a great deal of interpretation. However, values of K_o can be estimated by use of the Pressuremeter [B22]. Alternatively, values of K_o can be estimated based on a knowledge of the stress history of the soils [B107]. Since most soils have some degree of overconsolidation an estimated value of $K_0 = 0.5$ would generally be conservative. On this basis, K for low displacement H driven piles or drilled or augered piles would vary from 0.4 to 0.6 and for large displacement (pipe, precast concrete) driven piles would vary from 0.5 to 1.0.

b) Single Pile - Cohesive Soil (Undrained Loading)

Estimating the bearing capacity of a pile in clay is based on the undrained shear strength of the soil. A typical formula for calculating the ultimate bearing capacity of piles in clay is as follows:

$$Q_u = Q_t + Q_s = q_0 A_t + \alpha c_{\text{avg}} A_s$$

where Q_u, Q_t and Q_s are as before and q_o = ultimate unit bearing capacity at the pile tip and is equal approximately to $9 \times c$ (for general shear) where c is the undrained shear strength at the pile tip. Since this is typically a small percentage of the total pile capacity it is frequently omitted.

c_{avg} is average undrained shear strength along the length of the pile.
α is adhesion factor = ratio of skin friction to the undrained shear strength.

A modification of this formula by Semple and Rigdon [B141], to account for progressive failure of long slender piles is as follows:

$$Q_u = q_0 A_p + \alpha F_1 c_u A_s$$

where

F_l is a correction factor based on the overall aspect ratio (L/D) of the pile,
c_u is the maximum undrained shear strength,
L is pile length,
D is pile diameter.

Values of α versus c_u/σ_v' and F_l versus L/D (l/d) are given in Figure 65.

Vesic [B148] has shown that the time required for friction piles to attain their maximum capacity is a function of the time rate of the radial consolidation of the clay. Figure 66 indicates the increase in bearing capacity with time for several friction piles in clay. This indicates the importance of testing friction piles over a period of several weeks after driving to establish the increase in strength with time.

c) Group bearing capacity and settlement

Pile groups should be analyzed for both excessive settlements and bearing capacity failure. Foundations supported by friction piles are normally assumed to transfer their load to a horizontal plane at a depth equal to 2/3 the embedded length of the pile. End bearing piles are assumed to distribute their loads within the bearing stratum. Both assumptions are illustrated in Figure 67, parts a and b. Methods of calculating elastic and consolidation settlements are discussed in Clause 4. In addition to those settlements contributed by the soil, consideration should also be given to the elastic compression or elongation of the piles, which may be calculated by $\Delta L = PL/AE$, where P is the axial load, A is the area of the pile, and E is the modulus of elasticity of the pile. This must be modified by the distribution of skin friction along the pile, i. e., a friction pile will have less elastic compression than an end bearing pile, all other things being equal.

Copyright © 2001 IEEE. All rights reserved.

Copyright The Institute of Electrical and Electronics Engineers, Inc.
Provided by IHS under license with IEEE
No reproduction or networking permitted without license from IHS Not for Resale

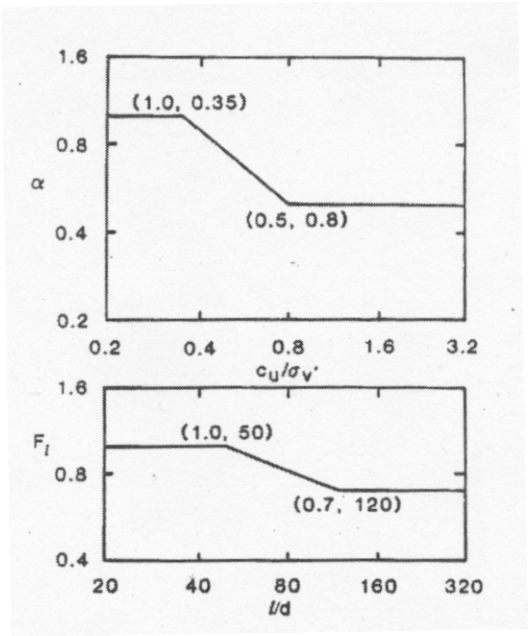

Figure 65—Criteria for axial pile capacity [B66]

Typically settlement of end bearing piles in granular soils is ignored, provided there is no compressible stratum below the pile tips within the zone of influence of the loaded area.

The ultimate bearing capacity of pile groups in sand has been generally found to exceed the bearing capacity of the sum of the individual pile capacities for center to center spacing of piles ranging from 2–6 times the diameter. The ratio of the ultimate capacity of a pile group to the sum of the individual ultimate capacities of all piles is the group efficiency. Model tests by Hyde [B81] and Stuart et al [B150] have shown a maximum group efficiency of 2 for a pile spacing of two diameters, with the efficiency decreasing to 1 for a pile spacing of 6 diameters. Vesic [B148] reports a maximum group efficiency of 1.7 at a pile spacing of 3–4 diameters, with group efficiency reducing with increased pile spacing. The greater group capacity is attributed to the overlap of the individual soil compaction zones near the piles, which will increase skin friction, while point bearing is unaffected by the adjacent piles.

Tomlinson [B156] has found that the group efficiency of piles founded in clay is equal to one for a spacing greater than 8 diameters; but at a spacing less than that, block failure should be considered using the following formula given by Terzaghi and Peck [B154]:

$$Q_{ult} = 2L(W + B)f_s + 1.3c_u N_c WB$$

where

Q_{ult} is ultimate capacity of the pile group,
L is depth of piles,
W is width of pile group,
B is length of pile group,
f_s is average shear resistance of soil, per unit of area, along pile length,
c_u is undrained shear strength at bottom of pile group,
N_c is bearing capacity factor.

If the bearing stratum is underlain by a weaker deposit within a distance equal to 1.5 times the average width of the pile group, its strength must be considered in calculating the group capacity.

Copyright © 2001 IEEE. All rights reserved.

Copyright The Institute of Electrical and Electronics Engineers, Inc.
Provided by IHS under license with IEEE
No reproduction or networking permitted without license from IHS
Not for Resale

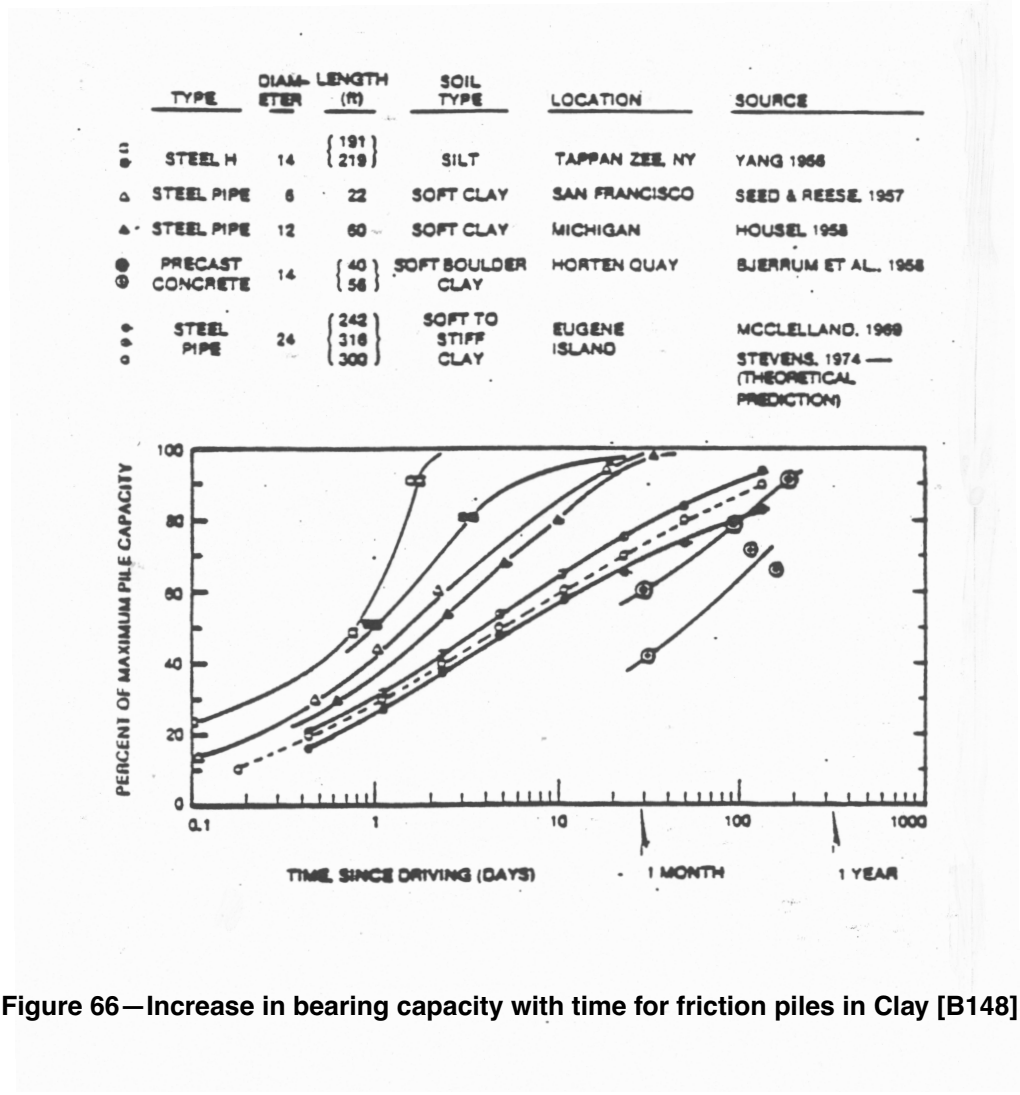

Figure 66—Increase in bearing capacity with time for friction piles in Clay [B148]

6.3.1.2 Uplift capacity

a) *Single pile*. The ultimate uplift capacity of single piles should be calculated by considering only the skin friction component of the capacity as discussed in 6.3.1.1. Field tests indicate that full frictional resistance is mobilized at pile butt movements in excess of approximately 2.5 mm–12.5 mm (0.1–0.5 in).

b) *Group effects*. The ultimate uplift capacity of a pile group may be equal to or less than the sum of the capacities of the individual capacities of the individual piles, depending upon the pile spacing. The ultimate uplift capacity of a pile group should be checked for block failure, which may be calculated by multiplying the vertical surface area of the envelope of the pile group by the average unit skin friction. The average unit skin friction may be determined as described in 6.3.1.1.

6.3.1.3 Lateral load capacity

Piles typically have a low resistance to lateral loads and should be battered if large shear loads are expected. A general solution for determining moments and displacements of a vertical pile subjected to lateral load and moment in sandy soils has been developed by Matlock and Reese [B102]. This method is based upon modeling a pile as a beam on an elastic foundation supported by Winkler springs.

Copyright © 2001 IEEE. All rights reserved.

Copyright The Institute of Electrical and Electronics Engineers, Inc.
Provided by IHS under license with IEEE
No reproduction or networking permitted without license from IHS
Not for Resale

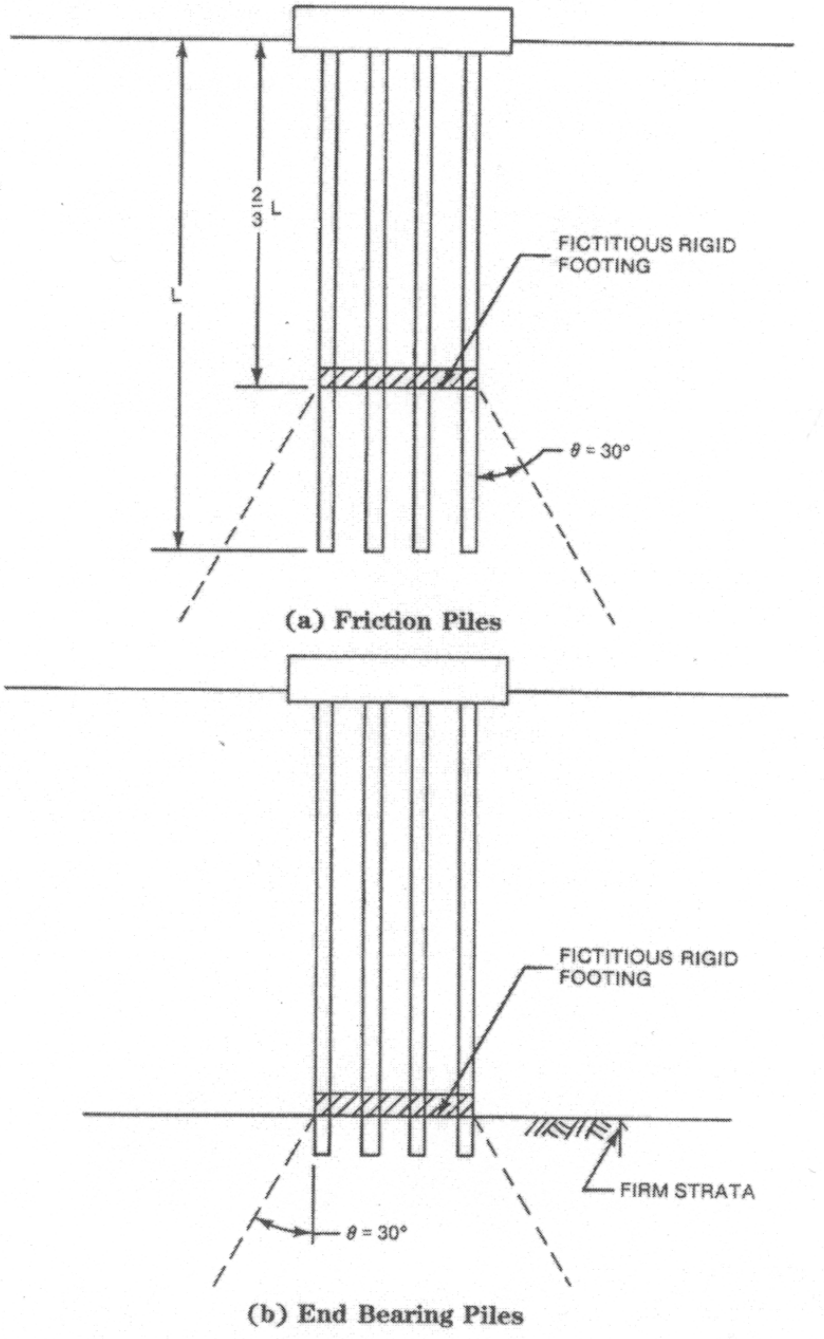

Figure 67—Assumed load distribution for settlement analysis

Copyright © 2001 IEEE. All rights reserved.

Copyright The Institute of Electrical and Electronics Engineers, Inc.
Provided by IHS under license with IEEE
No reproduction or networking permitted without license from IHS
Not for Resale

When a pile is subjected to a lateral load, P_l, and a moment, M, at the surface of the ground, the pile deflection at any depth [x_z (z)] can be expressed as:

$$x_z(z) = A_x \frac{P_1 T^3}{E_p I_p} + B_x \frac{MT^2}{E_p I_p}$$

The slope of a pile at any depth [θ_z, (z)] can be expressed as:

$$\theta_z(z) = A_\theta \frac{P_1 T^2}{E_p I_p} + B_\theta \frac{MT}{E_p I_p}$$

The moment of a pile at any depth [M_z (z)] can be expressed as:

$$M_z(z) = A_m P_1 T + B_m M$$

The shear force on the pile at any depth [p_z(z)] can be expressed as:

$$p_z(z) = A_v P_1 + B_p \frac{M}{T^2}$$

where

P_1 is shear load applied at the ground surface,
M is moment applied at ground surface.

and A_x, B_x, A_θ, B_θ, A_m, B_m, A_v, B_v, A_p, and B_p are coefficients and

$$T = \sqrt[5]{\frac{E_p I_p}{n_h}}$$

where n_h is the constant of modulus of horizontal subgrade reaction. Values of n_h are given below:

Soil type	n_h(kN/m^3)
Dry or moist sand	Loose: 1800–2200
	Medium: 5500–7000
	Dense: 15 000–18 000
Submerged sand	Loose: 1000–1400
	Medium: 3500–4500
	Dense: 9000–12 000
NOTE 1kN/m^3 = 6.36 lb/ft^3	

Copyright © 2001 IEEE. All rights reserved.

Copyright The Institute of Electrical and Electronics Engineers, Inc.
Provided by IHS under license with IEEE
No reproduction or networking permitted without license from IHS
Not for Resale

Values of the A and B coefficients versus the non-dimensional depth coefficient Z are given in Table 15, where Z = z/T, and z is the depth below ground. These values are intended to be used for a free headed pile, i.e., unrestrained against rotation at the pile butt. A complete selection of design curves for free, fixed and partially fixed pile heads for both sandy and clayey soils is given in Design Manual 7.2 [B161]. A limitation of this method is that it is only capable of handling a single soil layer. Since Davisson [B132] has demonstrated that the soil within 4 or 5 diameters of the ground surface has the greatest influence on pile performance, it is normally not necessary to go beyond the single layer solutions.

The limitation of the analytical method is not nearly as great as the uncertainties in selecting the appropriate subgrade moduli. Fortunately, the accuracy of the soil modulus is not critical in determining the maximum moment. Matlock and Reese point out that a 32 to 1 variation in the modulus is necessary to produce a 2 to 1 variation in the maximum moment.

More sophisticated computer analyses capable of handling multiple soil layers are available.

The best method for determining soil design parameters is by a combination of subsurface investigations, laboratory testing, and appropriate field load tests as discussed in Clauses 3 and 8. The extent to which this is carried out depends upon the relative costs of the field test program and the estimated potential saving in foundation costs.

a) Group effects

The action of pile groups under lateral loads is not well understood, in part because they cannot be easily modeled mathematically, and in part because few group load tests have been performed. Based on theoretical analysis and review of load test data, Poulos [B128] concluded that the major variables influencing horizontal movements and lateral load distribution within a pile group are pile spacing and pile stiffness. The width of the pile group was also observed to have a greater influence on lateral displacement than the number of piles in the group, so that considerable economy can be achieved by using a relatively small number of piles at relatively larger spacing. Reese, [B117], has reported that the maximum moments in pile groups may exceed the calculated moment for a single pile at the same lateral load by as much as 70% for pile spacings of 3 pile diameters. The explanation for this is that the interior piles have less lateral soil resistance than the outer piles, and consequently higher bending moments.

In addition to the geometry of the pile group, the design of the pile cap will also influence the lateral load capacity of the group. For pile caps embedded below the ground surface, passive earth pressure and friction (or adhesion) on the sides will also contribute to the ultimate capacity. The depth of embedment of the pile into the cap will determine the rotational restraint placed on the butt of the pile. As the rotational restraint increases, the lateral capacities of the individual piles will increase, thus increasing the lateral capacity of the group. However, as the fixity of the pile against rotation increases, so does the bending moment and the stress due to bending. Consequently, for a given deflection, a pile fixed against rotation at the butt will have twice the stresses due to bending moment of the pile which is pinned at the top, and, provided it has sufficient strength, it will also have more resistance to lateral load.

6.3.1.4 Batter piles

Battering the pile is an effective way to resist shear loads. Normally, when batter piles are used to carry shear loads, all piles are assumed to carry only axial loads.

The simplest type of batter pile foundation consists of one or several batter piles driven at the same batter as the applied load, and treated as if they were axially loaded piles. Batters of one horizontal to three or four vertical are typical, but piles have been driven to batters of one to one with special equipment.

Copyright © 2001 IEEE. All rights reserved.

Copyright The Institute of Electrical and Electronics Engineers, Inc.
Provided by IHS under license with IEEE
No reproduction or networking permitted without license from IHS
Not for Resale

Table 15—Values of A and B coefficients for laterally loaded piles and free end condition [B166]

Z	A_x	A_θ	A_m	A_v	$A_{p'}$	B_x	B_θ	B_m	B_v	$B_{p'}$
0.0	2.435	–1.623	0.000	1.000	0.000	1.623	–1.750	1.000	0.000	0.000
0.1	2.273	–1.618	0.100	0.989	–0.227	1.453	–1.650	1.000	–0.007	–0.145
0.2	2.112	–1.603	0.198	0.956	–0.422	1.293	–1.550	0.999	–0.028	–0.259
0.3	1.952	–1.578	0.291	0.906	–0.586	1.143	–1.450	0.994	–0.058	–0.343
0.4	1.796	–1.545	0.379	0.840	–0.718	1.003	–1.351	0.987	–0.095	–0.401
0.5	1.644	–1.503	0.459	0.764	–0.822	0.873	–1.253	0.976	–0.137	–0.436
0.6	1.496	–1.454	0.532	0.677	–0.897	0.752	–1.156	0.960	–0.181	–0.451
0.7	1.353	–1.397	0.595	0.585	–0.947	0.642	–1.061	0.939	–0.226	–0.449
0.8	1.216	–1.335	0.649	0.489	–0.973	0.540	–0.968	0.914	–0.270	–0.432
0.9	1.086	–1.268	0.693	0.392	–0.977	0.448	–0.878	0.885	–0.312	–0.403
1.0	0.962	–1.197	0.727	0.295	–0.962	0.364	–0.792	0.852	–0.350	–0.364
1.2	0.738	–1.047	0.767	0.109	–0.885	0.223	–0.629	0.775	–0.414	–0.268
1.4	0.544	–0.893	0.772	–0.056	–0.761	0.112	–0.482	0.688	–0.456	–0.157
1.6	0.381	–0.741	0.746	–0.193	–0.609	0.029	–0.354	0.594	–0.477	–0.047
1.8	0.247	–0.596	0.696	–0.298	–0.445	–0.030	–0.245	0.498	–0.476	0.054
2.0	0.142	–0.464	0.628	–0.371	–0.283	–0.070	–0.155	0.404	–0.456	0.140
3.0	–0.075	–0.040	0.225	–0.349	0.226	–0.089	0.057	0.059	–0.213	0.268
4.0	–0.050	0.052	0.000	–0.106	0.201	–0.028	0.049	–0.042	0.017	0.112
5.0	–0.009	0.025	–0.033	0.015	0.046	0.000	–0.011	–0.026	0.029	–0.002

Precise mathematical modeling of batter pile groups is not currently available due to the large number of variables involved, including the following:

— Rigidity of pile cap
— Degree of end restraint
— Effective length of pile
— Lateral loads carried by the pile cap
— Distribution of vertical and lateral loads carried by the piles

An approximate mathematical model has been developed for a computer solution and is presented by Bowles [B133]. Other structural analysis programs such as STRUDL can also be used to provide an approximate solution to a batter pile problem.

Copyright © 2001 IEEE. All rights reserved.

Copyright The Institute of Electrical and Electronics Engineers, Inc.
Provided by IHS under license with IEEE
No reproduction or networking permitted without license from IHS
Not for Resale

Hand calculation methods of solving relatively simple batter pile group problems that make no attempt to evaluate the soil structure interaction have been presented by Brill [B29] and Hrennikoff [B79]. One method that does incorporate soil moduli and pile stiffness and rigidity factors has been presented by Vesic [B148].

6.3.2 Dynamic methods of analysis

Driving criteria based upon resistance to penetration are valuable and often indispensable in ensuring that each pile is driven to a relatively uniform capacity. This helps eliminate possible causes of differential settlement of the completed structure due to normal variations in the subsurface conditions within the pile area. In effect, adherence to an established driving resistance permits each pile to seek its own required capacity regardless of variations in depth, density and quality of the bearing strata or variation in the pile length.

The most widespread method of estimating the capacity of piles is the use of some form of dynamic pile driving formula relating the measured permanent displacement of the pile at each blow of the hammer to the pile capacity. Driving formulas are based on an energy balance between the driving energy and the static capacity of the pile. These formulas are empirical and their use may result in ultra conservative or unsafe results.

The use of driving formula correlated with load tests will determine the applicability of the formula to a specific pile-soil system and driving conditions. In some areas dynamic formulas have been successfully used when applied with experience and good judgement, and with proper recognition of their limitations. In general, such formulas are more applicable to cohesionless soils.

A superior alternative to the conventional dynamic formula is the wave equation [B58]. The wave equation analysis is based on using the stress wave generated from the hammer impact to determine the displacements and stresses in the pile due to driving. Such information is useful to ensure that the pile is not overstressed during installation. Solutions to the wave equation for a given hammer and pile may also be used to evaluate the pile capacity and equipment compatibility.

Under certain subsoil conditions penetration resistance as a measure of pile capacity could be misleading, since it does not reflect soil phenomena such as relaxation or freeze that could either reduce or increase the final static pile capacity. Relaxation or soil freeze can be checked by retapping piles several hours to several days after driving. The possibility of these phenomena occurring should be anticipated by the foundation engineer as a result of the site investigation.

6.4 Pile deterioration

All types of piles are subject to deterioration. This deterioration is discussed in the following paragraphs, including protective measures that may be taken to control these problems.

6.4.1 Steel piles

Steel piles are subject to severe corrosion when exposed to salt water. Those areas normally most severely corroded are the steel in the tidal zone and the steel just at or below the mud line. The estimated rate of corrosion for uncoated steel in the North American continent, due to exposure to seawater is 0.15–0.2 mm/y (0.006–0.008 in/y) ([B38], [B138]).

Steel piles embedded in undisturbed natural soils below the groundwater table normally do not corrode [B138]. Piles embedded in manmade fills or in undisturbed soils above the water table corrode a minor amount, 1%–3% in 20 years, in the zones of worst corrosion activity. There are rare exceptions to this in the case of highly corrosive chemicals in fill or in pervious natural soils. These areas should be identified during the soil investigation by knowledge of prior use of the site as well as soil and groundwater tests for acidity.

Copyright © 2001 IEEE. All rights reserved.

Copyright The Institute of Electrical and Electronics Engineers, Inc.
Provided by IHS under license with IEEE
No reproduction or networking permitted without license from IHS
Not for Resale

Stray direct currents may also be a source of corrosion: however, such cases for pile foundations are not documented and consequently, must be quite rare.

Protection of steel piles in a corrosive environment may be accomplished by one or several of the following methods:

— Increasing the cross-sectional area of steel
— Protective coatings such as epoxy coal tar paint, cold applied bituminous coatings, or bituminous emulsions.
— Reinforced concrete jacket
— Cathodic Protection

If corrosion protection of some form must be provided, it is important to consult with a corrosion protection engineer to establish the most economical methods. A more detailed discussion of corrosion to piling and methods of protection are given by Romanoff [B138] and Chellis [B38].

Pipe piles are less susceptible to damaging corrosion than H piles because of their uniform cross section results in a more uniform distribution of corrosion. In addition, pipe piles may be filled with concrete, and the pile may be designed to carry only a very low load or no load in the steel.

6.4.2 Concrete piles

Deterioration of concrete piles in soils is not considered significant, provided the concrete is designed to resist attack by a corrosive environment. This is normally provided by using sulphate resisting cement (Type II or Type V), if required. Exposed concrete piles are susceptible to deterioration, which may be caused by one or several of the following:

— *Abrasive action*. Ice, debris, wind, water, and spray cause serious deterioration in even the best quality concrete.
— *Mechanical action*. This may result if freezing water in the pores causes progressive deterioration.
— *Chemical decomposition*. Chemical decomposition of concrete in seawater is promoted by the presence of cracks, and will ultimately expose the reinforcing steel to corrosion in the air or oxygen-bearing water.

6.4.3 Wood piles

Decay in untreated wood piles is caused by fungus growth that breaks down the cellular structure of the wood. Wood piles are also subject to attack by termites that eat the untreated wood cellulose. Marine borers also attack the wood piles in seawater. The most common form of treatment of wood piles is creosote that poisons the food supply of fungi, marine borers, and termites. Creosote must be applied by a pressurized process, and its effectiveness is measured by the balance of penetration and degree of absorption as described in AWPA C-3 [B20]. Creosoted wood piles have an estimated life of 33 years above ground, 100–150 years when buried below ground, and 8–50 years in seawater. Untreated wood piles will not deteriorate if buried in soil below the groundwater table. In southern sea waters, it is customary to use waterborn salts (CCA) for treatment because in this climate creosote is not effective against marine borers.

Copyright © 2001 IEEE. All rights reserved.

Copyright The Institute of Electrical and Electronics Engineers, Inc.
Provided by IHS under license with IEEE
No reproduction or networking permitted without license from IHS Not for Resale

6.5 Construction considerations

6.5.1 Site access

The decision to utilize a pile foundation can present unique accessibility problems. Generally, the pile foundation design is selected due to overlying soft soils. Piles, whether wood, concrete, or steel, and installation equipment (driving hammers, leads, and cranes) are items of considerable weight. If the surface soils are soft, steps must be taken to provide an access of adequate bearing capacity to enable this equipment to be moved to the structure site. This may consist of simply adding gravel and a reinforcing fabric to stabilize the soil, or may require the use of mats to reduce the bearing pressure.

Environmental requirements also must be considered. Early construction input can assist the engineer in providing an installation of minimal cost to the owner.

6.5.2 Handling and installation

During transportation to the construction site, care should be exercised in handling to prevent deformation of steel pipe piles and cracking of wood and concrete piles. Significant handling stresses for long piles can result from large bending moments developed during pickup, depending on the location of the pickup point. Tensile stresses developed in concrete or wood piles can result in structural damage to the pile (for example, cracking). Bending moments depend heavily on the location of the pickup points. They should be determined based on allowable stresses and clearly marked.

Initial alignment of the piles is most important in reducing the subsequent possibility of creating undesirable bending stresses. Drilling of a pilot hole or spudding may be necessary to remove or displace obstructions near the surface. The use of fixed leads is desirable to eliminate sway at the head and to ensure an axial hammer blow. Driving heads to distribute the blow of the hammer and cap blocks to prevent damage to the pile and hammer are necessary for impact driving. Overdriving of a pile may cause structural damage and should be avoided.

7. Design of anchors

7.1 Anchor types

An anchor is a device that will provide resistance to an upward (tensile) force transferred to the anchor by a guy wire or structure leg member. An anchor may be a steel plate, wooden log, or concrete slabs buried in the ground, a deformed bar or a steel cable grouted into a hole drilled into either soil or rock, or one of several manufactured anchors that are either driven, drilled or rotated into the ground. Anchorage may also be provided by vertical or battered drilled shafts or piles. Typical types of anchors are shown in Figure 68.

7.1.1 Prestressed and deadman anchors

Anchors may be classified as either deadman or prestressed. Deadman anchors are defined as those anchors that are not loaded until the structure is loaded. Prestressed anchors are loaded to specified load levels during installation of the anchor. Most of the initial strains of the prestressed anchor system are removed before the structural load is applied. Therefore, the full capacity of the anchor can be attained at very small deformation [movements of less than 6 mm (0.25 in) in soil are typical]. Prestressed anchors are proof-loaded to their design load at the time of installation. Shallow prestressed anchors may obtain additional strength by the increased effective stress created by the influence of the cap on the soil adjacent to the anchors as shown in Figure 69. There is some question as to the effect time will have on this increased capacity. Seeman et al. [B140] reported satisfactory load tests on 2224 kN (500-kip) capacity prestressed anchors installed for a 1100-kV test line. Prestressed anchors are generally more expensive than deadman anchors and should not

Copyright © 2001 IEEE. All rights reserved.

Copyright The Institute of Electrical and Electronics Engineers, Inc.
Provided by IHS under license with IEEE
No reproduction or networking permitted without license from IHS
Not for Resale

be used in soils which exhibit time dependent compressibility. Deadman anchors may include any of the systems shown in Figure 68. Initial strains in deadman anchors may be reduced by as much as 50% by prestressing them to their design load at the time of installation [B4].

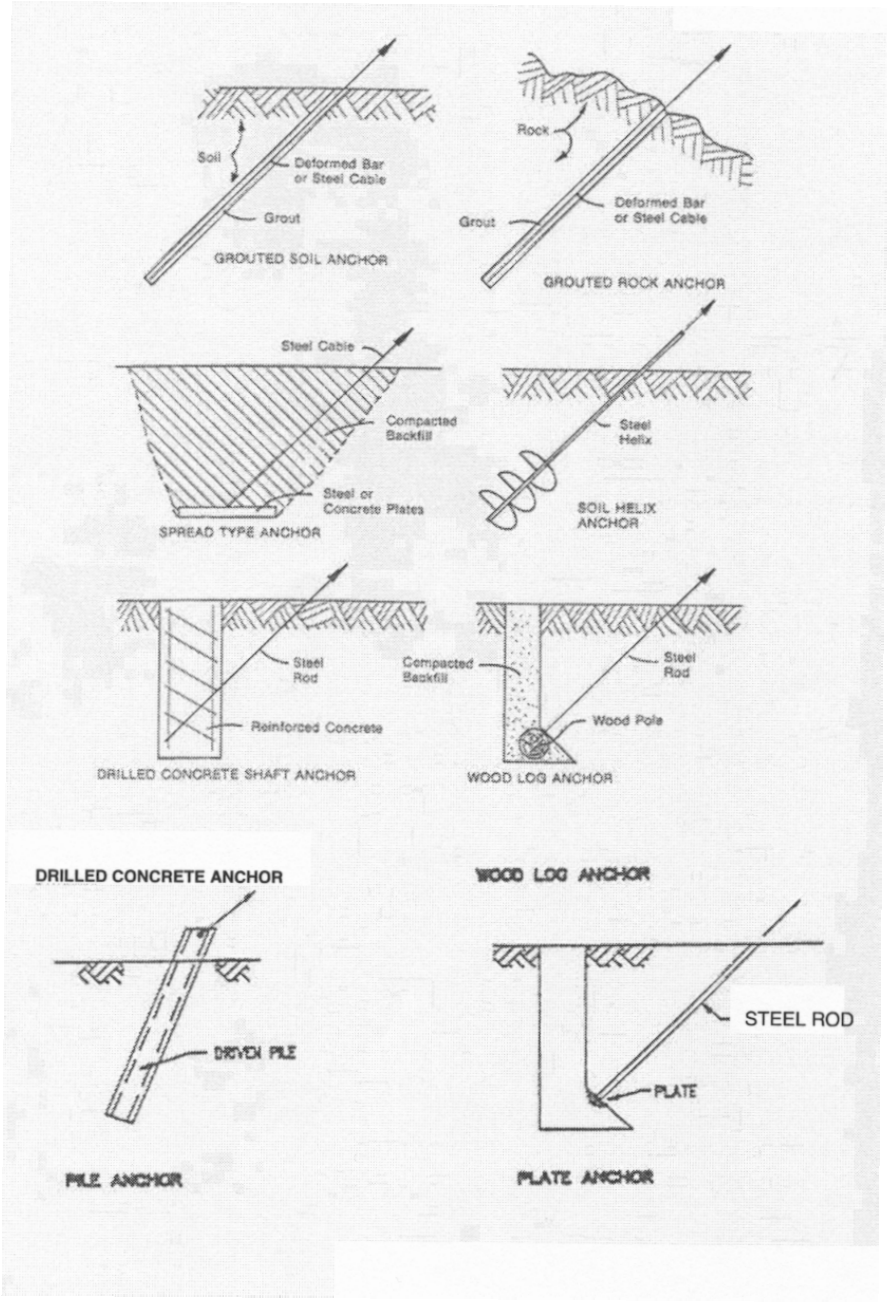

Figure 68—Typical anchors

Copyright © 2001 IEEE. All rights reserved.

Copyright The Institute of Electrical and Electronics Engineers, Inc.
Provided by IHS under license with IEEE
No reproduction or networking permitted without license from IHS
Not for Resale

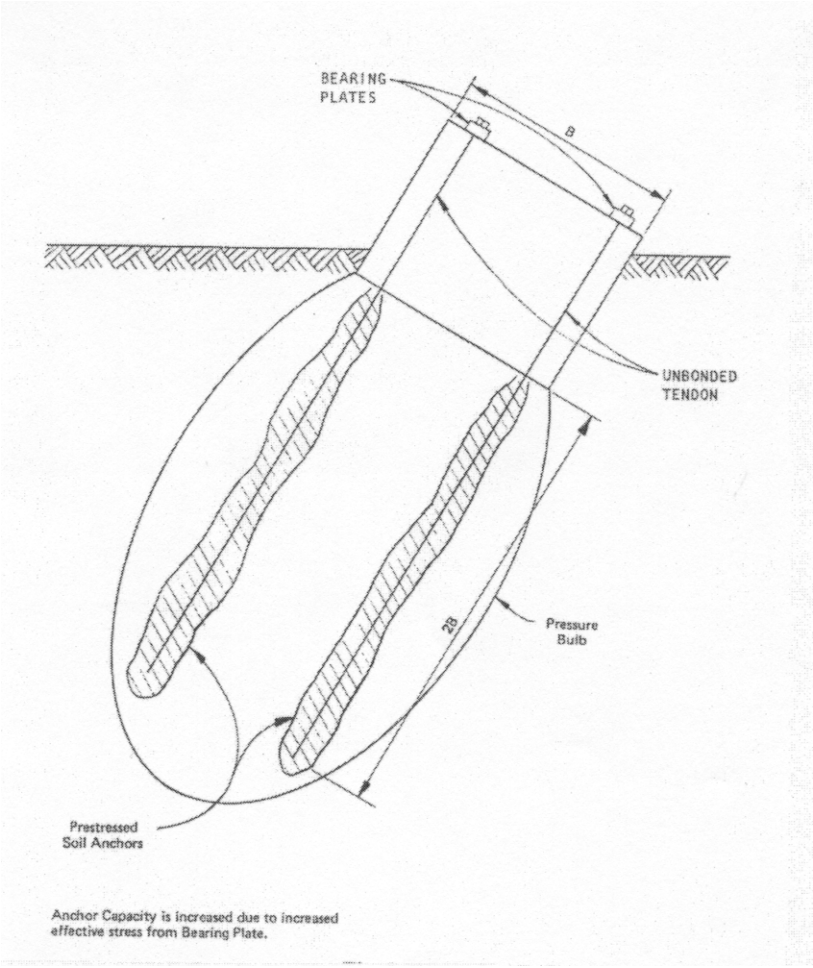

Figure 69—Prestressed anchors

7.1.1.1 Grouted rock anchors

A grouted rock anchor consists of a steel tendon (either steel bar, wire, tower leg angle, or steel cable) placed into a hole drilled into the rock. One rock anchorage system develops anchorage by grouting the void around the tendon in the rock. Another type of rock anchor develops anchorage with a mechanical expandable locking mechanism that expands into the surrounding rock at the anchor tip. All rock anchors are grouted either before or after installation. The grout may be injected either under gravity or at greater pressure.

7.1.1.2 Grouted soil anchors

A grouted soil anchor consists of a steel tendon (either steel bar, wire, or steel cable) placed into a hole drilled into the subsoil that is subsequently filled with cement grout under pressure. Loads are transferred through the tendon to the grout at a depth where the overburden pressure and shear strength of the soil are sufficient to resist the uplift force placed on the tendon. Grouted soil anchors are installed with a minimum disturbance of the in-situ soils, thereby preserving the natural soil strength. The in-situ stresses may be considerably increased by high-pressure grouting, contributing to a high anchor capacity. These factors tend to make grouted soil anchors cost effective, particularly with capacities in excess of 445 kN (100 kips). Grouted soil anchors may not be economical where many boulders are expected to be encountered.

Copyright © 2001 IEEE. All rights reserved.

Copyright The Institute of Electrical and Electronics Engineers, Inc.
Provided by IHS under license with IEEE
No reproduction or networking permitted without license from IHS
Not for Resale

7.1.1.3 Helix soil anchors

A helix soil anchor consists of one or more helically deformed plates attached to a central core or hub. The anchor is installed by rotating it into the ground, usually with a truck-mounted power auger. The anchorage is developed by transmitting the load in the hub to the soil surrounding the helices. Helix anchors can be designed for compression loads as well as for tension.

7.1.1.4 Spread anchors

Spread anchors are defined as those anchors that develop their resistance to uplift by the weight of the anchor, plus the weight and strength of the soil above it in the same manner as the spread foundations covered in Clause 4. Typical spread anchors include grillage, pressed plate, dome, pad, and pyramid. Some commonly used materials are steel, reinforced concrete, precast concrete, fiber-reinforced plastic and cast iron. Spread anchors are constructed in a pit or trench. Compacted backfill, usually with the same material that was excavated, is placed over the anchor. If the insitu material cannot be easily compacted, this factor should be considered in the design. A spread anchor is preferable in dry soils containing boulders where drilled or helix anchors cannot be readily installed. It is important to ensure that the backfill above the anchor is properly compacted, or the anchor will not develop its full capacity.

7.1.1.5 Plate anchors

Plate and log anchors are defined as anchors that require separate excavations for the anchor and anchor rod. The load is applied through the anchor rod to the anchor causing the anchor to bear upon relatively undisturbed earth (Figure 70). One plate-type anchor utilizes a wood log and anchor rod as shown in Figure 70, part a. This anchor is widely used because of the ease in obtaining material. The holding capacity of this anchor is limited by the strength of the wood log or the connection between the rod and the log. The patented Nevercreep anchor (which is no longer in widespread use) shown in Figure 70, part b substitutes a curved steel plate for the wood log and special fitting key to allow for easier installation of the rod.

A crossed steel plate, Figure 70, part c, was developed to increase holding capacity. The plate or log anchor capacity can be increased by substituting a reinforced concrete anchor in place of the steel plate or wood log. The holding capacity of plate and log anchors are usually limited by the strength of the connecting device.

7.1.1.6 Drilled shaft anchors

A reinforced concrete shaft may be used as an anchor. The shaft may extend to the ground surface or terminate at some point below the top of the ground. A steel rod or cable transmits the load to the shaft. Drilled shafts may be installed vertically or battered in the line with the applied force. The movement of the shaft is resisted by its weight plus the friction or adhesion resistance of the surrounding soil plus lateral bearing resistance in the case of vertical installations.

7.1.1.7 Pile anchors

Piles may also be used as anchors in a manner similar to the drilled shaft anchor.

7.2 Anchor application

Anchors are used to permanently support guyed structures, as well as too temporarily support other structure types during erection and stringing. The legs of lattice towers can be anchored directly by rock anchors or helix-type anchors. The uplift capacity of spread foundations may be increased through the use of anchors, as shown in Figure 71. Guys and anchors are also used to terminate wire loads on wood structures and to increase wood structure capacity for high transverse loading. Guys and anchors may be utilized to provide additional longitudinal strength. Anchors may be used to increase the load capacity of existing foundations.

Copyright © 2001 IEEE. All rights reserved.
--`,,`-`-`,,`,,`,`,,`---
Copyright The Institute of Electrical and Electronics Engineers, Inc.
Provided by IHS under license with IEEE
No reproduction or networking permitted without license from IHS
Not for Resale

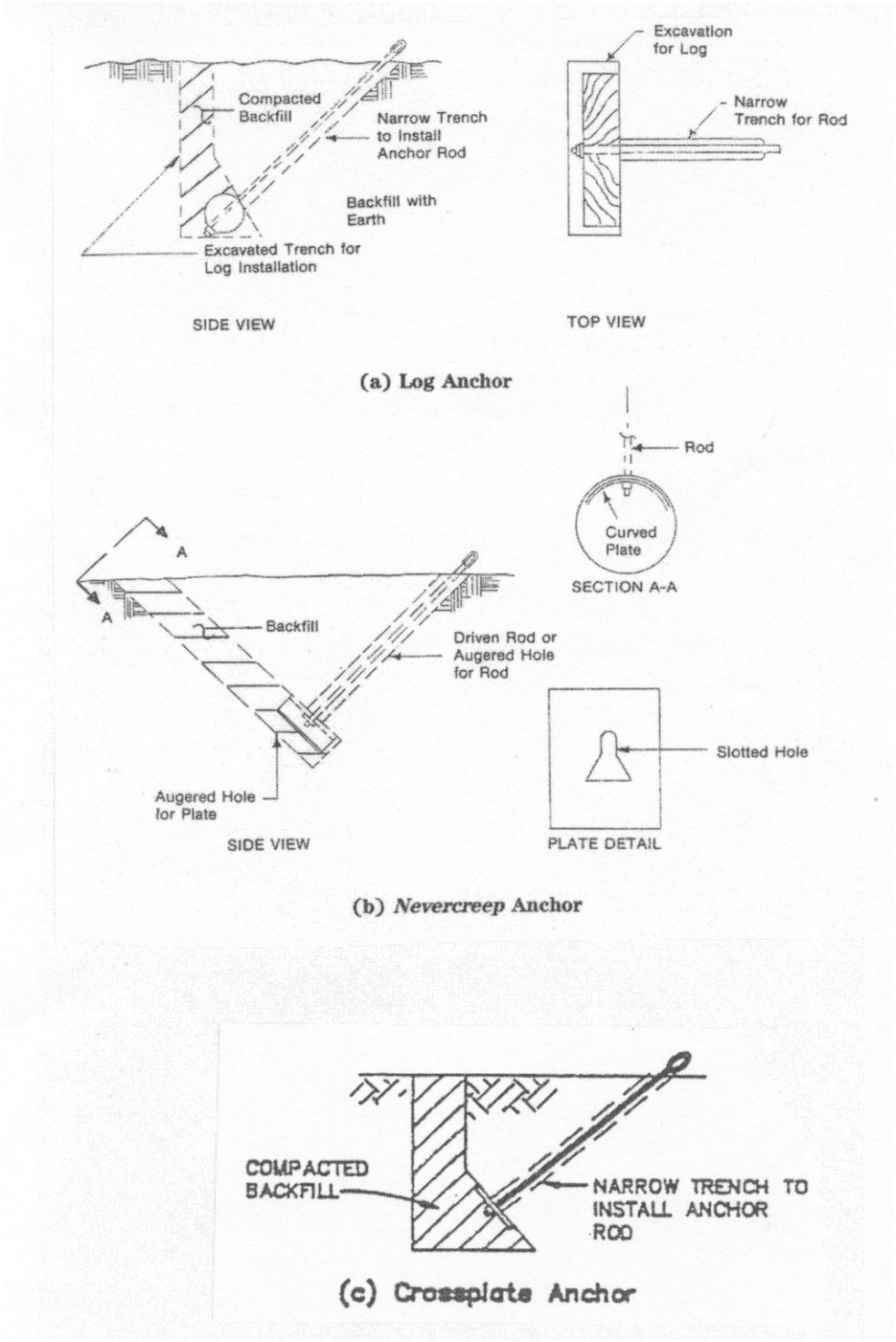

Figure 70—Typical plots and log anchors

Copyright © 2001 IEEE. All rights reserved.

Copyright The Institute of Electrical and Electronics Engineers, Inc.
Provided by IHS under license with IEEE
No reproduction or networking permitted without license from IHS
Not for Resale

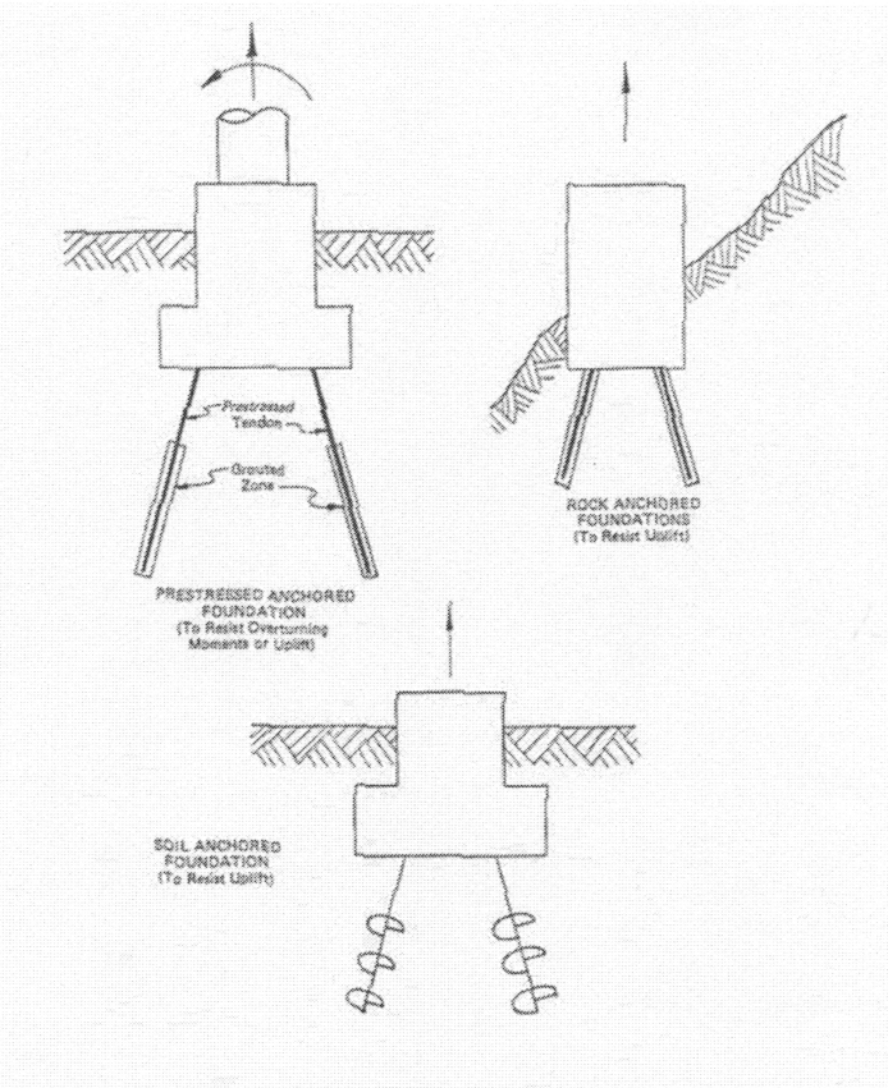

Figure 71—Typical spread foundations

7.3 Design analysis

The design analysis of an anchor depends upon a knowledge of the peak and residual shear strength properties of the soil or rock in which it is embedded. In rock, it is important to know the degree and depth of any weathering that may have occurred, together with the orientation and spacing of joints and foliation. A discussion of the investigation required to obtain these properties is contained in Clause 3. An understanding of the load characteristics, the structure deflection and the guy cable elongation tolerance is required in selecting and designing anchors. Anchor pullout tests are often conducted to confirm design assumptions where prior experience is lacking. See Clause 8 for a discussion of testing.

Copyright © 2001 IEEE. All rights reserved.

Copyright The Institute of Electrical and Electronics Engineers, Inc.
Provided by IHS under license with IEEE
No reproduction or networking permitted without license from IHS
Not for Resale

7.3.1 Design of grouted rock anchors

Rock anchors are designed to transfer uplift loads on transmission structure foundations or guys to the underlying rock strata. The ultimate uplift capacity of grouted rock anchors is determined by the following critical interfaces:

— Rock mass
— Grout-rock bond
— Grout-steel bond
— Steel tendon or connections, or both

See References [B23], [B65], and [B93] for more detailed discussion of rock anchor design.

7.3.1.1 Rock mass

The determination of whether a rock formation is suitable for assuming a rock mass failure is an engineering judgment based on a number of factors (such as RQD) that are discussed in Clause 3. Test borings, field inspection of excavations, knowledge of the local geology, past experiences, and load tests are important considerations in this evaluation. Since the rock characteristics can have a significant influence on the pull-out capacity of the rock mass, pullout tests or prestressing are often performed at questionable rock locations to confirm design assumptions. A generally used method for determining the load capacity of an anchor in heavily jointed or very weak rock is to assume that the rock mass fails with little rock resistance, and the load resistance is equal to the weight of rock contained within a specified volume that is often assumed to be a cone having its apex beginning at the anchorage and extending to the top of the rock mass, plus the shear strength of the rock along the assumed failure plane. This method should be used cautiously for design because the failure plane is complex and highly dependent on rock quality designation, resulting in a wide scattering of anchor capacities.

7.3.1.2 Grout-rock bond

An equation often used to establish ultimate uplift capacity of the anchor based on the grout-rock bond is:

$$T_u = \pi B_s L_s S_r \tag{141}$$

where

T_u is ultimate uplift capacity,
L_s is length of anchor shaft,
B_s is diameter of anchor shaft,
S_r is average shaft resistance per unit area of bond surface.

Some typical values of shaft resistance, S_r, for various rock types are summarized in Table 16.

Adams et al. [B4] conducted a number of tests to determine the rock-grout bond stress and concluded that the ultimate bond strength between rock and grout is a function of the relative shear strength of the grout or the rock, whichever is less. Horvath and Kenney [B78] developed relationships between shaft resistance and unconfined compressive strength of the weakest bonded material, either rock or grout, f'_w. All values in psi.

a) Large diameter [dia > 40.6 cm (16 in)]

$$S_r = (2 \text{ to } 3)\sqrt{f'_w} \tag{142}$$

b) Small diameter [dia < 40.6 cm (16 in)]

Copyright © 2001 IEEE. All rights reserved.

Copyright The Institute of Electrical and Electronics Engineers, Inc.
Provided by IHS under license with IEEE
No reproduction or networking permitted without license from IHS
Not for Resale

Table 16—Rock types and strength properties reported

Rock type	No of tests	Unconfined compressive strength MPa (psi)	Mobilized shaft resistance (S_r) MPa (psi)
Shale or mudstone	50	0.35 to 110 (50 to 16000)	0.12 to 3 + (17 to 400 +)
Sandstone	8	(7 to 24 +) (1000 to 3500 +)	0.52 to 6.5 (75 to 950)
Limestone or chalk	17	1 to 7 + (150 to 1000 +)	0.12 to 2.8 + (17 to 418)
Igneous	4	0.35 to 10.5 + (50 to 1500)	0.12 to 6.3 (18 to 920)
Metamorphic	8		0.47 to 2.3 + (68 to 273)
NOTE Grout/rock bond failures (shaft resistance) [B78]			

$$S_r = (3 \text{ to } 4)\sqrt{f'_w} \quad (143)$$

Figure 72 shows the relationship between shaft resistance and unconfined compressive strength of rock, and Figure 73 shows how shaft diameter affects shaft resistance.

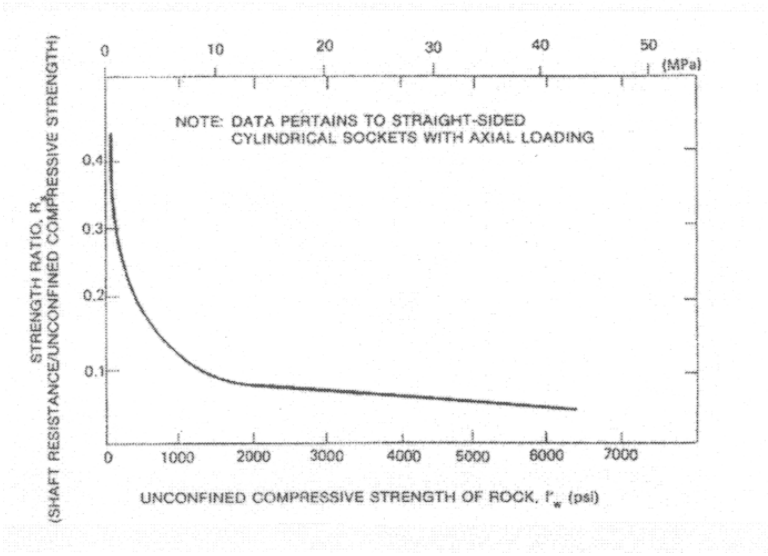

Figure 72—Straight ratio versus unconfined compressive strength for straight-sided sockets [B78]

7.3.1.3 Steel tendon

Normal reinforcing steel or high-strength steel wires, strands, cables, and bars are most commonly used for tendons. Often the choice of tendon type is determined by the method of installation or convenience of construction.

Copyright © 2001 IEEE. All rights reserved.

Copyright The Institute of Electrical and Electronics Engineers, Inc.
Provided by IHS under license with IEEE
No reproduction or networking permitted without license from IHS
Not for Resale

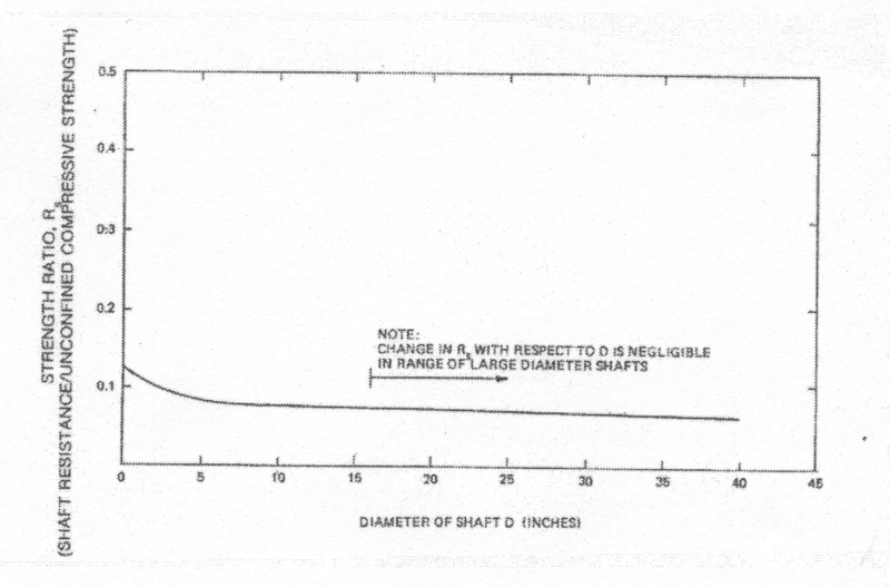

Figure 73—Average ratio for shafts of various diameters [B78]

7.3.1.4 Grout-steel bond

Grout-steel bond strengths depend upon the type of steel tendon used. The following steel tendon systems are discussed:

— Deformed steel bar
— Stranded wire cable
— Smooth steel bar

Table 17 lists typical properties and dimensions of steel wires, cables or strands, and bars commonly used for steel tendons.

Table 17—Typical steel properties and dimensions for tendons

Type of tendon	Diameter (in)	Bar size	Tensile stress f_u (ksi)	Yield stress f_y (% f_u)	Ultimate load (kips)	Yield load (kips)
Wire ASTM A421 [B7]	0.36		240	85[a]	11.8	10.0
Cables or strands ASTM A416 [B6]	0.25		250	85[a]	9.0	7.7
	0.50		270	85[a]	41.3	35.1
	0.60		270	85[a]	58.6	49.8

Copyright © 2001 IEEE. All rights reserved.

Copyright The Institute of Electrical and Electronics Engineers, Inc.
Provided by IHS under license with IEEE
No reproduction or networking permitted without license from IHS
Not for Resale

Table 17—Typical steel properties and dimensions for tendons (continued)

Type of tendon	Diameter (in)	Bar size	Tensile stress f_u (ksi)	Yield stress f_y (% f_u)[a]	Ultimate load (kips)	Yield load (kips)
Bars (deformed or plain) ASTM A615 [B10] Grade 40	0.75	6	70	57	30.8	17.6
	0.875	7	70	57	42.0	24.0
	1.00	8	70	57	55.3	31.6
	1.128	9	70	57	70.0	40.0
	1.27	10	70	57	88.9	50.8
	1.41	11	70	57	109.2	62.4
ASTM A616 [B11][b]	1.693	14	70	57	157.6	90.1
	2.257	18	70	57	280.1	160.0
ASTM A615 [B10] Grade 60	0.75	6	90	67	39.6	26.4
	0.875	7	90	67	54.0	36.0
	1.00	8	90	67	71.1	47.4
	1.128	9	90	67	90.0	60.0
	1.27	10	90	67	114.3	76.2
	1.41	11	90	67	140.4	93.6
	1.693	14	90	67	202.5	135.0
	2.257	18	90	67	360.0	240.0
Grade 75[c]	1.41	11	100	75	156.2	117.1
	1.693	14	100	75	225.1	168.8
	2.257	18	100	75	400.1	300.1

Copyright © 2001 IEEE. All rights reserved.

Copyright The Institute of Electrical and Electronics Engineers, Inc.
Provided by IHS under license with IEEE
No reproduction or networking permitted without license from IHS
Not for Resale

Table 17—Typical steel properties and dimensions for tendons (continued)

Type of tendon	Diameter (in)	Bar size	Tensile stress f_u (ksi)	Yield stress f_y (% f_u)[a]	Ultimate load (kips)	Yield load (kips)
ASTM A322 [B9]	0.50		160	85	34.1	29.0
	0.625		230	85	70.6	60.0
	1.00		150	85	122.8	108.6
	1.00		160	85	136.3	115.9
	1.25		150	85	187.5	159.4
	1.25		160	85	200.0	170.0
	1.375		150	85	234.0	198.9
	1.25		132	85	165.0	140.2
NOTE 1 in = 24.5 mm1; ksi = 6.898 N/ mm^2						

[a]90 for low relaxation steel
[b]ASTM A616 [B11] covers grade 50 and grade 60 only, maximum size #11 (1.41 in diameter)
[c]ASTM A615 [B10] no longer includes grade 75-90

7.3.1.4.1 Deformed steel bar

Deformed bars should be installed to at least the development lengths recommended in ACI 318 [B1].

7.3.1.4.2 Stranded wire cable

Stranded wire should have development lengths recommended in ACI 318 [B1] for development of prestressing strand. Additional bonding can be obtained by unstranding the wires at the end of the cable.

7.3.1.4.3 Smooth steel bar

Smooth bars should develop anchorage by using a mechanical device capable of developing the strength of the steel bar without damage to the grout. A nut-and-washer system at the rock end is one means of providing anchorage. Several mechanical rock anchors are available that provide a means for expanding the anchor into the rock. These devices use the rock to develop the uplift capacity required, and the grout is used to protect the steel tendon and seal the hole.

7.3.1.5 Unbonded and bonded tendons

Unbonded tendons transfer the entire load to a plate or point at the base of the anchor. The plate or point transfers all of the anchor load to the grout with no bond allowed to develop between the tendon and the grouted zone, except at the base of the anchor.

In a bonded anchor, the load transfer from the tendon to the grout is accomplished through the grout-steel bond acting over the surface of the tendon. Generally, the anchor geometry is such that no problems are encountered in obtaining the desired load in the tendon through the grout-steel bond. However, when bonding problems are encountered, the wires of cables may be unstranded at the end to ensure there is adequate

Copyright © 2001 IEEE. All rights reserved.

Copyright The Institute of Electrical and Electronics Engineers, Inc.
Provided by IHS under license with IEEE
No reproduction or networking permitted without license from IHS
Not for Resale

surface area for bonding. The tensile and shearing forces in the grout are larger for a bonded anchor, and hairline cracking in the anchor, which may lead to corrosion problems, has been observed in these anchor types [B119].

A partially bonded tendon is one in which a plate or point is fixed at the end of the tendon to help transfer the load. However, bonding of the tendon to the grout is permitted so that such anchors have the characteristics of both bonded and unbonded tendons.

7.3.2 Design of grouted soil anchors

Grouted soil anchors are designed to transmit uplift loads on transmission structure foundations or guys to the soil by the following mechanisms:

— Frictional resistance at the grout-soil interface.
— End bearing where anchors have a larger diameter than the initial drilled shaft diameter.

The actual load transfer mechanisms depend upon the anchor and soil type. Table 18 summarizes the basic grouted soil anchor types and the soils in which they are used.

7.3.2.1 Large diameter grouted soil anchors

Large diameter anchors are defined as any anchors whose shafts are larger than 40.6 cm (16 in) in diameter, and can be either straight-shafted, single-belled, or multi-belled. These anchors are commonly used in stiff-to-hard cohesive soils that are capable of remaining open when unsupported. Hollow flight augers can be used to install straight shafted anchors in less competent soils. Figure 74 shows typical large diameter grouted soil anchors.

The ultimate uplift capacity of large diameter straight-shaft and single-belled anchors can be estimated utilizing the formulae presented in 5.3.1.2 and 5.3.1.3. These formulae are largely empirical in nature, and field testing should be used to verify the ultimate uplift capacity.

7.3.2.2 Large diameter multi-belled grouted soil anchors

In relatively stiff cohesive soils, the ultimate uplift capacity of a belled-shaft anchor can be increased by increasing the number of bells as shown in Figure 74, part c. The ultimate uplift capacity T_u may be expressed as:

$$T_u = \pi B_s \sum_{0}^{L_s} \alpha C_u \Delta L + W'_f + \pi \omega C_u \left[\frac{1}{4}(B_b^2 - B_s^2) N_c + B_b L_u \right] \quad (144)$$

where

B_s is diameter of anchor shaft,
B_b is diameter of anchor bell,
L_s is distance from top of anchor to first bell,
L_u is distance from first bell to end of anchor.
W_f' is effective weight of anchor,
ω is shear strength reduction factor due to under reaming disturbances (ω has a value between 0.75 and 1.0)[B23],[B98],
α is strength reduction factor for adhesion,
ΔL is incremental length of anchor,
C_u is undrained shear strength,
N_c is bearing capacity factor (N_c = 9) [B65].

Copyright © 2001 IEEE. All rights reserved.

Copyright The Institute of Electrical and Electronics Engineers, Inc.
Provided by IHS under license with IEEE
No reproduction or networking permitted without license from IHS Not for Resale

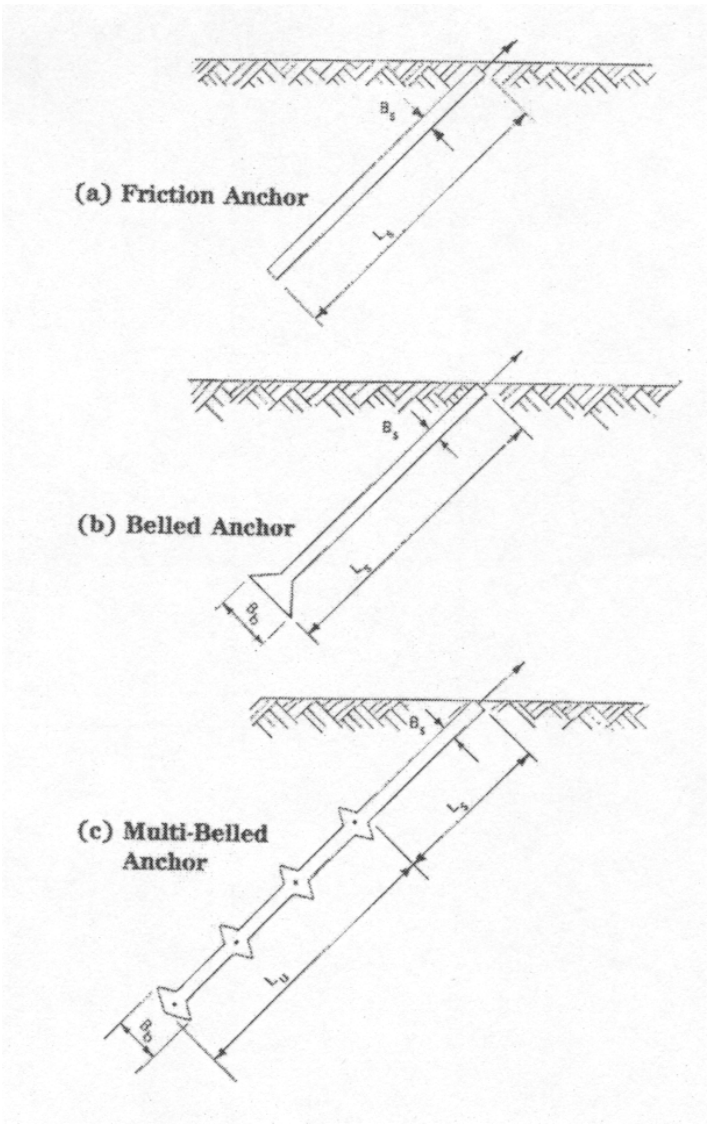

Figure 74—Typical large diameter grouted soil anchors

For failure to occur along a cylinder with a diameter B_b, the bells must be spaced from no more than 1.5 to 2.0 times the bell diameter with the bell diameter equal to 2 to 3 times the shaft diameter [B118].

7.3.2.3 Small diameter grouted soil anchors

Small diameter anchors are usually grouted under high pressure [usually greater than 1035 kN/m^2 (150 psi)]. The ultimate uplift capacity of the anchor will depend upon the soil type, grouting pressure, anchor length, and anchor diameter.

The interaction of these factors to determine capacity is not clear; therefore, the load predicting techniques are often approximate. The following theoretical relationships, in combination with empirical data, may be used to estimate ultimate uplift capacity. Figure 75 shows typical small diameter grouted soil anchors.

Copyright © 2001 IEEE. All rights reserved.

Copyright The Institute of Electrical and Electronics Engineers, Inc.
Provided by IHS under license with IEEE
No reproduction or networking permitted without license from IHS
Not for Resale

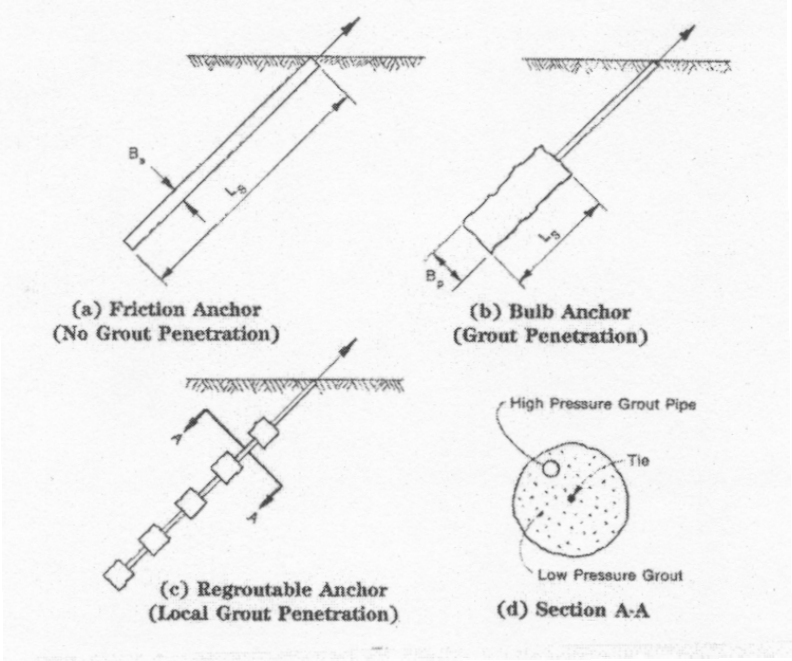

Figure 75—Typical small diameter grouted soil anchors

7.3.2.3.1 No-grout penetration into soil [B98], [B118]

For the condition of no-grout penetration into the surrounding soil, the ultimate uplift capacity T_u of small diameter grouted soil anchors may be estimated as:

$$T_u = P_i \pi B_s L_s \tan\bar{\phi} \quad (145)$$

where

B_s is diameter of anchor shaft,
L_s is length of anchor shaft,
$\bar{\phi}$ is effective friction angle between soil and grout (see 5.3.1.2),
P_i is grout pressure.

The following simplified formula is often used:

$$T_u = L_s n_i \tan\bar{\phi} \quad (146)$$

where

n_i is 8.7 to 11.1 kips/ft [B98].

Copyright © 2001 IEEE. All rights reserved.

Copyright The Institute of Electrical and Electronics Engineers, Inc.
Provided by IHS under license with IEEE
No reproduction or networking permitted without license from IHS
Not for Resale

Table 18—Summary of grouted anchor types and applicable soil types

Method	Diameter in cm (in)					
	Shaft type	Bell type	Gravity concrete	Grout pressure kN/m^2 (psi)	Suitable soils for anchorage	Load transfer mechanism
Low pressure						
Straight shaft friction (solid stem auger)	30 to 60 (12 to 24)	NA[a]	A[b]	NA	Very stiff to hard clays. Dense sands.	Friction
Straight shaft friction (hollow-stem auger)	15 to 45 (6 to 18)	NA	NA	200 to 1035 (30 to 150)	Very stiff to hard clays. Dense sands. Loose to dense sands.	Friction
Underreamed single bell at bottom	30 to 45 (12 to 18)	75 to 105 (30 to 42)	A	NA	Very stiff to hard cohesive soils. Dense sands. Soft rock	Friction and bearing
Underreamed multi-bell	10 to 20 (4 to 8)	20 to 60 (8 to 24)	A	NA	Very stiff to hard cohesive soils. Dense sands. Soft rock	Friction and bearing
High pressure - Small diameter						
Not regroutable[c]	7.5 to 20 (3 to 8)	NA	NA	1035 (150)	Hard clays. Sands. Sand-gravel formations. Glacial till or hard pan.	Friction or friction and bearing in permeable soils.
Regroutable[d]	7.5 to 20 (3 to 8)	A	NA	1380 to 3450 (200 to 500)	Same soils as for not regroutable anchors plus: stiff to very stiff clay varied and difficult soils	Friction and bearing
NOTE Grout pressures are typical.						

[a]NA Not applicable
[b]A Applicable
[c]Friction from compacted zone having locked in stress. Mass penetration of grout in highly pervious sand/gravel forms bulb anchor.
[d]Local penetration of grout will form bulbs which act in bearing or increase effective diameter.

7.3.2.3.2 Grout penetration into soil

When the surrounding soil is pervious enough to permit grout penetration, the ultimate uplift capacity, Tu, of small diameter grouted soil anchors may be computed as:

$$T_u = P_a \bar{\sigma}_v \pi B_p L_s \tan\bar{\phi} + N_b \bar{\sigma}_{v@\text{end}} \frac{\pi}{4}(B_p^2 - B_d^2) \quad (147)$$

Copyright © 2001 IEEE. All rights reserved.

Copyright The Institute of Electrical and Electronics Engineers, Inc.
Provided by IHS under license with IEEE
No reproduction or networking permitted without license from IHS
Not for Resale

where

B_p is diameter penetration,
$\overline{\sigma}_v$ is average vertical effective stress over entire anchor length,
$\overline{\sigma}_{v@end}$ is vertical effective stress at shallow anchor end,
P_a is contact pressure at anchor soil interface divided by effective vertical stress $\overline{\sigma}_v$ (Littlejohn [B98] reports typical values of P_a ranging between 1 and 2),
N_b is bearing capacity coefficient similar to Terzaghi's bearing capacity coefficient N_q but smaller in magnitude.

B_s, L_s, and $\overline{\phi}$ are as defined in Equation (145)

A value of $N_b = 0.71$ to $0.77\ N_q$ is recommended, provided the depth of anchor is greater than 25 times the diameter of penetration B_p. Since the values for B_p, P_a, and N_b are often not available, the above formula is not usually utilized to estimate ultimate uplift capacity.

Littlejohn [B98] suggests the following simplified formula:

$$T_u = L_s N_2 \tan\phi \tag{148}$$

where

ϕ is angle of internal friction.

This formula is valid for values of L_s from 0.9 to 3.7 m (3 to 12 ft). N_2 varies from 380 to 580 kN/m (26 to 40 kips/ft) and assumes a diameter of penetration from 400 to 610 mm (15 to 24 in) and depth to anchor from 12.2 to 15.1 m (20 to 45 ft).

Permeation of the cement grout will not occur for permeability, K, below 10^{-2}cm/sec, and the no-grout penetration formula should be used in this case.

7.3.2.3.3 Empirical relationships

Figure 76 presents an empirical plot of the capacity of anchors founded in cohesionless soils. This figure was developed by Ostermayer [B119] and represents the range of anchor capacities that may develop in soils of varying densities and gradations.

7.3.2.3.4 Regroutable anchors

Regroutable anchors are small diameter anchors that allow the load-carrying capacity of the anchor to be improved after installation and testing. Figure 75, part c, illustrates a regroutable anchor. Jorge [B84] reported an improvement of anchor load capacity in both cohesionless and cohesive soils with a regroutable anchor. Figure 77 presents a summary of the results with data on very stiff clay from Ostermayer [B119]. A summary of data on cohesive soils for regroutable anchors is presented in Table 19. These values can be used to estimate regroutable anchor loads.

Copyright © 2001 IEEE. All rights reserved.

Copyright The Institute of Electrical and Electronics Engineers, Inc.
Provided by IHS under license with IEEE
No reproduction or networking permitted without license from IHS
Not for Resale

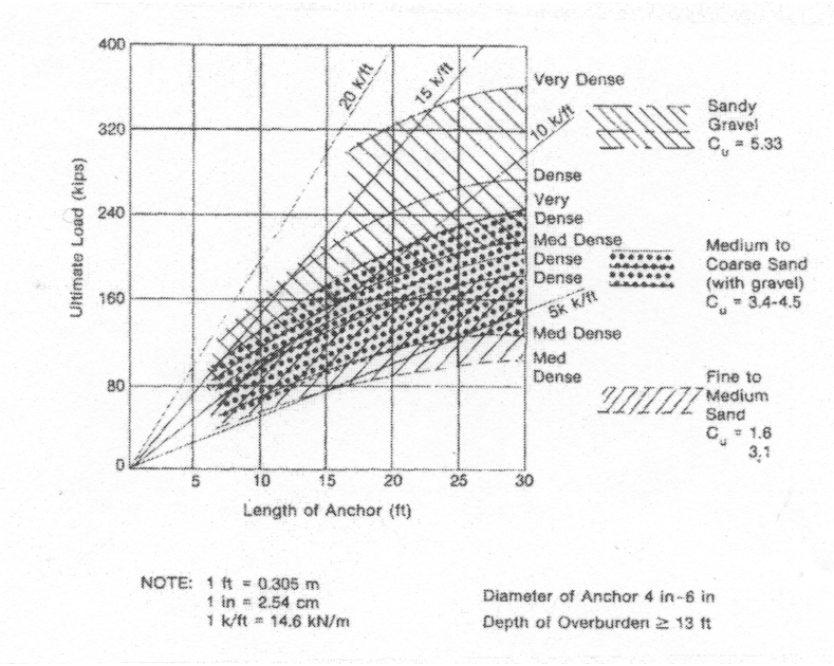

Figure 76—Load capacity of anchors in cohesionless soil showing effects or relative density, gradation, uniformity, and anchor length [B119]

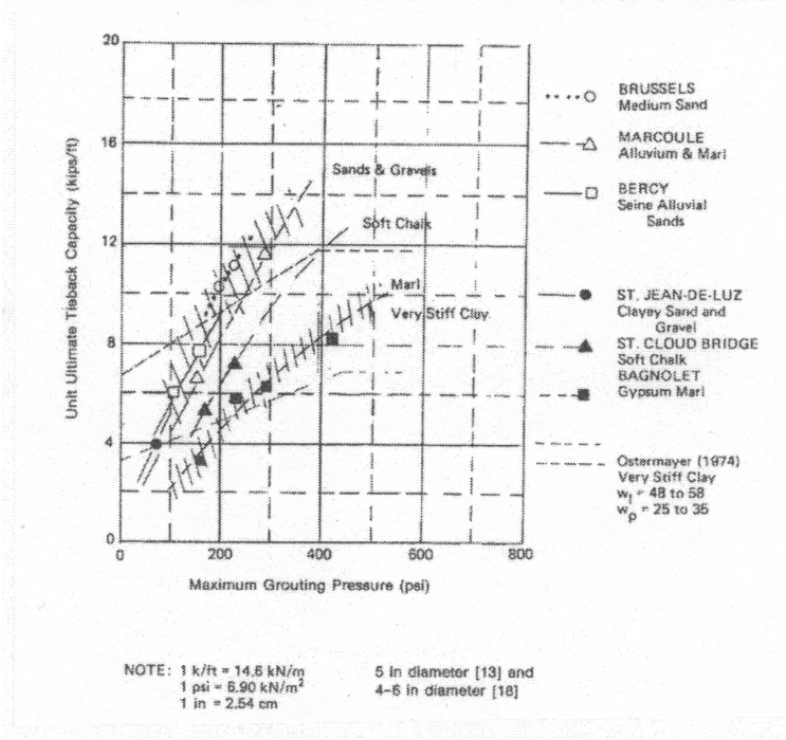

Figure 77—Ultimate anchor capacity as a function of grout pressure ([B84], [B119])

Copyright © 2001 IEEE. All rights reserved.

Copyright The Institute of Electrical and Electronics Engineers, Inc.
Provided by IHS under license with IEEE
No reproduction or networking permitted without license from IHS
Not for Resale

Table 19—High-pressure small-diameter tiebacks in cohesive soil [B119]

Soil type	Typical skin friction [kPa (lb per ft^2) of grouted zone]	
	Without post-grouting	With post-grouting
Marl clay medium plastic (W_l = 32 to 45; W_p = 14 to 25)		
Stiff	105—168 (2200—3500)	
Very stiff	168—311 (3500—6500)	
Marl sandy silt medium plastic (W_l = 45; W_p = 22)		
Very stiff to hard	311—407 (6500—8500)	407—503 (8500—10 500)
Clay - medium to highly plastic (W_l = 45 to 59; W_p = 16 to 35)		
Stiff	24—96 (500—2000)	
Very stiff	96—144 (2000—3000)	144—263 (3000—5500)

NOTES:
a) Tiebacks 90 mm to 152 mm (3-1/2 in to 6 in) o. d.
b) Values are for lengths in marl 4.6 m to 6.1 m (15 to 20 ft) and for lengths in clay 7.6 m to 9.1 m (25 to 30 ft).

7.3.3 Design of helix soil anchors

Commonly accepted practice for determination of uplift capacity of helical anchors is based on experience and empirical relationships that correlate installation torque to uplift capacity. The resulting anchor designs are not based on an evaluation of site conditions, subsurface stratigraphy, soil strength parameters or engineering principles. However, this approach has, in most cases, proved satisfactory. To this end the reader is directed to the various manufacturer's literature for information. Helix anchors are not normally prestressed; consequently, movement of several centimeters is common at the maximum design load. Testing each anchor to the design load is encouraged to verify capacity and reduce in-service movement under load.

To theoretically predict ultimate uplift capacity, Adams et al. [B4], Mitsch et al. [B114], Mooney et al. [B115] and Kulhawy [B87] have derived expressions based on bearing capacity theory above the top helix for multiple helix anchors and frictional cylinder theory between the top and bottom helices. Equations are presented for both cohesionless [B114] and cohesive soils [B115].

The general theory presented by the above references all note a distinct change in failure mode below a depth of from 3 to 5 helix diameters. Current practice for transmission line anchors recommends helix depth greater than 5 helix diameters, therefore, only the theory for deep foundations (D/B > 5) is presented. Cohesive soils are subdivided into clay and silt.

Copyright © 2001 IEEE. All rights reserved.
--`,,`-`-`,,`,,`,`,,`---
Copyright The Institute of Electrical and Electronics Engineers, Inc.
Provided by IHS under license with IEEE
No reproduction or networking permitted without license from IHS
Not for Resale

For deep foundations, the failure mode for a single helix is assumed to be a local bearing failure at the top of the helix. Multiple helices assume that the soil between the top and bottom helix acts as a soil plug which fails in shear along a cylinder of soil formed by the lower helix which is a larger diameter than the helices above it. This movement also results in local bearing failure on the top helix similar to a single helix. The skin friction of the shaft will also offer some resistance to uplift. All formulae below assume homogeneous soils and must be adjusted for soil changes.

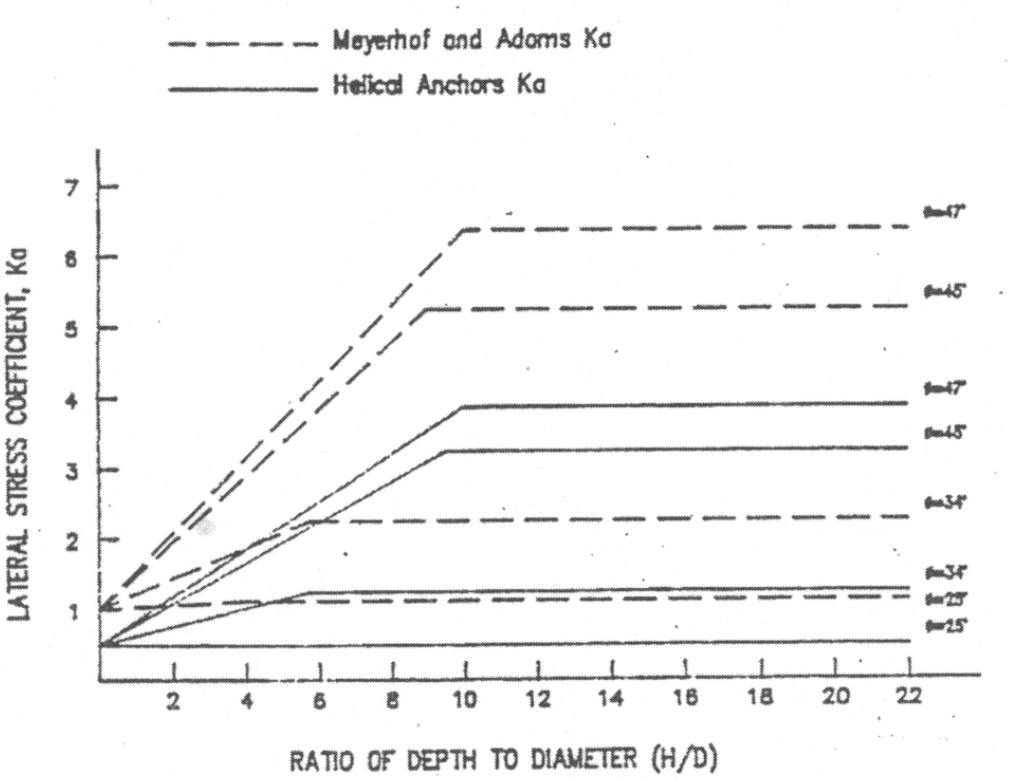

Figure 78—Recommended lateral stress values (Ka) for helical anchors and foundation in uplift

7.3.3.1 Cohesionless soils

7.3.3.1.1 Single helix :

$$T_u = \gamma D N_q A + P_s D \gamma \left(\frac{D}{2}\right) K_u \tan\phi \quad (149)$$

where

T_u is ultimate uplift capacity,
γ is effective unit weight of soil,
D is depth of helix,
N_q is uplift capacity factor (see Figure 79),

Copyright © 2001 IEEE. All rights reserved.

Copyright The Institute of Electrical and Electronics Engineers, Inc.
Provided by IHS under license with IEEE
No reproduction or networking permitted without license from IHS
Not for Resale

A is area of helix,
P_s is perimeter of shaft,
K_u is lateral earth pressure coefficient in uplift (see Figure 78),
ϕ is angle of internal friction.

7.3.3.1.2 Multiple helices

The shaft and helices below the top helix are assumed to act as a single cylindrical column with a diameter equal to the average diameter of the helices below the top helix. Total resistance capacity is found be adding this additional capacity (Q_a) to the capacity of the top helix previously calculated.

$$Q_a = \pi B_{ave} D_b K_u \gamma \left(D_a + \frac{D_b}{2} \right) K_u \tan\phi \quad (150)$$

where

B_{ave} is average diameter of the helix plates below the top helix,
D_a is depth above the top helix,
D_b is depth below the top helix.

K_u, γ, and ϕ are as above

7.3.3.2 Cohesive soils

7.3.3.2.1 Single helix-clay

Mooney's [B115] equations are presented below. They are similar to those of Adams and Hayes [B2] and Adams et al.[B4] but the bearing capacity factor N_c is replaced by an uplift factor N_{cu}. A reduction factor is applied to the undrained shear strength, C_u, to determine the shaft adhesion, C_a. Depending on the clay, C_a may vary from 0.3 C_u (for stiff clays) to 0.9 C_u (for soft clays).

$$T_u = AC_u N_{cu} + P_s D C_a \quad (151)$$

where

T_u is ultimate uplift capacity,
A is area of helix,
N_{cu} is uplift capacity factor for cohesive soils a value of 9 is recommended for deep foundations. (see Figure 80),
C_u is undrained shear strength,
P_s is perimeter of anchor shaft,
D is depth of helix,
C_a is adhesion on anchor shaft.

Copyright © 2001 IEEE. All rights reserved.

Copyright The Institute of Electrical and Electronics Engineers, Inc.
Provided by IHS under license with IEEE
No reproduction or networking permitted without license from IHS Not for Resale

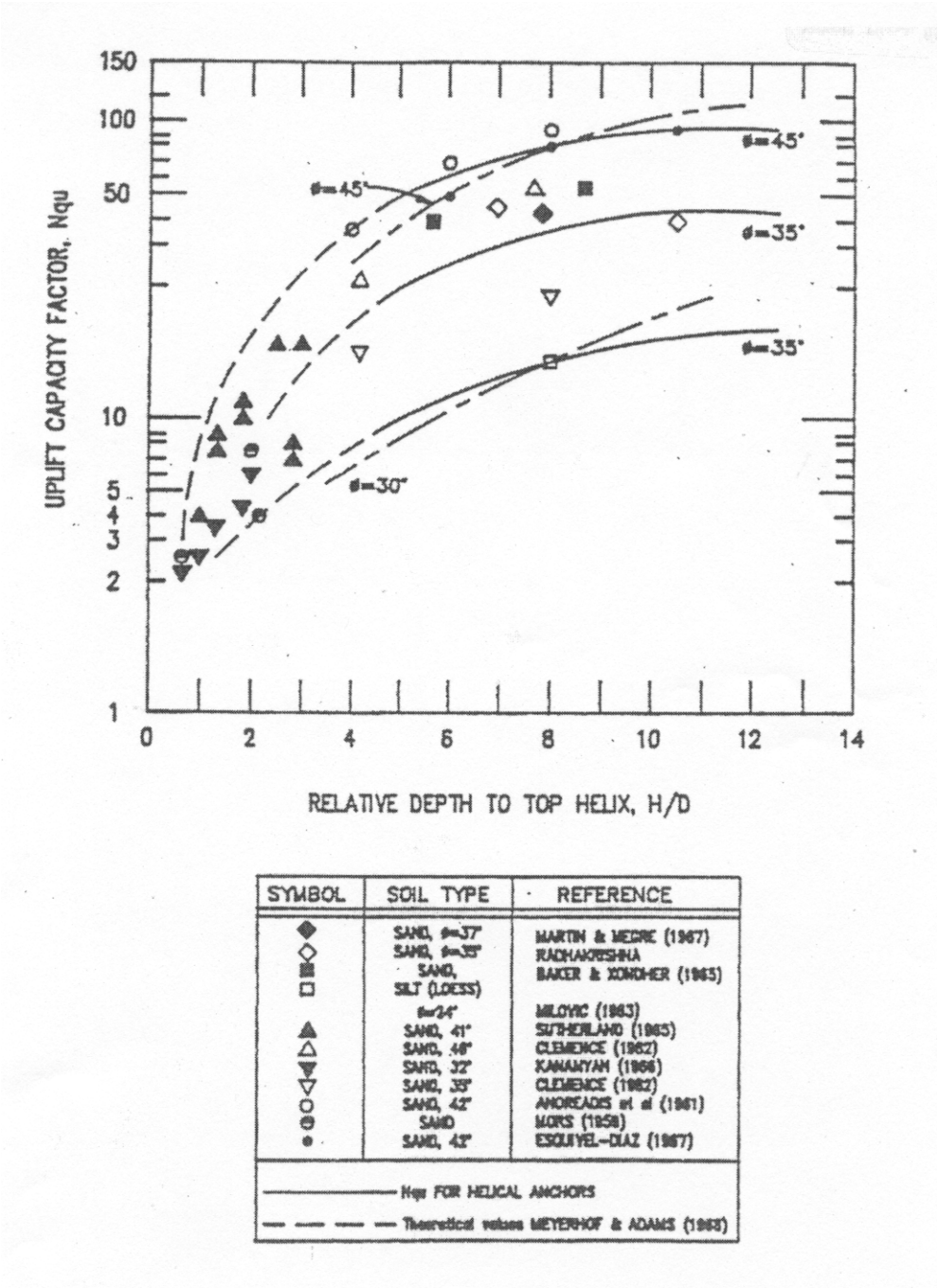

Figure 79—Uplift capacity factor, Nqu, versus H/D ratio for helical anchors in sand

Copyright © 2001 IEEE. All rights reserved.

Copyright The Institute of Electrical and Electronics Engineers, Inc.
Provided by IHS under license with IEEE
No reproduction or networking permitted without license from IHS
Not for Resale

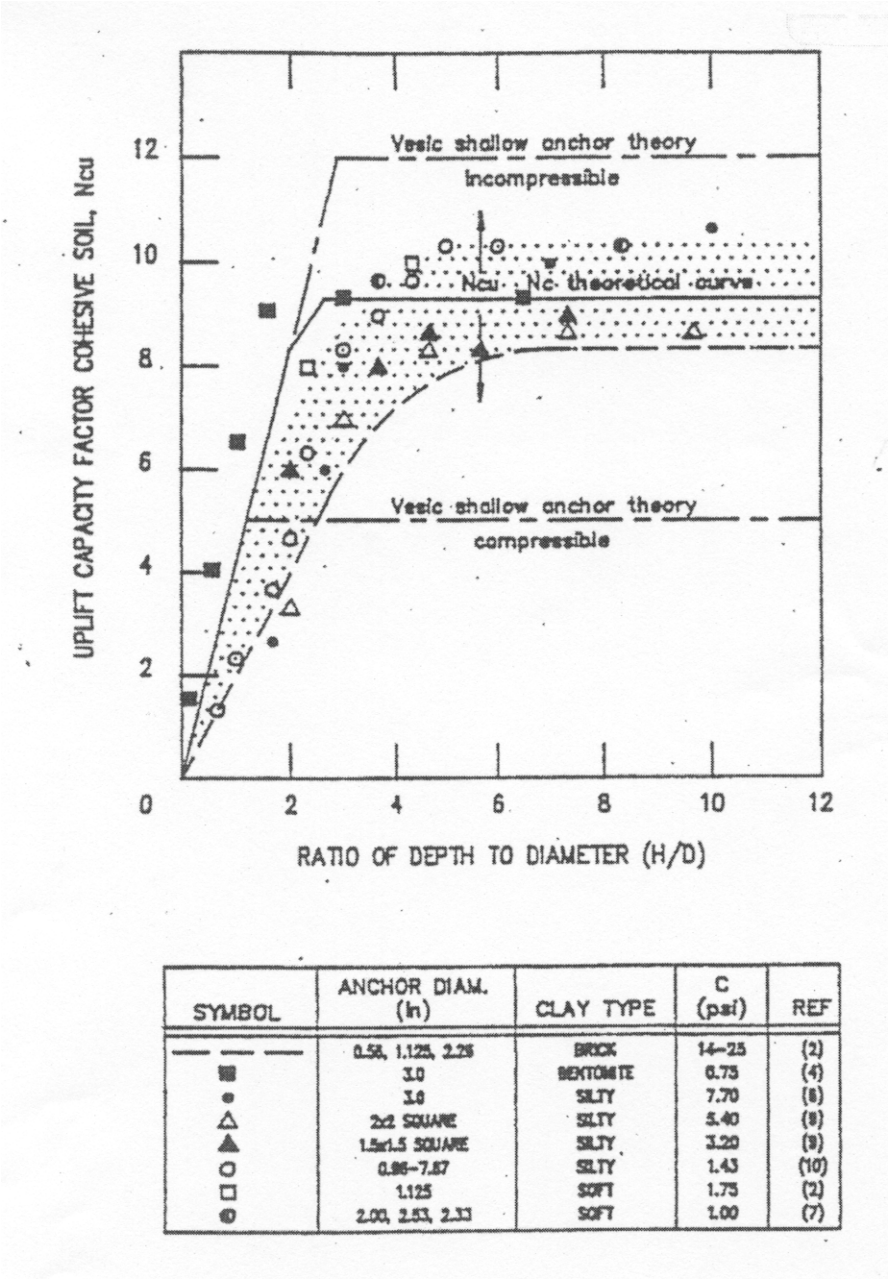

SYMBOL	ANCHOR DIAM. (in)	CLAY TYPE	C (psi)	REF
— — —	0.56, 1.125, 2.25	BRICK	14–25	(2)
■	3.0	BENTONITE	0.75	(4)
●	3.0	SILTY	7.70	(8)
△	2x2 SQUARE	SILTY	5.40	(9)
▲	1.5x1.5 SQUARE	SILTY	3.20	(9)
○	0.86–7.87	SILTY	1.43	(10)
□	1.125	SOFT	1.75	(2)
◐	2.00, 2.53, 2.33	SOFT	1.00	(7)

Figure 80—Uplift capacity factor, N_{cu}

Copyright © 2001 IEEE. All rights reserved.

Copyright The Institute of Electrical and Electronics Engineers, Inc.
Provided by IHS under license with IEEE
No reproduction or networking permitted without license from IHS
Not for Resale

7.3.3.2.2 Single helix-silt

The major difference between ultimate anchor capacity in clay and silt is the additional strength of the silt due to its frictional component.

$$T_u = \gamma D N_\phi A + A C_u + P_s D^2 \left(\frac{\gamma}{2}\right) K_o \tan\phi + P_s D C_a \quad (152)$$

where

γ is effective unit weight,
N_q is uplift capacity factor for cohesionless soils,
K_o is coefficient of lateral earth pressure in uplift (cohesionless soils).

T_u, A, N_{cu}, C_u, P_s, D, and C_a are as above.

7.3.3.2.3 Multiple helices

As with cohesionless soils, the shaft and helices below the top helix are assumed to act as a single cylindrical column with a diameter equal to the average diameter of the helices below the top helix.

7.3.3.2.3.1 Clay:

$$Q_a = \pi B_{ave} C_u D_b \quad (153)$$

where

Q_a is additional capacity,
B_{ave} is average diameter of helix plates below top helix,
C_u is undrained shear strength,
D_b is length of anchor below top helix.

7.3.3.2.3.2 Silt:

$$Q_a = \pi B_{ave} D_b K_o \gamma \left(D_a + \frac{D_b}{2}\right) \tan\phi + \pi B_{ave} C_u D_b \quad (154)$$

where

K_o is coefficient of lateral earth pressure in uplift (cohesionless soils),
γ is effective unit weight,
D_a is depth of top.

Q_a, B_{ave}, C_u, and D_b are as above

7.3.3.3 Correlation between uplift capacity and installation torque

Ghaly, Hanna, et al [B60][B61][B62][B63][B64] derived the following equation that relates installation torque to ultimate uplift capacity. This equation is limited to single pitch screw anchors:

Copyright © 2001 IEEE. All rights reserved.

Copyright The Institute of Electrical and Electronics Engineers, Inc.
Provided by IHS under license with IEEE
No reproduction or networking permitted without license from IHS
Not for Resale

$$T_u = 2\gamma A_s D\left[\frac{\tau}{\gamma A_s D p}\right] \quad (155)$$

where

T_u is ultimate uplift capacity,
γ is effective unit weight,
A_s is top surface area of helix blade,
D is depth of helix plate,
τ is installation torque,
p is pitch of screw anchor.

7.3.4 Design of spread anchors

Spread anchors develop their ultimate uplift capacity from the dead weight of the anchor plus the resistance of the soil above the anchor. The vertical component of the anchor uplift load may be analyzed by a number of different methods which are discussed in 4.2. Matsuo [B104] has performed model tests on spread foundations with a vertical pedestal that indicate as much as a 50% reduction in vertical capacity with an uplift load inclined 30° from the horizontal on pedestal-type spread foundations.

7.3.5 Design of plate anchors

In designing plate anchors, the soil uplift resistance, tendon strength, and tendon-to-plate connection strength are important considerations [B69], [B100].

7.3.5.1 Soil resistance

Design of plate anchors differ from spread anchors because the in situ strength of the soil can be used in calculating uplift capacity. Martin [B100] found that the failure mechanism changes from a soil failure resulting in movement of the soil mass above the anchor for shallow (D/B < 3) and medium depth (3 < D/B < 6) anchors to a localized soil failure at greater depths (D/B > 6); where D is the depth of the anchor and B is the minimum plate dimension. The strength in uplift is also dependent on

— The dimensions of the plate
— Depth and inclination of the plate
— Soil properties

The uplift resistance increases with depth and slope, but is also inversely proportional to the length-to-width ratio of the plate. Martin [B100] developed solutions for plate type anchors.

7.3.5.2 Tendon and connection design

Tendon design is covered in 7.3.1.4. The tendon to plate connection is often the critical design limitation for plate anchors. All forces and moments acting on the connection shall be considered. Full-scale testing of the connection for prototype plate anchors is recommended.

7.3.6 Design of drilled shaft anchors

The ultimate uplift capacity of drilled shaft anchors is covered in 5.3.1.

7.3.7 Design of pile anchors

The ultimate uplift capacity of pile anchors is covered in 6.3.1.2.

Copyright © 2001 IEEE. All rights reserved.

Copyright The Institute of Electrical and Electronics Engineers, Inc.
Provided by IHS under license with IEEE
No reproduction or networking permitted without license from IHS Not for Resale

7.4 Group effect

The capacity of a group of anchors depends upon the medium in which the anchor is embedded, the anchor spacing, and the depth of embedment. Each design should be checked for group failure; assuming the material is cohesive or granular soils, the group would be analyzed as a block of soil whose uplift capacity is equal to the weight of soil within the block plus the shearing resistance along the periphery of the block. The method of analysis would be one of the alternate methods for the uplift capacity for spread foundations discussed in 4.2.4. The method of analysis for the capacity of a group of rock anchors would be the same as given for single rock anchor in 7.3.1.1. An illustration of the method of analysis for a group of anchors is shown in Figure 81.

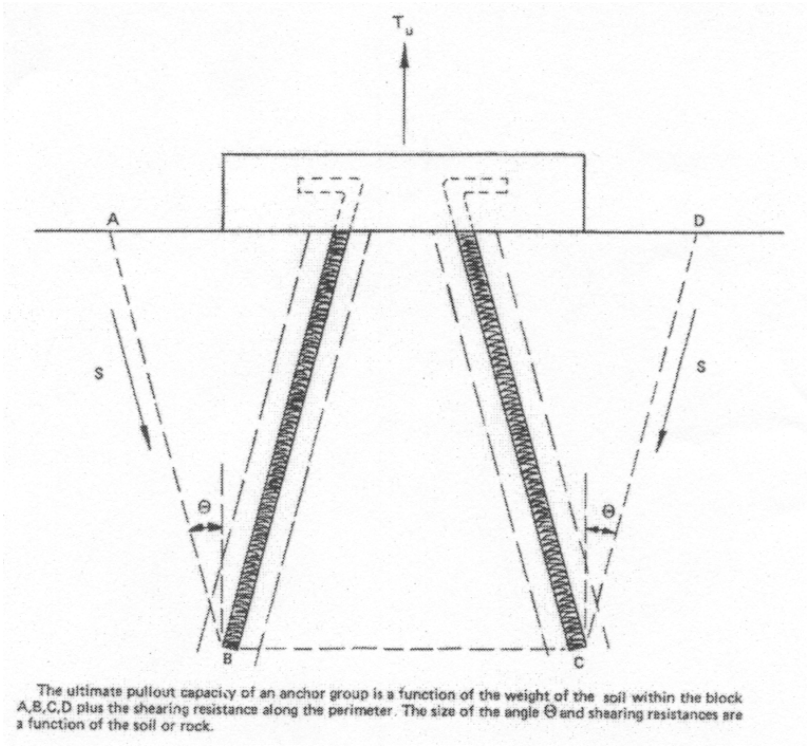

Figure 81—Ultimate uplift capacity of anchor groups

7.5 Grouts

7.5.1 Resin

Resin grouts are used because of their quick setting times of 10-20 min for 80-90% of ultimate strength. This allows anchor testing shortly after installation, opposed to other grouts which generally require 24 hours or more before testing. The strength of the resin grouts is comparable to that of concrete or cement grout. The major disadvantage of resin grouts is their relatively high cost. One method of installation for these grouts is placement of the grout and the activator in separate packages in the anchor hole. The anchor is then pushed down the hole breaking the packages. The setting process begins the instant the two compounds come in contact.

Copyright © 2001 IEEE. All rights reserved.

Copyright The Institute of Electrical and Electronics Engineers, Inc.
Provided by IHS under license with IEEE
No reproduction or networking permitted without license from IHS
Not for Resale

7.5.2 Cement

Cement grouts are commonly used in pressure grouted anchors, but they may also be placed under hydrostatic pressures as well. Generally, cement is mixed with water to form a neat cement grout. High early-strength grout may be used when quick setting is required. The strength of the grout usually is not critical, provided it has a compressive strength greater than 27 620 kPa (4000 psi). The anchors may be tested after 20 715 kPa (3000 psi) strength is reached. Cement grouts are most common for both earth and rock anchors. While expansive additives have been used in grouts, recent experience has shown that such additives may not be necessary for the satisfactory performance of the grout or anchor.

7.5.3 Concrete

In large diameter anchors [greater than 20 cm (8 in) diameter], the anchor is generally grouted under low pressure with a mixture of high early-strength cement, water, and sand or fine gravel. The sand or gravel filler is more economical than cement and does not appreciably reduce the strength of the grout. The aggregate in the concrete may prevent grout penetration and therefore reduce anchor capacity in permeable soils. However, large diameter anchors generally derive their resistive force in friction or end bearing, and do not rely upon grout penetration to increase capacity. The main concern for large diameter anchors is to assure a concrete-to-soil interface exists the full length of the anchor.

7.6 Construction considerations

7.6.1 Grouted rock anchors

Small diameter grouted rock anchors [8–20 cm (3–8 in)] typically are installed by advancing a casing down to the surface of the rock using conventional soil drilling equipment, and removing the soil with water or a combination of air and water. A hole is then drilled into the rock using either a rotary or percussion drill. After the grout holes are drilled, a temporary plug should be used to keep the holes from becoming fouled. A tendon is then inserted into the hole, and the hole is tremie grouted using a grout pipe or hose. The casing should not be removed until grout fills the entire hole and is seen at the ground surface. Grout should be pumped into the hole while the casing is being removed. Holes are often water-pressure tested to see if the hole will retain the grout. When drilling holes for grouted dowels, the location and batter of the grouted dowels (Figure 82) that anchor the concrete anchor into the deeper sound rock zones should be determined to provide adequate transfer of stress from the concrete to the underlying rock. This flexibility in hole location and batter cannot be tolerated for the grouted stub angle rod of the grouted type rock anchor (Figure 83). For this installation, the location and batter of the hole must be precise enough to accurately position the stub angle within the tolerances prescribed for accurate erection of the tower.

7.6.2 Grouted soil anchors

7.6.2.1 Straight-shaft large diameter grouted soil anchors

The method of installation depends upon the equipment used. A solid-stem continuous-flight auger may be used only if the hole is drilled in cohesive soil so that the hole will remain open when the flight is removed. If a hollow-stem auger is used, the auger remains in place during placement of the tendon. A detachable point is located in the auger tip to which the tendon is attached. The auger stem centers the tendon in the hole. Grouting with cement grout is done through the hollow stem as the auger is withdrawn. Grouting can be done under pressure, but the pressures are usually less than 1034 kPa (150 psi). A hollow-stem auger should be used in granular soils.

Copyright © 2001 IEEE. All rights reserved.

Copyright The Institute of Electrical and Electronics Engineers, Inc.
Provided by IHS under license with IEEE
No reproduction or networking permitted without license from IHS Not for Resale

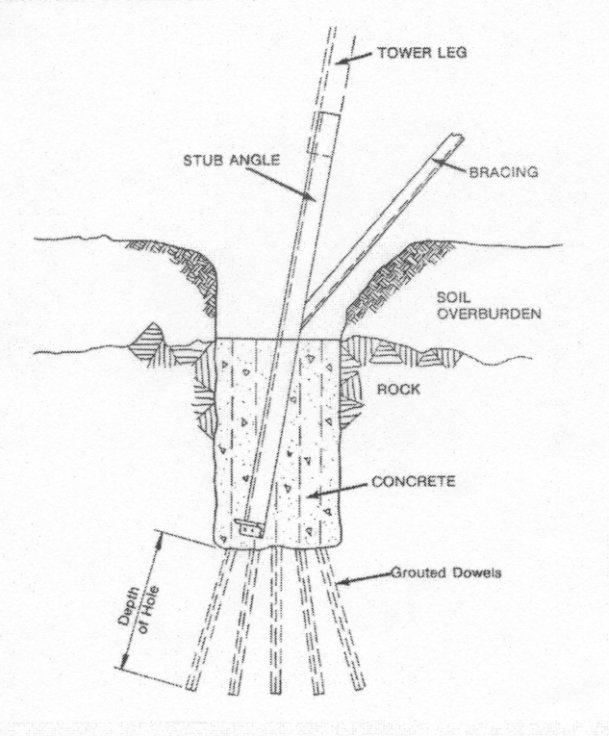

Figure 82—Tower stub rock anchor (with grouted dowels)

7.6.2.2 Multi-belled large diameter anchors

Multi-belled anchors are formed by drilling a straight shaft (either cased or uncased) to the point of the first bell, then withdrawing the drilling tools and inserting the belling tools. By repeating this procedure, a series of closely spaced bells is formed. Belling can only be done in self-supporting (cohesive) soils. Difficulties with the installation of this type of anchor have resulted in some contractors preferring to install longer straight shafted anchors rather than belled anchors. The bottom bell should be oversized to allow for loose material from upper bells that cannot be easily removed.

7.6.2.3 Small diameter anchors

An advantage of small diameter anchors is that the installation equipment is lightweight, readily available, maneuverable, and usable in poor site conditions.

7.6.2.3.1 Driven anchors

For this anchor type, a casing is driven into the ground with a detachable point at the end of the casing. After the casing is driven to the predetermined anchor length, the tendon is attached to the point and the point is separated from the casing. Grouting at pressures in excess of 1034 kPa (150 psi) begins as the casing is withdrawn. High grout pressures are most effective in soils where the grout can penetrate the surrounding soil.

7.6.2.3.2 Drilled anchors

Drilled anchors are the same as driven anchors, except that the hole is advanced by drilling using devices such as continuous-flight solid- or hollow-stem augers rather than by driving the casing.

Copyright © 2001 IEEE. All rights reserved.

Copyright The Institute of Electrical and Electronics Engineers, Inc.
Provided by IHS under license with IEEE
No reproduction or networking permitted without license from IHS
Not for Resale

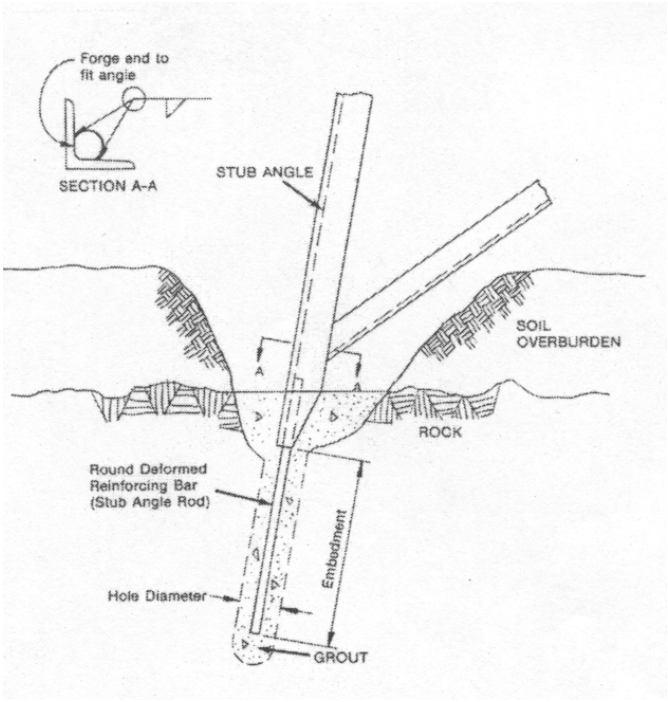

Figure 83—Grouted type rock anchor tower stub

7.6.2.3.3 Regroutable anchors

The installation procedures for regroutable anchors are similar to those for driven or drilled small diameter anchors. However, a grout pipe is affixed to the tendon prior to installing the tendon into the anchor hole. When the tendon is in place, grout is pumped in at low pressures to fill the voids between the tendon and the wall of the anchor hole while the casing is withdrawn. After the grout has set up, a second grouting is performed at higher grout pressures through the grout pipe that has ports at convenient intervals. The entire pipe can be grouted at once, or the ports can be isolated and grouted separately by means of packers. The high pressures [often as great as 4100 kPa (600 psi)] crack the initial grout and allow localized penetration into the soil. Once the initial grout has been cracked, the grout pressure drops off markedly, and the effective soil grouting pressures are in the range of 690 to 3450 kPa (100 to 500 psi). If the grout pipe is cleaned out, the procedure can be carried out several more times. The advantage of this procedure is that anchors failing to carry the load initially can be regrouted to increase their load carrying capability. Regroutable anchors require more sophisticated equipment and are more expensive than anchors with only a single grouting stage.

7.6.3 Helix soil anchors

Helix soil anchor installation requires adequate equipment and an experienced operator who installs the anchor at a constant rotational speed, with proper down pressure and with a constant anchor angle to ensure continued anchor advancement throughout the installation. Constant rotational speed is important because it makes it easier for the operator to provide the proper down pressure and constant anchor angle. If the speed is increased, it will be difficult to maintain proper down pressure. The result could be spinning the anchor. Spinning an anchor disturbs the soil and reduces the holding capacity, and installation must continue below the disturbed soil to an adequate depth to ensure the required design capacity. Constant speed also allows the

Copyright © 2001 IEEE. All rights reserved.

Copyright The Institute of Electrical and Electronics Engineers, Inc.
Provided by IHS under license with IEEE
No reproduction or networking permitted without license from IHS
Not for Resale

operator to determine changes in soil conditions that the anchor encounters. The constant speed should be slow enough to allow the ground man to visually monitor the anchor and tooling during installation. This would provide time to stop or correct the installation procedure if problems occur, such as encountering rocks or gravel. Proper down pressure should be 450 or 900 kg (1000 or 2000 lb). There are few devices in the field to measure this load. The result is that the operator controls the applied down pressure by feel. Too little down pressure can result in the anchor spinning, with results as mentioned above. Excessive down pressure can cause the helix to close, preventing further penetration. Excessive pressure can also cause hub breakage because it induces a bending stress. The combination of bending stress with shear stress induced by rotation can cause a failure below the torque rating of the anchor. Installations in rocky soils are particularly susceptible to excessive down pressure because of the combination stresses induced when a rock is encountered. In a soil free of rocks and obstructions, digger derricks can seldom apply excessive down pressure. Only the bed-mounted equipment, for example, Highway, Sterling, or Texhoma diggers, will apply excessive down pressure. In rocky and very stiff soils, it is very important to control down pressure and maintain proper alignment of the anchor, wrench, and kelly bar. Rotational speed should be slowed down to allow better control and feel when installing in rocky soils. Maintaining a constant anchor angle is important. If the anchor angle were continually changed during installation, bending stresses would be induced into the helix, weld, and hub and would promote failure. It is conceivable that if the angle changed, the installing tool or shaft could develop friction against the soil, which may cause inaccurate torque readings. Severely changing the anchor angle could cause inaccurate torque readings, and excessive wear on the installing tools and rotary equipment. Repeated use in this manner could substantially shorten the life of all equipment.

7.6.4 Spread anchors, Drilled Shaft Anchors, and Pile Anchors

Construction considerations for spread, drilled shaft, and pile anchors are similar to construction considerations for spread foundations, drilled shaft foundations, and pile foundations, respectively.

7.6.5 Corrosive water conditions

When anchor tendons are exposed to corrosive surface or subsurface water conditions, additional protective coating or grout encasement should be provided.

8. Load tests

8.1 Introduction

8.1.1 Reasons for load testing

Transmission line structure foundations are load tested for the following reasons:

— Verification of the foundation design for a specific transmission line
— Verification of the adequacy of foundations after construction, i.e., proof load tests
— Assistance in research investigations

Load tests conducted as part of a foundation investigation for a particular transmission line help the engineer determine the most cost-effective foundation for support of transmission line structures. These tests would be performed after the preliminary subsurface investigation of the right-of-way and preferably before final design of the foundations. Testing prior to final design allows for adjustment in the design in the event that the actual failure load is less or greater than the design load. However, it may be impractical to install a test foundation prior to the actual construction of the line.

Copyright © 2001 IEEE. All rights reserved.

Copyright The Institute of Electrical and Electronics Engineers, Inc.
Provided by IHS under license with IEEE
No reproduction or networking permitted without license from IHS
Not for Resale

Proof load tests conducted as a check on the adequacy of foundations after construction verify that foundations at a number of sites can withstand a particular load. These tests are performed routinely on grouted soil or rock anchors to ensure their capacity. It may be necessary to load test existing foundations if higher loads are proposed—for example, as a result of "reconductoring."

Load tests may be conducted on transmission line structure foundations to improve general knowledge of foundation behavior. Results of these research studies lead to improved transmission line structure foundation design methods and, in the long term, help reduce foundation costs.

Many load tests have been performed in such a manner that the results are of little value to the engineering profession. For example, the literature contains many examples of load test results which do not include an accurate and complete description of the soil or rock in which the load tests were performed.

This section is intended to guide engineers to develop testing programs which provide a sufficient quantity and quality of information to make the tests more useful to the individual engineer and to the engineering profession in general. Additional information on load testing is presented in Hirany and Kulhawy [B75] and Kulhawy, Trautmann, Beech, O'Rourke, McGuire, Wood, and Capano [B175].

8.1.2 Benefits

In general, information provided by load tests reduces the uncertainties inherent in the design of foundations, resulting in more reliable designs. A load test program should be evaluated by comparing the expected cost of the load test program against the potential benefits of the information obtained from the load tests.

Examples of the benefits of load tests are

a) *Cost savings*. When large numbers of foundations are to be constructed, the cost of a load test program may be relatively small when compared to the foundation cost savings that might result from the load test information.

b) *Efficient designs*. Variations of soil/rock properties result in uncertainties in determining foundation behavior. One accurate way to determine foundation behavior in a particular soil type is to perform full-scale load tests. Results of load tests performed in one soil type may allow the efficient design of foundations in similar soil types.

c) *Improve design methods*. It may be cost-effective or prudent to verify the validity of an existing, modified, or new design method. For a particular foundation type, whether it be conventional or unique, there may be several design methods which seem applicable, but result in different foundation dimensions. Foundation load test results can lead to the selection of the appropriate method.

d) *Improve construction techniques*. The construction technique used to build a specific foundation may have a major effect on the behavior of the foundation. It may not be possible to know in advance to what degree a particular construction technique will affect certain soil types. Foundations constructed using several techniques could be tested to determine the actual effect of each construction technique on the load capacity of the foundation.

   Another important benefit for performing foundation testing prior to final design can be the determination of the feasibility and efficiency of the construction technique.

e) *Optimize structure design*. Foundation load tests may be performed to determine if a cost-efficient structure design can be used. It is possible that these tests could be done in conjunction with any of the above.

Copyright © 2001 IEEE. All rights reserved.

Copyright The Institute of Electrical and Electronics Engineers, Inc.
Provided by IHS under license with IEEE
No reproduction or networking permitted without license from IHS Not for Resale

8.1.3 Types of load tests

Load tests can be classified on the basis of the type of load applied. Generally, the load types are as follows:

— Uplift
— Compression
— Lateral
— Overturning (Moment)

The engineer should decide whether to

a) Apply one type of load to the test foundation, making it easier to interpret foundation response to loading; or,

b) Apply several types of loads simultaneously, simulating an actual tower loading condition, but making interpretation of the foundation response more difficult.

8.2 Instrumentation

The type of instrumentation required will depend on the data which must be obtained to meet the needs of the test program. As a minimum, loads applied to the foundation and movements of the foundation should be measured. The necessity-for measuring other parameters such as stresses in the soil and foundation, movements of soil and/or rock in the zone of influence of the foundation, and pore water pressures in the soil near the foundation should be evaluated.

Selection of the proper instruments to obtain the desired measurements should be done by a qualified engineer who is fully aware of the advantages and disadvantages of available instruments. Descriptions, principles of operation, and a thorough inventory of various geotechnical instruments to measure load, deformation, soil stress, pore pressure, and temperature has been compiled by Dunnicliff [B56]. Seldom will one manufacturer have all of the instruments best suited to the test program.

A well-planned instrumentation system should consider the following (Dunnicliff [B56]):

a) *The variables to be measured*. In order of their importance, the most common types of measurements made during load tests are: loads, displacements, stresses, and pore water pressures.

b) *The physical phenomenon employed in the measuring system*. The technique by which a measurement is made will have an influence on the attributes which follow.

c) *Durability.* The intrinsic ability of the instrument to survive in its environment—resistance to impact, prolonged submergence, corrosive substances, temperature variations, etc.

d) *Sensitivity.* The smallest significant change in the variable being measured which the instrument will detect.

e) *Response time*. The ability of the measuring system to detect rapid changes in the value of the variable being measured. This is very important in dynamic measurements and in pore water pressure measurements.

f) *Range*. The difference between the maximum and minimum quantities that can be measured by a particular instrument without undergoing any alteration.

g) *Reliability.* The ability of an instrument to retain its specified measuring capabilities with time.

Copyright © 2001 IEEE. All rights reserved.

Copyright The Institute of Electrical and Electronics Engineers, Inc.
Provided by IHS under license with IEEE
No reproduction or networking permitted without license from IHS
Not for Resale

h) *Environmental calibration*. In many cases, the presence of an instrument alters the behavior of the soil or rock in the vicinity of the instrument. The environmental calibration is the relationship between the real measurement and the ideal measurement where the ideal measurement is the value the measured variable should have had if the instrument was not present.

i) *Accuracy*. Accuracy can be defined as the tolerance of the instrument, tolerance being the value added to or subtracted from a particular reading such that the resulting computed range of readings bounds the actual value of the variable.

j) *Data reliability*. The ability to check for erroneous readings by comparison with a separate instrument installed in a similar position or the ability to recalibrate in situ and check a reference or zero reading.

Generally, the best instruments for field use are those which are of a simple, basic design, and reliable. When new or innovative instruments are used, it is prudent to have reliable backup instruments until the new instruments have proven themselves. Elaborate instrumentation programs have often failed to produce useful results because of the use of unsuitable instruments installed and operated by unskilled personnel.

Attention to detail in the installation of the instruments is of upmost importance. The process of installation and in situ calibration should be reviewed well in advance of installation. Problems during installation should be anticipated and contingency plans developed to cope with the problems.

When tests are to be performed, stable reference points are usually required for monitoring vertical and/or horizontal movements. The reference points should be founded well outside the expected zone of influence of the foundation.

8.3 Scope of test program

8.3.1 Literature review

The first step toward a successful load test is a review of the literature, including available standards, to determine how tests have been performed in the past. Past load test results may give an indication of expected movements and stresses of foundations under loads similar to those proposed for the test program.

When reviewing load test literature, some of the important questions to consider are the following:

— What foundation type was tested and how does it compare to the proposed test foundation?
— How was the foundation constructed?
— What type and magnitude of loads were applied and how were the loads measured?
— What were the subsurface conditions at the test site?
— What parameters were measured and what instruments were used to measure them?
— What was the reliability of the instruments?
— What were the values of the measured parameters and how do they compare to predicted values?
— What were the conclusions of the test program and are they reasonable?
— Is there enough information to draw your own conclusions?

8.3.2 Development of field testing program

The major elements to consider in developing a field testing program are listed below. More detailed criteria are given by Hirany and Kulhawy [B75].

Copyright © 2001 IEEE. All rights reserved.

Copyright The Institute of Electrical and Electronics Engineers, Inc.
Provided by IHS under license with IEEE
No reproduction or networking permitted without license from IHS Not for Resale

a) *Foundation types to be tested*. The foundation types to be tested will depend on which foundations are most promising for supporting the proposed design loads in the subsurface conditions at the structure locations. One or several foundation types can be tested. The foundation(s) may be conventional or unique, designed by established, modified, or new techniques.

b) *Location of test sites*. Selecting proper sites for testing is of extreme importance. The main goal here is to choose site(s) having subsurface conditions representative of those that are expected to be encountered along the proposed transmission line corridor. If subsurface conditions vary considerably on the right-of-way, the engineer should consider the benefits of conducting tests in each of the subsurface conditions. Access to the site(s) should be as easy as possible, and if more than one test is to be performed at a particular site, adequate space should be available to allow sufficient distance between individual test foundations to eliminate influence of one foundation on another.

c) *Number of test foundations*. The number of foundations to be tested should be determined by cost and benefit considerations. The number required is related to the selection of test sites.

d) *Geotechnical investigations*. The data obtained from the test program will be of value to the profession only if the subsurface soil/rock properties and construction procedures and equipment are defined thoroughly.

   The soil/rock properties at each test site should be known with sufficient accuracy to interpret the test results. Commonly, the preliminary subsurface exploration will provide the index properties of the soil and/or rock along the right-of-way. To permit adequate evaluation of the test results, test sites require a thorough geotechnical investigation and documentation of all construction details.

   When possible, undisturbed soil samples should be obtained from the immediate test site. Complete soil descriptions should be made and appropriate index property tests should be performed on all samples. Engineering properties of the soil should be measured and, when appropriate, in situ tests of important soil properties, such as soil modulus, should be made.

   This subsurface information will be important to the interpretation of the test results and will also allow other engineers to assimilate the results with their own experience.

e) *Type of tests to perform*. The types of tests which may be performed are given in 8.1.3. The test types required should be based on the expected combination of loads to be applied to the transmission line foundations as installed. Much more information is obtained if the foundation is loaded to failure.

f) *Construction techniques*. The method and materials used to construct test foundations should be the same as those anticipated to be used to construct the production foundations. Some test programs center around the use of the various construction techniques to determine which one is best suited for constructing a large number of foundations. In this case, each technique employed for the test program should be capable of being repeated for construction of the foundations on the project.

g) *Instrumentation*. Deciding on the number and type of instruments to use and the appropriate locations of the instruments is a critical step in the test program (see 8.2). The engineer should determine the critical parameters reflecting foundation behavior and select instruments to measure these parameters.

   In designing the instrumentation system, it is helpful to anticipate the data that will be obtained and try to draw conclusions from the use of these data. This “rehearsal” often reveals areas of the foundation which are under- or over-instrumented. This would lead to a rearranging of the instruments to obtain a better end result.

h) *Load application system*. The method for applying the required load to the test foundation should be evaluated early in the development of the test program. The load application system should be designed to safely apply the required test loads, and preferably, be designed to enable foundation failure to be achieved.

   There are many methods used to apply loads to transmission structure foundations. Some actual test setups are shown on Figure 84, Figure 85, and Figure 86.

Copyright © 2001 IEEE. All rights reserved.

Copyright The Institute of Electrical and Electronics Engineers, Inc.
Provided by IHS under license with IEEE
No reproduction or networking permitted without license from IHS
Not for Resale

Any reaction structure should be placed far enough from the test foundation so that the zones of ground movement caused by each do not overlap. The method for measuring applied loads should be determined in conjunction with the design of the load application system.

i) *Order of testing*. In large programs, it may be possible to use the results of initial tests to determine what type of tests should be conducted in later phases of the program. For example, if initial test results indicate that a particular foundation size has excessive capacity, the design should be re-evaluated and subsequent tests made on smaller foundation sizes. Testing programs which can be done in phases tend to be more efficient than programs where tests are performed concurrently.

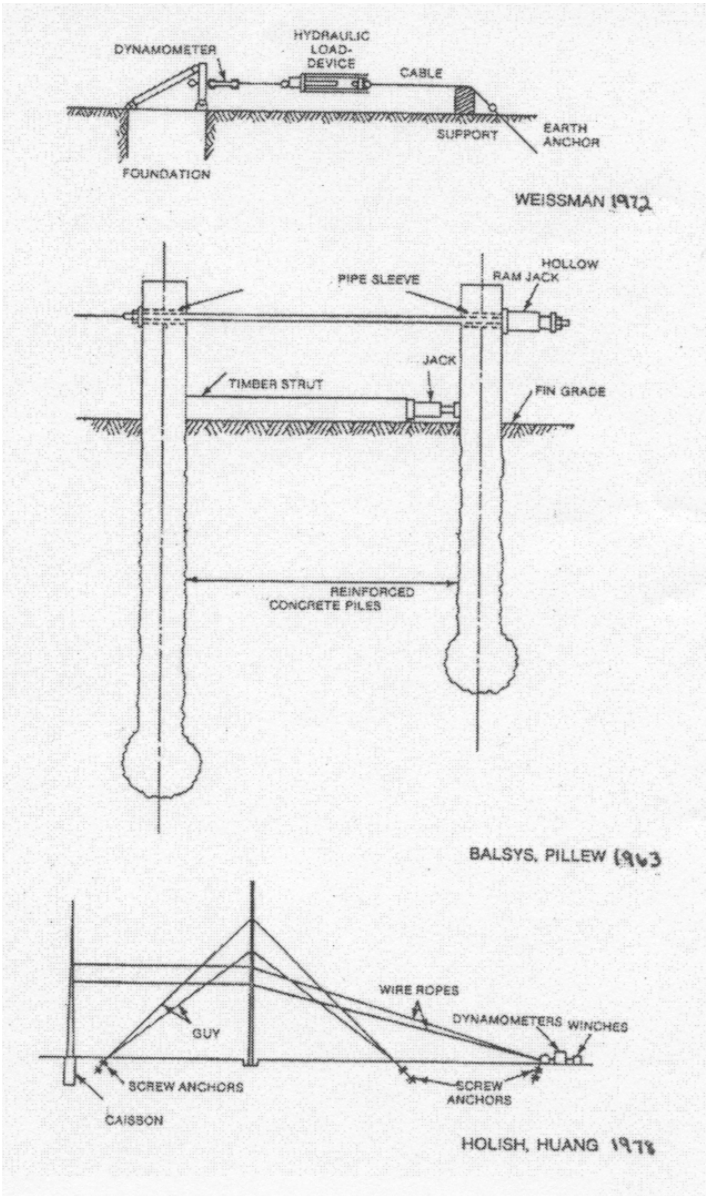

Figure 84—Examples of test setups for moment and shear loads [B75]

Copyright © 2001 IEEE. All rights reserved.

Copyright The Institute of Electrical and Electronics Engineers, Inc.
Provided by IHS under license with IEEE
No reproduction or networking permitted without license from IHS
Not for Resale

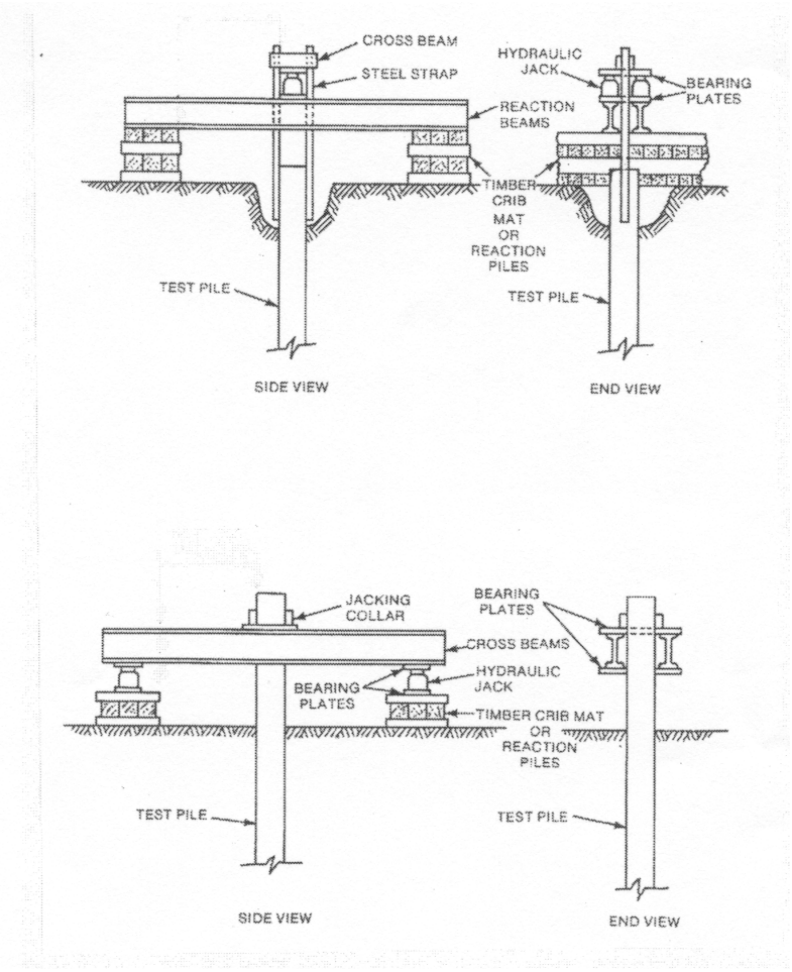

Figure 85—Examples of test setups for uplift loads [B163]

8.3.3 Construction of test foundation

Before construction of the test foundations, the contractor should be made aware that the foundation will be instrumented and be warned of possible delays in the construction in order to install the instruments.The engineer and contractor should meet to discuss the construction techniques and the method for installing instruments in a safe and reliable way. Coordination with the construction operation can be just as important as the detailed procedures of the tests themselves.

Details of construction operations should be well-documented by the engineer for the following reasons:

— To verify that the desired foundation geometry and composition were achieved
— To determine if some part of the construction operations can explain an unusual finding
— To establish the details of construction
— To provide future reference

Copyright © 2001 IEEE. All rights reserved.

Copyright The Institute of Electrical and Electronics Engineers, Inc.
Provided by IHS under license with IEEE
No reproduction or networking permitted without license from IHS
Not for Resale

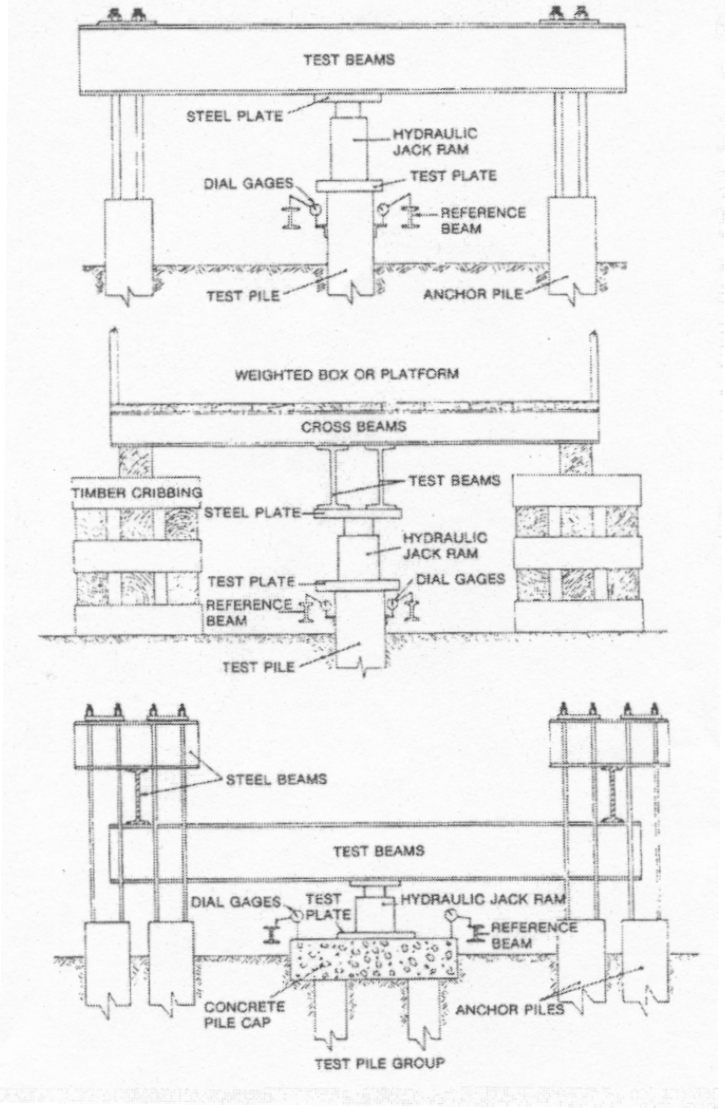

Figure 86—Examples of test setups for compression loads [B12] [B163])

Excavations for construction of the test foundations are helpful in accurately determining the subsurface conditions at the test site. The subsurface conditions revealed by construction operations should be described in detail. Photographs of the construction operations and subsurface conditions should be taken frequently. Care should be taken to protect vulnerable instrument parts during construction.

Instruments should be monitored often during the construction phase. Initial “no-load” readings on instruments should be taken in the field after sufficient time has elapsed for the instruments to adjust to field moisture and temperature conditions. Electrical instruments should be protected from moisture.

--`,,`-`-`,,`,,`,`,,`---
Copyright © 2001 IEEE. All rights reserved.
Copyright The Institute of Electrical and Electronics Engineers, Inc.
Provided by IHS under license with IEEE
No reproduction or networking permitted without license from IHS
Not for Resale

8.3.4 Test performance

Preferably, the test should be conducted in good weather. If this is not possible, adequate protection for the instruments should be provided. The accuracy of the instrumentation system should be judged on the day of the test; some instruments perform poorly in inclement weather. Before any loads are applied to the foundation, a set of zero, or "no-load", readings should be taken on all instruments. Electrical readout instruments often require a warmup time to obtain stable readings.

The loading and unloading schedule depends on the requirements of the test program and should be established in advance of the test. The loads should be applied in increments and readings of the instruments taken during each increment. The criteria for proceeding to the next load increment should be established. This is usually done by plotting, during the test, displacement of the foundation as a function of time for a given load. If in the opinion of the test engineer, displacements with time become insignificant, then the next load is applied. A plot of load versus displacement should be made as the test progresses to obtain immediate indications of the foundation behavior under load.

It is important to have good communication between the personnel applying the loads to the foundation, personnel taking readings of instruments, and test supervisor. If the instrument readings indicate an unsafe situation, the personnel taking readings must be able to direct the loads to be dropped immediately. Loads should be applied to the foundation only by order of the test supervisor. This requirement is to ensure safety and to enable instruments to be read on schedule.

Loads applied to test foundations for transmission structures can be large. Therefore, it is absolutely necessary to proceed with caution and to provide for the safety of all.

When the performance of a load test requires unusual or difficult timing in applying loads and reading instruments, it is recommended that a "mock" test be performed to familiarize the test personnel with the required procedures.

Photographs should be taken during the test for documentation purposes.

Some test programs will require post-test excavations to inspect the foundation and the mode of failure in the surrounding soil and/or rock. These excavations should be well planned, so that information critical to the investigation will not be inadvertently destroyed.

8.3.5 Analysis and documentation

Analyses of test results can be divided into two parts

a) Those performed while the test is in progress, and
b) Those performed after completion of the tests.

Analyses performed while the test is in progress give an immediate indication of the behavior of the foundation and allow better control of the test program. For example, in a static load test, the time required for sustaining each load increment can be judged by a displacement versus time plot made in the field while the foundation is under a particular load. Usually, the next load increment is applied after a certain time rate of displacement for the foundation has been reached. Applying the next load too soon may cause the load versus displacement curve to be erroneous.

Plotting measures in the field can help to point out anomalous readings. These readings can be double-checked to determine if a simple error has occurred or to verify the reading.

Copyright © 2001 IEEE. All rights reserved.

Copyright The Institute of Electrical and Electronics Engineers, Inc.
Provided by IHS under license with IEEE
No reproduction or networking permitted without license from IHS
Not for Resale

If an actual transmission structure is used to apply loads to the test foundation, the engineer should consider instrumenting the structure to better understand its behavior under actual loading conditions. The decision to instrument the structure should be based on a cost/benefit analysis in the same manner as the foundation test program.

Some instrument readings may give an indication of impending failure of a structural member of the test setup. These instruments should be monitored frequently and the readings analyzed to determine if it is safe to continue the test.

It is helpful in analyzing data to put it in a graphical form. For example, a table of lateral displacement values along the length of a drilled shaft, tends to be difficult to interpret, whereas a figure showing displacement profiles at each load increment provides a good visual indication of the lateral displacement behavior. Visually depicting the data obtained during the test helps to identify trends in the foundation behavior and allows other engineers to quickly grasp the essential elements of the test.

The results of the tests should be interpreted in a manner which satisfies the requirements of the test program. Some tests will require only a simple determination of whether a foundation moved less than an allowable value under the maximum design load. Others will require sophisticated analyses to arrive at a new method of designing a particular foundation. The analyses should consider the actual subsurface conditions at the test sites including additional subsurface information obtained during excavation for the foundation.

The behavior of the foundation predicted by analytical methods should be compared to the actual behavior of the foundation determined on the basis of test results. This comparison should give an indication of the adequacy of a particular design method for the foundation type and subsurface conditions at the test site.

The analyses should take into account the recent climatic history for the test area—that is, wet, dry, or frozen ground.

When extrapolating the results of load tests to the design of actual foundations on the line, it must be realized that subsurface conditions will not be known at the actual structure sites to the degree of accuracy that they are known at test sites. Also, construction control at structure sites will probably be much less strict than at the test sites. The engineer has the option to add a degree of conservatism in the design of foundations to account for the variability of subsurface conditions and probable variances in construction technique.

In foundation engineering, the accumulation of experience from full-scale load tests is an extremely important asset. However, test results lose their value to the engineering profession unless the experiences gained can be summarized in a manner that can be assimilated readily. One important aspect of reporting test results is to present complete and accurate subsurface information.

The test report should be presented such that an engineer unfamiliar with the test can easily follow the procedures and the behavior of the foundation and surrounding ground. The techniques used to construct and test the foundation should be explained fully.

Copyright © 2001 IEEE. All rights reserved.

Copyright The Institute of Electrical and Electronics Engineers, Inc.
Provided by IHS under license with IEEE
No reproduction or networking permitted without license from IHS
Not for Resale

Annex A

(informative)

Bibliography

[B1] ACI 318, Building Code Requirements for Reinforced Concrete.

[B2] Adams, J. I., and Hayes, D. C., "The uplift capacity of shallow foundations," *Ontario Hydro Research Quarterly*, vol.19, no. 1, 1967.

[B3] Adams, J. I., and Radhakrishna, H. S., "The uplift capacity of footings in transmission tower design," IEEE Paper A 76 124-8, Jan. 30, 1976.

[B4] Adams, J. I., Radhakrishna, H. S., and Klyn, T. W., "The uplift capacity of anchors in transmission tower design," *IEEE/PES Winter Meeting and Tesla Symposium*, New York, Jan. 25–30, 1976.

[B5] ANSI/ASCE 10-97, ANSI approved Dec. 9, 1997, Design of steel latticed transmission structures.

[B6] ANSI/ASTM A416, Specification for Uncoated Seven-Wire Stress-Relieved Steel Strand for Prestressed Concrete.

[B7] ANSI/ASTM A421, Specification for Uncoated Stress-Relieved Wire for Prestressed Concrete.

[B8] "Arctic and subarctic construction TM5-85288," Department of the Army Technical Manual on Terrain Evaluation in Arctic and Subarctic Regions.

[B9] ASTM A322, Specification for Steel Bars, Alloy, Strands and Grades.[3]

[B10] ASTM A615, Specification for Deformed and Plain Billet-Steel Bars for Concrete Reinforcement.

[B11] ASTM A616, Specification for Rail-Steel Deformed End Plain Bars for Concrete Reinforcement.

[B12] ASTM D1143, Method for Testing Piles Under Static Axial Compressive Load.

[B13] ASTM D1194, Test Method for Bearing Capacity of Soil for Static Load on Spread Footings.

[B14] ASTM D1586, Method for Penetration Test and Split-Barrel Sampling of Soils.

[B15] ASTM D2488, Practice for Description and Identification of Soils (Visual-Manual Procedure).

[B16] ASTM D3441, Standard Test Method for Deep, Quasi-Static, Cone and Friction-Cone Penetration Tests of Soil.

[B17] ASTM D3689, Method for Testing Piles Under Static Axial Tensile Load.

[B18] ASTM D3966, Method for Testing for Vertical/Batter Piles for Load-Deflection Relationships for Lateral-Axial Load.

[3]ASTM publications are available from the American Society for Testing and Materials, 1916 Race Street, Philadelphia, PA 19103, USA.

Copyright © 2001 IEEE. All rights reserved.

Copyright The Institute of Electrical and Electronics Engineers, Inc.
Provided by IHS under license with IEEE
No reproduction or networking permitted without license from IHS
Not for Resale

[B19] ASTM D4719, Test Method for Pressuremeter Testing in Soils.

[B20] AWPA C-3, 1984, Piles, Preservation Treatment by Pressure Process.

[B21] Balsys, V., and Pellew, T. W., "The civil and structural features of the 500-kV transformer stations in Ontario," *Proceedings of the Institution of Civil Engineers*, London, pp. 285–300, 1963.

[B22] Baqueling, F., Jazequel, J. F., and Shields, P. H., *The Pressuremeter and Foundation Engineering*. Trans Tech Publications, 1978.

[B23] "Basset, Discussion," *Conference on Ground Engineering*, Institution of Civil Engineers, London, 1970.

[B24] Bishop, A. W., and Henkel, D. J., *The Measurement of Soil Properties in the Triaxial Test*. London: Edward Arnold, 1962.

[B25] Bowles, J. E., *Analytical and Computer Methods in Foundation Engineering*. New York: McGraw-Hill, 1974.

[B26] Bowles, J. E., *Foundation Analysis and Design*, 2nd ed. New York: McGraw-Hill, 1977.

[B27] Bowles, J. E., *Foundation Analysis and Design*, 4th ed. New York: McGraw-Hill, 1988.

[B28] Bragg, R. A., DiGioia, A. M. Jr., and Rojas-Gonzalez, L. F., "Direct embedment foundation research," Electric Power Research Institute, Palo Alto, CA, Report EL-6309, July 1988.

[B29] Brill, M. I., "Practical formulas for loads and moments in battered pile foundations," *Civil Engineering*, pp. 56, June 1972.

[B30] Broms, B. B., "Lateral resistance of piles in cohesive soils," *Journal of the Soil Mechanics and Foundations Division, ASCE,* vol. 90, no. SM2, part 1, pp. 27–63, Mar. 1964.

[B31] Broms, B. B., "Lateral resistance of piles in cohesionless soils," *Journal of the Soil Mechanics and Foundations Division, ASCE,* vol. 90, no. SM3, part 2, pp. 123–156, May 1964.

[B32] Broms, B. B., "Design of laterally loaded piles," *Journal of the Soil Mechanics and Foundations Division, ASCE,* vol. 91, no. SM3, pp. 79–99, May 1965.

[B33] Callahan, J. F., and Kulhawy, F. H., "Evaluation of procedures for predicting foundation uplift movement," Electric Power Research Institute, Palo Alto, CA, Report EL-4107, page 124, Aug. 1985.

[B34] Caquot, A., and Kerisel, J., "Traite de Mecanique des Sols," Paris, France, 1949.

[B35] Caquot, A., and Kerisel, J., "Sur le terme de surface dans le calcul des foundations en milieu pulverulent," *Proceedings, 3rd International Conference on Soil Mechanics and Foundation Engineering,* vol. 1, Zurich, Switzerland, pp. 336–337, 1953.

[B36] Casagrande, A., "The structure of clay and its importance in foundation engineering," *Journal of the Boston Society of Civil Engineers,* vol. 19, no. 4, pp. 16–25, 1932. (Reprinted in *Contributions to Soil Mechanics, 1925-1940*. Boston Society of Civil Engineers, 1940.)

[B37] Casagrande, A., "Classification and identification of soils," *ASCE Transactions,* vol. 113, p. 901, 1948.

[B38] Chellis, R. D., *Pile Foundations*. New York: McGraw-Hill, 1961.

 Copyright © 2001 IEEE. All rights reserved.

Copyright The Institute of Electrical and Electronics Engineers, Inc.
Provided by IHS under license with IEEE
No reproduction or networking permitted without license from IHS Not for Resale

[B39] Cook, R. D., *Concepts and Applications of Finite Element Analysis,* 2nd ed. New York: John Wiley and Sons, 1981.

[B40] Coyle, H. M., and Castello, R. R., "New design correlations for piles in sand," *Journal of the Geotechnical Engineering Division, ASCE,* vol. 107, no. GT7, 1981.

[B41] Crowther, C. L., *Load Testing of Deep Foundations*. New York: John Wiley and Sons, 1988.

[B42] DAS, B. M., *Resistance of Shallow Inclined Anchors in Clay, Uplift Behavior of Anchor Foundations in Soil*. New York: ASCE, pp. 86–101, Oct. 1985.

[B43] Davidson, H. L., "Laterally loaded drilled shaft research," vols. I and II, Electric Power Research Institute, Palo Alto, CA, Report El-2197, 1981.

[B44] Davisson, M. T., and Gill, H. L., "Laterally loaded piles in a layered soil system," *Journal of the Soil Mechanics and Foundations Division, ASCE,* vol. 89, no. SM3, pp. 63–94, May 1963.

[B45] Davisson, M. T., and Prakash, S., "A review of soil-pole behavior," *Highway Research Record*, no. 39, pp. 25–46, 1963.

[B46] Deere, D. U., and Deere, D. W., "Rock quality designation (RQD) after twenty years," U.S. Army Engineer Waterways Experiment Station, Vicksburg, MS, Contract Report GL-89-1, 1989.

[B47] Deere, D.U., et al., "Design of surface and near surface construction in rock," *Proceedings, 8th Symposium on Rock Mechanics*. New York: The American Institute of Mining, Metallurgical and Petroleum Engineering, 1967, pp. 237–302.

[B48] Demello, V. F. B., "The standard penetration test," *Proceedings, 4th Panamerican Conference on Soil Mechanics and Foundation Engineering,* vol. 1, pp. 1–86, 1971.

[B49] "Design of guyed electrical transmission structures," ASCE Manual, no. 91, 1997.

[B50] "Design of steel transmission pole structures," ASCE Manuals and Reports on Engineering Practice, no. 72, 1990.

[B51] DiGioia, A. M. Jr., and Rojas-Gonzalez, L. F., "TLWorkstation™ Code: Version 2.0 Volume 17: MFAD Manual (Revision 1)," Electric Power Research Institute, Palo Alto, CA Dec. 1991.

[B52] DiGioia, A. M. Jr., Donovan, T. D., and Cortese, F. J., "A multi-layered/pressuremeter approach to laterally loaded rigid caisson design," *Seminar on Lateral Pressures Related to Large Diameter Pipe, Piles, Tunnels, and Caissons,* ASCE, Dayton, OH, Feb. 1975.

[B53] DiGioia, A. M. Jr., Rojas-Gonzalez, L. F., and Newman, F. B., "Statistical analysis of drilled shaft and embedded pole models," *Foundation Engineering: Current Principles and Practices,* edited by F. H. Kulhawy. New York, ASCE, pp. 1338–1352, 1989.

[B54] Doughty, H. C., and Young, R. A., "Stabilizing steel transmission poles," *Transmission and Distribution,* pp. 70–72, Feb. 1969.

[B55] Downs, D. I., and Chieurzzi, R., "Transmission tower foundations," *Journal of the Power Division,* ASCE, vol. 92, no. PO3, pp. 91–114, Apr. 1966.

[B56] Dunnicliff, J. (1988). Geotechnical Instrumentation for Monitoring Field Performance, John Wiley and Sons, New York.

Copyright © 2001 IEEE. All rights reserved.

Copyright The Institute of Electrical and Electronics Engineers, Inc.
Provided by IHS under license with IEEE
No reproduction or networking permitted without license from IHS
Not for Resale

[B57] EPRI EL-6800, Project 1493-6, Section 5, Final Report, "Manual on estimating soil properties for foundation design," Aug. 1990.

[B58] Federal highway Administration, 1986, Wave Equation Analysis of Pile Foundations, Contract No. DTFH61 - 84 - C - 00100, National Technical Information Service, Springfield, Va., 22161.

[B59] Gambin, M., "Calculation of Foundation Subjected to Horizontal Forces Using Pressuremeter Data," Soils-Sols, Paris, No. 30/31, 1979, pp. 17–59.

[B60] Ghaly, Ashraf, Hanna, Adel, and Hanna, Mikhail, Uplift Behavior of Screw Anchors in Sand. I: Dry Sand, ASCE, New York, Journal of Geotechnical Engineering, Vol. 117, No. 5, May, 1991.

[B61] Ghaly, Ashraf, Hanna, Adel, and Hanna, Mikhail, Uplift Behavior of Screw Anchors in Sand. II: Hydrostatic and Flow Conditions, ASCE, New York, Journal of Geotechnical Engineering, Vol. 117, No. 5, May, 1991.

[B62] Ghaly, Ashraf, Hanna, Adel, Ranjan, Gopal, and Hanna, Mikhail, Helical Anchors in Dry and Submerged Sand Subjected to Surcharge, ASCE New York, Journal of Geotechnical Engineering, Vol. 117, No. 10, October, 1991.

[B63] Ghaly, Ashraf, Hanna, Adel, and Hanna, Mikhail, Installation Torque of Screw Anchors in Dry Sand, Japanese Society of Soil Mechanics and Foundation Engineering, Soils and Foundations, Vol. 31, No. 2, 77–92, June 1991.

[B64] Ghaly, Ashraf, and Hanna, Adel, Experimental and Theoretical Studies on Installation Torque of Screw Anchors, Canadian Geotechnical Journal, Vol 28, No. 3, 1991, pp353–364.

[B65] Goldberg, D. T., W. E. Jaworski, and M. D. Gordon, Lateral Support Systems and Underpinning, Design and Construction, Vol. I, prepared for Federal Highway Administration, US Department of Commerce, publication PB-257 210, April 1, 1976.

[B66] Grand, E. B., "Types of Piles: Their Characteristics and General Use," Highway Research Record, 1977, pp. 3–15.

[B67] Grandholm, H., "On the Elastic Stability of Piles Surrounded by a Supporting Medium," Handigar Ingeniors Vetenskaps Akademien, No. 89, 1929.

[B68] Guidelines for Electrical Transmission Line Structural Loading, Manuals and Reports on Engineering Practice, No. 74, American Society of Civil Engineers, 1991.

[B69] Hanna, T. H., and R. W. Carr, The Loading Behavior of Plate Anchors in Normally and Overconsolidated Sands. Proceedings, 4th Conference on Soil Mechanics, Budapest, 1971, pp. 589–600.

[B70] Hansen, J. B., "A Revised and Extended Formula for Bearing Capacity," Bulletin No. 28, Danish Geotechnical Institute, Copenhagen, 1970, pp. 5–11.

[B71] Hansen, J. B., "The Ultimate Resistance of Rigid Piles Against Transversal Forces," Danish Geotechnical Institute, Bulletin No. 12, 1961, pp. 5–9.

[B72] Harr, M. E., Mechanics of Particulate Media - A Probabilistic Approach, McGraw-Hill Book Company, New York, New York, 1977.

[B73] Harrington, P. A., Tolbert, W.C., and Fisher, H.E., "New Foundations are Key to 230 kV Circuit Savings," Electrical World, September 29, 1969.

Copyright © 2001 IEEE. All rights reserved.

Copyright The Institute of Electrical and Electronics Engineers, Inc.
Provided by IHS under license with IEEE
No reproduction or networking permitted without license from IHS
Not for Resale

[B74] Hentenyi, M., "Beam on Elastic Foundation," The University of Michigan Press, Ann Arbor, MI, 1946, 255 p.

[B75] Hirany, A. and Kulhawy, F. H. (1988), "Conduct and Interpretation of Load Tests on Drilled Shaft Foundations," Report EL 5915, Volume 1 and Volume 2, Electric Power Research Institute, Palo Alto, CA.

[B76] Holish, L. L. and Huang, W. (1978). "Foundation Design Based on Field Test." Transmission and Substation Conference Paper T&S - P28 Chicago, IL.

[B77] Horvath, R. G., Kenney, T. C., and Kozicki, P., "Methods of Improving the Performance of Drilled Piers in Weak Rock," Canadian Geotechnical Journal, Vol. 20, No. 4, 1983, pp. 758–772.

[B78] Horvath, R. G., and T. C. Kenney, Shaft Resistance of Rock- Socketed Drilled Piers, ASCE Conference Paper, Atlanta, October 23–25, 1979 (Preprint 3698).

[B79] Hrennikoff, A., "Analysis of Pile Foundations with Batter Piles," Transactions, ASCE, Vol. 115, 1950, pp. 351–382.

[B80] Hvorslev, M. J. The Present State of the Art of Obtaining Undisturbed Samples of Soils, Committee on Sampling and Testing, Soil Mechanics and Foundation Division, ASCE, March, 1940[4].

[B81] Hyde, A. 1957, "Bearing Capacity of Piles and Pile Groups," Proceedings of the Fourth International Conference on Soil Mechanics and Foundation Engineering, Vol. 2, pp 46–51.

[B82] Ismail, N. F. and Klym, T. W., ASCE - Journal of Geotechnical Engineering Division, Vol. 105, No. GT5, May 1979, "Uplift and Bearing Capacity of Short Piers in Sand."

[B83] Ivey, D. L., "Theory, Resistance of a Drilled Shaft Footing to Overturning Loads," Texas Transportation Institute, Austin, TX, Research Report No. 105-1, February 1968.

[B84] Jorge, G. R., LeTirant IRP Reinjectable Special pour Terrains Meubles, Karstique ou a Faibles Characteristics Geotechniques. Proceedings, Seventh International Conference on Soil Mechanics and Foundation Engineering, Mexico City, August 25–29, 1969.

[B85] Koutsoftas, D. and Fischer, J.A. In-Situ Undrained Shear Strength of Two Marine Clays. Journal, Geotechnical Engineering Division, ASCE, Vol.102, GT9, 1976, pp 989-1005.

[B86] Kulhawy, F. H., "Drained Uplift Capacity of Drilled Shafts," Proceedings, 11th International Conference on Soil Mechanics and Foundation Engineering, San Francisco, CA, August 1985, pp. 1549–1552.

[B87] Kulhawy, F. H., Uplift Behavior of Shallow Soil Anchors - An Overview, Uplift Behavior of Anchor Foundations in Soil, ASCE, New York, pp. 1–25, October 1985.

[B88] Kulhawy, F. H. and Goodman, R. E., "Foundations in Rock," Chap. 55 in Ground Engineer's Reference Book, Ed. by F. G. Bell, Butterworths, London, 1987, pp. 55/1–55/13.

[B89] Kulhawy, F. H., and Jackson, C. S., "Some Observations on Undrained Side Resistance of Drilled Shafts," "Foundation Engineering: Current Principles and Practices," Ed., F. H. Kulhawy, ASCE, New York, NY 1989, pp. 1011–1025.

[4]Copies of this report are available from the Engineering Societies' Library, 345 East 47th Street, New York, NY 10017.

Copyright © 2001 IEEE. All rights reserved.

Copyright The Institute of Electrical and Electronics Engineers, Inc.
Provided by IHS under license with IEEE
No reproduction or networking permitted without license from IHS
Not for Resale

[B90] Kulhawy, F. H., and Jackson, C. S., and Mayne, P. W. "First-Order Estimation of Ko in Sands and Clays," "Foundation Engineering: Current Principles and Practices," Ed. F.H. Kulhawy, ASCE, New York, NY, 1989, pp. 121–134.

[B91] Kulwahy, F. H., Kozera, D. W., and Withian, J. L., "Uplift Testing of Model Drilled Shafts in Sand," Journal of Geotechnical Engineering Division, article number 14301 GT1.

[B92] Kulhawy, F. H., and Mayne, P. W. "Manual on Estimating Soil Properties for Foundation Design, "Report EL-6800, Electric Power Research Institute, Palo Alto, CA, July 1990, 300 p.

[B93] Kulhawy, F. H., and Pease, K. A., Load Transfer Mechanisms in Rock Sockets and Anchors, Electric Power Research Institute, Report EL-3777, Palo Alto, California, November, 1984, 102p.

[B94] Kulhawy, F. H. and Peterson, M. S., "Behavior of Sand-Concrete Interfaces," Proceedings, 6th Pan-American Conference on Soil Mechanics and Foundation Engineering, Vol. 2, Lima, 1979, pp. 225–236.

[B95] Kulhawy, F. H., Trautmann, C. H., Beech, J. F., O'Rourke, T. D., McGuire, W., Wood, W. A., and Capano, C., "Transmission Line Structure Foundations for Uplift-Compression Loading," Report EL-2870, Electric Power Research Institute, Palo Alto, CA, February 1983, 412 pp. 5–47.

[B96] Lambe, T. W., Soil Testing for Engineers. New York: John Wiley and Sons, 1951.

[B97] Lambe, T. W. and Whitman, R. V., Soil Mechanics. New York: John Wiley & Sons, 1968.

[B98] Littlejohn, G. S., Soil Anchors, Proceedings of a Conference Organized by the Institution of Civil Engineers, London, pp. 33–44, June 1970.

[B99] Marcuson, W.F.III and Bieganousky, W.A. SPT and Relative Density in Course Sands. Journal of the Geotechnical Engineering Division, ASCE, Vol.103, GT11, 1977, pp 1295-1309.

[B100] Martin, D., Design of Anchor Plates, CIGRE Paper CSC 22-74 (WG 07)-11, revised March 28, 1977.

[B101] Matlock, H., "Correlations for Design of Laterally Loaded Piles in Soft Clay," Proceedings, 2nd Annual Offshore Technology Conference, Houston, TX, 1970, American Institute of Mining, Metal, and Petroleum Engineering, pp. 577–594.

[B102] Matlock, H., and Reese, L. C. (1960), "Generalized Solution for Laterally Loaded Piles," Journal of the Soil Mechanics and Foundation Division, ASCE, vol. 89, No. SM5, Part I, pp. 479–482.

[B103] Matlock, H., and Reese, L. C., "Generalized Solutions for Laterally Loaded Piles," Journal of the Soil Mechanics and Foundations Division, ASCE, New York, NY, Vol. 86, No. sm5, October, 1969, pp. 63–91.

[B104] Matsuo, M., Study on Uplift Resistance of Footings (I). Soils and Foundations, Vol. VII, 1967, pp. 1–37.

[B105] Matsuo, M., Study on Uplift Resistance of Footings (I). Soils and Foundations, Vol. VIII, No. 4, 1967, pp. 1–37.

[B106] Matsuo, M., "Study on the Uplift Resistance on Footing (II), Soil and Foundations.

[B107] Mayne, P. W., and Kulhawy, F. H., "K_0-OCR Relationships in Soil," Journal of the Geotechnical Engineering Division, ASCE, Vol. 2, Dec. 1979, pp 225 - 236.

Copyright © 2001 IEEE. All rights reserved.

Copyright The Institute of Electrical and Electronics Engineers, Inc.
Provided by IHS under license with IEEE
No reproduction or networking permitted without license from IHS Not for Resale

[B108] Mayne, P. W., and Kulhawy, F. H., "K_0-OCR Relationships in Soil," Journal of the Geotechnical Engineering Division, ASCE, New York, NY, Vol. 108, No. GT6, June 1982, pp. 851–872.

[B109] Menard, L. The Interpretation of Pressuremeter Test Results. Sols Soils, No.26, 1975, pp 7-43.

[B110] Mesri, G. and Godlewski, P. M., Time and Stress Compressibility Interrelationship, ASCE Geotechnical Journal May 1977.

[B111] Mesri, G. and Choi, Y. K., Settlement Analysis of Embankments on Soft Clays, Journal of Geotechnical Engineering ASCE Vol.111, No. 4, and April 1985 page 441 to 464.

[B112] Meyerhof, G. C. and Adams, J. l., "The Ultimate Uplift Capacity of Foundations," Canadian Technical Journal, Vol. V, No. 4, 1968, pp. 225–244.

[B113] Mindlin, R. D., Force at a point in the interior of a Semi-infinite Solid. Journal of Applied Physics, Vol. 7, No. 5, pp 195-202, 1936

[B114] Mitsch, M. P., and S. P. Clemence, The Uplift Capacity of Helix Anchors in Sand. Uplift Behavior of Anchor Foundations in Soil, Editor S. P. Clemence, American Society of Civil Engineers, New York, NY, October, 1985, pp 26–47.

[B115] Mooney, J. S., S. Adamczak, Jr., and S. P. Clemence, Uplift Capacity of Helical Anchors in Clay and Silt. Uplift Behavior of Anchor Foundations in Soil, Editor S. P. Clemence, American Society of Civil Engineers, New York, NY, October, 1985, pp 48–72.

[B116] Mors, H., "Methods of Dimensioning for Uplift Foundations of Transmission Line Tower," Conference Internationale Des Grande Resequx Electriques a Haute Tension, Paris, Session 1964, No. 210.

[B117] National Electrical Safety Code, Institute of Electrical and Electronics Engineers, Inc., Secretariat, 1997

[B118] Neely, W. T., and J. M. Montague, Pullout Capacity of Straight Shafted and Underreamed Ground Anchors. Die Swiele Ingenieur, South Africa, Vol. 16, April 1974, pp. 131–134.

[B119] Ostermayer, H., Construction, Carrying Behavior and Creep Characteristics of Ground Anchors. Conference on Diaphragm Walls and Anchorages, Institution of Civil Engineers, September, 1974.

[B120] Palmer, L. A., and Thompson, J. B., "The Earth Pressure and Deflection Along Embedded Lengths of Piles Subjected to Lateral Thrust," Proceedings, 2nd International Conference on Soil Mechanics and Foundation Engineering, Rotterdam, 1948, ISSMFE, Vol. 5, pp. 156–161.

[B121] Parker, F., Jr., and Reese, L. C., "Experimental and Analytical Studies of Behavior of Single Piles in Sand Under Lateral and Axial Loading," Research Report 117-2, Center for Highway Research, The University of Texas at Austin, TX, November 1970.

[B122] Pease, K.A., and Kulhawy, F.H., "Load Transfer Mechanisms is Rock Sockets and Anchors," Report EL-3777, Electric Power Research Institute, Palo Alto, CA, November 1984, 102 p.

[B123] Peck, R.B. and Bazaraa, A.R.S.S. Discussion. Journal of the Soil Mechanics and Foundation Division, ASCE. vol 95, SM5, 1969, p. 905-909.

[B124] Peck, R. B., Hanson, W. E., Thornburn, T. H., Foundation Engineering, John Wiley and Sons, Inc., New York, New York, 2nd Edition, 1974.

Copyright © 2001 IEEE. All rights reserved.

Copyright The Institute of Electrical and Electronics Engineers, Inc.
Provided by IHS under license with IEEE
No reproduction or networking permitted without license from IHS
Not for Resale

[B125] Penner, E., and Gold, L. W., 1971, Transfer of Heaving Forces by Adfreezing to Columns and Foundation Walls in Frost-Susceptible Soils, Canadian Geotechnical Journal, 8, pp. 514–526.

[B126] Potyondy, J. G., "Skin Friction Between Various Soils and Construction Materials," Geotechnique, Vol. 11, No. 4, Dec. 1961, pp. 339–353.

[B127] Poulos, H. G., "Ultimate Lateral Pile Capacity in Two-Layer Soil," Geotechnical Engineering, Asian Institute of Technology, Volume 16, No. 1, June 1985.

[B128] Poulos, H. G., 1971, "Behaviour of Laterally Loaded Piles: 11 Pile Groups". Journal of the Soil Mechanics and Foundations Division, ASCE, Vol. 97, May 1971, pp 733 - 751.

[B129] Poulos, H. G. and Davis, E. H. Elastic Solutions for Soil and Rock Mechanics, New York, John Wiley & Sons, 1974.

[B130] Poulos, H. G., and Davis, E. H., "Pile Foundation Analysis and Design," John Wiley and Sons, New York, NY, 1980, 147 p.

[B131] Reese, L. C., Discussion of "Soil Modulus for Laterally Loaded Piles," by B. McClelland and J.A., Focht, Jr., Transactions, ASCE, New York, NY, Vol. 123, Paper No. 2954, 1958, pp 107–074.

[B132] Reese, L. C., "Design and Construction of Drilled Shafts," Journal of the Geotechnical Engineering Division, ASCE, New York, NY, Vol. 104, No. GT1, 1978, pp. 95–116.

[B133] Reese, L. C., Cox, W. R., and Kiip, F. D., "Analysis of Laterally Loaded Piles in Sand," Proc. 6th Annual Offshore Technology Conference, Vol. 2 No. 2080, Houston, TX 1974, pp. 473–483.

[B134] Reese, L. C., and Matlock, H., "Nondimensional Solutions for laterally Loaded Piles with Soil Modulus Assumed Proportional to depth," Proceedings, 8th Texas Conference on Soil Mechanics and Foundation Engineering, Austin, TX, 1956.

[B135] Reese, L. C., O'Neill, M. W., and Touma, F. T., "Bored Piles installed by Slurry Displacement," Proceedings, Eighth International Conference on Soil Mechanics and Foundation Engineering, Moscow, Vol. 2.1, 1973, pp. 203–209.

[B136] Reese, L. C., and Welch, R., "Lateral Loading of Deep Foundations in Stiff Clay," Journal of the Geotechnical Engineering Division, ASCE, New York, NY, Vol. 1010, No. GT7, July 1975, pp. 633–649.

[B137] Rodgers, T. E. Jr., H. Singh, and J. Judwari, A Rational Approach to the Design of High Capacity Multi-Helix Screw Anchors, 7th IEEE/PES Transmission and Distribution Conference and Exposition, April 1–6, 1979.

[B138] Romanoff, M., 1962, "Corrosion of Steel Piling in soils," National Bureau of Standards, Monograph 58.

[B139] Schmertmann, J. H., "Static Cone to Compute Static Settlement Over Sand," Journal Soil Mechanics and Foundation Division, ASCE, 96, No. SM3.

[B140] [Seeman, T. and R. Gowans, Guy Anchor Test Project for Lyons 1100 kV Test Line. IEEE/PES Winter Meeting, New York, NY, January 30–February 4, 1977.

[B141] Semple, R. M., and Rigden, W. J., "Shaft Capacity of Driven Piles in Clay," Ground Engineering, January, 1986.

Copyright © 2001 IEEE. All rights reserved.

Copyright The Institute of Electrical and Electronics Engineers, Inc.
Provided by IHS under license with IEEE
No reproduction or networking permitted without license from IHS
Not for Resale

[B142] Sheikh, S. A., O'Neil, M. W., and Mehrazarin, M. A., "Expansive Concrete Drilled Shafts," Canadian Journal of Civil Engineering, Vol. 12, No. 2, 1985, pp. 382–295.

[B143] Sheikh, S. A., O'Neil, M. W., and Venkatesan, N., "Behavior of 45-Degree Under-reamed Footings," Research Report 83-18, University of Houston, TX, November 1983, 126 p.

[B144] Smith, E. A. L., 1960, "Pile Driving Analysis by the Wave Equation," ASCE Journal of the Soil Mechanics and Foundations Division, Vol. 86, SM4, pp. 35–61.

[B145] Sowa, V. A., "Pulling Capacity of Concrete Cast In Situ Bored Piles," Canadian Geotechnical Journal, 1970, pp. 482–493.

[B146] Sowers, G. B. and Sowers, G. F. Introductory Soil Mechanics and Foundations. 3rd ed. New York, MacMillan, 1970.

[B147] Stas, C. V., and Kulhawy, F. H., "Critical Evaluation of Design Methods for Foundations Under Axial Uplift and Compression Loading," Report EL-3771, Electric Power Research Institute, Palo Alto, CA, November 1984, 198 p.

[B148] Stern, L. I., Bose, S. K., and King, R. D., The Uplift Capacity of Poured-in-Place Cylindrical Caissons, IEEE Paper A 76 053-9, January 30, 1976.

[B149] Stewart, J. P., and Kulhawy, F. H., "Experimental Investigation of the Uplift Capacity of Drilled Shaft Foundations in Cohesionless soil," Contract Report B-49(6), Niagara Mohawk Power Corporation, Syracuse, NY, May 1981, 422 p. Geotechnical Engineering Report 81-2, Cornell University.

[B150] Stuart, J. B., Hannah, T. H., Naylor, A. H., 1960, "Notes on Behaviour of Model Pile Groups in Sand," Symposium on Pile Foundations, Stockholm.

[B151] Subsurface Investigation for Design and Construction of Foundations of Buildings. ASCE, Manual 56, 1976.

[B152] Symposium on Vane Shear Testing of Soils. ASTM Special Technical Publication, No.193, 1956.

[B153] Terzaghi, K., "Evaluation of Coefficient of Subgrade Reaction," Geotechnique, London, Vol. 5, 1955, pp. 297–326.

[B154] Terzaghi, K., and Peck, R. B., 1967, Soil Mechanics in Engineering Practice, John Wiley and Sons.

[B155] Tomlinson, M. J., "Adhesion of Piles Driven in Clay Soils," Proceedings 4th International Conference in Soil Mechanics and Foundation Engineering, Vol. 2, London, 1959, pp. 66–71.

[B156] Tomlinson, M.J., 1977, Pile Design and Construction Practice, Viewpoint Publications.

[B157] Trautmann, C. H., and Kulhawy, F. H., "Data Sources for Engineering Geologic Studies," Bulletin of the Association of Engineering Geologists, Vol. 20, No. 4, November 1983, pp. 439–454.

[B158] Trautmann, C. H. and Kulhawy, F. H., "Uplift Load-Displacement Behavior of Spread Foundations," Journal of Geotechnical Engineering, ASCE 1988 and Uplift Load Displacement Behavior of Grillage Foundations ASCE Geotechnical Division Pub. No. 40, 1994.

[B159] Trautmann, C. H., and Kulhawy, F. H., "TLWorkstation Code: Version 2.0, Volume 16: CUFAD Manual," Report EL-6420, Vol 16, Electric Power Research Institute, Palo Alto, CA, 1990, 133 p.

Copyright © 2001 IEEE. All rights reserved.

Copyright The Institute of Electrical and Electronics Engineers, Inc.
Provided by IHS under license with IEEE
No reproduction or networking permitted without license from IHS
Not for Resale

[B160] Tucker, K. D., "Uplift Capacity of Drilled Shafts and Driven Piles in Granular Material," "Foundations for Transmission Line Towers" Ed., J-L Briaud, ASCE Geotechnical Special Publication No. 8, New York, NY, 1987,pp. 142–159.

[B161] United States Department of the Navy, Naval Facilities Engineering Command, 1982, NAVFAC DM 7.2, Foundations and Earth Structures, Government Printing Office, Washington.

[B162] Vesic, A. S., "Bearing Capacity of Shallow Foundations," Chapter 3 in Foundation Engineering Handbook, Ed. by H. Winterkorn and H. Y. Fang, Van Nostrand Reinhold Company, New York, 1975, pp. 121–147.

[B163] Vesic, A. S. (1977). Design of Pile Foundations, National Cooperative Highway Research Program, Synthesis of Highway Practice 42, Transportation Research Board, National Research Council, Washington, DC.

[B164] Weissman, G. F. (1972). Tilting Foundations, Journal, "Soil Mechanics and Foundations Division." ASCE. SM159-78.

[B165] Winterkorn, H. F. and Fang, H. Foundation Engineering Handbook. New York, Van Nostrand Reinhold, 1976.

[B166] Woodward, R. J., and Gardner, W. S., 1972, Drilled Pier Foundations, McGraw - Hill.

[B167] Woodward, R. J., Gardner, W. S., and Greer, D. M., "Drilled Shaft Foundations," McGraw-Hill, New York, NY, 1972, 287 p.

[B168] Zobel, E. S., McKinnon, W. H., Ralson, P., King, R. D., and Engimann, J. C., Transmission Structure Foundation Test Results for Various Types and Locations, IEEE Paper A 76 185-9, January 30, 1976.

Copyright © 2001 IEEE. All rights reserved.
Copyright The Institute of Electrical and Electronics Engineers, Inc.
Provided by IHS under license with IEEE
No reproduction or networking permitted without license from IHS
Not for Resale